



*National University of Science and Technology
POLITEHNICA Bucharest
Faculty of Industrial Engineering and Robotics*



Journal of Industrial Engineering and Robotics

2024, Volume 8, Issue 2

Scientific Committee of Journal of Industrial Engineering and Robotics

Prof.dr.ing.	AMZA Catalin
Conf.dr.ing.	BACIU Florin
Conf.dr.ing.	CATANA Madalin-Gabriel
S.l.dr.ing.	DIJMARESCU Manuela-Roxana
S.l.dr.ing.	NICULAE Elisabeta
Conf.dr.ing.	POPA Laurentiu
S.l.dr.ing.	POPESCU Adrian
Prof.dr.ing.	SEVERIN Irina
S.l.dr.ing.	TUDOSE Daniela Ioana
Conf.dr.ing.	UNGUREANU Liviu Marian

Editorial board of Journal of Industrial Engineering and Robotics

Prof.dr.ing.	DUMITRESCU Andrei
Conf.dr.ing.	PARPALA Radu
S.l.dr.ing.	RADU Constantin
S.l.dr.ing.	ROTARU Alexandra
S.l.dr.ing.	TUDOSE Virgil

Editors

Prof.dr.ing.ec.	DOICIN Cristian
Conf.dr.ing.	APOSTOL Dragoş

RESEARCH ON THE DEVELOPMENT OF AN AUTOMATIC TRANSMISSION

ORGHIDEAN Rareș-Vasile¹, DIJMĂRESCU Manuela-Roxana², IONESCU Nicolae²

¹Faculty of Industrial Engineering and Robotics, Study Program: Industrial Engineering,
Year of Study: 4, email: rares_orghidean@yahoo.ro

²Faculty of Industrial Engineering and Robotics, Manufacturing Engineering Department,
POLITEHNICA Bucharest

ABSTRACT: *The project will provide a comprehensive overview of the approach taken to develop and design an automatic transmission, delving into the intricate details of the engineering and design processes involved. It will showcase the meticulous steps taken to ensure that the automatic transmission not only meets but exceeds customer expectations in terms of performance and reliability.*

KEYWORDS: *product design, product development, automatic transmission.*

1. Introduction

In today's society automatic transmissions represent a crucial part of everyday transport, marking it a necessity for millions of people, thus efficiency and performance are the driving factors for the automotive industry in designing and producing highly efficient, low cost and durable transmissions for people all around the world.

By implementing advanced automatic transmission, the goal is not only to make driving easier and to reduce accidents but also to offer the driver a better and more comfortable driving experience. Thus, particular attention will be given to optimizing the transfer and retrieval of forces all around to ensure the vehicle lasts as long as possible with the minimum number of repairs.

To achieve these objectives, a detailed and analytical approach is required, including a comprehensive assessment of the current situation and specific requirements. Only through a deep understanding of the needs and the context in which the automatic transmission will be implemented can the optimal solution be identified and implemented, with a significant impact on overall efficiency and performance of the industrial process.

2. Business strategy

To understand what we need to obtain from an automatic transmission we need to understand its characteristics and functions and more importantly to know what the customer wants to find in the product. In order to make sure we adhere to the customers' needs we have conducted a questionnaire to find out exactly what to focus on while developing the transmission. Table 1 shows the clients' needs, the parameter that influences the need and the solution to the problem.

Table 1. Needs and needs interpretation.

Client need	Parameter	Solution
I want it to last as long as possible	Material	Steel (gears)
I need a light transmission	Material	Aluminium (casing)
I want a silent transmission	Lubricant	Special Transmission Lubricant
I need a quick acceleration	Gear ratios (Low gear)	4.20:1 (1 st gear)
I want to optimize fuel consumption	Gear ratios (Overdrive gear)	0.62:1 (6 th gear)

3. Functional analysis

In this analysis, primary and secondary functions of the automatic transmission were examined. The importance of selected functions was assessed on a scale from 1 to 10 (refer to Table 2) to determine critical operations requiring specific attention and those suitable for optimization aimed at cost efficiency.

Table 2. Product functions

Primary/Secondary	Functions	Rating
Primary	Gear Selection: Selecting the appropriate gear ratio based on vehicle speed, load, and driver input.	10
Primary	Power Transmission: Transmitting power from the engine to the wheels efficiently.	10
Primary	Torque Conversion: Converting engine torque to usable output torque.	9
Secondary	Fluid Cooling: Cooling transmission fluid to maintain optimal operating temperatures.	8
Secondary	Shift Timing: Timing the gear shifts to ensure smooth transitions between gears.	8
Secondary	Manual Override: Allowing manual control over gear selection for driver preference or specific driving conditions.	6
Secondary	Traction Control: Modulating power delivery to the wheels to optimize traction and stability.	7

Based on this analysis, it becomes evident that while all the mentioned functions are essential, their impact on vehicle performance or driver safety varies. Understanding this, adjustments can be made to the transmission to align with the specific requirements of the vehicle, thereby optimizing the entire process for efficiency and cost-effectiveness.

4. Concept development

Aiming for the best experience and versatility while driving, the transmission will feature 6 speeds, assuring a seamless transition between gears, adaptable for different driving conditions. Additionally, it will include a reverse gear for maneuvering and parking and a neutral gear for towing or idling.

The transmission will be composed of 5 clutches (see figure 1) from which C1 and C2 will be driven by two shift forks so that C1 will engage the sun gears of C4 and C5 and C2 will engage the planet carrier of C4 and the ring gear of C5. C1, C2 and C3 will be permanently engaged regardless of if C1 or C2 are engaged or not. The remaining C3, C4 and C5 are all planetary gear assemblies allowing for a great number of possible outputs depending on the engagement of the clutches.

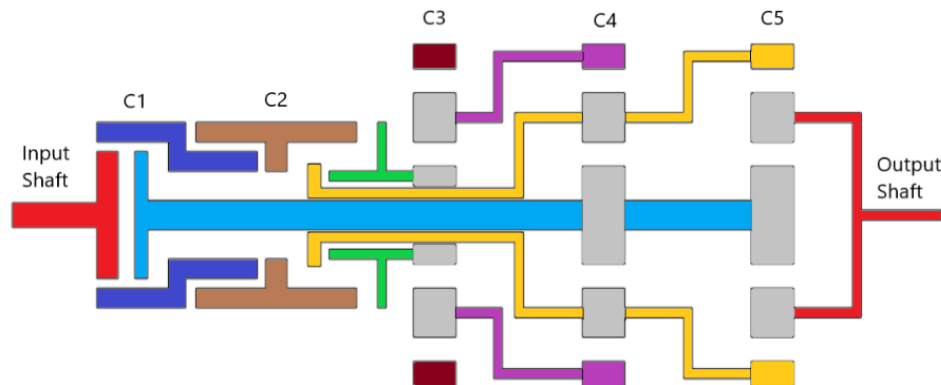


Fig. 1 Plan the Transmission depicting the different clutches. (C1,2,3,4,5 - Clutches)

5. Technical solution development and prototyping

The clutches C1 and C2 will be composed of a mechanism closely resembling the shifting of a manual transmission the only it will engage or disengage the clutches and they can be driven at the same time.

The C1 and C2 components seen in Fig. 1 (dark blue and brown) will be the synchroniser sleeves in the C1 C2 clutches. They will serve the purpose of synchronisation and lock of the Input shaft and middle shaft (light blue) in the case of C1 and the input shaft and the C5 ring gear C4 planet carrier assembly. Another thing that differs the C1 C2 clutches from a manual transmission is that the sleeves are directly connected to the input shaft as opposed to the hubs (Fig. 2). This results in the sleeves having to undertake the task of driving the C3 sun gear and the middle shaft (in the case of C1) simultaneously. For a better efficiency and to avoid shocks in the system a synchronizer ring is placed between the sleeve and the hub to ensure a smooth and synchronized gear change as seen in Fig. 3.

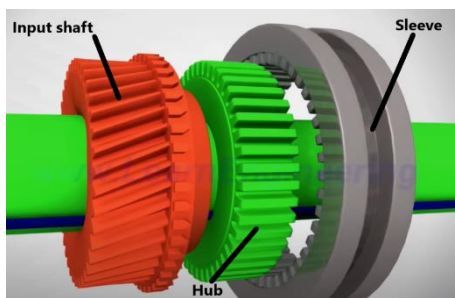


Fig. 2 Manual transmission input shaft, hub, sleeve assembly [1]

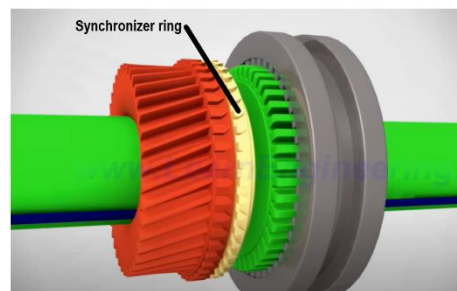


Fig. 3 Synchronizer ring [1]

assembly

part of the planetary gears' assemblies.

Spur gears [2] while being the simplest gear types in terms of geometry they are a fundamental part of the calculation for other types of gears. The spur gears consist of a cylindrical base with teeth that are straight and parallel to the axis. The gear teeth not only for spur but for all gear types mesh together to transmit a rotational motion and power between shafts. Gears can change the rotational speed and or the direction of the power transmitted.

Helical gears [3] are a type of gear very similar to spur gears but with noticeable differences. The most notable difference is the angle at which the teeth are cut in regard to the gear axis. This angle is called the helix angle Fig.6, this arrangement of teeth ensures a gradual engagement of the teeth, thus providing a quicker and smoother operation.

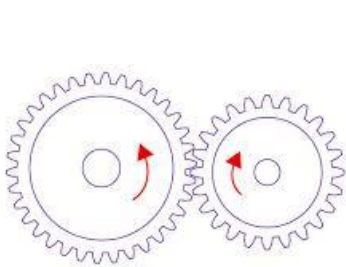


Fig. 5. Spur gears [2]

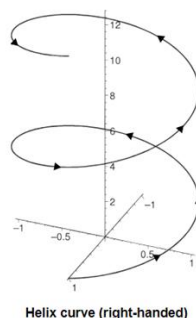


Fig. 6. Helix curve [3]



Fig. 7. Internal gear [4]

Internal gears are composed of a circular ring base and having the teeth on the inside of the circle. Internal gears teeth have a concave or re-entrant shape exactly opposite of the convex shape of the spur or helical gear types. Internal gears are often used in Planetary gear assemblies due to the number of options available for locking the gear, thus offering more control to the planetary assembly.

Planetary gears or also called epicyclic gears are practically a system in which one or more so called planet gears rotate around one central gear called sun gear. While conventional gears are fixed in position when mounted planetary gears offers trough the possible movement of its gears and mounting supports called planet carriers, more possible gear ratios thus saving on space and weight.[3] The planetary gears used composed of one central helical gear as the sun gear, three helical gears as the planet gears and one internal helical gear as the ring gear, the planetary gears will be held together by a planet carrier.

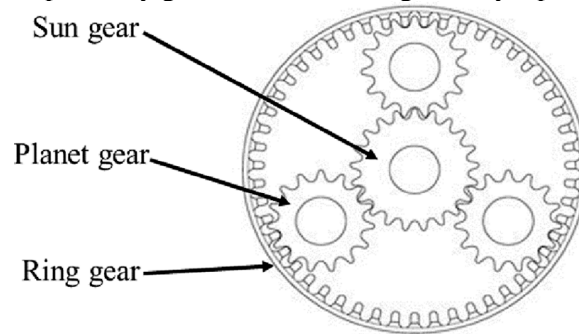


Fig. 8 [5]

For a faster and more reliable way for calculations a program in excel has been made to automatically calculate the gear ratios of the planetary gears and the final gear ratios of the transmission, as seen in Fig. 9. Since the module of the gears only influence the size of the gears we can insert only the number of teeth for the sun and ring gears and the program calculates the needed planet carrier. The neutral gear is obtained by locking only the C5 clutch, and no force driven on the middle shaft thus the transmission has no output, and the vehicle can be freely moved. The Reverse gear is obtained by locking the C5 ring gear which also locks the C4 planet carrier which together with the input resulted from locking the C3 results in rotating the C5 sun gear in a reversed direction.

			Carrier theoretic	Carrier actual			
Clutch	Sun	Ring	Sun + Ring	(Ring-Sun)/2			
3	28	50	78	11			
4	20	52	72	16			
5	20	64	84	22			
whole divider							
	sd/rb (s/c)	sd/cb (s/r)	rd/sb (r/c)	cd/sb (c/r)	rd/cb (r/s)	cd/rb (c/s)	s = Sun
3	0.358974	0.56	0.641025641	1.56	1.785714	2.785714	r = Ring
4	0.277778	0.384615	0.722222222	1.384615385	2.6	3.6	c = Carrier
5	0.238095	0.3125	0.761904762	1.3125	3.2	4.2	sd = Sun driven
							sb = Sun blocked
							cd = Carrier driven
							cb = Carrier blocked
							rd = Ring driven
							rb = Ring blocked
Gear	Clutch	Ratio:1	1/Ratio				
1	C1+C5	4.2	0.238095238				
2	C1+C4	2.223529	0.44973545				
3	C1+C3	1.544959	0.647266314				
4	C1+C2	1	1				
5	C2+C3	0.715909	1.396825397				
6	C2+C4	0.617647	1.619047619				
R	C3+C5	4.5	0.222222222				
N	C5						

Fig. 9

The calculations for the gear geometry have been made after the equations from the KHK Gears site [6] and an Excel program has been made in order to make much faster and reliable calculations as seen in Fig. 10.

No.	Item	Symbol	Formula	Example	
				Sun(R)	Carrier(L)
1	Module	m	Set Value	3	
2	Reference Pressure Angle	α		20	
3	Number of Teeth	z		20	22
4	Center Distance	a	$(z_1 + z_2) m / 2$	63	
5	Reference Diameter	d	zm	60	66
6	Base Diameter	d_b	$d \cos \alpha$	56.38155725	62.01971297
7	Addendum	h_a	1.00m	3	3
8	Tooth Depth	h	2.25m	6.75	6.75
9	Tip Diameter	d_s	$d + 2m$	66	72
10	Root Diameter	d_r	$d - 2.5m$	52.5	58.5

Fig. 10 Calculations for the C5 sun gear right hand and carrier gear Left hand

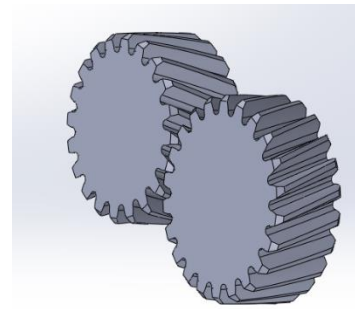


Fig. 11 Assembly of C5 sun and planet carrier gears

Calculations for the sun and planetary carrier gears will be made for the C3, C4 and C5 planetary gears along side with central holes for every gear as a way to fixate them inside the transmission assembly. The C3 sun gear will have a big circular central hole because the middle shaft and the C5 ring/C4 Planet carrier will be connected to the C2 clutch trough the C3 sun central hole and will not be connected to anything except the C3 planetary gears. C4 and C5 sun gears will be connected to the central shaft thus rotating together.

Item	Symbol	Formula	Example	
			External gear (1)	Internal gear (2)
Module	m	Set Value	3.00	
Reference pressure angle	α		20.00	
Number of teeth	z		22.000	64.000
Profile shift coefficient	x		0.000	0.000
Involute function α_w	$\text{inv } \alpha_w$	$2 \tan \alpha \left(\frac{X_2 - X_1}{Z_2 - Z_1} \right) + \text{inv } \alpha$	0.014904	
Working pressure angle	α_w	https://planetcalc.com/993/	20.00	
Center distance	y	$\frac{Z_2 - Z_1}{2} \left(\frac{\cos \alpha}{\cos \alpha_w} - 1 \right)$	0.000	
modification coefficient				
Center distance	a	$\left(\frac{Z_2 - Z_1}{2} + y \right) m$	63.00	
Reference diameter	d	zm	66.000	192.000
Base diameter	d_b	$d \cos \alpha$	62.020	180.421
Working pitch diameter	d_w	$\frac{d_b}{\cos \alpha_w}$	66.000	192.000
Addendum	h_{s1}	$(1 + x_1) m$	3.000	3.000
	h_{s2}	$(1 - x_2) m$		
Tooth depth	h	2.25m	6.75	
Tip diameter	d_{s1}	$d_1 + 2h_{s1}$	72.00	186.00
	d_{s2}	$d_2 - 2h_{s2}$		
Root diameter	d_{r1}	$d_{s1} - 2h$	58.50	199.50
	d_{r2}	$d_{s2} + 2h$		

Fig.12 Calculations for the C5 ring gear

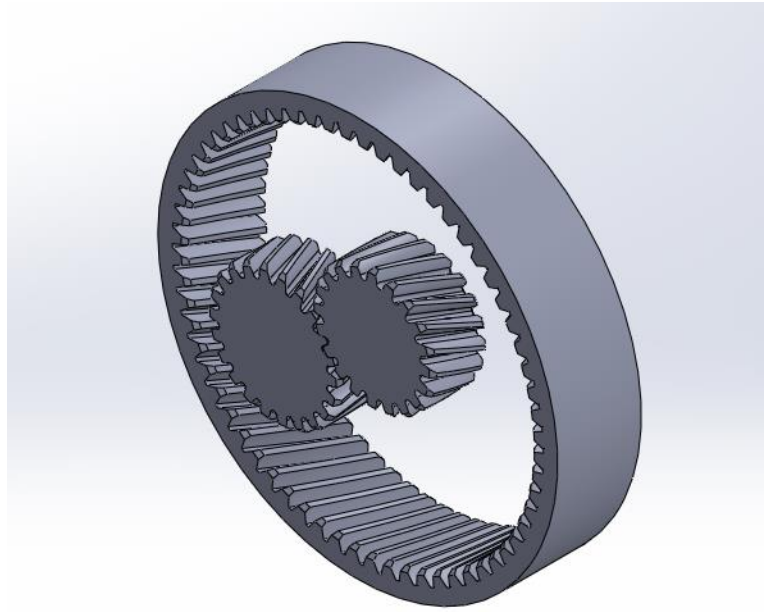


Fig. 13 C5 planetary gear assembly

6. Conclusions

As the research concludes on the development of an automatic transmission, several key insights emerge, shaping the trajectory and outcomes of our project.

Primarily, market awareness plays a pivotal role. A comprehensive analysis of customer preferences and industry dynamics guides our development endeavours, ensuring alignment with market demands.

Moreover, staying abreast of cutting-edge technology is paramount. Incorporating the latest advancements enables us to enhance the performance, fuel efficiency, and longevity of our automatic transmissions, distinguishing them in a competitive market landscape.

Furthermore, maintaining flexibility and adaptability is essential. Given the diverse range of vehicles desired by consumers, produced at various times and volumes, adopting flexible manufacturing approaches allows us to meet these demands while upholding quality standards.

7. References

- [1]. Lesics. (2015, March 4). Manual Transmission, How it works? [Video]. YouTube. <https://www.youtube.com/watch?v=wCu9W9xNwtI> (05.05.2024)
- [2]. <https://uk.rs-online.com/web/content/discovery/ideas-and-advice/spur-gears-guide> (05.05.2024)
- [3]. Glinisky, C. (2020, July 19). Helical Gears - Geometry of helical gears and gear meshes. <https://drivetrainhub.com/notebooks/gears/geometry/Chapter%20%20-%20Helical%20Gears.html#Geometry-/-Helical-Gears> (05.05.2024)
- [4]. Internal Gears | High-Precision Internal Spur Gear Manufacturing | WM Berg. (n.d.). <https://www.wmberg.com/products/gears/internal-gears> (05.05.2024)
- [5]. https://www.researchgate.net/figure/Simple-planetary-gear-set_fig1_33864194 (05.05.2024)
- [6] Kanri, K. W. (n.d.). Calculation of gear dimensions | KHK Gears. KHK Gears. https://khkgears.net/new/gear_knowledge/gear_technical_reference/calculation_gear_dimensions.html (05.05.2024)

RESEARCH ON ULTRASONIC AIDED ECM POLISHING

**CONSTANTIN A.C. Paul-Andrei, PELENGICĂ P.C. Paul-Mihai, SANDU C.M.
Constantin-Andrei, Liviu Daniel GHICULESCU, ENCIU Cornel**

Faculty of Industrial Engineering and Robotics, Specialization: Manufacturing Engineering,
Year of study: IV, e-mail: paulandrei001@yahoo.com

ABSTRACT: *This paper presents the current state of the art of ultrasonic aided electrochemical polishing, which involves anodic dissolving of the machined material predominantly around the microgeometry peaks of the machined surface, ultrasonic depassivation of the neutral layer deposited on the machined surface and roughness (Ra) reduction by ultrasonic removal of the microgeometry protrusions. Numerical simulations of ultrasonic concentrators integrating different tool sizes and different thicknesses of the electrical insulating layer to achieve the resonance condition are performed. Numerical simulations are also developed on the process of material removal and depassivation when machining a stainless steel. The results of the numerical simulations are validated by experimental results obtained, which show the correct operation of the ultrasonic chains and finding an optimum value of ultrasonic power (pressure) for maximum Ra reduction.*

KEYWORDS: *electrochemical polishing, ultrasound, numerical simulation.*

1. Introduction

Electrochemical Machining (ECM) is the controlled removal of (electrically conductive) material from a workpiece based on the principle of anodic dissolution according to Faraday's laws of electrolysis [1]. ECM is used for machining complex shapes from conductive materials, which are difficult to machine with other conventional methods [10, 11]. The process is not affected by the hardness of the material and has the following advantages: obtaining a good surface quality and a very high productivity, up to $10^5 \text{ mm}^3/\text{min}$ (similar to milling) [2, 3]. During electrochemical machining in ultrasonic field (Electrochemical Machining Aided by Ultrasonics - ECM+US), US waves create gas microbubbles on the surface of the workpiece which, by imploding, produce a large amount of energy that brings advantages on improved depassivation of the neutral layer formed on the machined surface, as well as roughness reduction by removing the peaks of the surface microgeometry [7].

2. Current status

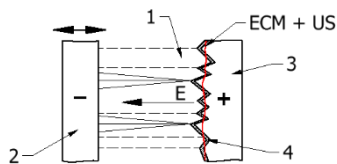


Fig. 1. ECM +US polishing mechanism scheme [adapted from 2]

In ECM polishing (or finishing), the phenomenon of anodic dissolution (Fig. 1), which occurs in the electrolytic medium (1) as a result of the electric field of intensity E created between the tool (2) (cathode) and the workpiece (3) (anode), has the following explanation: on the surface of the workpiece, the passivated layer (4) is formed, the thickness of which is smaller in the region of the micro-peaks [2].

The oscillating movement of the tool in the ultrasonic field causes gas bubbles to form in the machining gap. By approaching the tool, they implode and produce a large amount of energy (ultrasonic cavitation). When these micro-implosions of bubbles occur, the material is removed by reducing the peaks of the micro-geometries present on the surface of the part. A higher quality of surface and improved

depassivation of the neutral layer is achieved [6, 9]. Ultrasonic assist of ECM also yields increased productivity by improving electrolyte flow through the machining gap [8]. ECM+US also brings advantages when using low energy compared to conventional ECM [12] where electrolyte pressures of 20-25 atm are used for depassivation [4, 5].

3. Ultrasonic chains used to assist ECM polishing

The construction of the US chains is as shown in Figure 2 [2]:

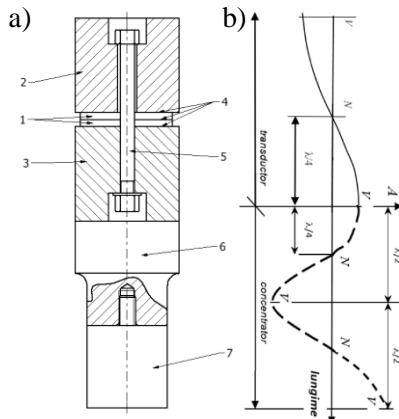


Fig. 2. Ultrasonic chain and stationary wave formation [2]

The US processing system consists of a US generator, which converts the industrial frequency of 50 Hz AC current from the main grid into an ultrasonic frequency, $f_{US}=20-40\text{KHz}$ applied to the transducer of the ultrasonic chain - fig. 2. a, example of the construction of a US chain, used at USM, where: 1 - discs made of piezoceramic material; 2 - steel reflecting bushing; 3 - duralumin radiating bushing; 4 - 0.2...0.3 mm thick copper blades (through which the transducer is connected to the US generator); 5 - clamping screw; the pre-bending force (of tone force magnitude) is controlled so that the piezoceramic material transmits the oscillations with minimum losses; 6 - concentrator; 7 - tool, included in the US chain.

In the ultrasonic chain, standing waves are formed resulting from the superposition of elementary waves of the same frequency travelling in opposite directions, Fig. 2.b. [2]. Some points oscillate with minimum amplitude, knots (N), others with maximum, peak amplitude (V).

The ECM+US polishing surfaces for which numerical simulations were performed are shown in Fig. 3, 4, 5:

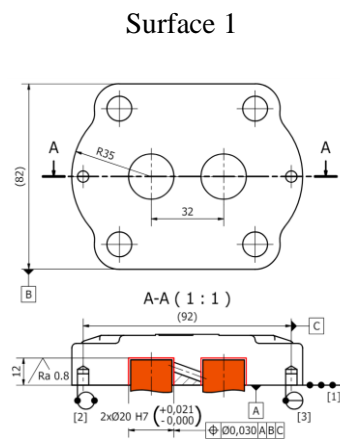


Fig. 3. Operation sketch, workpiece 1

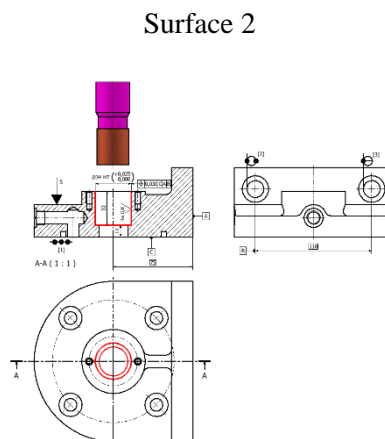


Fig. 4. Operation sketch, workpiece 2

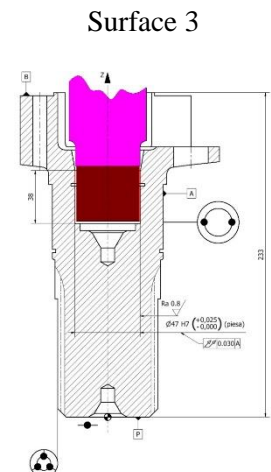


Fig. 5. Operation sketch, workpiece 3

4. Numerical simulation steps for ultrasonic concentrator

Simulation of the US concentrator is performed in COMSOL Multiphysics by representing the US concentrator, which integrates the tool and helps to determine the eigenfrequency. This is used to obtain the resonance condition, the operating condition of the US chain, the equilibrium between the eigenfrequency of the concentrator and the transducer. In Fig. 6, the model parameters are shown. In fig. 7. is shown the discretization of the ultrasonic chain into free triangular finite elements. In fig. 11, the

boundary conditions for determining the eigenfrequency of the concentrator are shown - without mechanical constraints.

Name	Expression	Value	Description
l1	54.64[mm]	0.05464 m	Length of radiating bushing
r1	26 [mm]	0.026 m	Radius of radiating bushing
l2	60 [mm]	0.06 m	Length of concentrator
r2	15.17[mm]	0.01517 m	Radius of concentrator
densitate	7950 [kg/m ³]	7950 kg/m ³	Steel Density
modulE	2.1*10 ¹¹	2.1E11	Young's Module for Steel
hscula	32[mm]	0.032 m	Length of Tool
rscula	r2	0.01517 m	Radius of Tool
hg1	10[mm]	0.01 m	Stud 1 Hole Length
rg1	4[mm]	0.004 m	Stud 1 Hole Radius
hp1	8[mm]	0.008 m	Stud 1 Length
hg2	6[mm]	0.006 m	Stud 2 Hole Length
rg2	3[mm]	0.003 m	Stud 2 Hole Radius
hp2	5[mm]	0.005 m	Stud 2 Length
roCu	8940 [kg/m ³]	8940 kg/m ³	Copper Density
modulECu	1.532E11 [Pa]	1.532E11 Pa	Young's Module for Copper
gv	0.6[mm]	6E-4 m	Thickness of paint

Fig. 6. Numerical simulation parameters

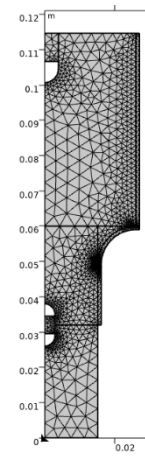


Fig. 7. Discretization of the ultrasonic concentrator

The model has been assigned materials according to figures 8, 9 and 10 where the three zones of the ultrasonic chain are illustrated, the concentrator has been assigned the physical-mechanical properties of C45 (density, $\rho = 7950$ [kg/m³], Young's modulus, $E = 2.1 \cdot 10^{11}$ Pa, Poisson's ratio, $\nu = 0.28$), the electrode-tool of copper (density, $\rho = 8940$ [kg/m³], Young's modulus, $E = 1.532 \cdot 10^{11}$ Pa, Poisson's ratio, $\nu = 0.034$), and the insulation layer was assigned the properties of epoxy paint (density, $\rho = 1600$ [kg/m³], Poisson's ratio, $\nu = 0.7$).

As the concentrator is made of a steel (C45) it is electrically conductive, so the insulation layer aims to eliminate the electric field between the tool and the workpiece on the surface not intended for machining.

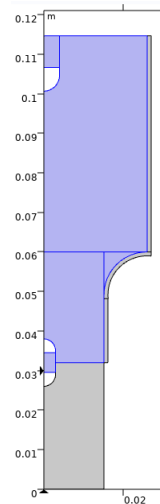


Fig. 8.
Concentrator,
C45

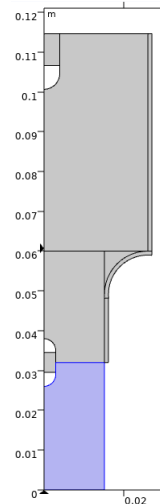


Fig. 9.
Electrode – tool,
Cu

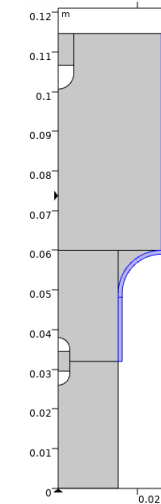


Fig. 10. Isolation
layer, epoxy paint

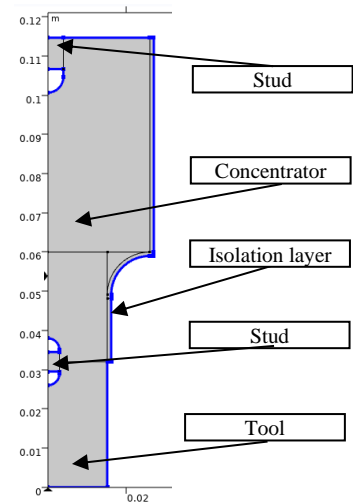


Fig. 11. Boundary
conditions for
determining
eigenfrequency

5. Analysis of results for the eigenfrequency of the ultrasonic concentrator

The simulation results provide information about the natural frequency of the ultrasonic chain. The length of the concentrator and the integrated tool will be determined in order to have at the tip of the tool a frequency of 20100 Hz which is the frequency of the transducer (target frequency) for the thickness of the 0.6 mm insulating layer (to be applied on the real concentrator).

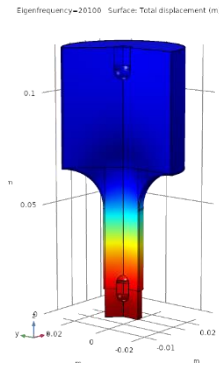


Fig. 12. Simulation results
Tool radius = 8,17 mm

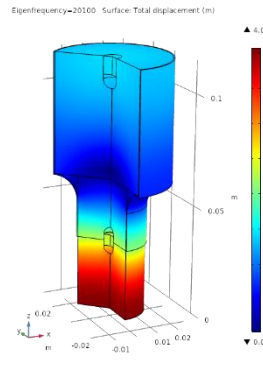


Fig. 13. Simulation results
Tool radius = 15,17 mm

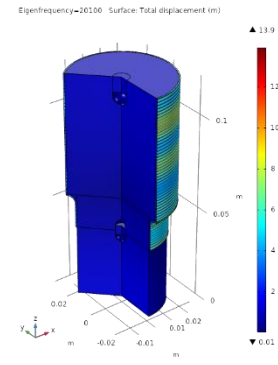


Fig. 14. Simulation results
Tool radius = 21,67 mm

The results of the simulations are shown in Figures 12, 13 and 14, these represent the three cases, where the tool parameters, radius (R) and length, vary with the surface to be machined.

After analyzing the data from the first simulation it is determined how the eigenfrequency varies with the thickness of the insulating layer. Thus, it decreased with increasing thickness of the insulating layer in the range 0.2 - 1 mm. The results are centralized in Figure 15. It can be seen that the resonant frequency, 20100 Hz, was obtained at an insulating layer thickness of 0.6 mm for all three US chains studied.

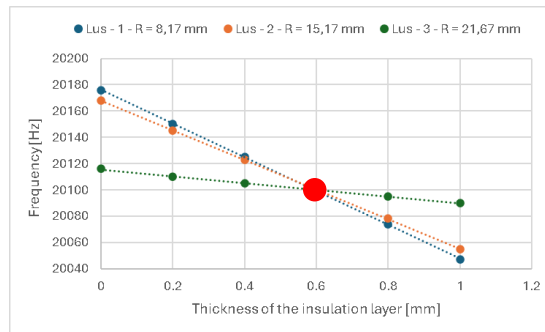


Fig. 15. Eigenfrequency of the concentrator as a function of the insulating layer

6. Determination of the nodal plane height

In the following, the same three cases of ultrasonic chains with different tool electrode radius will be analyzed to determine the nodal plane position (fig. 16 - tool radius = 8.17 mm; fig. 17 - tool radius = 15.17 mm; fig. 18 - tool radius = 21.67 mm).

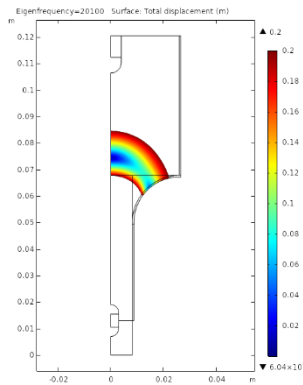


Fig. 16. Simulation results
Tool radius = 8,17 mm

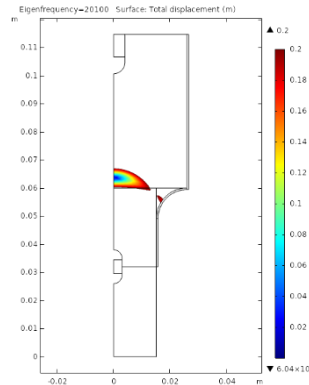


Fig. 17. Simulation results
Tool radius = 15,17 mm

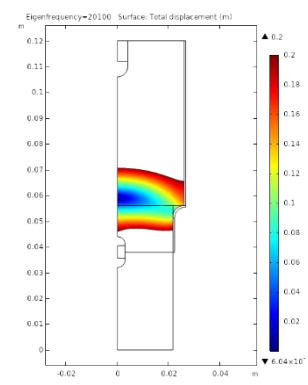


Fig. 18. Simulation results
Tool radius = 21,67 mm

The results of the simulations are shown in Table 1:

Table 1 – Simulation results

Electrode radius	R = 8,17 mm	R = 15,17 mm	R = 21,67 mm
Nodal plane height	74,32 mm	63,68 mm	58,9 mm

The purpose of these simulations was to find the height at which the nodal plane is located, in order to create a nodal channel that will be used for the radial fastening of the US chain.

7. Stages of simulated ultrasonic cavitations

The formation, development and collective implosion of gas bubbles as a result of ultrasonic cavitations in the machining gap is represented during a period (cycle) of ultrasonic oscillation in Fig. 19. It can be seen that the collective implosion of gas bubbles occurs at the end of the tool lifting half-period (stretching of the electrolytic liquid), at which time high pressures with the magnitude of 100 MPa are developed, forming directed shock waves along the machining gap, parallel to the machined surface. Implosion time is calculated to be 0.8 μ s for a machining gap of 0.1 mm [2].

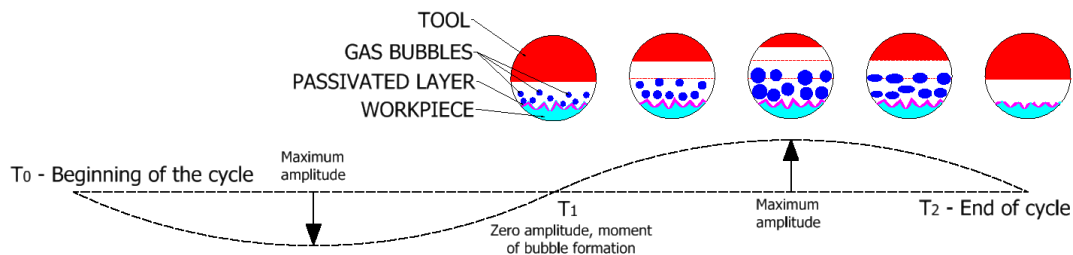


Fig. 19. The implosion cycle of gas bubbles on the level of microgeometry

Numerical simulation was performed in COMSOL Multiphysics, 2D axis symmetric, in the solid mechanics module using a time-dependent study, over the time of 0.8 μ s implosion. The stress produced by the bubble implosion was simulated using a contact pressure on the surface of the microdepression (SM). In Fig. 20 the parameters of the model are presented. In order to achieve geometry of the piece, the materials that will be assigned to the model were taken into account, namely: at the bottom is a stainless steel (SS 41003 alloyed with 12% Cr), and an iron oxide is formed on the SM (Fe_2O_3) – electrically neutral layer – resulting in electrochemical processes through combining the positive ions of the part with the negative ions in the electrolyte solution. In Fig. 21 are presented boundary and loading conditions of the model: the piece is placed on a flat surface (fixed base on the bottom surface of the model in simulation) and on the SM a pressure of contact produced by the force exerted during the implosion of gas bubbles. Due to the

small size of interstitial surface processing, the direction of these forces is horizontal, parallel to the processed surface on the sense negative of the OX axis.

Name	Expression	Value	Description
hp	5[mm]	0.005 m	Workpiece Hight
lp	10[mm]	0.01 m	Workpiece Length
Ra	0.636e-6	6.36E-7	Rughness before the ECM+US process
PRa	0.1[mm]	1E-4 m	Microneragularity's Pitch
pf	0.5e-6	5E-7	Thickness of the pasivated layer
tus	0.8e-6	8E-7	Cavitation bubble implosion time
modulinox	200[GPa]	2E11 Pa	Young's Module for Stainless steel
nuinox	0.29	0.29	Poisson's Ratio for Stainless Steel
tau0	313.6	313.6	Braking strength shear fatigue [MPa] C120
pus	200[MPa]	2E8 Pa	Cavitationl US pressure
modulFe2O3	300[GPa]	3E11 Pa	Young's Module for iron oxide
roFe2O3	4345	4345	Density of Iron oxide
nuPFFe2O3	0.24	0.24	Poisson's Ratio for Iron Oxide
tau0Fe2O2	57.6	57.6	Braking stregh shear fatigue [MPa] Iron oxide

Fig. 20 – Simulation parameters

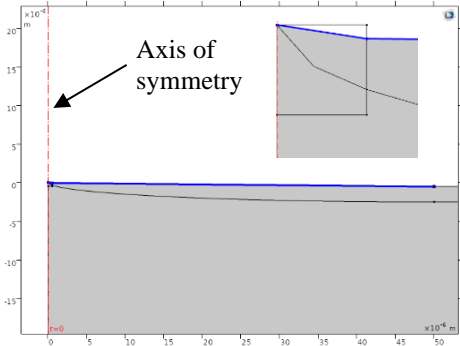


Fig. 21 – Boundary conditions – pressure of contact on the surface of the cavity

The geometry of the model was created taking into account the distribution of iron oxide especially at the tip of the roughness as shown in Figure 22 (mechanical properties of Fe2O3 are: density, $\rho = 4345$ [kg/m³], Young's modulus, $E = 300 \cdot 10^{11}$ Pa [14], Poisson's ratio, $\nu = 0.24$). Figure 23 shows how the rest of the part is made of SS 41003 with the following mechanical properties: density, $\rho = 7800$ [kg/m³], Young's modulus, $E = 2 \cdot 10^{11}$ Pa, Poisson's ratio, $\nu = 0.29$.

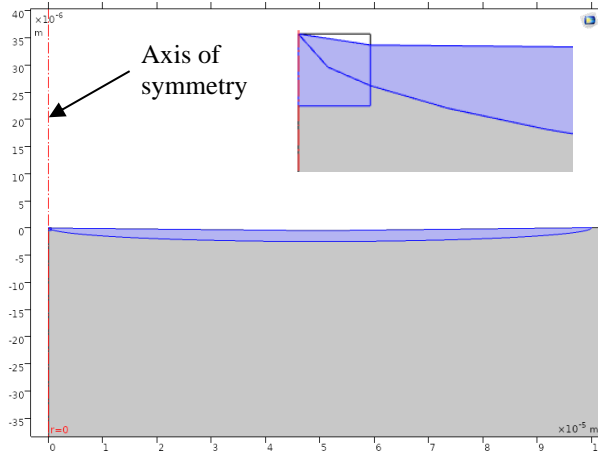


Fig. 22 – The area of the passive layer at the tip of the microgeometry

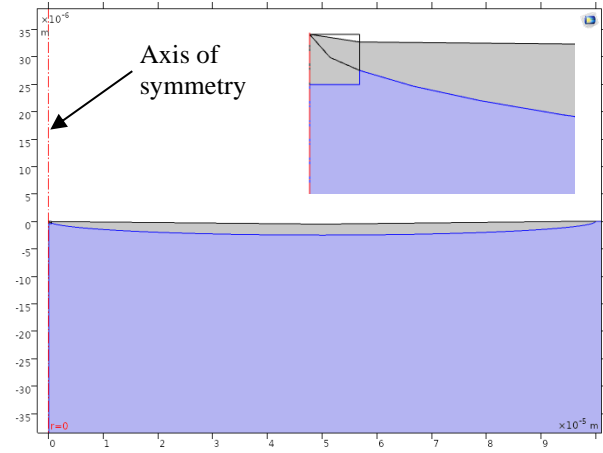


Fig. 23 – Stainless Steel material area

8. Results

The following will analyze two simulation cases in which the cavitationl US pressure varies.

In the first case, a relatively low pressure of 50 MPa is applied. This aims at removing the neutral layer (depassivation). The simulation results were compared with the shear fatigue strength (τ_0) of iron oxide determined using the relations [13].

$$\begin{aligned}\tau_0 &= 0,6 * 1,6 * \sigma_r \text{ [MPa]} \\ \sigma_r &= 60 \text{ MPa} \\ \tau_0 &= 0,6 * 1,6 * 60 \\ \tau_0 &= 57,6 \text{ MPa,}\end{aligned}\tag{1}$$

where, σ_r is the static breaking strength.

This highlights the area where the ultimate tensile strength is higher than the admissible one: 57.6 MPa. These results are shown in Figures 24 and 25. Therefore, these areas are removed as a result of ultrasonic cavitation.

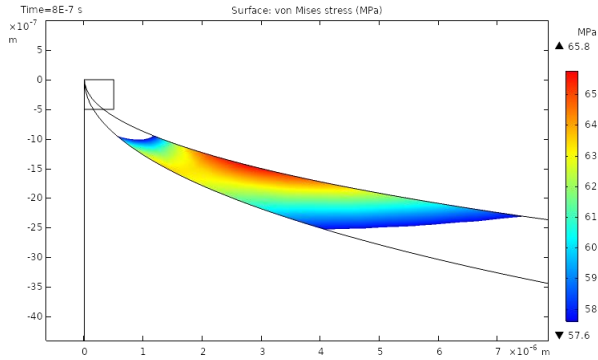


Fig. 24 – 2D representation of the removed material

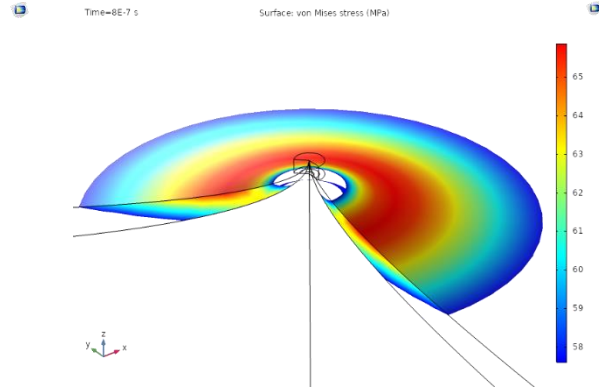


Fig. 25 – 3D representation of the removed material

In the second case, the cavitation US pressure is increased to 200 MPa in order to simulate the removal of the passivated layer, but also the microgeometry peaks to reduce the roughness.

The simulation results were compared with the fatigue shear strength of stainless steel determined with the relations [13].

$$\tau_o = 0,6 * 1,6 * \sigma_r [MPa] \quad (2)$$

$$\sigma_r = 550 MPa$$

$$\tau_o = 0,6 * 1,6 * 550$$

$$\tau_o = 440 MPa$$

Thus, the points where the breaking stress is higher than the admissible one (440 MPa) are highlighted. These results can be seen in Figures 26 and 27. So, these areas are removed in following implosions produced by US cavitation.

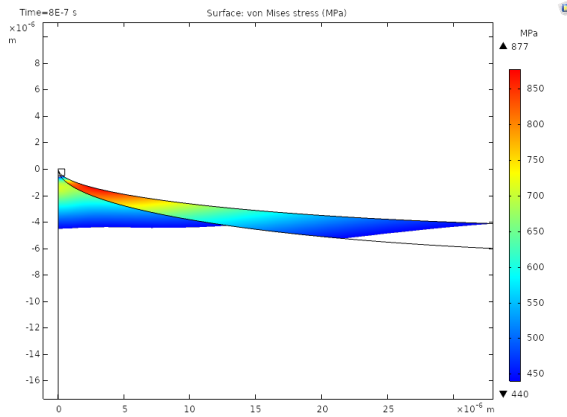


Fig. 26 – 2D representation of the removed material

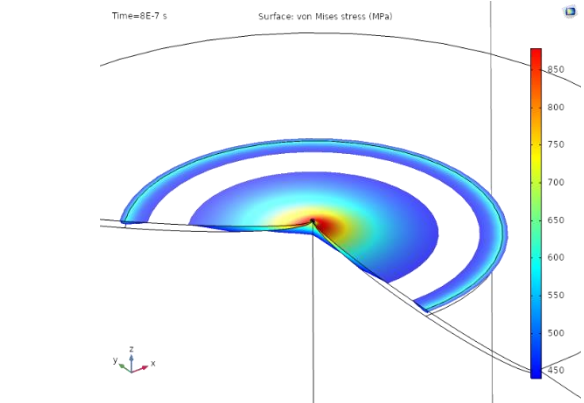


Fig. 27 – 3D representation of the removed material

Figure 28 shows the variation of the depth of the sampled layer depending on the ultrasonic pressure, after several runs of the model. Thus, the pressure (which corresponds to an optimal value of the power of the US generator), so that the roughness of the processed surface is minimized.

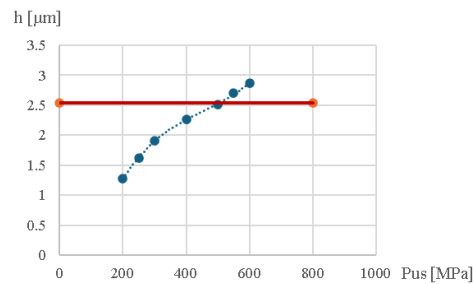


Fig. 28. The influence of pressure on the processing depth

The depth of the initial microdepression (2.544 μm) was marked with the horizontal line. Increasing the pressure results in a deeper depth of material being removed, which increases the initial roughness (R_a 0.636 μm). This corresponds to the R_a measured on the workpiece.

9. The stand and experimental results

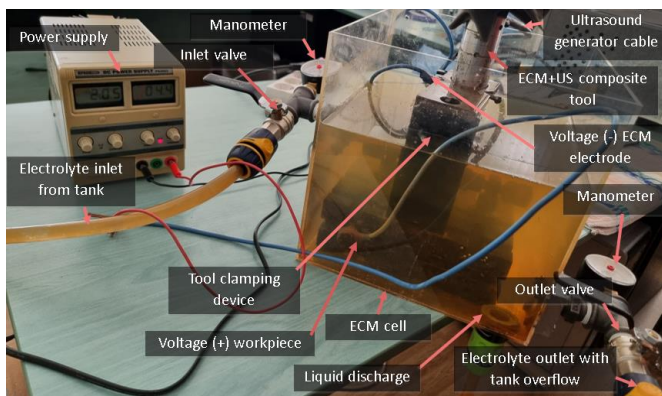


Fig. 29. Experimental stand - electrolytic cell



Fig. 30. ECM+US machining area

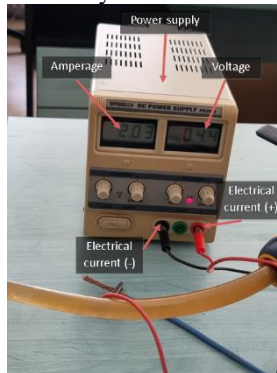


Fig. 31. Power supply

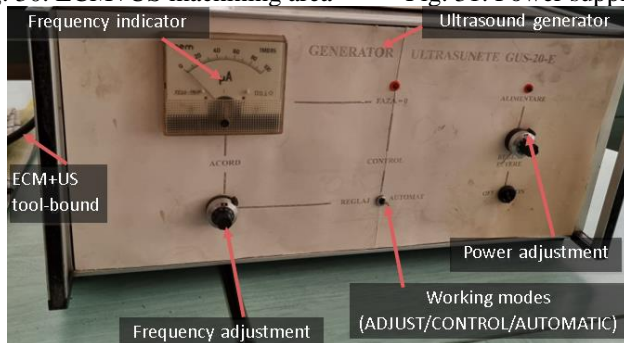


Fig. 32. Ultrasound generator

The experimental stand was made by drd. eng. As. C. Enciu for successive ECM+US machining.

The machining steps were:

- positioning and clamping the 12% Cr Stainless Steel part in the working station;
- bringing the ultrasonic concentrator into working position, frontal gap $s_F=0.7$ mm (fig. 30);
- starting the electrolyte tank pump;
- filling the electrolyte cell with electrolyte fluid (fig. 29);
- switching on the source and setting the working parameters (1A and 0,44 V) (fig. 31);
- ECM of a 4,9 cm^2 area, for 3 min;
- switching off the power supply;
- recirculation of electrolyte for 30s to wash the machined surface of impurities;
- switching on the US generator (fig. 32);
- generator adjustment at resonant frequency, $f_0 = 20100$ Hz and power consumption, $P_{\text{cus}} = 93\text{-}119$ W;
- US machining for 3 min
- switching off the US generator;
- emptying the counterpressure chamber of electrolytic fluid;
- US chain release;
- removal of the workpiece;
- cleaning the workpiece.

Several machining operations were performed with the values of power consumption, P_{cus} of the US generator, in the above-mentioned range and the experimental results are shown in the table 2. Ra values were measured with the ISR-C002 INSIZE universal roughness tester.

Table 2. Experimental results

$J = 0.25 \text{ [A/cm}^2\text{]}, S=4.9 \text{ cm}^2$		Start	End, ECM, US $t=3 \text{ min}$	
P_{cus} [W]	I [A]	Ra [μm]	Ra [μm]	Ra reduction [%]
95	1	0.916	0.735	19.8
103	1	0.488	0.341	30.1
109	1	0.636	0.419	34.1
114	1	0.808	0.586	27.5
119	1	0.863	0.707	18.1

The graphical representation of the variation of roughness as a function of power consumption (P_{cus}) on the machined surface (Fig. 33) shows that the maximum reduction, 34% of Ra is obtained at $P_{cus}=109 \text{ W}$. A SEM QUANTA INSPECT F50 scanning electron microscope image of the machined surface (Fig. 34) shows a non-uniform removal of the material due to the existence of the usual (light-colored) Cr carbide particles smaller than 500 nm in the stainless steel. Cavities resulting from ultrasonic erosion are also observed, with dimensions of about $1\text{-}2 \mu\text{m}$.

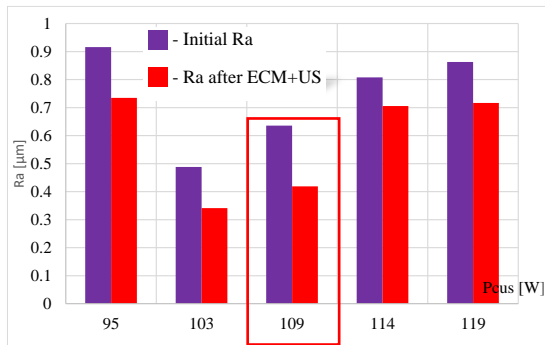


Fig. 33. Variation of Ra as a function of ultrasonic power P_{cus}

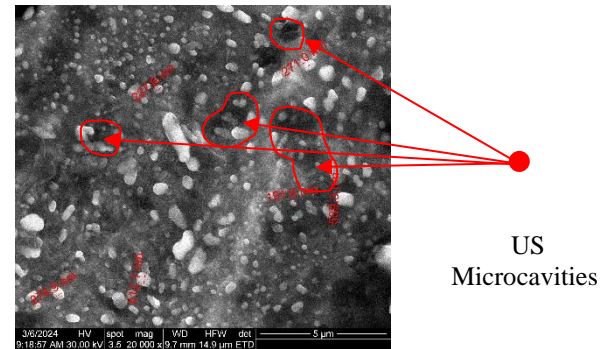


Fig. 34. SEM image of the machined surface

10. Summary

The contributions of the study are: numerical simulation to obtain the eigenfrequency resonance condition of ultrasonic concentrators, integrating tools of different sizes with different electrical insulating layer thicknesses, used to assist ECM polishing; numerical simulation of Fe_2O_3 layer depassivation and ultrasonic material removal in ultrasonic-assisted ECM polishing of 12% Cr stainless steel; validation of the models obtained by numerical simulation by experimental data showing the correct operation of the ultrasonic chains and finding an optimum US generator power for maximum roughness reduction after a single cycle of operation.

Future research directions are: modelling material removal by introducing submicrometer Cr carbide particles, which influence the process; improving the experimental stand by adjusting the frequency range of the US generator and adaptive control to maintain the resonant frequency during processing; correlating US removal with ECM by repeating the operating cycle and further reducing the roughness of the machined surface.

11. Bibliography

- [1]. El-Hofy, H. (2019), "Vibration-assisted electrochemical machining: a review, *The International Journal of Advanced Manufacturing Technology*, ISSN 0268-3768;
- [2]. Ghiculescu, D. (2023), Tehnologii neconvenționale, Curs Universitatea Politehnica București, Available at: <https://curs.upb.ro/2023>, Accessed at 28.03.2024.
- [3]. Rajkumar, KP. Poovazhagan, L. Saravanamuthukumar, P. Javed Syed Ibrahim S, Santosh S (2015) Abrasive assisted electrochemical machining of Al-B4C nanocomposite. *Appl. Mech. Mater.* 787:523–527.
- [4]. Davydov AD, Volgin VM, Lyubimov VV (2004) Electrochemical machining of metals: fundamentals of electrochemical shaping. *Russ. J. Electrochem.* 40(12):1230–1265.
- [5]. Rajurkar, K.P, Kozak, J, Wei B, McGeough JA (1993) Study of pulse electrochemical machining characteristics. *CIRP Ann. Manuf. Technol.* 42(1):231–234
- [6]. Jigar B. Patel, Zhujian Feng, Pedro P. Villanueva, Wayne N.P. Hung, (2017), "Quality Enhancement with Ultrasonic Wave and Pulsed Current in Electrochemical Machining", *Procedia Manufacturing*, ISSN 2351-9789.
- [7]. Nicoară, Dan & Hedes, Alexandru & Șora, Ioan. (2006). Ultrasonic enhancement of an electrochemical machining process. *Universitatea Politehnica din Timișoara* 5. 213-218.
- [8]. Skoczypiec, Sebastian. (2011). Research on ultrasonically assisted electrochemical machining process. *The International Journal of Advanced Manufacturing Technology*. 52. 565-574. 10.1007/s00170-010-2774-4.
- [9]. Liu, Jia & Liu, Yan & Zhang, Zhe & Wang, Hao. (2022). Parameter Optimization and Experimental Study on Tool-Vibration-Assisted Pulsed Electrochemical Machining of γ -TiAl TNM Blades. *Applied Sciences*. 12. 8042. 10.3390/app12168042.
- [10]. Xiangming, Z. Yong, L. Jianhua, Z. Kan, W. Huanhgai, K. (2020). Ultrasonic-assisted electrochemical drill-grinding of small holes with high-quality, *Journal of Advanced Research*, ISSN 2090-1232.
- [11]. Yongcheng, G. Wangwang, C. Yongwei, Z. (2021), Experimental Study on Ultrasonic Assisted Electrochemical Micro-Machining of Micro-Dimple Array Structure, *International Journal of Electrochemical Science*, ISSN 1452-3981, <https://www.sciencedirect.com/science/article/pii/S1452398123007903>, Accessed at 31.03.2024
- [12]. SINGH, Tarlochan, (2021) Experimental investigations of energy channelization behavior in ultrasonic assisted electrochemical discharge machining. *Journal of Materials Processing Technology*, 293: 117084.
- [13]. Drobotă, V. Rezistentă materialelor, *Editura tehnică*, 1982
- [14]. A. Ouglova, Y. Berthaud, M. François, F. Foct, Mechanical properties of an iron oxide formed by corrosion in reinforced concrete structures, *Corrosion Science*, Volume 48, Issue 12., p. 3988-4000, 2006

RESEARCH ON ELECTROLYTE FLOW UNIFORMITY IN ELECTROCHEMICAL POLISHING

**BUNEA Ionuț-Alexandru, ENCIU Cornel Cristian, GHICULESCU Liviu Daniel, PĂUN
Albert-Georgian, RĂDUCUȚĂ Ioana-Ruxandra**

Faculty: Industrial Engineering and Robotics, Department: Machine Construction Technology,
Year of degree: IV, e-mail: ioana.raducuta@stud.fiir.upb.ro

ABSTRACT: The paper presents the current state of the electrochemical polishing process (Electro Chemical Machining – ECM), using the intermittent flow method of the electrolytic liquid. The uniformity of the flow rate on the machined surface was aimed for, a key condition for ECM polishing. The logical scheme of the study and numerical simulations of the flow were developed for three different machining surfaces, in the following cases: laminar flow, turbulent flow and flow stop. The distributions of flow velocities in the machining gap were determined. The results of the simulations were validated by experimental data that determined an optimal value for the current density on the machined surface at which a maximum reduction in roughness was achieved.

KEYWORDS: electrochemistry, electrolyte flow, rugosity, numeric simulation

1. Introduction

Electrochemical machining (ECM) is based on the principle of anode dissolution to remove material at the atomic level, thus obtaining a high-quality surface [1],[3]. It is a non-contact machining method, with the advantages of manipulating materials of any hardness, without inducing tool wear and internal stress in the surface layer, but limited to electrically conductive materials. In ECM, the high velocity and pressure of the electrolyte in the work gap (the space between the tool and the part) is important to remove gas bubbles, heat, dissolved (precipitated) material from the part and to maintain the stability of the ECM (electrochemical reactions). In case of uneven flow of the electrolytic liquid on the processed surface, striations appear. Therefore, keeping the electrolyte flow under control is very important in the ECM process [4].

ECM has a wide range of applications in fields such as: electronic, automotive, aerospace, medical, food, nuclear, etc. through the ability of ECM to create mirror-like surfaces [1], [5].

The work aims to develop an intermittent processing method, which includes several phases: the first phase involves a high flow rate of the electrolyte, for washing the processing interstices, and the second phase, a reduced flow rate during the current pulses, to allow a controlled polishing of the surface and to discourage the formation of the passivated layer [2].

2. Current status regarding process influence

Schematically, an ECM process contains a tool - cathode and a workpiece - anode, with the electrolyte introduced under pressure through the gap between them. The electrolyte outlet section (adjustable by valve) allows flow control. The fluid flow in the interstitium is usually turbulent, which prevents the uniformity of the machining process [1, 2, 3, 5].

Patent EP 0 471 086 A1 (fig. 1) presents an innovative device and process for the electrochemical polishing of metal surfaces, through an uniform distribution of electric current and the introduction of electrolytic liquid intermittently with varying flow rates. The patented technical solutions ensure a laminar

type of flow during the electrical impulses to process the part uniformly, as well as a turbulent type of flow between them to ensure the adequate washing of the interstitium [3]. In fig. 3, the logic diagram of the numerical simulation is presented, while in fig. 4, the equipment with which the operation will be performed is presented.

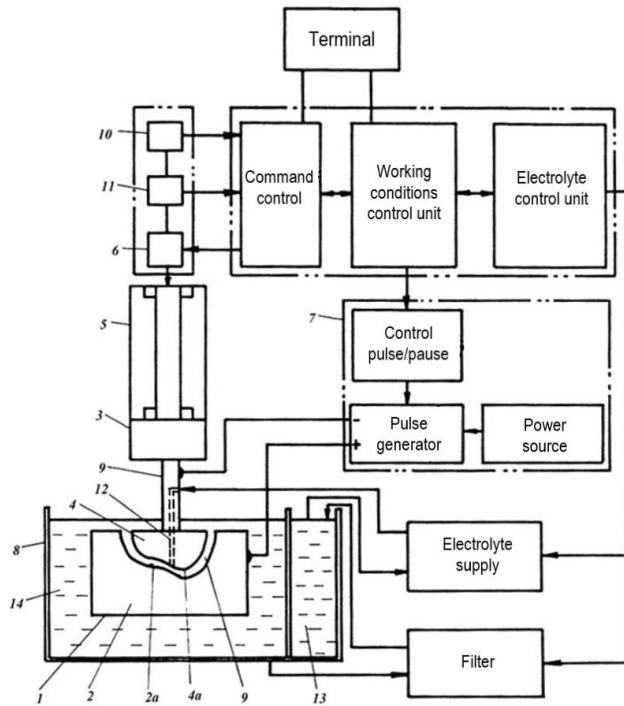


Fig. 1 Intermittent ECM processing device [2,3]

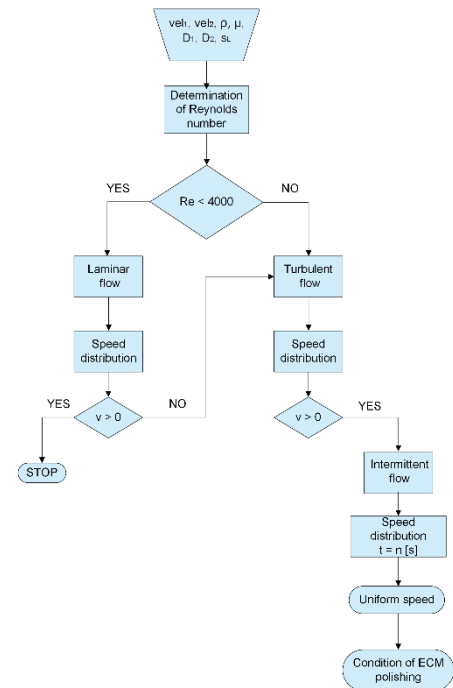


Fig. 2. Logical diagram of the numerical simulation process

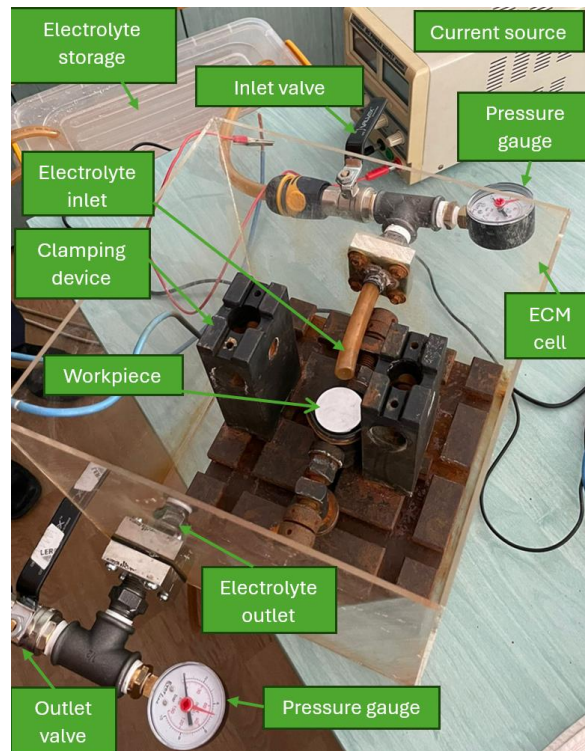


Fig. 3. The equipment for electrochemical polishing (As. Drd. Ing. C. Enciu)

Fig. 3 shows the equipment used for experiments, made by As. Dr. Eng. C. Enciu, and figures 4, 5, 6 show the polished ECM surfaces for which the numerical simulations were carried out.

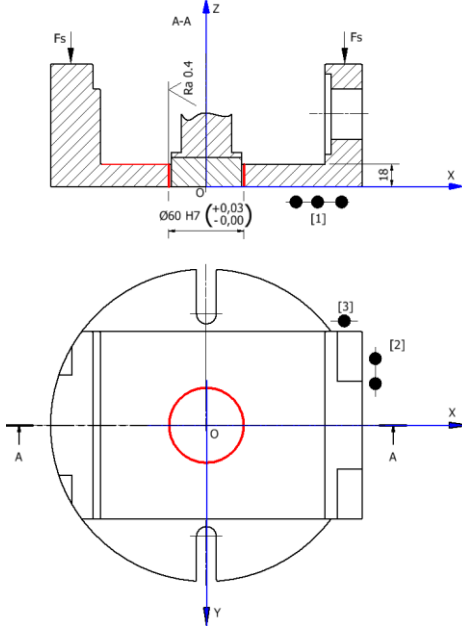


Fig. 4. The machined surface for workpiece 1

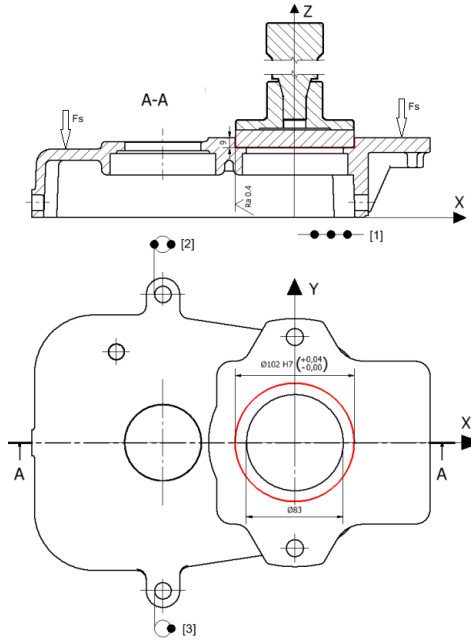


Fig. 5. The machined surface for workpiece 2

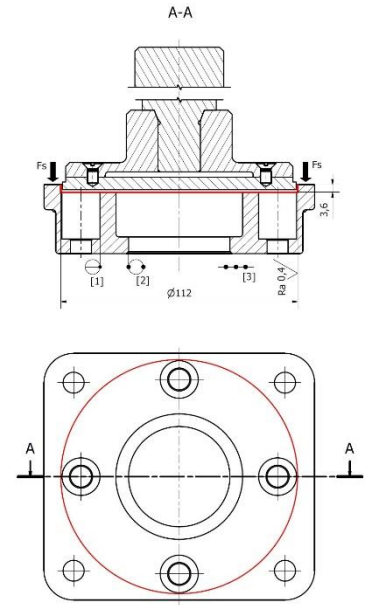


Fig. 6. The machined surface for workpiece 3

3. Determining Reynolds number

The Reynolds number is calculated, which determines the type of flow (laminar or turbulent) using relation (1). For $Re < 4000$, the flow is laminar, respectively turbulent for $Re \geq 4000$ [1]:

$$Re = \frac{\rho \cdot vel \cdot l}{\mu} \quad (1)$$

where: ρ – fluid density [kg/m^3]; vel_1, vel_2 – electrolyte inlet flow speed [m/s]; l – characteristic length [m]; μ – dynamic viscosity of the liquid [$Pa \cdot s$].

Two values of the flow velocity are introduced and used in the numerical simulation, from relation (1), $vel_1 = 1.5$ m/s, respectively $vel_2 = 0.02$ m/s:

$$Re_1 = \frac{\rho \cdot vel_1 \cdot l}{\mu} = \frac{1031 \cdot 1.5 \cdot 0.054}{0.00079} = 111583 > 4000 \Rightarrow \text{Rezultă curgere turbulentă}$$

$$Re_2 = \frac{\rho \cdot vel_2 \cdot l}{\mu} = \frac{1031 \cdot 0.02 \cdot 0.054}{0.00079} = 1049.5 < 4000 \Rightarrow \text{Rezultă curgere laminară}$$

The use of the two values vel_1 and vel_2 aimed at adequate washing of the machining gap, by ensuring that the velocity does not cancel out in the machining gap, but to obtain an uniform flow (relatively close values of the velocity distribution on the machined surface).

5. Numerical simulation of the electrolyte fluid flow through the working gap

The steps required for modeling using COMSOL Multiphysics 4.2 are described:

- A. The **3D module** is chosen as the **workspace**, then **Fluid Flow, Laminar Flow**, and as **Time dependent** regime, in case 1, for vel_1 . [2], [8].
- B. **Parameterization of the model and introduction of the characteristics** of the electrolyte liquid is done according to fig. 7 respectively fig. 8:
5% NaCl electrolyte properties are introduced:

Parameters			
Name	Expression	Value	Description
rp	30 [mm]	0.03 m	Raza alezaj piesa
hp	18 [mm]	0.018 m	Inaltime prelucrata
vel1	0.02 [m/s]	0.02 m/s	Viteza de intrare 1 - Prelucrare
tc1	5 [s]	5 s	Timpul de curgere sub vel1
vel2	1.5 [m/s]	1.5 m/s	Viteza de intrare 2 - Spalare
tc2	5[s]	5 s	Timpul de curgere sub vel2
tc3	1 [s]	1 s	Timpul de curgere sub vel = 0 m/s
xl	0.69 [mm]	6.9E-4 m	Interstitiul de lucru lateral
pout	2000000 [Pa]	2000000.0 Pa	Presiunea la iesire a lichidului
hi	30 [mm]	0.03 m	Inaltimea alezajului de intrare

Fig. 7. Modeling parameters from Global definitions

Property	N...	Value	Unit	Property group
✓ Density	rho	1031	kg/m^3	Basic
✓ Dynamic viscosity	mu	0.79/1000	Pa*s	Basic

Fig. 8. Introduction of electrolyte properties (5% NaCl)

- C. **Creating the flow geometry** parameterized by the prior step sizes (fig. 9) and **discretizing** it by fine-sized *free tetrahedral* finite elements in the geometry node of the Model builder (Fig. 10.)

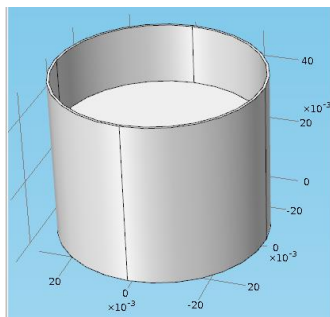


Fig. 9. Creation of the geometry of the processing gap

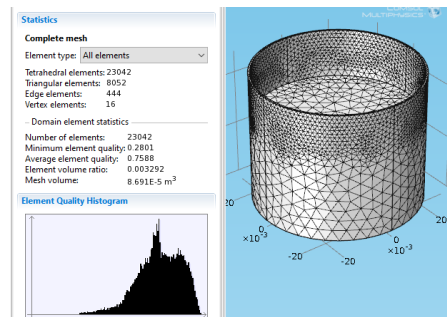


Fig 10. Discretization of geometry in finite elements

- D. **Setting boundary conditions**, presented in fig. 11, in the form of a velocity (vel_1/vel_2) input and the output under pressure (pout) of the liquid (fig.12) in the case of laminar flow:

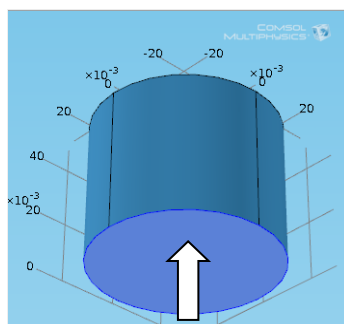


Fig. 11. Selecting the inlet

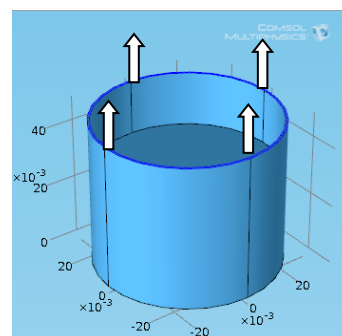


Fig. 12. Selecting the outlet

E. **Flow simulation** is done from the **Study** module, for each flow. Time parameters can be chosen in the case of the time dependent study for laminar flow (Study 1) (fig. 13). The second study is set for turbulent flow (Study 2) (fig. 14). We also set the flow for the case of cancellation of the inlet flow velocity, whose input data are the results of the previous simulation (Study 2), the turbulent flow (fig. 15).

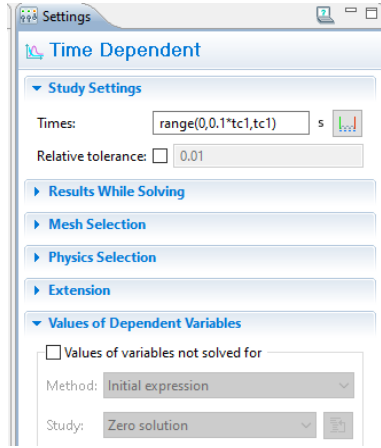


Fig. 13. Setting the laminar flow

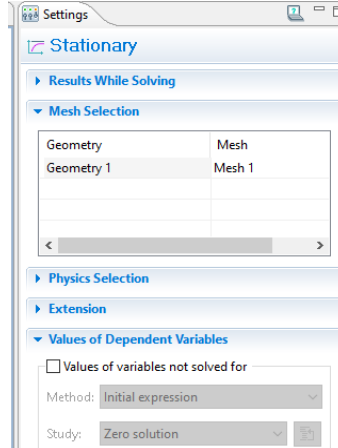


Fig. 14. Setting the turbulent flow

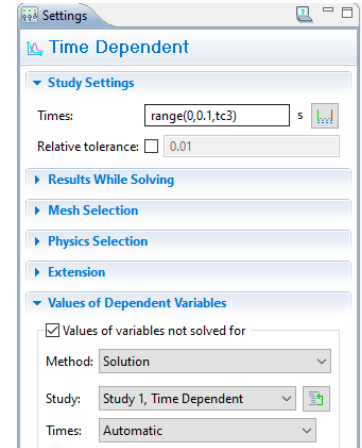


Fig. 15. Setting the laminar flow stop

5. Interpretation of the results

In laminar flow, it is found that the velocity is canceled in certain areas of the processing gap [2], [6], [7], (Fig. 16.). In fig. 17, the pressure reduction on the flow path from the processing gap is highlighted. Therefore, the turbulent flow solution is adopted, by increasing the inlet velocity, at vel_1 . It can be seen from fig. 19 that the flow velocity does not cancel, which allows washing of the machining gap, but the velocity distribution is not uniform over the machined surface. Finally, the flow velocity at the electrolyte inlet is canceled and the flow velocity distribution is obtained after a time of 5 s, fig. 20. Even if the velocity is not constant, its values are so small that the electrolytic liquid is considered stationary. At this point, one can proceed to the ECM polishing phase (the flow uniformity condition being met). Figures 18 and 21 show the distribution of velocities along the electrolyte path. The sequence shown is repeated for models 2 and 3, shown in Figures 22-27, respectively 28-33.

Model 1 – The machined surface for workpiece 1

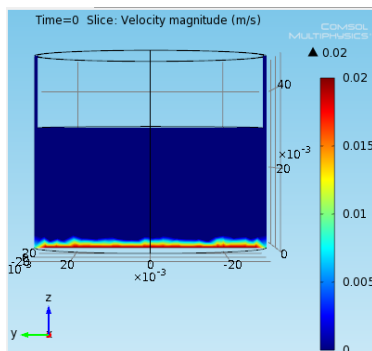


Fig. 16. Electrolyte velocity distribution in the machining gap, in *laminar* flow

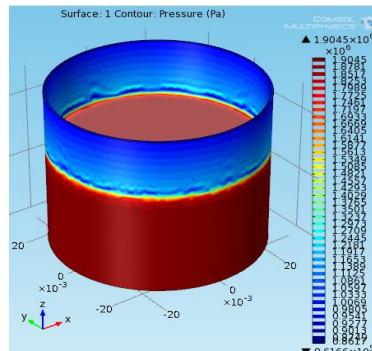


Fig. 17. Fluid pressure during *turbulent* flow

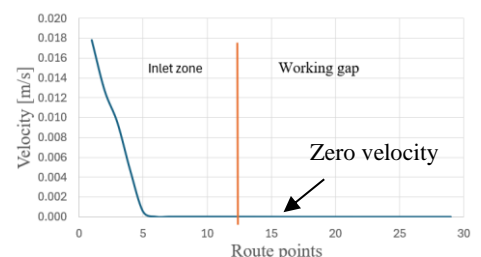


Fig. 18. Velocity distribution along the electrolyte path for *laminar* flow ($vel_1 = 0.02$ m/s)

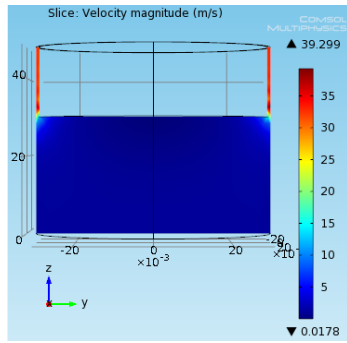


Fig. 19. Electrolyte velocity distribution in the machining gap, *turbulent flow*

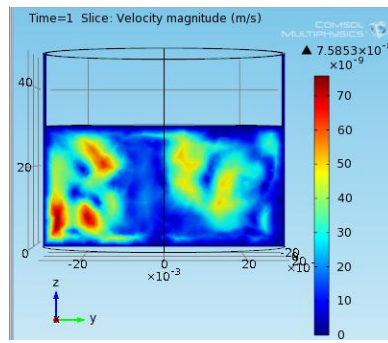


Fig. 20. Velocity distribution in the machining gap after canceling the input velocity, at $t = 5$ s

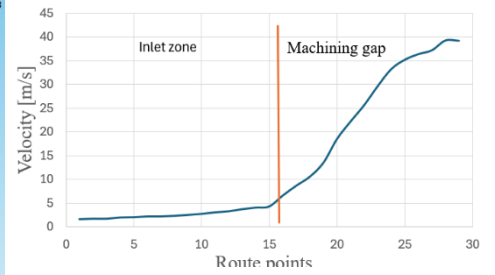


Fig. 21. Velocity distribution along the electrolyte path for *turbulent flow* ($vel_2 = 1.5$ m/s)

Model 2 – The machined surface for workpiece 2

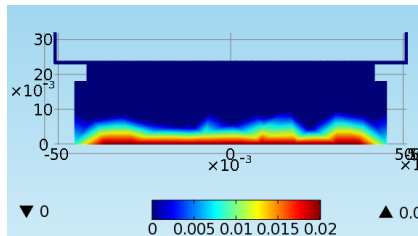


Fig. 22. Electrolyte velocity distribution in the machining gap, in *laminar flow*

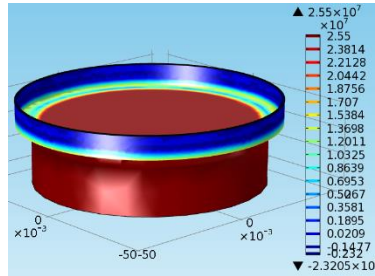


Fig. 23. Fluid pressure during *turbulent flow*

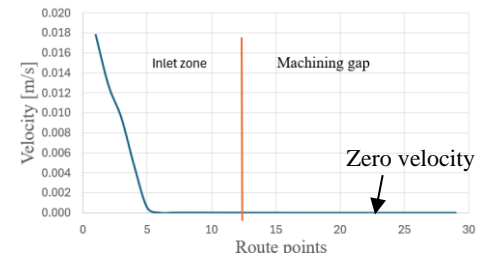


Fig. 24. Velocity distribution along the electrolyte path for *laminar flow* ($vel_1 = 0.02$ m/s)

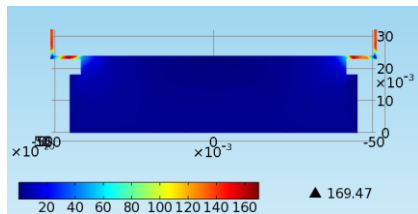


Fig. 25. Electrolyte velocity distribution in the machining gap, *turbulent flow*

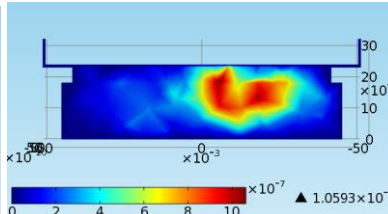


Fig. 26. Velocity distribution in the machining gap after canceling the input velocity, at $t = 5$ s

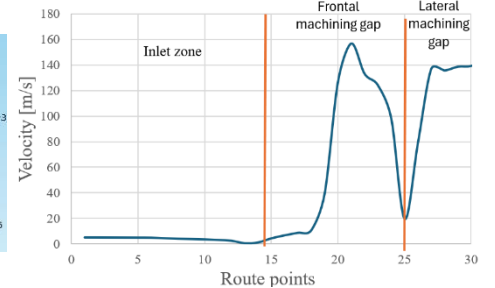


Fig. 27. Velocity distribution along the electrolyte path for *turbulent flow* ($vel_2 = 2$ m/s)

Model 3 – The machined surface for workpiece 3

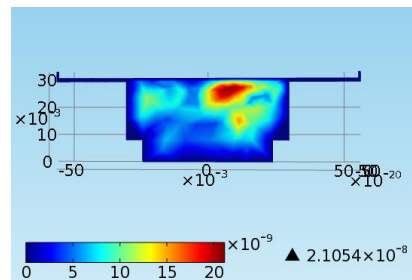


Fig. 28. Electrolyte velocity distribution in the machining gap, in *laminar flow*

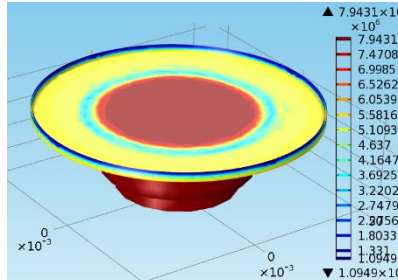


Fig. 29. Fluid pressure during *turbulent flow*

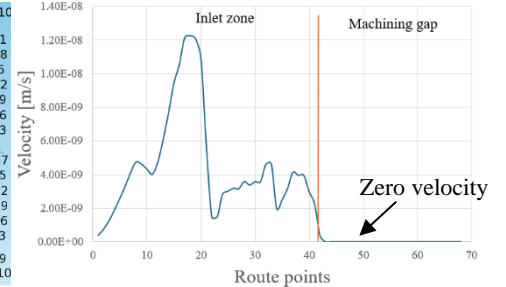


Fig. 30. Velocity distribution along the electrolyte path for *laminar flow* ($vel_1 = 0.02$ m/s)

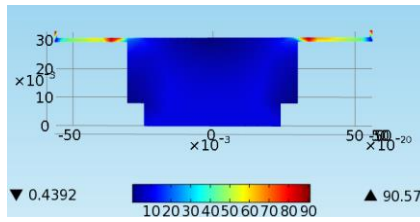


Fig. 31. Electrolyte velocity distribution in the machining gap, *turbulent* flow

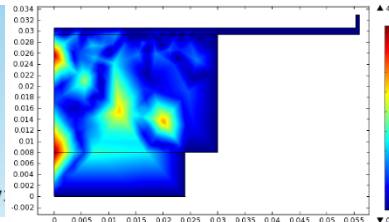


Fig. 32. Velocity distribution in the machining gap after canceling the input velocity, at $t = 5$ s

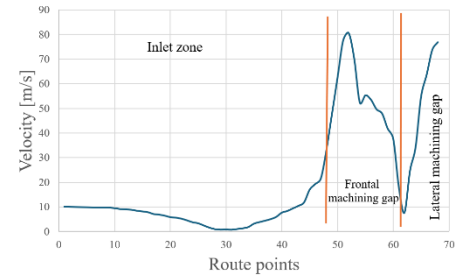


Fig. 33. Velocity distribution along the electrolyte path for *turbulent* flow ($vel_2 = 10$ m/s)

6. Experimental results

The experimental results obtained by the method of intermittent electrolyte flow and ECM finishing, 3 min, an area of 4.9 cm^2 of a stainless steel with 12% Cr, (see fig. 3) are presented in table 1:

Table 1. ECM Model, $t = 3$ min

J [A/cm ²]	I [A]	Initial Ra [μm]	Final Ra [μm]	Ra reduction [%]
0.1	0.5	0.298	0.258	13.4
0.15	0.75	0.356	0.278	21.9
0.2	1	0.3	0.223	25.7
0.3	1.5	0.449	0.318	29.2
0.4	2	0.44	0.373	15.2

The graphical representation of the roughness as a function of the current density (J) on the machined surface (fig. 28) shows that the maximum reduction of Ra is obtained at $J=0.3 \text{ A/cm}^2$. An SEM QUANTA INSPECT F50 image of the machined surface (fig. 29) shows uneven sampling of the material due to light-colored Cr carbide particles less than $1 \mu\text{m}$ in size, usual in the composition of stainless steel with 12% Cr.

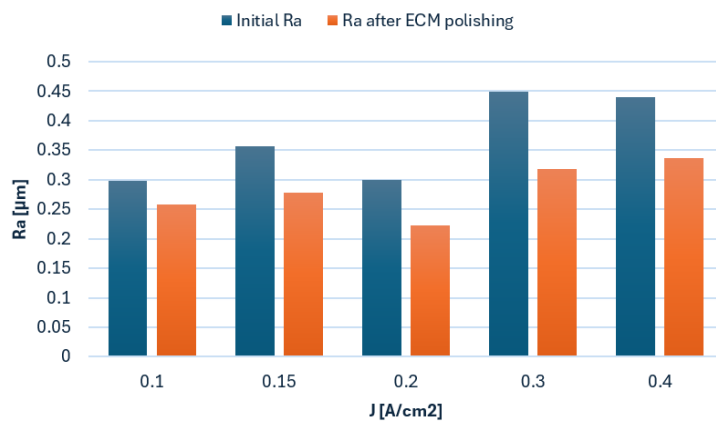


Fig. 28. Variation of Ra as a function of current density J

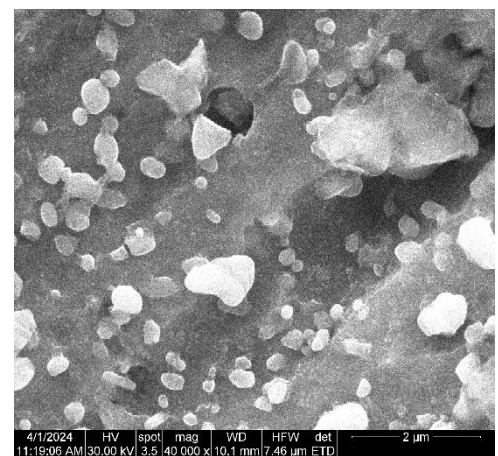


Fig. 29. SEM image of the machined surface

7. Summary

The contributions of the work are the numerical simulation of the electrolyte flow during the polishing (finishing) of the ECM, according to a logical scheme that aimed to smooth the flow on the processed surface. This was achieved by applying the following phases:

- Laminar flow simulation to check the speed distribution in the processing area.
- Turbulent high-speed flow for washing the processing interstitium, respectively removing the resulting ECM products.
- Stopping the flow after 5s and proceeding with ECM for 3 minutes.

The experimental results obtained, which validated the numerical simulations, highlight the reduction of about 25% of Ra by this method of ECM over a stainless steel with 12% Cr. SEM images show non-uniform material sampling due to Cr-carbide particles in the stainless-steel composition.

Future research directions are:

- Optimizing the current density on the processed surface.
- The use of a more efficient electrolyte for stainless steel processing.
- Optimizing its concentration and temperature.
- Optimizing the processing gap.
- Improvement of the experimental stand (electrolyte filtration, temperature, and pH control in real time).

8. Bibliography

- [1]. Ghiculescu D. (2024). „*Tehnologii de fabricare electrochimice*”, course Universitatea Politehnica București. Available at: curs.upb.ro/2023, accessed at: 28.03.2024.
- [2]. Ghiculescu D. (2024). „*Procese avansate de fabricare 2*”, course Universitatea Politehnica București. Available at: curs.upb.ro/2023, accessed at: 02.04.2024.
- [3]. Kuwabara Y, Hukuroi-shi S. „*Electrolytic finishing method*”, EP 0 471 086 A1;
- [4]. Hongping L, Dahai M. (2019), “Characteristics of ECM polishing influenced by workpiece corner feature and electrolyte flow”, în: M. Kunieda, R.K. Leach: *Precision Engineering*, vol. 56, Elsevier, pag. 330-342, ISSN: 1873-2372.
- [5]. Chagnes A. (2015), "Chapter 2 - Fundamentals in Electrochemistry and Hydrometallurgy", în: A. Chagnes, J. Światowska: *Lithium Process Chemistry*, pag. 41-80, Elsevier, ISBN: 978-0-12-801417-2.
- [6]. L.G. Leal. (1992), "*Laminar Flow and Convective Transport Processes*", 143030, Elsevier, ISBN: 978-0-7506-9117-8.
- [7]. R.K. Shah, A.L. London. (1978), "*Laminar Flow Forced Convection in Ducts*", Elsevier, ISBN: 978-0-12-020051-1.
- [8]. T. Cebeci (2013), "*Analysis of Turbulent Flows with Computer Programs*", Elsevier, ISBN: 978-0-08-098335-6.

RESEARCH ON THE DEVELOPMENT OF A SMART BOOKSHELF

AMMAR Abdul Karim¹, DIJMĂRESCU Manuela-Roxana², IONESCU Nicolae²

¹Faculty of Industrial Engineering and Robotics, Study Program: Industrial Engineering,
Year of Study: 4, email: abedammar4321@gmail.com

²Faculty of Industrial Engineering and Robotics, Manufacturing Engineering Department,
POLITEHNICA Bucharest

ABSTRACT: *This research study presents the design and development of a bookshelf, aiming to enhance it into a smart product. The main objective is to create a smart bookshelf capable of autonomously executing various tasks without physical human intervention. Having as a starting point the specification resulted from the need and functional analysis, concepts have been explored to demonstrate how such a smart bookshelf can operate solely through voice commands or touch input on a dedicated tablet application designed specifically for its control. The concepts were analyzed, and the optimal solution was further developed by making its numerical model in CATIA software.*

KEYWORDS: *product design, product development, smart bookshelf.*

1. Introduction

Bookshelves have a significant history, with significant breakthroughs occurring every century. They have long been an essential piece of furniture in homes, serving not only as storage units but also as symbolic repositories of knowledge, imagination, and personal identity [1,2]. In our ever-evolving digital age, where technology continues to shape the way we interact with our environment, the traditional bookshelf is undergoing a transformation into its smarter counterpart [3]. This transition heralds a new era of convenience, efficiency, and interconnectedness, while maintaining the timeless charm and functionality of its predecessors [2,3].

The creation of smart technology has surely revolutionized each component of our lives, and bookshelves are no exception [3]. A smart bookshelf integrates present day functions and connectivity alternatives to decorate its functionality, convenience, and versatility [4,5].

The main aim of this research paper is to introduce the design and development process of an innovative smart bookshelf. This bookshelf aims to fulfill human needs by allowing users to relax their hands, eliminating the need to manually retrieve books, and enabling the bookshelf to respond to user commands promptly.

2. Business Strategy

2.1. Need Analysis

Understanding the specific requirements and priorities of users is essential for the optimal design and functionality of the smart bookshelf. In conducting the need analysis, several specific needs were identified as presented in table 2.1. The table also outlines the crucial components of the smart bookshelf alongside their importance levels, accompanied by a detailed description of each need and a recommended solution to address it.

Table 2.1. Need analysis for the smart bookshelf

Need	Description	Importance (1-5)	Solution/Feature
Space Optimization	Maximize storage capacity while minimizing physical space	5	Adjustable shelves, compact design
Organization	Efficiently categorize and locate books	4	Radio Frequency Identification tags, barcode scanning, sorting algorithms

Need	Description	Importance (1-5)	Solution/Feature
Accessibility	Easily reach and retrieve books	5	Motorized shelves, voice commands, app-controlled access
Aesthetic Appeal	Enhance the visual appeal of the living space	4	Sleek design, customizable finishes, LED lightning
Smart Features	Incorporate technology for added convenience and automation	5	IoT integration, app connectivity, voice assistant
Security	Protect valuable or rare books from theft or damage	4	Locking mechanism, security cameras, alarm system
Connectivity	Enable integration with other smart home devices	3	Wi-Fi connectivity, compatibility with smart hubs
Power Efficiency	Reduce energy consumption and environmental impact	3	Energy-efficient components, standby mode

2.2. Functional Analysis

A functional analysis of a product includes breaking down its features, components, and talents to recognize the way it fulfills its meant motive and meets consumer needs [6]. This evaluation specializes in the features carried out via way of means of the product in preference to its bodily attributes or layout aesthetics. It facilitates picking out the important thing functionalities, checking their effectiveness, and finding possibilities for development or innovation [6-7].

Table 2.2 shows the environmental elements with their actions and main functions that connect them to the product.

Table 2.2. Functional Analysis

Environmental elements	Actions of the environmental element	Main functions
User	Helps the bookshelf detect the name of the book by saying its name	1. Makes the function work well
Tablet	Helps achieve the commands by tapping on the book wanted	1. User interface for the smart bookshelf
Gripper	Get the commands from the tablet	1. Handle books to the user

2.3. Market Segmentation

Market segmentation for smart bookshelves is vital for efficaciously focused on various client agencies with tailor-made advertising and marketing strategies. Demographic segmentation identifies awesome agencies primarily based totally on elements like age, income, and occupation. For instance, younger experts in city settings may prioritize space-saving functions and smooth designs, whilst households with youngsters might also additionally seek outsmart bookshelves with childproofing measures and academic content. Table 2.3 shows the segmentation categories of the smart bookshelf.

Table 2.3. Market Segmentation of a Smart Bookshelf

Segmentation Category	Examples
Demographic	Age: Young professionals, families with children, seniors.
	Income: Affluent individuals, middle-income households.
	Occupation: Tech enthusiasts, busy professionals.
Psychographic	Lifestyle: Minimalists, tech-savvy individuals
	Personality: Early adopters, convenience seekers.
	Values: Sustainability advocates, organization enthusiasts.
Behavioral	Usage Occasion: Home use, office use, educational settings.
	Purchase Behavior: Impulse buyers, research-oriented buyers.
	Benefits Sought: Convenience, space-saving, aesthetics.
Usage Context	Home Environment: Apartments, suburban homes, luxury residences.
	Work Environment: Home offices, corporate offices, coworking spaces.
	Educational Environment: Schools, colleges, libraries.

Some of the contradictions highlighted in the roof of the quality house (negative and strong negative correlations) were analyzed and solved by formulating them as technical contradictions, using the contradictions matrix, the 40 inventive principles and the 39 TRIZ parameters.

While traditional bookshelves typically encounter few issues due to their simplicity, the advent of smart bookshelves introduces challenges related to energy consumption and programming. To mitigate these issues, it's crucial to analyze the following aspects:

- ### 3.2. Technical contradictions

- TC1: When the number of applications increases (P33), the energy consumption is increased (P20).
- TC2: When the number of applications increases (P33), the barcode integration decreases (P33).4
- TC3: When the energy consumption is decreased (P20), the program efficiency is decreased (P27).
- TC4: When the energy consumption is decreased (P20), the Security (User Authentication) is decreased (P35).
- TC5: The Services are increased (P27), the Security (User Authentication) is decreased (P35).
- TC6: When the program efficiency is decreased (P27), the Security (User Authentication) is increased (P35).
- TC7: When the Security (User Authentication) is increased (P35), the voice control efficiency is decreased (P33).
- TC8: When the Security (User Authentication) is increased (P35), the internet of things (IoT) connectivity is decreased (P21).

Table 3.1. Improving and worsened parameter for the considered technical contradictions

Contradiction no. (TC)	Improving parameter			Worsened parameter			
	Parameter name	Improving desired direction/Taguchi Type	TRIZ equivalent parameter (P1...P39)	Parameter name	Improving desired direction/Taguchi Type	Unwanted effect	TRIZ equivalent parameter (P1...P39)
TC1	No. of applications on the tablet	GTB	P33. Ease of operation	Energy Consumption	NTB	Increasing	P20. Use of energy by stationary object
	TC1: When the number of applications increases (P33), the energy consumption is increased (P20).						
TC2	No. of applications on the tablet	GTB	P33. Ease of operation	Barcode Integration	GTB	Decreasing	P33. Ease of operation
	TC2: When the number of applications increases (P33), the barcode integration decreases (P34).						
TC3	Energy Consumption	NTB	P20. Use of energy by stationary object	Program	GTB	Decreasing	P27. Reliability
	TC3: When the energy consumption is decreased (P20), the program efficiency is decreased (P27).						
TC4	Energy Consumption	NTB	P20. Use of energy by stationary object	Security (User Authentication)	GTB	Decreasing	P35. Adaptability or versatility

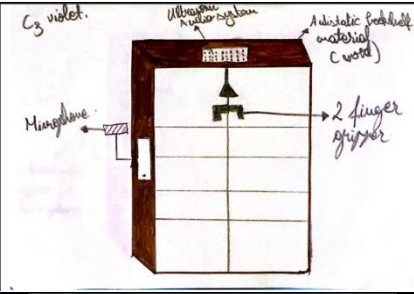
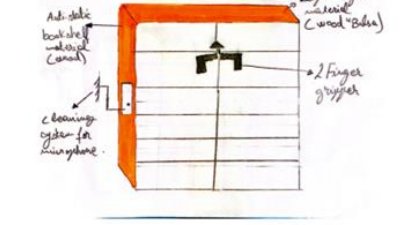
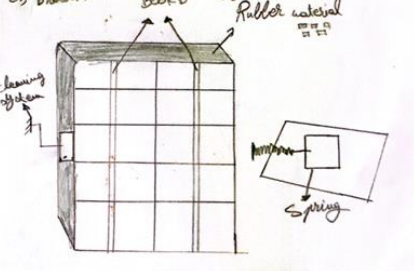
Contradiction no. (TC)	Improving parameter			Worsened parameter			
	Parameter name	Improving desired direction/Taguchi Type	TRIZ equivalent parameter (P1...P39)	Parameter name	Improving desired direction/Taguchi Type	Unwanted effect	TRIZ equivalent parameter (P1...P39)
TC5	TC4: When the energy consumption is decreased (P20), the Security (User Authentication) is decreased (P35).						
	Services	GTB	P27. Reliability	Security (User Authentication)	GTB	Decreasing	P35. Adaptability or versatility
TC6	TC5: The Services are increased (P27), the Security (User Authentication) is decreased (P35).						
	Security (User Authentication)	GTB	P35. Adaptability or versatility	Program	GTB	Decreasing	P27. Reliability
TC7	TC6: When the program efficiency is decreased (P27), the Security (User Authentication) is increased (P35).						
	Security (User Authentication)	GTB	P35. Adaptability or versatility	Voice Control	GTB	Decreasing	P33. Ease of operation
TC8	When the Security (User Authentication) is increased (P35), the voice control efficiency is decreased (P33).						
	Security (User Authentication)	GTB	P35. Adaptability or versatility	Internet of things (IoT) connectivity	GTB	Decreasing	P21. Power
TC8: When the Security (User Authentication) is increased (P35), the internet of things (IoT) connectivity is decreased (P21).							

4. Conceptual design

Having as a basis the functions and specifications developed and presented above, five concepts were generated from the smart bookshelf, as presented in table 4.1.

Tabel 4.1. Concepts presentation

Concept no.	Concept sketch	Concept description
1		There was a microphone added to the tablet, an extra shelf was added at the bottom, and it has 12 shelves with the shelf that had the automatic drawer compared to the bookshelf with 10 shelves in page nr. 2, plus the rubber material that was applied to the surface of the bookshelf.
2		There was a cleaning system added to clean the microphone below the microphone itself, it was connected to the tablet directly. It has 12 shelves with a shelf that had an automatic drawer compared to the bookshelf with 10 shelves on page nr. 2, plus the rubber material that was applied to the surface of the bookshelf.

Concept no.	Concept sketch	Concept description
3		There was a microphone added to the tablet, with an ultrasonic audio system at the top of the bookshelf. The bookshelf's outer surface contained anti-static material (wood), and we added a 2-finger gripper to help grab the book and give it to the people.
4		There was a cleaning system added to clean the microphone below the microphone itself, it was connected to the tablet directly. The bookshelf's outer surface contained anti-static material (wood) but we also chose the wood type to be balsa to make it a lightweight material, and we added a 2-finger gripper to help grab the book and give it to the people.
5		There was a cleaning system added to clean the microphone below the microphone itself, it was connected to the tablet directly. The rubber material that was applied to the surface of the bookshelf. A book divider was added to divide the genre in the book. Also, a spring was added to push the books from back to front, so people don't have to push their hands inside to get a book.

After an analysis of the developed concepts, it has been decided that the best one was the third concept. This concept numerical model has been designed in CATIA V5 (see fig. 4.1) with a gripper added at the inside top of the bookshelf as shown in fig.4.2.

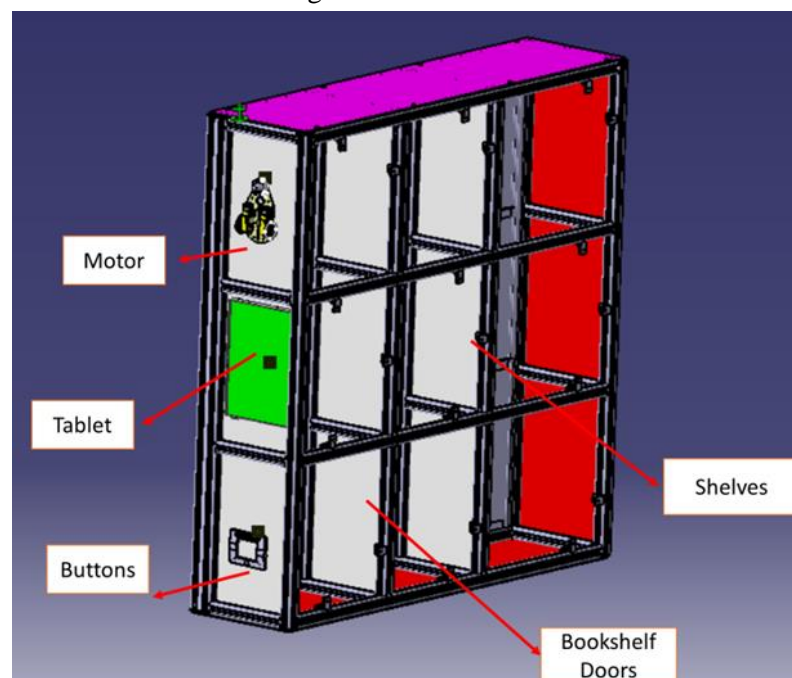


Fig. 4.1. Detailed Design of the Smart Bookshelf

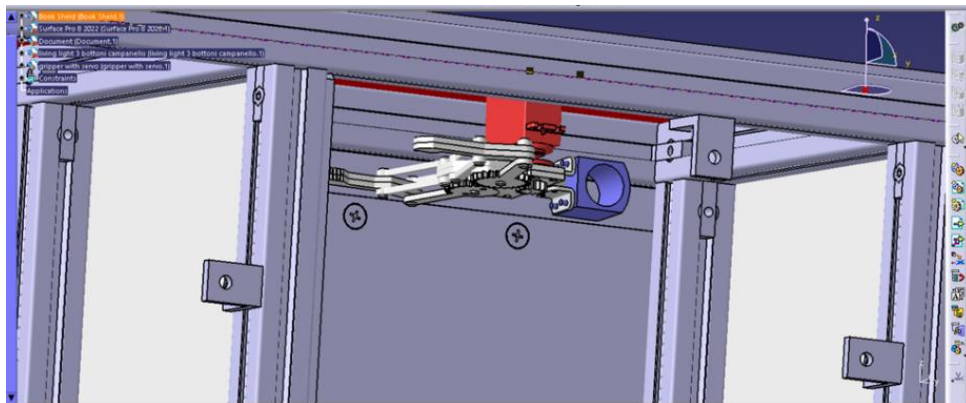


Fig.4.2. Smart Bookshelf with a gripper

The integration of technology and smart functionality is achieved through the implementation of a gripper mechanism, allowing users to access books without physically reaching into the bookshelf. This gripper operates in response to commands issued via a tablet interface, activated by a button press. Additionally, the incorporation of a separate microphone addresses issues related to voice recognition, overcoming limitations associated with relying solely on the tablet's built-in microphone.

5. Conclusions

The integration of technology and smart movement into the developed solution for a smart bookshelf represents a significant advancement in convenience and user experience. By incorporating a gripper mechanism controlled via tablet commands, users can effortlessly handle books without physically interacting with the bookshelf, streamlining organization and accessibility. The addition of an independent microphone addresses the challenge of voice recognition, ensuring accurate and responsive interaction by capturing commands more effectively. This innovative solution enhances the functionality and accessibility of the smart bookshelf, demonstrating our commitment to delivering intuitive and user-centric technology solutions. With these enhancements, users can enjoy a seamless and efficient experience, effortlessly managing their book collections with the convenience of voice commands and automated gripper functionality.

6. References

- [1]. Mattern, S., "Before Billy: A brief history of the bookcase", Harvard Design Magazine, available online at <https://www.harvarddesignmagazine.org/articles/before-billy-a-brief-history-of-the-bookcase/>, accessed on 01.05.2024.
- [2]. Ali, R., "The Importance of Bookshelves in Home Décor", Mediul, available online at <https://medium.com/@rubina.ali4560/the-importance-of-bookshelves-in-home-d%C3%A9cor-cb8e60eab1e5>, accessed on 01.05.2024.
- [3]. Hickerson, T.H., Lippincott, J.K. and Crema, L., *Designing Libraries for the 21st Century*, Association of College and Research Libraries, Chicago, Illinois 2022.
- [4]. Liu, Z. (2021), "Smart bookcase based on image recognition", Web of Conferences, Volume 223, article no. 04038.
- [5]. Xiaoyang, W., Hui, P., Ruixiang, O. (2017), "Library's Smart Bookshelf and Book Positioning System Based on ultra-high frequency RFID Technology", Advances in Engineering Research, Volume 123, pp. 219-222.
- [6]. Ionescu, N., Product Design and Development Project Guide, 2023-2024.
- [7]. Gurbuz, E. (2018), *Theory of New Product Development and Its Applications*. Marketing. InTech, available at: <http://dx.doi.org/10.5772/intechopen.74527>.

SMART PARKING FOR SMALL SPACES

**ȘTEFANIA-ADRIANA GHEORGHE¹, DUGĂEȘESCU ILEANA²,
ZAPCIU MIRON²**

¹Faculty of Industrial Engineering and Robotics, Specialization: Industrial Engineerig,
Studying year: IV, e-mail: adriana.gheorghe59@yahoo.ro

²Faculty of Industrial Engineering and Robotics, Manufacturing Engineering Department

³Faculty of Industrial Engineering and Robotics, Robots and Production Systems Department,
POLITEHNICA Bucharest

Abstract: With the rise in the number of cars, the parking of said cars creates some problems. Car accidents triggered by the small spaces and the inexperience of the drivers create unnecessary problems. Identifying this problem, a smart parking mechanism that aids the driver in manipulating the car is developed starting from the conceptualization stage, design, and validation.

Key words: parking, analysis, concept, mechanism, design.

1. Introduction

Since the invention of the car in 1886, people have started depending on it more and more. The vehicle helps in a faster transportation while also providing comfort. When it comes to personal cars, the automotive industry has been expanding tremendously in the last couple of years. The increase of personal cars caused the decrease in parking space available and constant traffic congestion. A notable example of how the increase of the number of cars affected the livelihood of people is U.S.A. In 2019, the average American spent around 54 h in traffic congestion [1], and that 20% of cars accidents are happening in the parking lots [2].

With the parking crisis, another problem joins the conversation: car accidents happening in the parking lot due to: clumsy drivers, lack of visibility, cramped parking spaces. Out of all the accidents, reverse driving accidents account for 25% of all parking lot collisions, 80% of bumper scratches occur during parking lot maneuvers, 41% of parking lot collisions involve vehicles hitting stationary objects, and vision obstruction is responsible for 27.5% such mishaps [2].

Parking issues significantly impact people's daily lives and lead to substantial energy consumption and space waste. To alleviate this problem, countries worldwide promote the use of multilevel parking facilities. The application of stereoscopic parking equipment has effectively eased the pressure on urban transportation. The lifting mechanism of the stereoscopic parking equipment, as the primary actuator, should have high stiffness, motion accuracy, load weight ratio, and a short transmission chain. A parallel mechanism can address safety and stability issues caused by the long transmission chain of conventional stereoscopic parking equipment. The parallel mechanism's frame-based actuation offers significant stiffness, short transmission chain, strong load capacity, high precision, small motion inertia, and easy control. The 6-DOF Gough/Stewart platform and the 4-DOF Delta robot are the most widely used and outstanding representatives of parallel mechanisms. Therefore, the development of the parallel lifting mechanism for stereoscopic parking robots is a crucial problem that needs to be addressed to improve the efficiency and safety of stereoscopic parking equipment [3].

What categorises the „smart parking mechanism” a „smart product” is the fact that the smart parking lot is going to aid the driver in manipulating the car in small spaces. The mechanism movement is similar to rotary table, therefore, it makes the car the hypothetical work piece which is rotated to the operator's desire, in this case, the driver. The numerous car accidents that happen while reversing the car, supports the creation of such a mechanism which aids the driver in properly manipulating the car so it avoids accidents.

The smart parking lot is an assembly formed by: a AC motor, a V-belt transmission, the rotating platform, supports, sensors, a camera, and encoder to receive inputs from the sensors and send them to the software the actions the parking mechanism. In this research, the product goes through concept development, computer aided design, and computer aided engineering. Going through those steps ensures the quality of the product and its credibility.

2. Development of the product

There are multiple types of parking spaces such as: public, private, and hypermarket parking spaces. The smart parking system has the potential to become part of all those types.

Although, development of parking gets more advance each day with the help of digitalization, there are no solutions that aid in positioning of the car. Both nationally and internationally, smart parking spaces limit themselves to sensors that show their availability, detectors for vehicles, smart signs, and smart maps that show the parking spots available in the city. In the end, the market and legal opportunities are big.

From a political point of view, the European affiliation and integration might encourage the development of such projects. In terms of research opportunities, the corporations focus on their own researches, and the small to medium companies can be attracted with the help of European funds.

For developing such a product, concept development was conducted and multiple concepts were created. The most relevant concepts were concept 1, as seen in figure 1. a), in which the platform has water channels that aid in draining the water off the platform, concept 2 which can be seen in figure 1. b), in which the platform has special cavities that will fix the car wheels while the rotation is undergoing, concept 3 which is illustrated in figure 1. c), it is similar to concept 2, however, instead of cavities, some special hooks fix the wheels, and concept 4 which is presented in figure 1. d), this concept has a rougher surface that provides a better grip of the wheels without adding other parts to the platform.

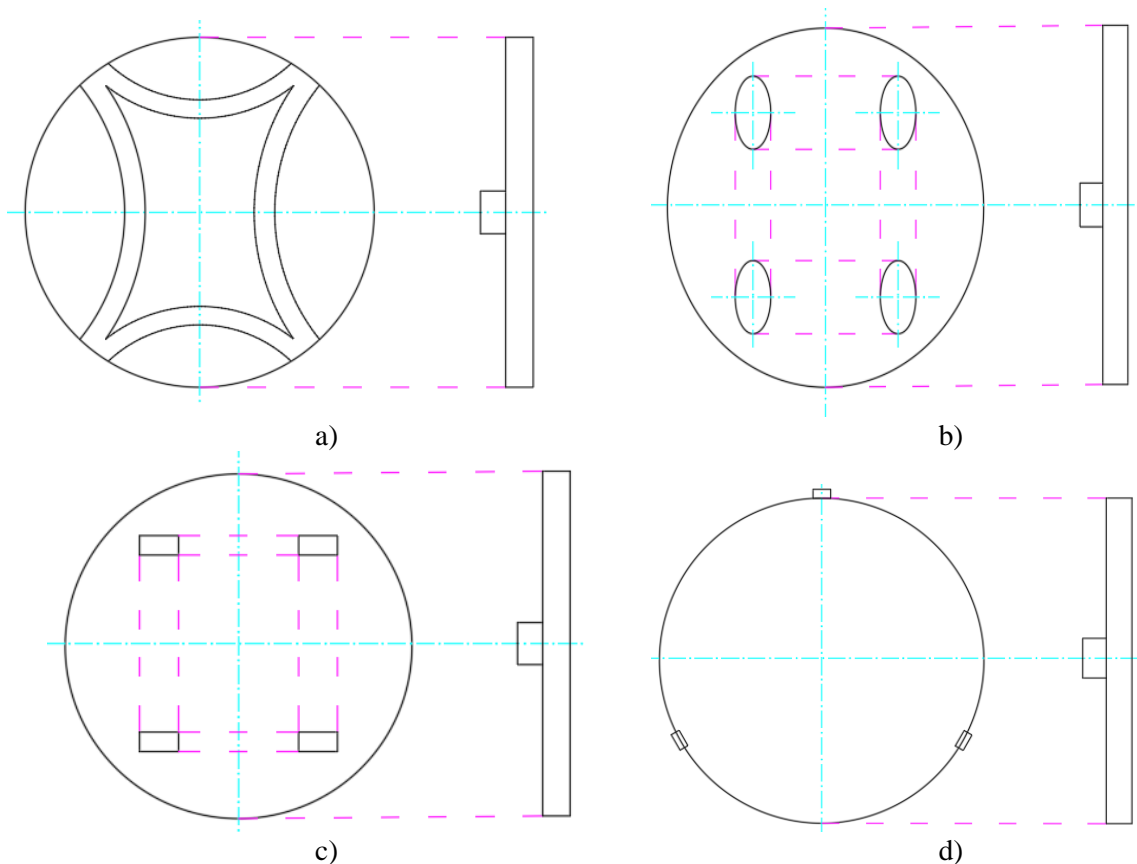


Figure 1. Concepts generated: a) Concept 1, b) Concept 2, c) Concept 3, d) Concept 4

Due to the fact that the final product is an assembly, its components are identified and designed using specialized software.

The computer aided design of the smart parking mechanism was created using the specialized software. Because of the nature of the program, the assembly parts went through a 3D-to-2D process in which the 2D drawings were based on the 3D parts previously created. In figure 2 it can be seen the 3D model of the assembly showcasing the positions of the parts.

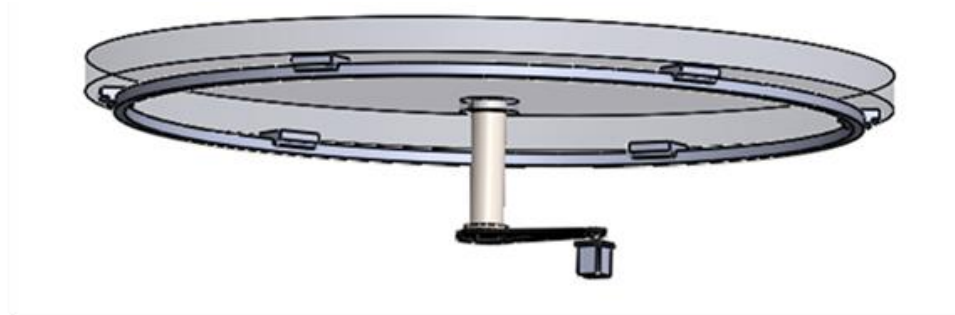


Fig. 2 The 3D design of the assembly

The motor, the pulleys, the V-belt, and the parallel key were designed using specialized calculus [4]. The guiding curve, the bearings and the shafts were designed using online catalogues [5], and catalogues provided during previous courses [4]. The important information regarding this assembly is that the platform has a diameter of 3500 mm.

The parts of the assembly were designed using the specialized software piece by piece, as seen in Figure 3:

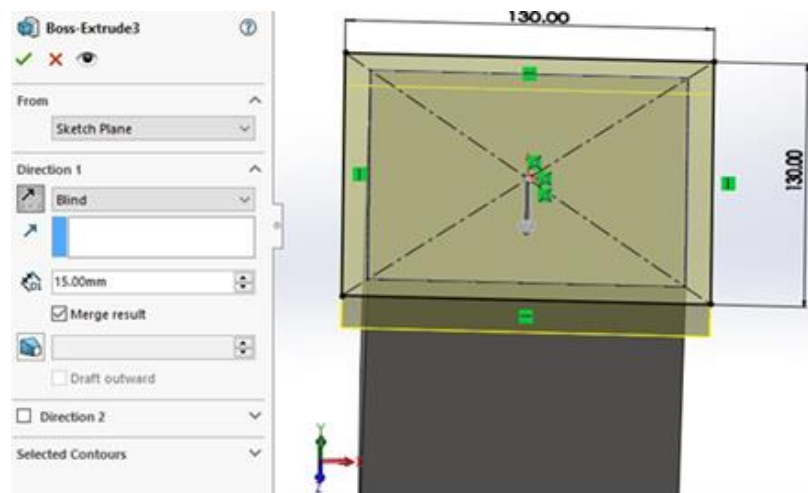


Fig. 3 The designing of the motor

In figure 4 it is presented the designing of the V-belt which will transmit the rotation coming from the motor to shaft which will rotate the platform.

The V-belt was designed using specialized calculations [4].

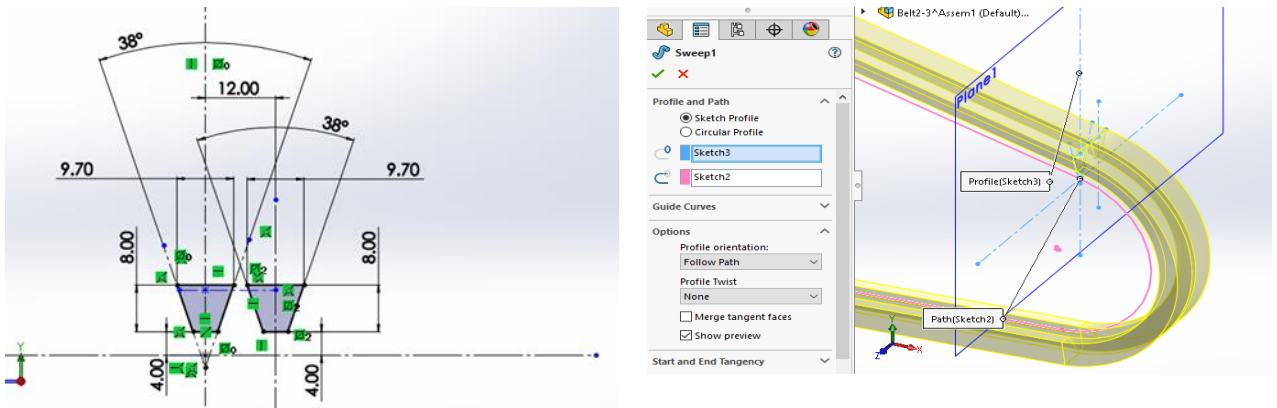


Fig. 4 Designing of the V-belt using the command Sweep and the sketch

The pulleys were designed according to the machine elements standards and with the help of commands such as: extrude and cut extrude, as seen in figure 5:

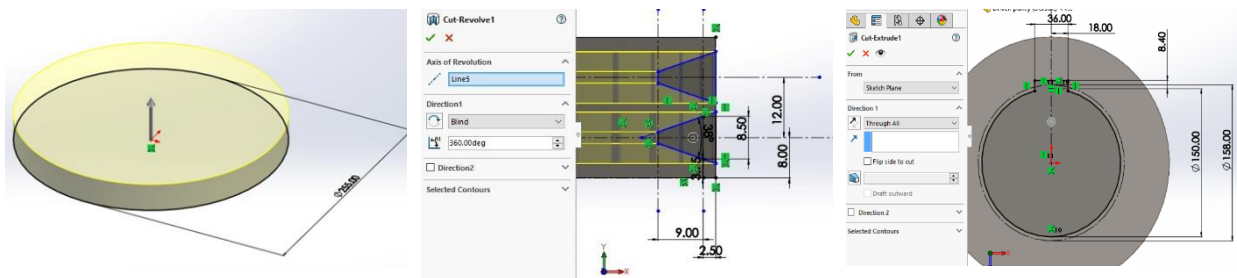


Fig. 5 Designing of one of the pulleys

The computer aided engineering was conducted only on the platform due to the fact that is the most important part of the assembly. For the analysis, only modal and harmonic response analyses were conducted because there are no other external factors that might influence the platform's behavior.

Modal analysis studies free vibration and it is used to determine the dynamic characteristics of the structures, namely the frequencies and the mode shapes. Natural frequencies have to be compared with the operating frequencies of the machine, to avoid resonances at natural frequencies harmonics. In comparison, Harmonic Response analysis is used for simulating how a structure will respond to applying dynamic loads sinusoidal. Sinusoidal dynamic loads are very common and can be found in the most unexpected places [6].

The material chosen for the platform is stainless steel with the following characteristics presented in the Table 1.

Table 1 Material characteristics of stainless steel [7]

Material	Stainless Steel(A36)
Characteristics	
Density (g/cm ³)	7.9
Tensile strength, ultimate(MPa)	400~550
Tensile strength, yield (MPa)	250
Elongation at break	10~20%
Modulus of elasticity	199947.9615
Poisson's ration	0.26
Hardness (Rockwell)	B67~83
Melting point(deg. C)	1510
Price	\$520/ton

The analysis starts with the mesh creation and validation, as seen in Figure 6:

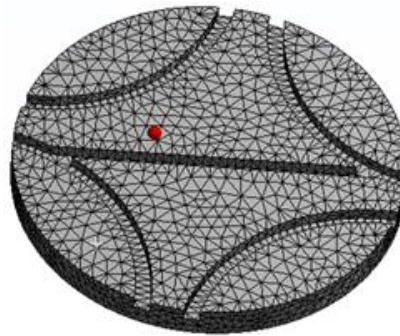


Fig. 6 Generated mesh

After adding some external factors that influence the structure, such as fixed supports, cylindrical supports, and surface pressure, components which can be seen in Figure 7:

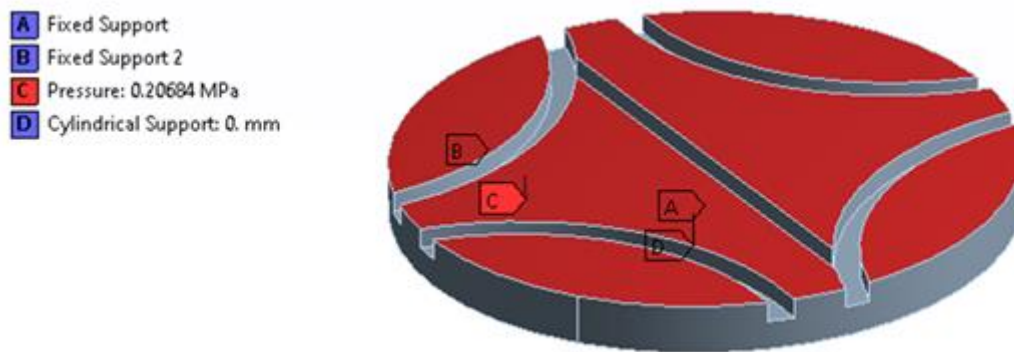


Fig. 7 The added components

In Figure 8 it is presented the frequencies resulted after the modal analysis was conducted:

•→ Modal analysis results:¶

A total of 6 modes were analyzed and the following frequencies resulted:¶

Table 3.2.1¶	
The frequencies resulted¶	
	75775¶
	75795¶
	75827¶
	76361¶
	77954¶
	78083¶

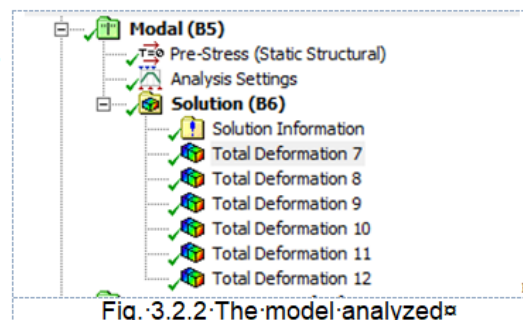
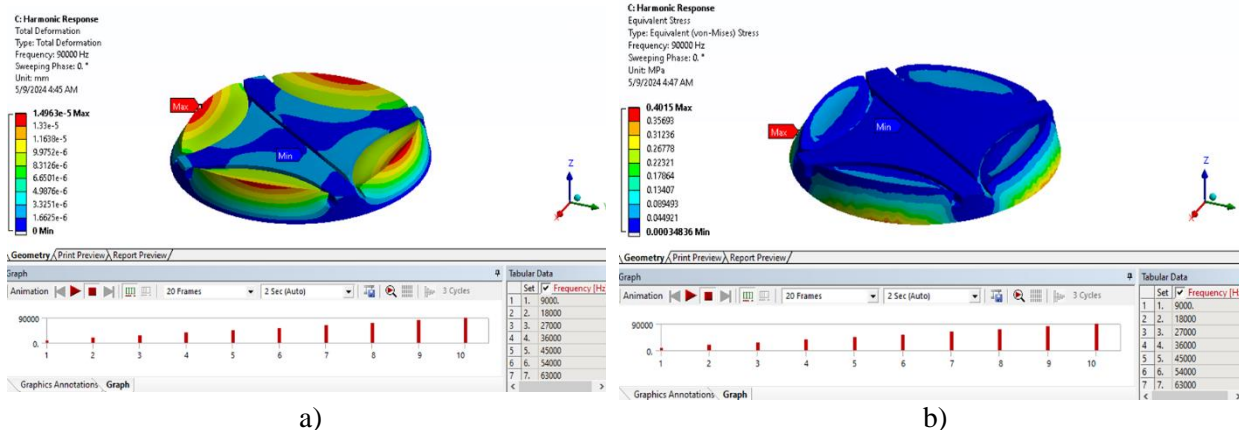


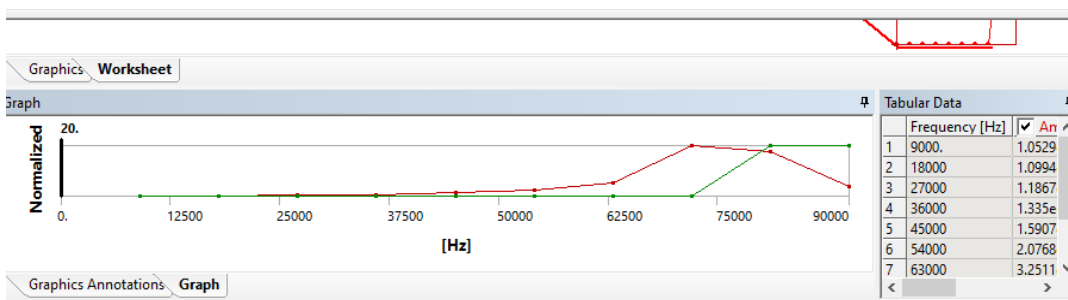
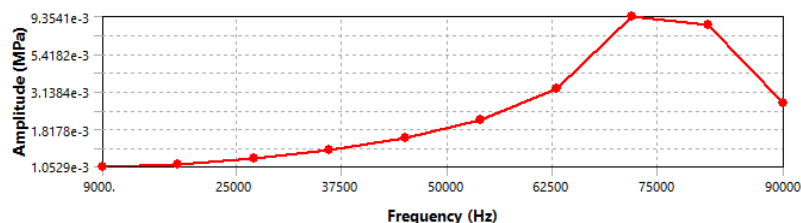
Fig. 3.2.2 The model analyzed¶

Fig. 8 Modal analysis results

The harmonic response analysis results can be seen in Figures 9 a), b) and c).



a) Frequency Response



c)

d) Fig. 9 Harmonic Response Analysis: a) The harmonic response analysis – Total deformation result, b) Harmonic response – Equivalent stress Response, c) The frequency response for the harmonic analysis

The results obtained were analyzed and the following conclusions emerged:

- The structure will resist the load done by the car, due to the fact that a car's natural frequencies are in the range of 1.2-1.8 Hz [8]
- Due to the high frequencies obtained, the material can be changed from stainless steel to a lighter and cheaper material, for example a 3D printing material such as Ultem 2100 or PEEK.
- Other designs of the platform can be taken into consideration, such as a grid type structure that will eliminate most of the weight of the platform

For further studies, a material properties comparison was conducted between the material chosen for the analyses and other possible materials. This comparison can be seen in Table 2:

Table 2 Material properties

Material	Stainless Steel(A36) [7]	Aluminium 5052 [9]	PEEK [10]	Ultem 1000 [11]	Ultem 2100 [11]
Characteristics					
Density (g/cm ³)	7.9	2.68	1.31	1.28	1.34
Water absorption, 24h (%)	-	-	0.10	0.25	0.21
Tensile strength, ultimate(MPa)	400~550	228	115	105	115.83192
Tensile strength, yield (MPa)	250	193	110	-	114
Elongation at break	10~20%	~12%	40%	40%	6%
Modulus of elasticity (GPa)	200	703000	4343.7	-	-
Poisson's ration	0.26	0.33	0.43	0.36	-
Hardness (Rockwell)	B67~83	H108	M100/R126	M112/R125	M114/R127
Melting point(deg. C)	1510	~607	340	340	340
Price	\$520/ton	\$500/ton	\$500/kg	\$59 for 6.35x305x305	1110 euros/25 kg

3. Conclusions

Although indispensable, cars have become a hassle to crowded cities and drivers. The increased number of cars has created traffic congestions, a constant need of parking lots, and parking lot accidents (see §1).

- Because the parking problem negatively impacts the citizens' daily life, countries worldwide started promoting the use of multilevel parking facilities. The application of stereoscopic parking equipment has effectively eased the pressure on urban transportation. The stereoscopic parking equipment's frame-based actuation offers significant stiffness, short transmission chain, strong load capacity, high precision, small motion inertia, and easy control (see §1).

- The „smart parking mechanism” is a „smart product” because it aids the driver in manipulating the car in small spaces. The mechanism movement is similar to rotary table, therefore, it makes the car the hypothetical work piece which is rotated to the operator's desire, in this case, the driver. The numerous car accidents that happen while reversing the car, supports the creation of such a mechanism (see §1).

- The mechanism opens the path to new researches on the parking problem. Those researches might create a new market and encourage the emergence of start-up companies that will focus on the creation of parking mechanisms (see §2).

- The designing of the parking mechanism undergoes several phases: product design and development, computer aided design and computer aided engineering. Those phases ensures the product quality and credibility (see §2).

- The computer aided design of the smart parking mechanism was created using the specialized software. Because of the nature of the program, the assembly parts went through a 3D-to-2D process (see §2).

- In the computer aided engineering phase, the platform undergoes two analyses: modal analysis and harmonic response analysis. Those analyses show the rotating platform behavior (see §2).

- The results of the analyses highlight the possibility of using different materials used for the platform (see §2).

- The smart parking mechanism was talked before in the engineering community, but this product, globally speaking, is only in the conceptualization era. With the present technology, this product is possible to

implement but really expensive to do it. The conceptualization, designing, validation, and production of it rises the price up and the implementation of it might highlight some economic aspects.

- With the creation of such product, both the market and the consumer behavior will change. By identifying a need, providing a solution for it, and implementing that solution will trigger other engineers and creators to develop something similar but better.

4. References

- [1]. Jie Hao, Viet Tuan Pham, Stuck in traffic: Do auditors price traffic congestion?, The British Accounting Review, Volume 56, Issue 2, 2024, DOI: 101279, ISSN 0890-8389, <https://doi.org/10.1016/j.bar.2023.101279>,
- [2]. Jannik Lindner, Parking Lot Accident Statistics [Fresh Research], Gitnux, last updated 16.12.2023, available at <https://gitnux.org/parking-lot-accident-statistics/>
- [3] Jingang Jiang, Dianhao Wu, Tianhua He, Yongde Zhang, Changpeng Li, Hai Sun, Kinematic analysis and energy saving optimization design of parallel lifting mechanism for stereoscopic parking robot, Energy Reports, Volume 8, 2022, Pages 2163-2178, ISSN 2352-4847, <https://doi.org/10.1016/j.egyr.2022.01.133>
- [4] Alexandru Valentin Radulescu, Machine Elements, Faculty of Mechanics and Mechatronics, Department of Machine Elements and Tribology, 2022
- [5] Henlich, Curve guides, available at https://www.hennlich.ro/fileadmin/_migrated/en__HCR__en_a01_336.pdf, last accessed at 09.05.2024
- [6]. Pupaza Cristina, Computer Aided Engineering, Department of Robotics and Production Systems, 2022
- [7] American Metals Co. , A36 Steel Technical Data Sheet, available at <https://www.metalshims.com/t-A36-Steel-Technical-Datasheet.aspx>, last accessed at 28.05.2024
- [8] Coker, A.J. (Ed), *Automobile Engineer's Reference Book*, 1959
- [9] Atla Steels, Aluminium Alloy Data Sheet, 2013, available at https://www.atlassteels.com.au/documents/Atlas_Aluminium_datasheet_5052_rev_Oct_2013.pdf, last accessed at 28.05.2024
- [10] Direct plastics, PEEK, available at <https://www.directplastics.co.uk/pdf/datasheets/PEEK%20Data%20Sheet.pdf>, last accessed at 28.05.2024
- [11] Laminated plastics, Technical Data Sheet Ultem (PEI), available at <https://laminatedplastics.com/ultem.pdf>, last accessed at 28.05.2024

DEVELOPING A WEB APPLICATION FOR SIMULATING INDUSTRIAL PROCESSES FOR MONITORING AND CONTROL

STAICU Andrei Alexandru, TUNSOIU Nicolae

Faculty: Industrial Engineering and Robotics, Specialization: Applied Computer Science in Industrial Engineering,

Year of study: II, e-mail: andyalexandru20045@gmail.com

ABSTRACT: Industrial automation has become a central element in modern manufacturing providing significant benefits. The current paper proposes an industrial application on three segments: Monitoring and Manual Control, Dimensional Control, and Automatic Control. The Manual Monitoring and Control Division represents a valuable asset within the manufacturing industry, providing workers with efficient monitoring procedures. This enables them to promptly respond to any detected issues, thereby enhancing both efficiency and safety within the factory environment. The Dimensional Control component assists in engineering and design, helping to verify the conformity of manufactured parts, leading to reduced errors and defects in production.

The Automatic Control division facilitates industrial automation, it can be implemented in production lines to automatically detect the presence or absence of certain objects, optimizing the production flow.

KEYWORDS: Automation, Control, Efficiency, Industry, Optimizations.

1. Introduction

Industry 4.0, also known as the "fourth industrial revolution" or "smart factory," represents a major transition in the industrial environment, where digital technologies are extensively integrated into production processes [1].

In today's highly competitive business environment, the industry is challenged by demands for productivity, quality, and safety. The role of information technology in achieving these objectives has become critical. Large and complex production systems cannot be efficiently and safely managed without advanced information management and process control [2].

This paper presents an application that integrates various web technologies for controlling and monitoring the digitization process in a factory, thus contributing to the expansion of Industry 4.0. The need for remote monitoring of processes in a factory has led to the development of an application that covers the supervision needs of existing processes and provides real-time workflow information.

Currently, there are numerous process monitoring applications on the market, but none contribute to a deeper understanding of monitoring and automation in a factory. This lack of understanding can lead to a decrease in workflow and company profit.

The application is structured into three sections, aiming to cover a wide range of processes encountered in a smart factory: Manual Monitoring and Control, Dimensional Control, and Automatic Control. The three divisions will be detailed, explaining the purpose and advantages that each solution brings to a company through its implementation.

2. The existing problems in a factory that require automation

We are witnessing the greatest transition in the history of the planet. We live in an era where factories are becoming "The Dark Factory," or better known as "Lights-out Factory" (operating with minimal human activity, allowing them to function in darkness without human intervention) [3].

Let's analyze a specific case, where we will compare the application with an existing monitoring solution in the industry. Paessler PRTG, developed by "Paessler The Monitoring Experts" [3], is recognized for monitoring processes in a factory. However, there are some aspects that can be improved. Although it supports IoT and PLC monitoring, the lack of more granular control can be a significant impediment. The interface, while intuitive, does not provide an accurate picture of the process nor does it allow for precise interventions in case of emergencies or anomalies. In comparison, my application stands out for its precision, detailed control, and the ability to react quickly to any unexpected situation in the factory. The following sections will present the application's features to highlight its superiority compared to other similar applications.

3. WEB Interface

The web application, named "Creative Ventures," is developed using HTML, CSS, JS, PHP, MySQL, LabVIEW, and NI Vision Assistant, along with various web protocols (HTTP, SMTP), ODBC connectivity, a local Apache server, and a small portion of C++. By using these technologies, we ensure that we can maximize the potential of each component for its specific purpose.

The first interaction with the application is through the Sign Up page (Fig. 1):

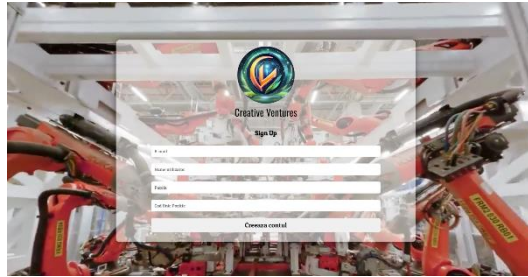


Fig. 1. Sign Up page

The user is required to provide personal data to complete the username, password, email address, as well as a unique code provided by the "employer" on the Sign Up page. This unique code serves as the website's response to the user, granting viewing rights and functionalities to different modules of the application. For example, if a company hires an intern, they will only have access to the Monitoring and Automatic Control module.

Upon creating the account, the information is sent through a connection to the MySQL database via PHP, where the existence of a similar account and the correspondence of the unique employer code will be verified. If the connection is successful, the provided data will be recorded in the database, and the user will be redirected to the Log In page to enter the application.

Once logged into the application, the user is greeted by a concept of a chatbot named Echo. Its role is to assist the engineer in completing their tasks. However, Echo remains a concept that can be integrated with artificial intelligence in the future. To simulate some of its capabilities, we have created a dedicated page where it can respond to a few predefined questions that an engineer might have (Fig. 2):

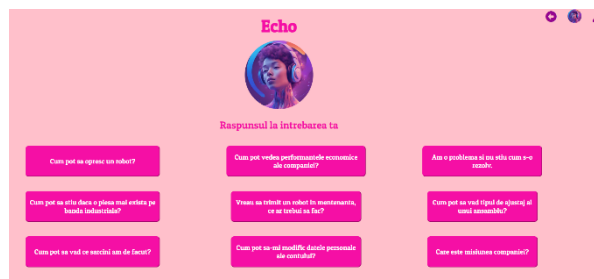


Fig. 2. Echo Page

Another option available to the user in this section is the "My Account" page, where they can view their account settings. This means they can see information regarding their account or "Submit a Ticket," meaning they can send an automated email to the IT Department for various issues.

3. Manual Monitoring and Control

The first section of the application is the Manual Monitoring and Control. The engineer accessing this section is greeted by the 5 robots of the pseudo-company (AssemblyLineBot, BoxConveyorBot, BottleLiftBot, DairyPackBot, and CrateCraftBot), as well as numerous functionalities (Stop/Restart Robot, Maintenance Report, Tasks, Economic Factors) that they can access (Fig. 3):

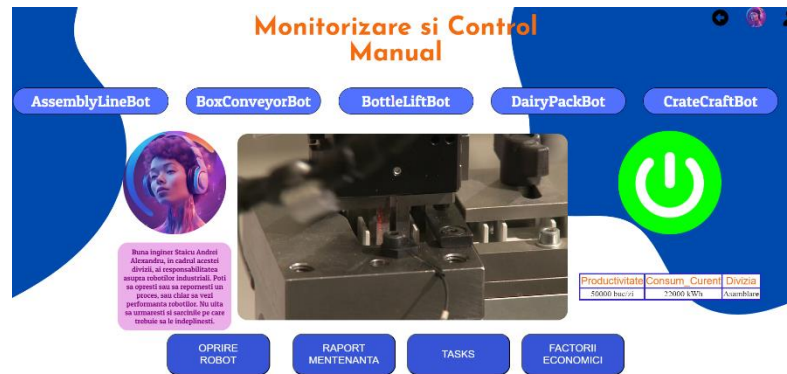


Fig. 3. Manual Monitoring and Control Interface

The process engineer has access to the 5 robots and can see if they are functional or stopped. They can also view details about each robot on the right side, extracted from the MySQL database. As this is a simulation of an industrial process, the 5 robots are represented by 5 videos, but instead, CCTV cameras could be used to monitor the process. This division is intended for processes where a process engineer can easily intervene on-site, as it is a large and open space. If we talk about processes that are automated and the engineer cannot easily intervene, we will cover this part in the Automatic Control chapter.

On another note, this process can be stopped, and information about the status of a robot is automatically sent to the database (Fig. 4):

ID	Denumire_robot	Stare	Productivitate	Consum_curent	Divizia
1	AssemblyLineBot	1	50000 buc/zi	22000 kWh	Asamblare
2	BoxConveyorBot	0	9500 buc/zi	12000 kWh	Impachetare
3	BottleLiftBot	1	14500 buc/zi	18700 kWh	Alimentara
4	DairyPackBot	0	13200 buc/zi	20900 kWh	Alimentara
5	CrateCraftBot	1	50000 buc/zi	26000 kWh	Impachetare

Fig. 4. Table "roboti" from the data base

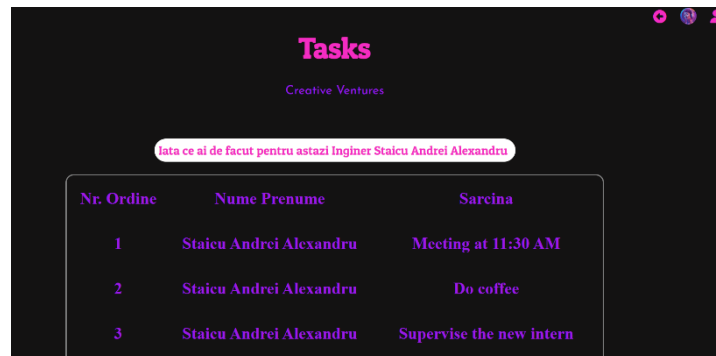
If the engineer notices an anomaly in the system or a malfunction, they can press the "Stop robot" button, where a pop-up will appear to confirm the decision. If they press the "Yes" button, the robot's status will be updated to 0. If they wish to restart the robot, they can press the "Restart robot" button, and the process will continue, updating the status to 1.

After the engineer has stopped the process, they have the option to generate a maintenance report by accessing the "Maintenance Report" button, where they are redirected to a dedicated page for creating the report. The engineer can describe the reason for sending the robot for maintenance, select its name, the industrial line it belongs to, as well as the names of the company's director and manager (Fig. 5):

Fig. 5. Maintenance Report

By pressing the "Print" button, a page that can be printed is generated. The name of the engineer preparing the report is automatically added, along with their position.

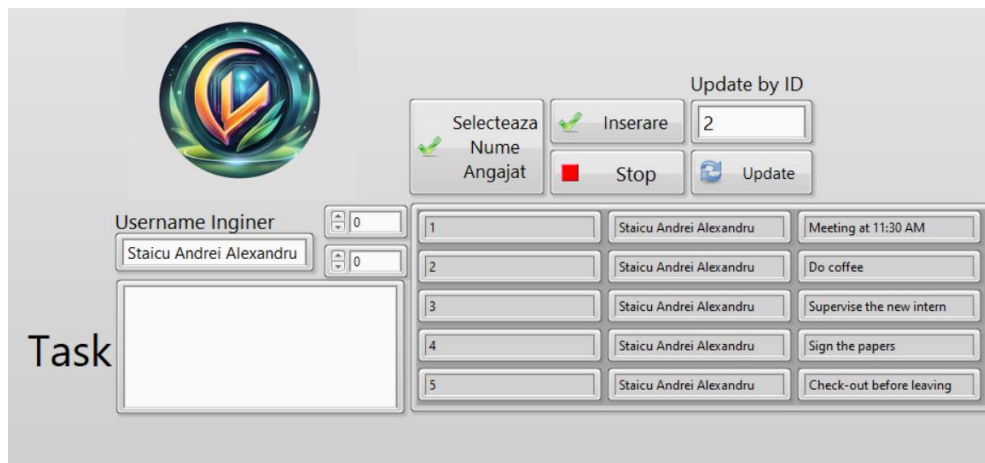
Another functionality is "Tasks," where the engineer can see the tasks they need to accomplish. This page is static, and the engineer cannot make any changes to it (Fig. 6):



Nr. Ordine	Nume Prenume	Sarcina
1	Staicu Andrei Alexandru	Meeting at 11:30 AM
2	Staicu Andrei Alexandru	Do coffee
3	Staicu Andrei Alexandru	Supervise the new intern

Fig. 6. Tasks Page

The engineer can only view information about the tasks he needs to perform, and this data is directly retrieved from the "tasks" table in the database. To change these tasks, we have developed a small LabVIEW application, a virtual instrument, intended for the employer. Only the employer can change the task-related data. The application connects to the database, can insert new tasks, can display all tasks of a particular employee, and can update an employee's task (Fig. 7):



Nr. Ordine	Nume Prenume	Sarcina
1	Staicu Andrei Alexandru	Meeting at 11:30 AM
2	Staicu Andrei Alexandru	Do coffee
3	Staicu Andrei Alexandru	Supervise the new intern
4	Staicu Andrei Alexandru	Sign the papers
5	Staicu Andrei Alexandru	Check-out before leaving

Fig. 7. Virtual Instrument for Assigning Tasks to an Employee

The last functionality of this Manual Monitoring and Control division is the "Economic Factors" section, dedicated to visualizing the company's economic performance. In this page, both engineers and employers can see economic details about the processes performed in a working day. They can directly view all active or inactive robots, as well as the productivity of each robot (data retrieved directly from the database, where each robot produces a certain number of products daily).

Through a basic algorithm in LabVIEW, we have displayed the company's productivity percentage on this page. With 5 robots, each represents 20% of productivity. For each inactive robot, productivity decreases. This aspect can be observed both in the productivity percentage section and in the bar chart.

Next, we have the revenue section. These revenues are read from the database and, being a simulation, are preset for robots working 24/7. When a robot is inactive, the revenue is \$0. In reality, these revenues vary depending on other factors, which can be integrated when this application is implemented by a company. After obtaining these revenues, through a simple calculation, we add up the total revenues and display them on the site (Fig. 8):



Fig. 8. Company Revenues

3. Dimensional Control

In Industry 4.0, our goal is to maximize production and minimize waste as much as possible to contribute to a more sustainable world. A crucial aspect in quality control industry is achieving the highest possible precision during material processing. Within the discipline of "Tolerances and Dimensional Control," we have noticed a complete lack of tools in this regard. Digitalization in this field is still limited. To illustrate this problem, we can consider a website that deals with the calculation of fits between two components (shafts and holes).

A relevant example is "Online calculation of fits" [4], developed by the Swiss company MESYS AG. It is an online platform for calculating deviations and tolerances for fits. The website uses the ISO 286 (2010) standard. However, it does not provide a very user-friendly solution for engineers. It is an old site that does not provide enough details about fits, probably to encourage users to purchase their dedicated software.

Our division deals with calculations that such free web applications do not offer. Our application requests the nominal size of the fit, the upper and lower deviations of the shaft and hole. The only difference between my site and the application offered by MESYS AG is that an engineer can directly input the tolerance field for the deviation calculation. In the future, our application could be equipped with such a database.

After the engineer submits the fit data to the web service, the program is ready to return the following information: nominal size, fit deviations (provided by the user), tolerances, dimensions, clearances, interferences, minimum and maximum values of the shaft and hole, average clearance and interference, clearance, and interference tolerance, and probable. Finally, the type of fit is displayed, as well as the corresponding clearances/interferences. To perform these calculations, we used the following formulas:

$$TD = ES - EI, Td = es - ei,$$

(1)

$$D_{max} = D_{nom} + ES, D_{min} = D_{nom} + EI$$

$$d_{max} = D_{nom} + es, d_{min} = D_{nom} + ei$$

(2)

$$J_{max} = ES - ei, J_{min} = EI - es,$$

$$J_{med} = (J_{max} + J_{min})/2$$

$$S_{max} = -J_{min}, S_{min} = -J_{max},$$

$$S_{med} = (S_{max} + S_{min})/2$$

(3)

(4)

$$T_j = J_{\max} - J_{\min}, T_s = S_{\max} - S_{\min}$$

$$T_{j\text{prob}} = \sqrt{TD * TD + T_d * T_d}$$

(5)

$$J_{\max\text{probs}} = J_{\max} - (T_j - T_{j\text{prob}})/2$$

$$J_{\min\text{probs}} = J_{\min} + (T_j - T_{j\text{prob}})/2$$

(6)

$$J_{\text{probu1}} = J_{\min} + (1/3) * T_j$$

$$J_{\text{probu2}} = J_{\max} - (2/3) * T_j,$$

$$S_{\max\text{prob}} = S_{\max} - (T_j - T_{j\text{prob}})/2$$

$$S_{\max\text{probs}} = S_{\max} - (T_s - T_{j\text{prob}})/2$$

(7)

$$S_{\min\text{probs}} = S_{\min} + (T_s - T_{j\text{prob}})/2$$

3. Automatic Control

The Automatic Control Division is the closest to the concept of a smart factory within Industry 4.0. This division is dedicated to automating processes, minimizing human intervention. We have chosen to present a simple type of application for the Automatic Control part in this paper, highlighting the potential to add a diverse range of applications within this division.

Thus, the chosen type of application is the recognition of a part on a conveyor belt. In case a part is not detected on the belt, its absence will be signaled on the main panel of the page, and an email will be automatically sent to notify about the event that occurred in the industrial belt area.

In Industry 4.0, sensors are no longer the only solution for monitoring a process. By using artificial intelligence, we can develop image processing applications to analyze various aspects. Therefore, for this application, we opted to use Vision Assistant, provided by National Instruments, as part of the LabVIEW suite.

We managed to identify the most efficient method for recognizing a part on a conveyor belt. One possible approach would have been to take numerous photos of the part from different angles and positions to provide the program with a varied range of data to analyze. However, this method is extremely slow and does not offer optimal performance. However, we have discovered a method with significantly higher efficiency, namely particle analysis and filtering (Fig. 9):

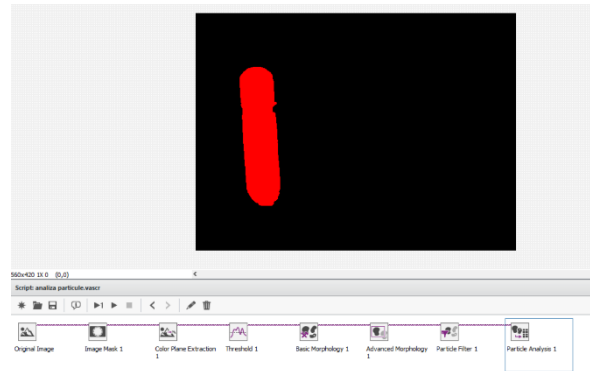


Fig. 9. Component recognition script in Vision Assistant

To develop this application, various functions of Vision Assistant were used to process the image. Firstly, an Image Mask was created to remove the camera tripod from the image, and then the image was compressed to 8 bits by extracting its color plane with Color Plane Extraction. A Threshold was applied to the image to delineate the area of interest and minimize the detection of noise in the image. As a result, a clear image with the object we want to identify was obtained, but some adjustments were still needed. To slightly dilate the object, the Basic Morphology function was used to ensure that we have a closed contour. Then, using Advanced Morphology, the holes in the contour were covered to avoid detecting multiple unwanted objects on the belt. This was crucial to eliminate confusion caused

by detecting unwanted objects on the belt. The Particle Filter function was used to define the exact area of the desired object, so that in case other smaller or larger objects appear, they are eliminated to not influence the final result. The last step consisted of Particle Analysis, which allowed us to extract the number of detected objects, confirming that there is only one object present on the belt.

To detect the absence of the piece, we implemented an efficient algorithm that, with the help of a camera, transmits real-time images to the LabVIEW application via IP, processes the images using Vision Assistant, and sends the result (1 or 0, depending on the presence or absence of the piece) to a file. Although we could transmit this data directly to a database, we chose this option for this work because it is faster. Then, these data are read, and when a 0 is detected (indicating the absence of the piece), a timer is initiated set to 10 seconds. If the piece is missing for 10 seconds, the time is counted, and at the tenth second, the timer is reset, and the algorithm to send an email to the user is initiated using the SMTP protocol to report the system anomaly (Fig. 10):

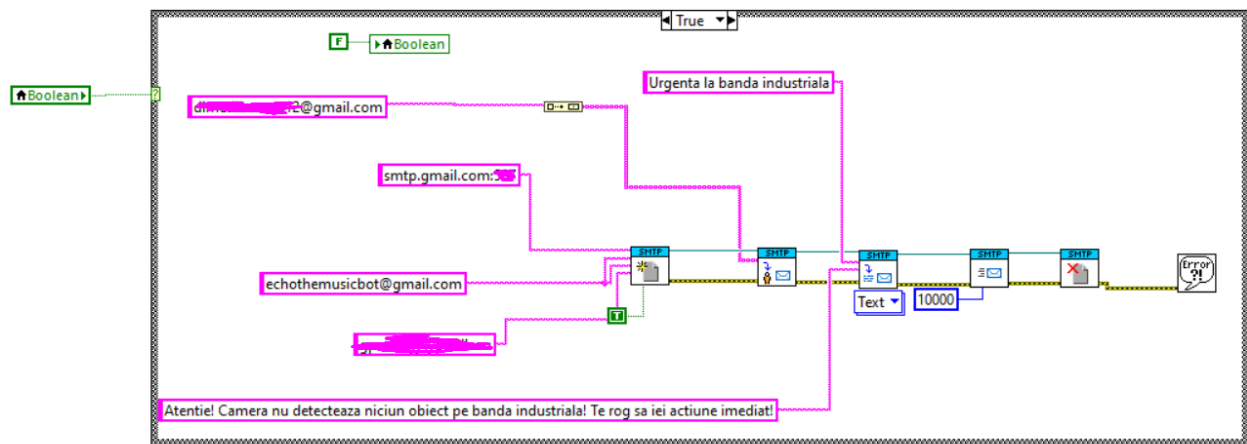


Fig. 10. SMTP Protocol

6. Conclusions

Process control and product quality assurance are crucial in the current context. Quality standards have significantly risen, and even the smallest control errors can have significant consequences. In this paper, we highlighted key points for increasing productivity in a factory, ensuring quality, and avoiding anomalies. Manual monitoring and control represent an efficient solution to ensure the flow of the process. Through dimensional control, engineers can be more confident that the parts are compliant, and process automation through automatic control offers high precision and maximum control over productivity.

Although this paper covers a wide range of applications usable in industry, there is always room for development. For example, the manual monitoring and control part will evolve together with artificial intelligence. Data about the products made in a factory will be managed by it. Technicians dealing with manual, difficult, and repetitive work in a factory will gradually be replaced by autonomous, bipedal robots. Moreover, all processes will be exclusively digital.

In conclusion, the implementation and continuous evolution of monitoring and control solutions in the industry are crucial for increasing efficiency, ensuring quality, and adapting to the continuously changing market requirements. By integrating emerging technologies, such as artificial intelligence and advanced automation, factories can transition to more efficient and reliable processes, thus contributing to the long-term success and competitiveness of industrial businesses.

8. Bibliography

- [1]. Oracle România, Aplicații, Managementul lanțului de aprovizionare, Manufacturing, Industry 4.0 – Prezentare generală, Ce este Industry 4.0?, <https://www.oracle.com/ro/scm/manufacturing/what-is-manufacturing/what-is-industry-4-0/> ;
- [2]. Tommila, T., Hirvonen, J., Jaakkola, L., Peltoniemi, J., Peltola, J., Sierla, S., & Koskinen, K. (2005). Next generation of industrial automation. Concepts and architecture of a component-based control system, VTT Technical Research Center of Finland, 58-63
- [3]. Siemens Digital Industries Software (28.04.2024), Technology, Lights-out factory, <https://www.sw.siemens.com/en-US/technology/lights-out-factory/> ;
- [4]. Paessler The Monitoring Experts (28.04.2024), Paessler PRTG, <https://www.paessler.com/industrial-it-monitoring> ;
- [5]. MESYS AG, Online fit calculator, Calculation of fits according ISO 286 (2010), <https://www.mesys.ch/calc/tolerances.fcgi?lang=en>;
- [6]. Autor, Teemu Tommila. și Autor, Juhani Hirvonen. (2005), “Next generation of industrial Automation, Concepts and architecture of a component-based control system”, in: VTT RESEARCH NOTES 2303, VTT Technical Research Centre of Finland, 6. Summary and conclusions, pagina 97

9. Notations

The following symbols are used within the paper:

T_D = bore tolerance [mm]; T_d = shaft tolerance [mm]; E_s = upper deviation of bore [mm]; E_l = lower deviation of bore [mm]; e_s = upper deviation of shaft [mm]; e_l = lower deviation of shaft [mm]; D_{max} = maximum size [mm]; D_{nom} = nominal size [mm]; D_{min} = minimum size [mm]; J_{max} = maximum clearance [mm]; J_{min} = minimum clearance [mm]; J_{med} = average clearance [mm]; S_{max} = maximum interference [mm]; S_{min} = minimum interference [mm]; S_{med} = average interference [mm]; T_j = clearance tolerance [mm]; T_{jprob} = probable clearance tolerance [mm]; $J_{maxprob}$ = probable maximum clearance [mm]; $J_{minprob}$ = probable minimum clearance [mm]; $S_{maxprob}$ = probable maximum interference [mm]; $S_{minprob}$ = probable minimum interference [mm]

MAKING AN EXPERIMENTAL MODEL OF A PALLET HANDLING AND TRANSPORT ROBOT

RĂILEANU Anton, DEMIAN Gabriel, DUGĂEȘESCU Ileana

Faculty: Industrial Engineering and Robotics, Specialization: Industrial Economic Engineering,
Year of studies: Year III, e-mail: anton.raileanu@stud.fiir.upb.ro

ABSTRACT: The design of an experimental robot model involved the identification of the required functionalities, the design of the corresponding elements and the identification of the necessary electrical components. The exterior shape of the model was inspired from the existing electric forklifts. The main functionalities of the robot are handling and transporting pallets and the appropriate mechanisms were designed to this end. The lifting system was conceived for vertical translation and angular motion, using electric motors and a servomotor. The chassis of the robot consists of three compartments to accommodate various elements and to ensure the correct operation of the system. The model's parts were fabricated using FDM technology and Z-Hips and PLA materials. The programming and the assembling were done meticulously, and the performance analysis showed that the model fulfils the expected functionalities. However, some aspects that need improvement were identified, such as the stiffness of the lifting system and the stability of the bluetooth connection. In conclusion, the experimental model is functional and ergonomic.

KEY WORDS: robot, transport, analysis, design, additive manufacturing.

1. Introduction

The subject of the paper consists in making a small-scale experimental model of an automated robot that, through its functionalities, can handle and transport pallets, and provide relevant information to the process. The established objective was achieved through a series of successive activities, starting with the design of the robot and manufacturing of the parts, followed by assembling the model and establishing the necessary electrical elements, and ending with programming of the instructions.

2. Current stage

The year 1867 was marked by the first patent for a device that could both lift and transport materials. The device was simple, consisting of a vertical frame, a lifting system and a cantilever platform. That system could be attached to a cart, which could then be moved to different sites [3].

In 1913 an invention was created that revolutionized the lifting systems, the hydraulic lift [3]. Although the construction of the forklifts in the 1920s allowed their logistical/industrial application, there was a significant limitation in terms of their utility: there were no standard dimensions for the pallets. Because of it, pallets could be either too small or too large for the forklifts to handle them. In the late 1930s, engineers solved this problem by standardizing the pallet sizes [3].

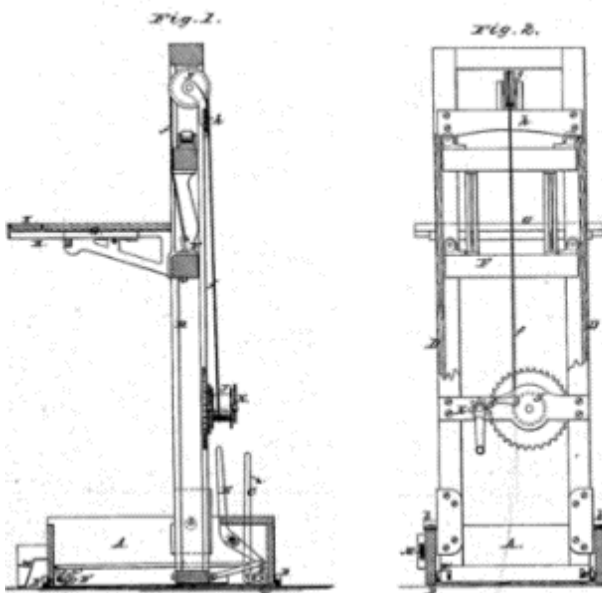


Fig. 1. Illustrations from the patent for the first portable lift, a precursor to the forklift mast [3].



Fig. 2. Forklift for non-standard pallets [3].

At present, automated forklifts make up a large share of the equipment of large industrial warehouses, being capable to adapt to specific requirements, these machines can be used in a variety of transport applications in factories, warehouses and in centres for distribution and order execution. Such vehicles that can handle and transport autonomously heavy objects or materials are known as Automated Guided Vehicles, AGV's, or Autonomous Mobile Robots, AMR's. They are equipped with sensors and a guidance system to ensure precise movements and eliminate the need for the manual control [4].

3. Designing the experimental model

In the initial phase of designing the robot, will be identified the functions which are necessary in order to fulfil the established requirements. In the next phase, using Autodesk Inventor [5], will be designed the

elements that will fulfil the identified functions. In the end, the designed parts will be manufactured using additive manufacturing technologies.

3.1. Analysis of the model's functions

The main functions of the robot consist in pallet handling and transporting. For handling the pallets, there is need for mechanisms to ensure the vertical translation of the forks carrying the pallets and a mechanism to ensure the angular motion of the lifting system in relation to the ground plane. In order to fulfil the transport function, a self-motion system is imposed to the robot. Given that the experimental model is not designed to be self-guided, its control function will be provided. A final additional function imposed to the robot is the transmission of visual and auditory signals, necessary to provide users or observers with information about the process.

Thus, the identified functions of the model are:

- F 1.* Vertical fork translation;
- F 2.* Angular motion of the lifting system;
- F 3.* Self-motion of the model;
- F 4.* Ensuring control;
- F 5.* Transmission of visual and audio signals.

3.2. Designing the lifting system

The lifting system is assigned the functions of vertical translation (F1) and angular motion of the forks (F2). The function of translation will be ensured by a system consisting of a fork carrier, guided on two vertical uprights, and moved by the means of a pulley system operated by an electric motor. The angular motion in relation to the ground plane of the lifting system will be carried out by the means of a servomotor that will actuate a mechanical arm. The dimensions of the elements will be designed so that handling of a pallet with 100 x 70 mm dimensions can be ensured.

Table 1. The component elements of the lifting mechanism

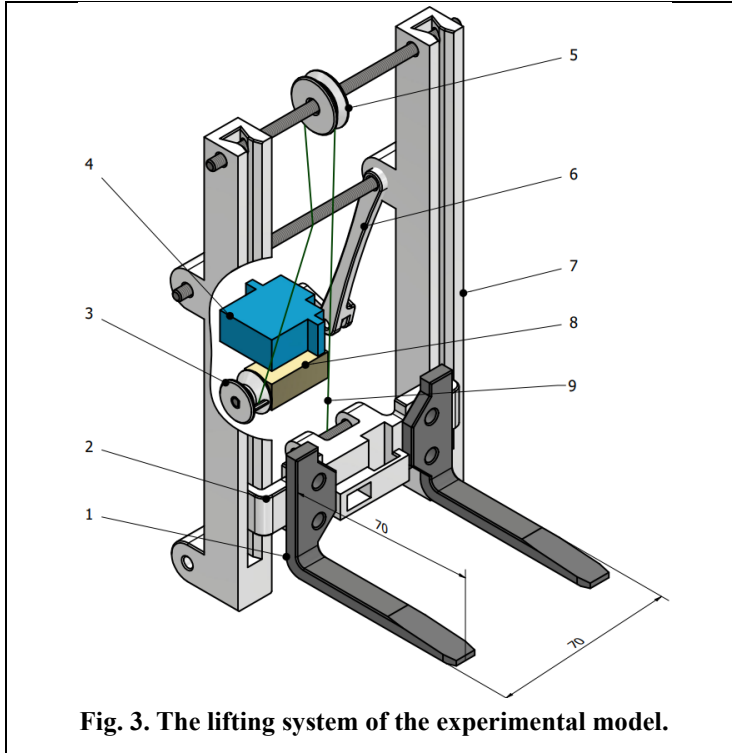
	No. crt.	Name	Unit	Type of parts
	1	Forks	2	Designed
	2	Fork carrier	1	Designed
	3	Main pulley	1	Designed
	4	Servomotor	1	Purchased
	5	Upper pulley	1	Designed
	6	Arm	1	Designed
	7	Upright	2	Designed
	8	Electric motor with a 50 RPM gear	1	Purchased
	9	Thread	1	Purchased

Fig. 3. The lifting system of the experimental model.

3.3. Designing the chassis elements

The chassis of the robot will be composed of three compartments in which the elements necessary to fulfil the F3, F4, F5 functions will be located. The lower compartment is composed of the supporting chassis on which the electric motors of the wheels, the electric element for motor control, the electric motor and the servomotor of the lifting system are fixed. The uprights of the lifting system are also placed on the supporting chassis. The middle compartment is on the lower frame that covers the supporting chassis. The *Arduino* control board will be placed in this compartment. The third compartment is above the upper frame, on which the breadboard with the related electrical elements and the battery for powering the electrical circuit will be located.

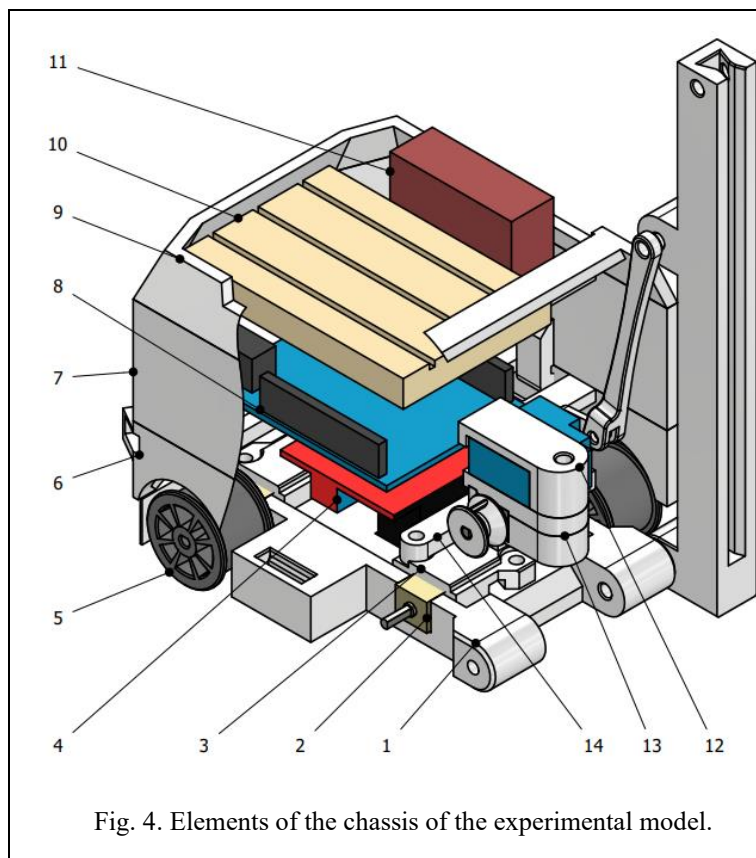


Table 2. The chassis components

<i>No. crt.</i>	<i>Name</i>	<i>Unit</i>	<i>Type of parts</i>
1	Chassis	1	Designed
2	200 RPM electric motor	4	Purchased
3	Motor fixing cover	2	Designed
4	L298N	1	Purchased
5	Wheel	4	Designed
6	Lower frame	1	Designed
7	Middle frame	1	Designed
8	Arduino board	1	Purchased
9	Upper frame	1	Designed
10	Breadboard	1	Purchased
11	9V battery	1	Purchased
12	Servomotor cover	1	Designed
13	Upper cover	1	Designed
14	Lower cover	1	Designed

4. Manufacturing the parts through TFA

The designed parts of the experimental model were manufactured using the FDM (Fused Deposition Modelling) additive manufacturing technology. This technology is recommended due to the fast-manufacturing time, the appropriate resistance of the manufactured parts, as well as to the possibility of obtaining complex surfaces. The chosen manufacturing technology imposes some particularities in the process of designing the parts, thus, the adjustments were prescribed 0.1...0.2 mm larger clearances, given that, following FDM manufacturing, considerable geometric changes are found in bores and shafts.



a)



b)

Fig. 5. a) Manufactured lifting system parts and b) chassis parts.

5. Assembling the parts of the experimental model

The robot parts were assembled by clamping and by the means of screws and nuts. The chassis was assembled with the lower, middle and upper frame elements by snap-fitting some designed geometries. The other parts are provided with holes to fit with assembling with $M4$ screws and nuts. Within the lifting system, cut up threaded $M4$ rods were used, $l = 110\text{ mm}$.

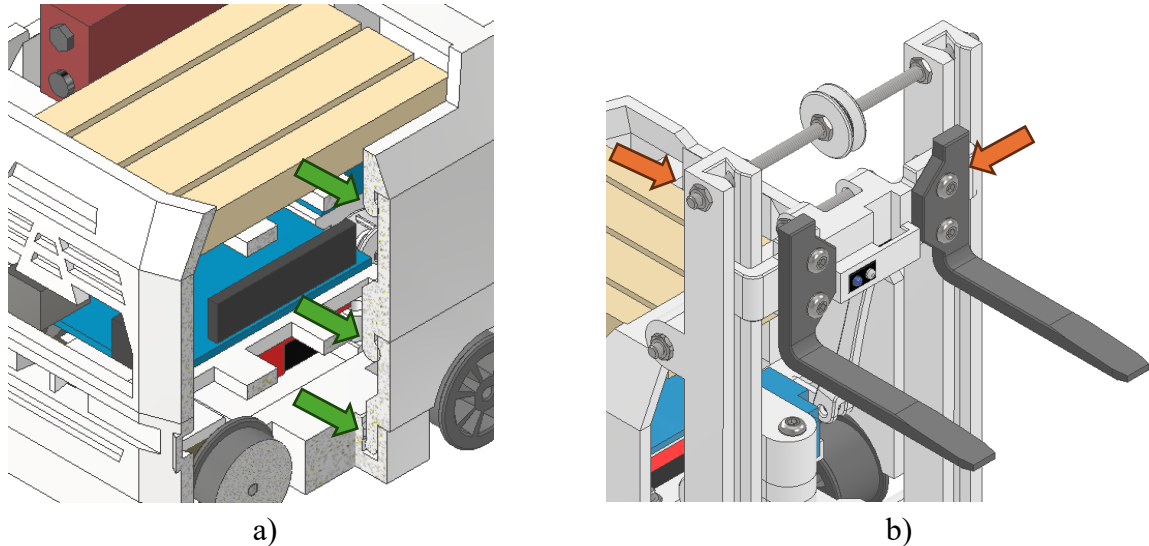





Fig. 6. a) Elements assembled through clamping, b) screw-nut assemblies.











6. Identification of the necessary electrical elements

In the lower frame, are identified the 4 electric motors necessary for self-propulsion, together with their control component, L298N. In the next frame will be the central component and the Arduino board to which the rest of the circuit elements are connected, directly or indirectly. In the upper frame will be located the power battery and a breadboard on which will be made the connections of the components for transmission of visual/auditory signals, of the bluetooth module and of the button.

The electronic elements of the lifting system, the electric motor and the servomotor will also be located on the chassis.

Table 3. The electrical elements of the experimental model

No. crt.	Name	Figure [7]	Unit	Function
1	Arduino UNO board		1	Process and transmit the programmed instructions towards the executing elements.
2	L298N H-Bridge		1	Control of the 4 motors required for self-propulsion of the model.
3	Electric motor with a 200 RPM gear		4	Ensure the rotational motion of the wheels (self-propulsion).

<i>No. crt.</i>	<i>Name</i>	<i>Figure [7]</i>	<i>Unit</i>	<i>Function</i>
4	Electric motor with a 50 RPM gear		1	Ensure the rotational movement of the main wheel of the lifting system.
5	Servomotor		1	Ensure the angular motion of the lifting system.
6	Breadboard		1	Provide support and connection for other electrical elements.
7	LED		1	Transmit the visual information about the state of the model.
8	Piezo buzzer		1	Transmit the auditory information about the state of the model.
9	Button		1	Ensure on-off control.
10	HC06 bluetooth module		1	Ensure the connection and the transmission of commands from the user interface.
11	Fire Dupont		~	Ensure the electrical connection between the elements.
12	220Ω, 10KΩ Resistor		~	Ensure the good operation of the electrical elements.
13	9V Battery		1	Power supply

7. Programming the instructions

Broadly, the written code consists of:

1. Defining the memories of the component elements and of the libraries necessary for code operation;
2. Pre-setting the initial states of the component elements and setting the data transmission/reception speed;
3. Main loop work function;
4. Secondary execution functions called by the main function.

To serve as an example, the setup code sequence is presented. Initially, this code sequence establishes the connection between the Arduino board and the involved circuit elements, then each pin is designated as INPUT/OUTPUT. At the end of the function, it calls the secondary execution functions to pre-set the initial positions/states of the robot's elements.

```
void setup() {
  Serial.begin(9600);
  pinMode(2, OUTPUT); //setting the first pin of the 50rpm motor as output
  pinMode(3, INPUT); //setting the button pin as input
  pinMode(4, OUTPUT); //setting the second pin of the 50rpm motor as output
  pinMode(5, OUTPUT); //setting the buzzer pin as output
  pinMode(6, OUTPUT); //setting the led pin as output
```

```

pinMode(7, OUTPUT); //setting the first left motors controlling pin as output
pinMode(8, OUTPUT); //setting the second left motors controlling pin as output
brat.attach(9); //setting the servomotor pin as (9)
pinMode(10, OUTPUT); //setting the first right motors controlling pin as output
pinMode(11, OUTPUT); //setting the second right motors controlling pin as output
digitalWrite(led,0); // LED pre-setting (off)
stop(); // calling the engine stop function
angle(u); // calling the function of setting the angular position of the servomotor
forks(0); // calling the function of lifting system control (inactive engine)
}

```

Once the Bluetooth module becomes a data receiver, the main loop function reads the received command and calls the secondary functions involved in performing the functionality intended by the operator. Each distinct operation of the model is characterized by lighting of the led with a certain intensity and a specific sound. In this way, the visual/audio management functionalities are also provided.

8. Performance analysis

As a result of making the robot and testing it in pallet transport and handling operations, it was found that it fulfils acceptably all the functionalities established at the beginning of the design. It can move through translational and rotational motion. The lifting system can perform both the vertical translational motion and the angular motion in relation with the ground plane of the fork carrier.

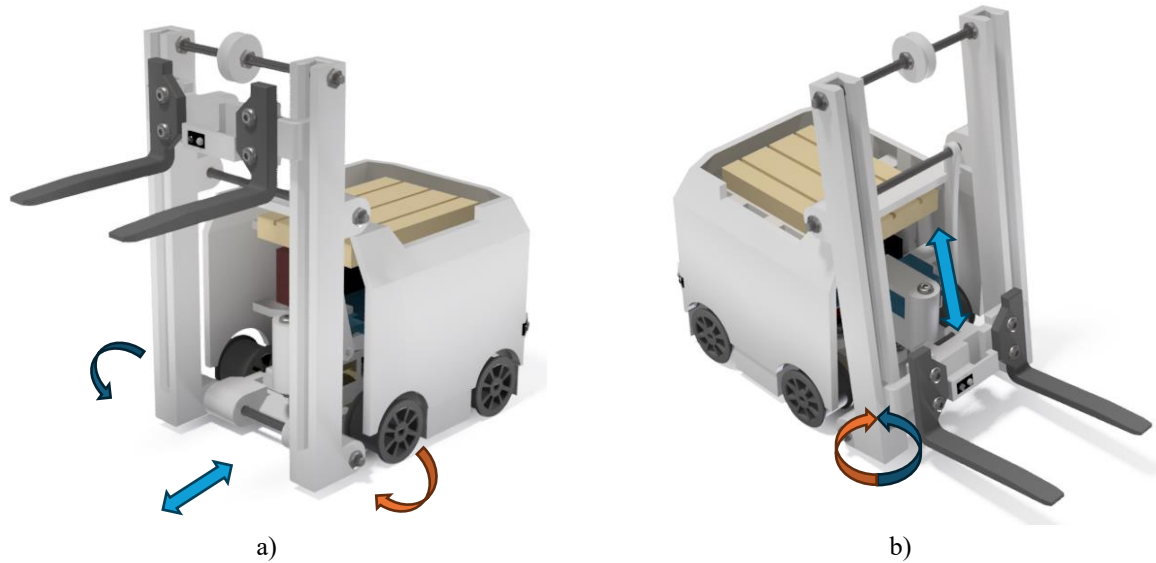
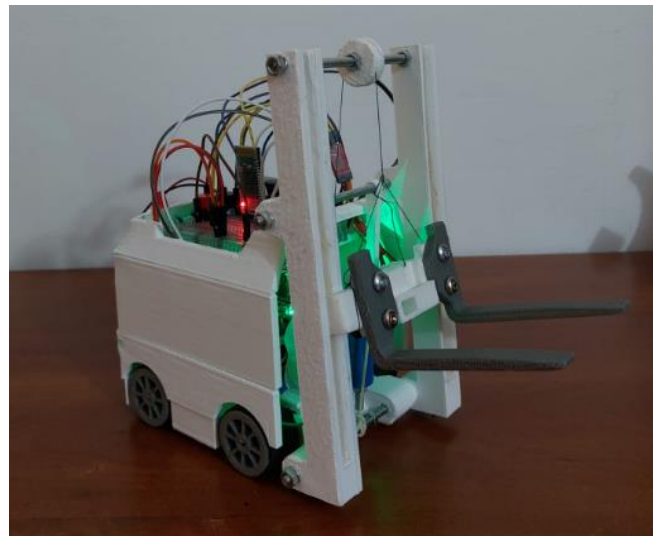


Fig. 7. a) Axis movements of the robot, b) movements of the lifting system.

As for the construction of the robot, the designed and manufactured parts form an ergonomic assembly.



a)



b)

Fig. 8a, b. The experimental model of pallet handling and transport robot, a) back and b) front views.

8. Conclusions

The designed experimental model is functional and ergonomic. The robot can perform pallet handling through the designed lifting system. Pallet transport is performed through self-propulsion of the chassis. At the same time, the robot provides the operator/observer with visual and auditory information about the current state of the robot, which increases its degree of ergonomics.

Bibliography

- [1] Martinez S. L., Stager G. S. Invent To Learn: Making, Tinkering, and Engineering in the Class. ISBN 10: 0-9891-5110-7, ISBN 13: 978-0-9891-5110-8.
- [2] Anghel, T. (2020). Programarea plăcii Arduino. Editura Paralela 45. ISBN: 978-973-47-3204-3.
- [3] <https://www.conger.com/forklift-history/>
- [4] <https://www.vecnarobotics.com/resources/what-are-automated-forklifts/>
- [5] <https://www.autodesk.com/products/inventor/overview?term=1-YEAR&tab=subscription>
- [6] <https://zortrax.com/3d-printers/m300-plus/>
- [7] <https://www.optimusdigital.ro/ro/>

DEVELOPMENT OF AN EXPERIMENTAL MODEL TO SIMULATE FINGER MOVEMENT

**Iustin IVAN¹, Ciprian-Robert CLIPICIOIU¹, Alexandra-Elena CARDAȘ¹,
Roxana-Gabriela GANEA¹, Tudor IGNAT¹, Ileana DUGĂEȘESCU², Alexandru
NICOLESCU²**

¹Faculty of Industrial Engineering and Robotics, Major: Industrial Informatics, Year of study: 2,

¹e-mail: iustinivan2002@gmail.com

²Faculty of Industrial Engineering and Robotics, Manufacturing Engineering Department

ABSTRACT: The proposed experimental device is an innovative tool designed to simulate finger movements of a hand. It supports reading the positions of all five fingers and setting individual limitations for each. By connecting to PCs via Bluetooth or cable, it provides real-time response and simulation of finger mobility limitations, allowing users to easily implement this experimental model in various other projects.

KEYWORDS: finger tracking, wireless communication;

1. Introduction

As digital technologies advance, there is a growing concern regarding the human ability to interact efficiently with these innovations. This project focuses on developing a simple and economically accessible system to enable people to control digital technologies through human interfaces. The proposed device represents a "do-it-yourself" (DIY) approach, integrating easily accessible components into 3D structures, thus facilitating its adoption in academic environments. The integration of electrical components in this tool optimizes user comfort and system efficiency. Through the open-source philosophy, the project encourages collaborative contributions, with the potential to enhance scientific research and accelerate innovations.

2. Current stage

In 2016, HTC released a virtual tracking system consisting of a VR headset, a pair of joysticks, and 2 satellites placed in separate corners of a room. This setup allowed for tracking both the user's head and hands in 3D space. Over time, companies shifted their focus to haptic or presence sensors, and then later began using a combination of these and images from cameras placed on VR glasses, thus projecting the position of hands and fingers more clearly into the virtual environment [3].

However, it can be observed in the market that gloves simulating the virtual environment in real life, limiting finger movement based on virtual factors, have had a slow increase in popularity due to their high price and limited availability.

3. Project description

The first stage of the project involved creating a prototype of the hardware system. Currently, there are several hardware integrations to ensure the proper functionality of the device. The hardware component is a critical aspect of the project, mediating the exchange of information between humans and machines. Potentiometers were attached to each finger joint to accurately capture finger movements. These potentiometers convert the mechanical motion into varying electrical signals, which are then processed by the ESP32 board. The board serves as the controller for the system, interpreting these signals and converting them into readable data.

Given the complexity of this interaction, ensuring robust hardware integration was essential. Each potentiometer had to be calibrated to provide precise input, and the Arduino code had to be optimized to

handle multiple inputs simultaneously without delay. This stage involved extensive testing and debugging to address any issues that arose, as any inaccuracies could make the system difficult to understand or use.

In the initial phase, the team focused on the finger position measurement mechanism, considering two options: using a potentiometer to control the rotational movement with the distance difference from the tip of an extended finger to the distance to the same fingertip when clenched into a fist.

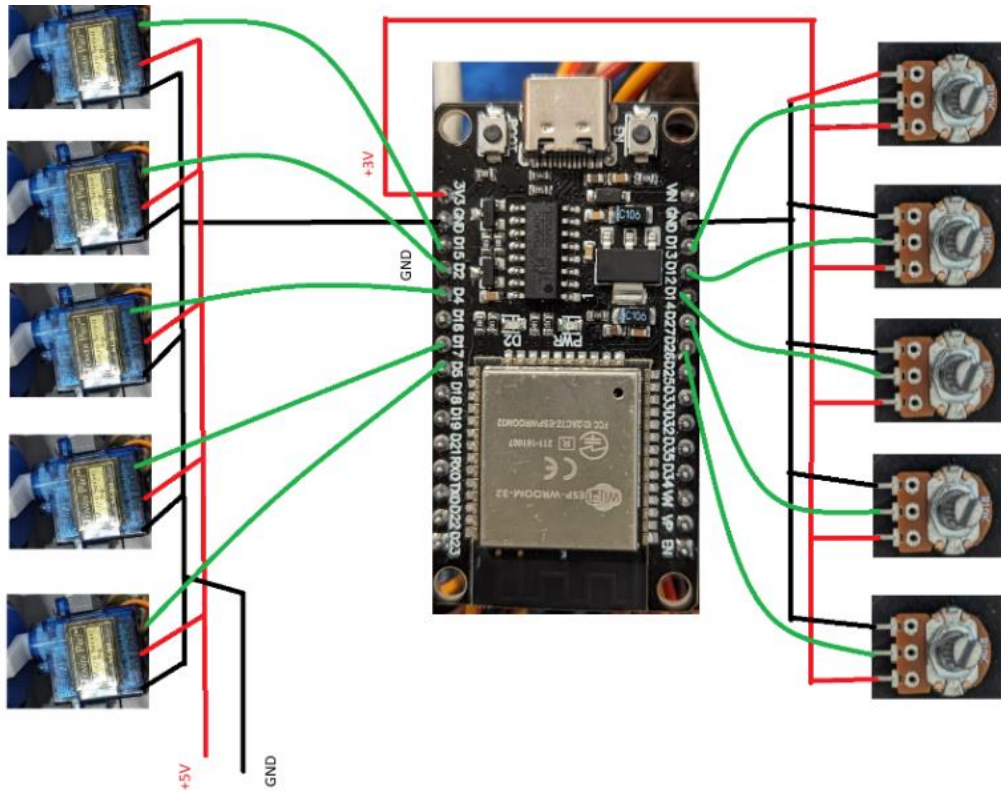


Fig. 1. Simplified model of the circuit

In the next stage, the design of a casing containing the components presented in Figure 1. The latter limits the rotation of the potentiometer, thus restricting the ability to move the finger and forming a fist. This simplified approach allows for the development of an accessible and functional device without unnecessarily complicating it with a more complex finger limitation mechanism.

To create the 3D printed case, specific design software was used. After completing the 3D model, specialized software was used to generate the necessary code for 3D printing the components. The material used for printing is PCTG (Polyethylene Terephthalate Glycol). The use of high-performance materials such as PCTG ensures resistance to constant demands, regardless of the heat generated by the electronic components. As for the printing parameters: Nozzle Diameter: 0.4 mm; Layer Height: 0.2 mm; Print Speed: 60 mm/s; Infill Density: 20% which provides sufficient strength for most prototypes and general-use items while minimizing material use and print time; Print Temperature: 210°C; Bed Temperature: 60°C this will reduce warping and ensures the print stays securely in place; Retraction Distance: 0.8 mm, leading to cleaner prints; Supports: Enabled, with a density of 15% and an overhang angle threshold of 60°.

In Figure 2 is presented the case which will be 3D printed and will contain all the individual components for each finger.

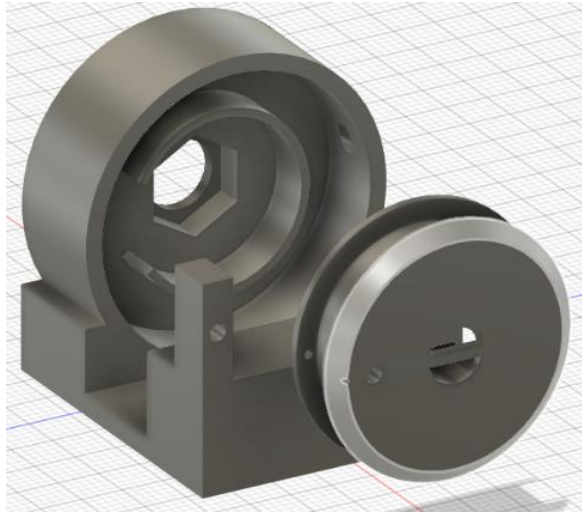


Fig. 2. 3D model of the case

In the Figure 3 is displayed a better view on how the potentiometers are mounted.

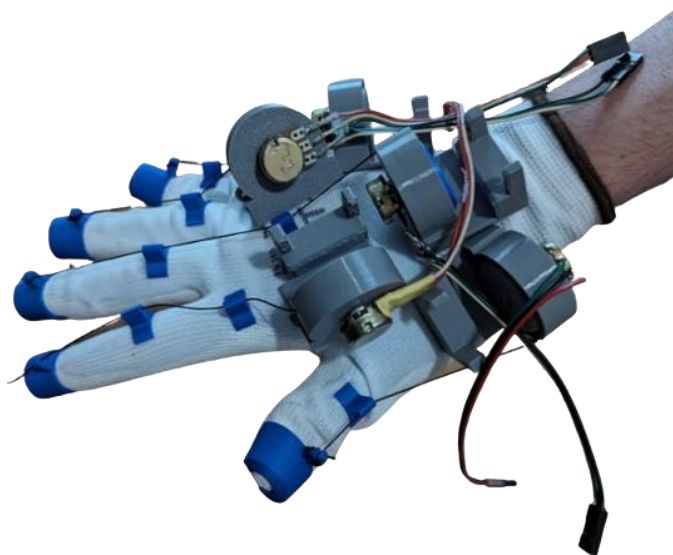


Fig. 3. The assembly of the components

After completing the prototype and assembling the electronic components, attention was given to software integration to utilize the data obtained from the potentiometers and control the servo motors. For this purpose, code was developed to read the analog values from the potentiometers and actuate the servo motors. Bluetooth technology was used for communication between the computer and the microcontroller, and the data was transmitted and received through serial communication.

Thus, the finger positions transmitted by the ESP32 (the microcontroller used) are in the format:

"XX-XX-XX-XX-XX"

where XX can vary from 0 to 100; a value of 100 indicates that the finger is fully extended, while a value of 0 indicates that the finger is clenched into a fist shape. The same format was used for transmitting the limitations on the position of the servo motor; a value of 0 representing the 0-degree position of the servo motor, and 100 indicating the 120-degree position.

The microcontroller program was written in a modular manner, thus creating a "FingerControl" class, in which the functions for controlling the servo motor (moveServo) and the potentiometer (fingerPos) were defined below.

Therefore, each finger of the glove has an object of type "FingerControl". To create this type of object, the constructor with the same name and parameters will be used: the servo motor pin on the microcontroller specific to the right finger and the pin of the potentiometer.

The potentiometer provides analog values read by the microcontroller with a resolution of 12 bits, so read values from 0 to 4095. For simplification, the map function was used to transform the values from 0 to 4095 into values from 0 to 100. The same principle was used for transmitting the position of the servo motor.

The primary code is the class object "FingerControl" that is explained in steps below:

1. Including the Header and Initializing the Servo:

```
...  
#include "FingerControl.h"  
Servo servo = Servo();  
...
```

The code begins by including the "FingerControl.h" header file, which contains the necessary definitions and declarations for the `FingerControl` class. A global `Servo` object is then initialized. This object will be used to control the servo motor that simulates finger movements.

2. Defining the `FingerControl` Constructor:

```
...  
FingerControl::FingerControl(int Servo_pin, int Pot_pin) : Servo_pin(Servo_pin),  
Pot_pin(Pot_pin) {  
    servo.attach(Servo_pin);  
}  
...
```

The `FingerControl` class is designed to manage the servo motor and potentiometer. The constructor takes two parameters: `Servo_pin` and `Pot_pin`, which represent the pins to which the servo motor and potentiometer are connected, respectively. Inside the constructor, the servo is attached to the specified pin, allowing the program to control it.

3. Reading Finger Position:

```
...  
int FingerControl::fingerPos() {  
    int pozitie = map(analogRead(Pot_pin), 0, 4095, 0, 100);  
    return pozitie; // Return the mapped position  
}  
...
```

The `fingerPos` function reads the current position of the potentiometer. It uses the `analogRead` function to get a value between 0 and 4095, which corresponds to the position of the potentiometer's knob. This value is then mapped to a percentage scale from 0 to 100, making it easier to interpret and use in further calculations. The function returns this mapped position as an integer.

4. Moving the Servo:

```
...
```

```

void FingerControl::moveServo(int percentage) {
    if (percentage < 0) {
        percentage = 0;
    } else if (percentage > 100) {
        percentage = 100;
    }
    int angle = map(percentage, 0, 100, 0, 180);
    servo.write(Servo_pin, angle);
}
...

```

The `moveServo` function is responsible for moving the servo motor to a specified position. It takes a percentage value as input, which represents the desired position of the finger. The function ensures that this value is within the valid range (0 to 100). It then maps the percentage to an angle between 0 and 180 degrees, which corresponds to the range of motion of the servo motor. Finally, the servo is instructed to move to the calculated angle.

The communication between the experimental device and a computer can be easily implemented in virtual reality programs, games, and other virtual environments through either a data cable (USB) or Bluetooth.

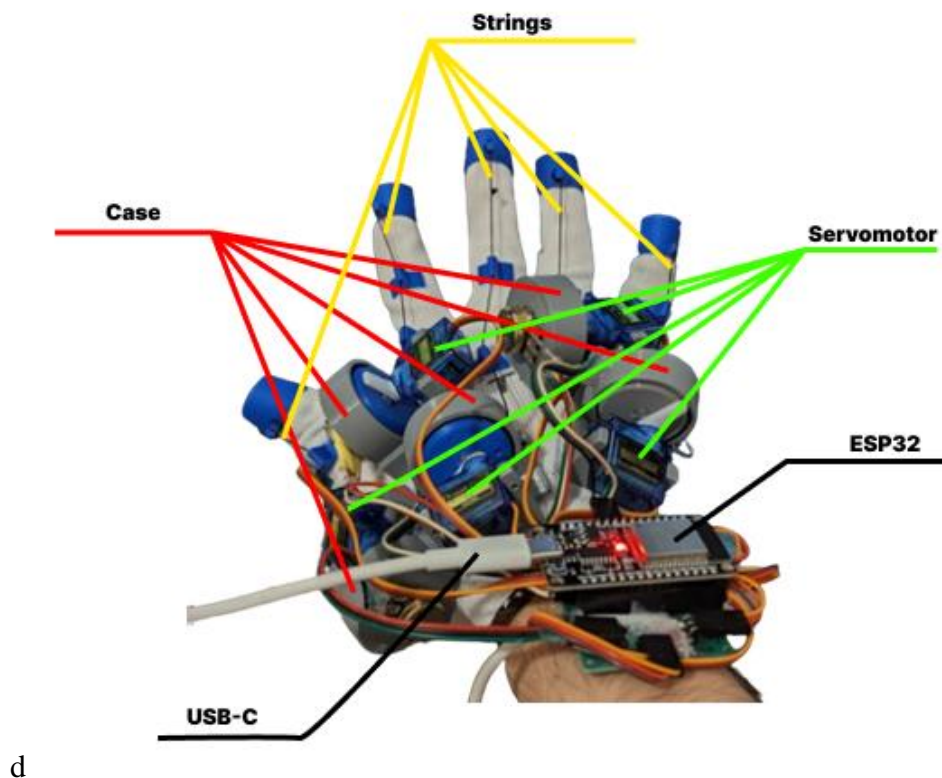


Fig. 4. The final stage of the experimental glove.

In the above image is presented the finished model with all the components installed and explained below:

Strings - Cables that run through the hand and connect to the servomotors. When the servomotors rotate, they pull on the strings which in turn move the fingers of the robotic hand.

Servomotors - Motors are designed to rotate a specific angle. In this case, they are used to move the fingers.

ESP32 - Microcontroller used to control the servomotors. It receives signals from a computer program and then sends instructions to the servomotors on how to move.

USB-C** - Connector that is used to power the robotic hand and to connect it to a computer.

4. Conclusions

The paper outlines the stages of developing an experimental model used for finger movement simulation. It focuses on integrating hardware and software to ensure the proper functionality of the device. Modularity and scalability were prioritized to allow adaptability to various usage scenarios.

To further develop this prototype, various sensors can be studied to improve precision and responsiveness to finger movements, along with integrating haptic feedback for a more immersive experience. Objectives include simplifying and reducing the size of the device, alongside continuous innovation to meet user needs and improve interaction in the virtual environment.

5. Bibliography

- [1]. Randy H. Shih (2020), *Parametric Modeling with Autodesk Fusion 360*, Editura SDC Publications, ISSN 978-1630573720
- [2]. Massimo Banzi și Michael Shiloh (2022), *Getting Started With Arduino: The Open Source Electronics Prototyping Platform*, Editura Make Community, ISSN 978-1680456936
- [3]. *** History of VR – Timeline of Events and Tech Development - <https://virtualspeech.com/blog/history-of-vr> (Accessed at 07.05.2024)
- [4]. *** I built VR Haptic Gloves to Control Robots - <https://www.youtube.com/watch?v=iPtgvh6fNdQ> (Accessed at 07.05.2024)
- [5]. *** How to build cheap VR Haptic Gloves to FEEL VR - <https://www.youtube.com/watch?v=2yF-SJcg3zQ&t=902s&pp=ygUIbnIgZ2xvdmU%3D> (Accessed at 07.05.2024)
- [6]. DIY Glove Controller With E-Textile Sensors - <https://www.instructables.com/DIY-Glove-Controller-With-E-Textile-Sensors/>
- [7]. Etextile VR Gloves for Vive Tracker - <https://www.instructables.com/Etextile-VR-Gloves-for-Vive-Tracker/>
- [8]. AI - <https://www.britannica.com/technology/artificial-intelligence>

6. Notations

The following symbols are used in the paper:

DIY = “Do it yourself”

COM = “communication port”

VR = “virtual reality systems”

AI = “artificial intelligence”

PCTG = Polyethylene Terephthalate Glycol, which is a type of thermoplastic material.

VIRTUAL INSTRUMENT FOR SIMULATING THE HOHMANN TRAJECTORY OF A ROCKET TRAVELLING TO A NEIGHBOURING PLANET

IONESCU Paul-Iosif , Paulina SPANU

Facultatea: Facultatea de Inginerie Industrială și Robotică, Specialization: Industrial Engineering,
Student Year: 1st, e-mail: paul_iosif.ionescu@stud.fiir.upb.ro

ABSTRACT: This paper describes the results obtained through designing and developing a virtual instrument using the LabVIEW program. The virtual instrument calculates the distance travelled by a spacecraft to a specific celestial body taking into account the trajectory of the original as well as the second planet, to create the optimum path, at maximum fuel efficiency. The virtual instrument allows the calculation of the distance from a point of origin to another celestial body, located in a revolutionary axis around a central star, accounting for its influence.

KEYWORDS: LabVIEW, calculator, trajectory, Hohmann transfer.

1. Introduction:

The very costly, and not-so-long-ago, novel prospect of aeronautical space travel is a topic almost synonymous with complex and painstakingly accurate calculations, which whilst taking a considerable amount of time, require a very slim margin of error. One that can simply not be left at the mercy of human error.

Calculations concerning the spacecraft trajectory especially, are hard to interpret, as those presuppose accounting for the movement of celestial bodies. In such cases, as calculations become more complex and elements more numerous, a visual-to-automatic calculator can reduce the number of erroneous results as well as lead to a clearer vision of the entire process.

The virtual simulation allows for quick and exact calculations as well as accounting for the constant shift in position of the two chosen planets, those being, the start and end points of the presentation, and the theoretical time a journey would take in a spacecraft.

As specified earlier, the model can account for all coordinates given for any of the two points of interest, including accounting for their adjustment in real-time.

2. Problem breakdown:

The model is composed of multiple parts, the starting position of our original planet, in this case, Earth, with an initial and a final position respectively, and an end-point planet, in this case, Mars, with its initial and final position (see Fig. 1):

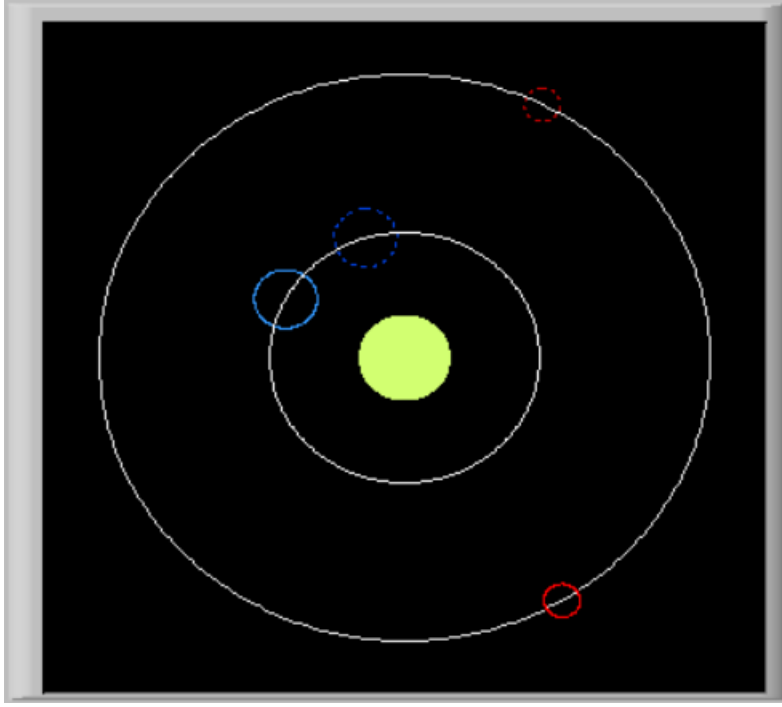


Fig. 1. Simplified Solar System

The revolution period of Earth is 365.25 days, and its location is mentioned in the tool-provided table section, the location of Mars, our endpoint, is yet unknown, with a revolution period of 686.96 days, but we must remember that this system is in constant motion; as such we need to find, how fast the bodies travel on their trajectory, the time a journey might take, and the projected distance our end-point will be when the spacecraft makes contact. To find their radius of trajectory for our end-point planet, we can use Kepler's Third Law^[1] (see Eq. 1).

$$\left(\frac{r_M}{r_E}\right)^3 = \left(\frac{T_M}{T_E}\right)^2 \quad (1)$$

After finding the radius, we ought to find the distance travelled by Mars and its radius speed using the equations for our axis of travel (see Eq. 2) and our orbital speed around the Sun (see Eq. 3):

$$s = 2\pi r_M \quad (2)$$

$$v_M = \frac{s}{T_M} \quad (3)$$

And finally, the length of the semi-major axis of the Hohmann transfer orbit ^[2] (see Eq. 4)

$$a = \frac{r_E + r_M}{2} \quad (4)$$

Where:

r_E – the radius of the trajectory of Earth

r_m – the radius of the trajectory of Mars

T_E – orbital period of Earth around the Sun

T_M – orbital period of Mars around the Sun

s – distance travelled by Mars

v_M – the speed of Mars

a – the length of the semi-major axis of the Hohmann transfer orbit

3. Description of the interactive interface:

The following segment will focus on the Input data required for the initialization and calculus of the spacecraft trajectory, as well as the Output data with tailored units for ease of understanding:

For our input data, we have the following controls adjustable from the front panel, type number: E1, M1, corresponding with the two bodies; and string type: Units, corresponding with the preferred output unit of measurements (see Fig. 2).

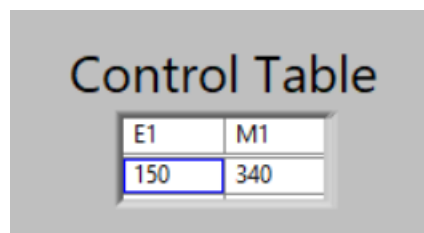


Fig. 2. The LabVIEW Control Table

When running continuously the virtual tool will display the numerical results on the front panel indicator for the following measurements: r_M , v_M , a , t , E_2 , M_2 , α_M , α_E (see Fig. 3).

The image shows a LabVIEW output table titled "Output Table". It has three columns: Result, Num Value, and Unit. The table contains eight rows of data.

Result	Num Value	Unit
r_M	227942729	m
a	188771365	m
v_M	24	km/s
t	6213	h
E_2	405	°
M_2	476	°
α_M	136	°
α_E	255	°

Fig. 3. The LabVIEW Output Table

Along with the visual simulation of a simplified solar system, presenting the aforementioned position of Earth, both initial and final, and Mars, likewise initial and final, along with a representation of a Hohmann trajectory, in the form of a half-ellipse (see Fig. 4).

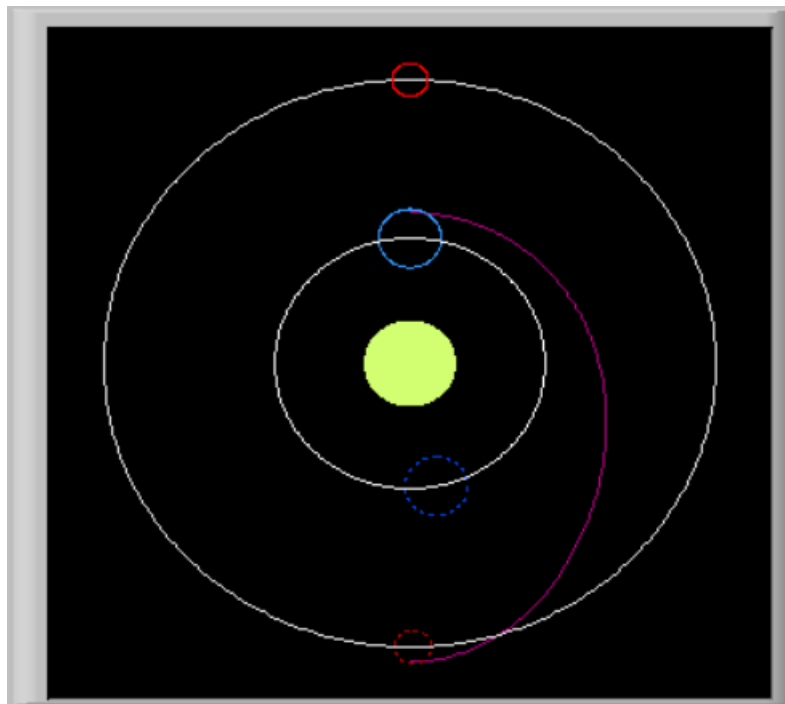


Fig. 4. Hohmann Trajectory

4. Description of the virtual calculator algorithm:

The virtual simulation allows for a variety of units of measurement which the user can modify in real time to guarantee a clear understanding of the mass of any measurements in an intuitive and relevant way for any of their purposes.

These units include angular degrees, minutes, and seconds, metric units from meters to kilometres, megametres, and gigametres, and units of time, such as hours, days, weeks and months (see Fig. 5).

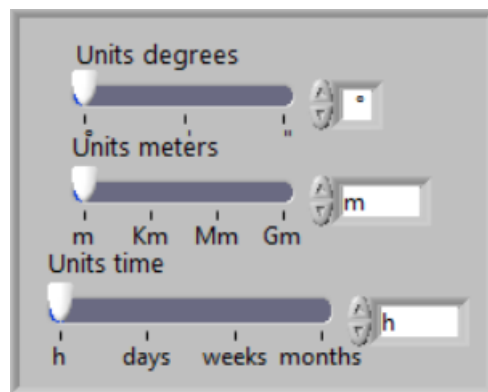


Fig. 5. Adjustable Units Parameters

The algorithm behind these (see Fig. 6) is a combination of “Case Structures”, indicators, arrays and “Build Array” structures that ensure all units are correctly displayed next to their relevant number counterparts (see Fig. 3)

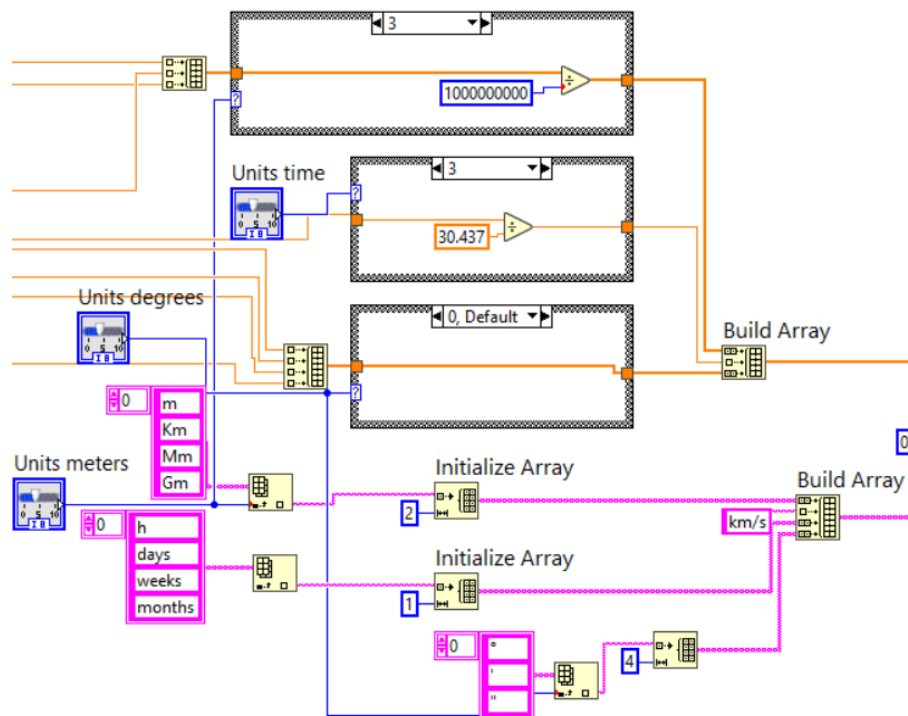


Fig. 6 The Units to Case Structure to Arrays to Display

In the virtual calculator diagram, the Formula Node function was used to compute the calculations by utilizing Equations 1 – 4, as they were introduced, the order of arithmetic operations was respected (see Fig. 7).

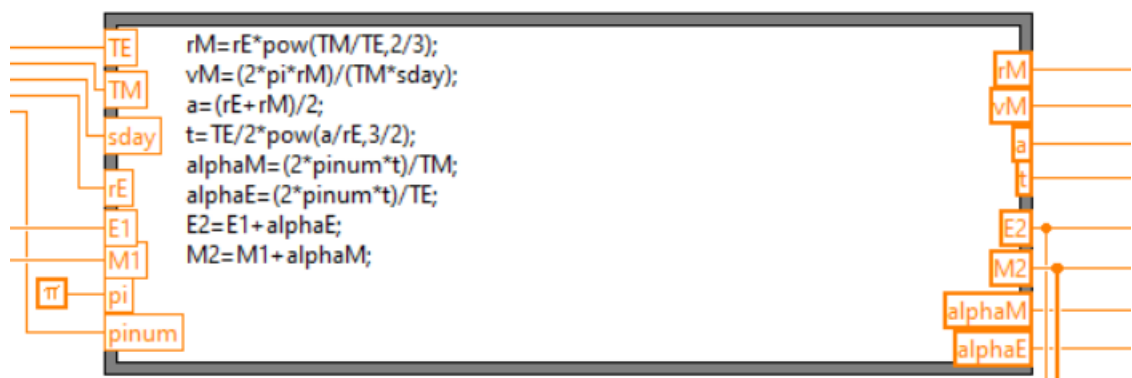


Fig. 7. Main Formula Node

The velocity and distance travelled by the end-point planet are calculated, as well as the semi-major axis, which gives us the distance a spacecraft is required to travel to contact the endpoint. The time is then computed, to correctly assess the end position of the first and second planet, and the distance travelled by both planets is expressed in radii, accounting for the expected distance travelled in the previously calculated time so that a final position for both plates can be displayed (see Fig. 1).

5. Conclusion:

With all this being said, the visual tool achieves its purpose through the use of the Laboratory Virtual Instrument Engineering Workbench or LabVIEW system with its many functions and extensive documentation, in simulating a complex operation known as Hohmann's Trajectory.

6. Biography:

- [1] – [Orbits and Kepler's Laws](#) *NASA Solar System Exploration*. Retrieved: 17/03/2024
- [2] – [NASA Technical Translation F-44, 1960; The Attainability of Heavenly Bodies](#) by *Walter Hohmann*; Pg. 78. Retrieved: 17/03/2024

DESIGN AND IMPLEMENTATION OF AN EXPERIMENTAL CONVEYOR MODEL FOR PRODUCT SORTING AND A PROCESS MONITORING APPLICATION

Stanciu Alexandru-Fabian, Maria Magdalena ROȘU

Faculty IIR, Field of Study:IAII, The Year of Study:IV, e-mail: scont34@yahoo.com

ABSTRACT: *The project focuses on the development of an automatic sorting system for products on a conveyor belt. The products, which have barcodes inscribed on them, are sorted into two different boxes with the help of sorting arms. These arms are powered by two NEMA17 motors. If a product is not in the database, it is left to fall freely at the end of the conveyor belt. The conveyor belt is powered by a NEMA23 motor and belt transmission. This automatic sorting system can have applications in improving efficiency and productivity in various industrial sectors.*

KEYWORDS: *CONVEYOR, SORTING, AUTOMATION, IMAGE PROCESSING, MONITORING.*

1. Introduction

In academic research, the paper titled "Design and implementation of an experimental conveyor model for product sorting and a process monitoring application" addresses a central issue in the field of industrial automation: the efficient sorting of products.

The paper proposes an automated sorting system that utilizes barcode technology to classify products on a conveyor belt. The system is composed of two main components: the hardware, which includes the conveyor belt, motors, and webcam, and the software, which includes the database and sorting algorithm.

Products are sorted into two different boxes using sorting arms driven by NEMA17 motors. If a product is not recognized by the system, it is allowed to fall freely at the end of the conveyor belt.

By implementing this system, the paper aims to demonstrate the potential of modern technology in improving efficiency and productivity in the industry. The results of this work can serve as a basis for the further development of automated sorting systems.

2. Current state

The innovation of this project was inspired by the needs of a parts manufacturing company, where operators had to manually sort each part based on a numerical code, as shown in Figure 2.1. This manual process was not only time-consuming but also prone to human errors. In this context, the project aims to automate this sorting process, also changing the labeling of the experimental parts, as illustrated in Figure 2.2.

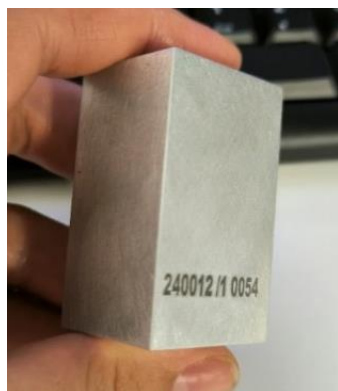


Figure 2.1 Example part from the company

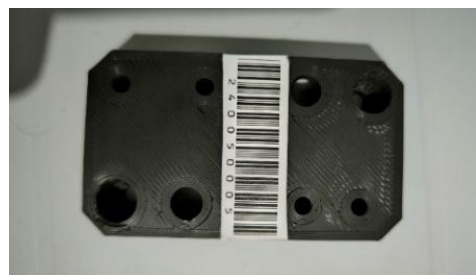


Figure 2.2 Example part

In the process of constructing the transport system, an aluminum bracket was used to secure the motor that drives the belt. This bracket was equipped with a vertical adjustment mechanism on screws, allowing for precise positioning of the motor. The toothed wheel was attached to the motor shaft with a screw, due to the cylindrical shape of the shaft, as shown in Figure 2.3.

Additional components, such as the rollers used for rotating the belt, the covers, and the toothed wheel located at the end of the main roller (as seen in Figure 2.4), as well as the manual focus system for the webcam, were manufactured using a Ultimaker Cura 3D printer. The material selected for these components was polylactic acid (PLA).

The choice of PLA as the printing material was determined by several factors, which will be discussed further:

- **Strength:** PLA is a sturdy material, making it ideal for printing parts such as gears, conveyor belt rollers, or roller covers.
- **Ease of Printing:** PLA is easy to print and requires a relatively low temperature, making it popular among 3D printer users.
- **Recyclability:** PLA is considered a more sustainable material because it does not come from finite resources such as petroleum but is derived from natural and renewable resources: corn starch, tapioca roots, or sugar cane.



Figure 2.3 Attaching the toothed wheel



Figure 2.4 3D printed parts

Within the construction process, the frames for securing the rollers were made from angle irons, as shown in Figure 2.5. Additionally, the support structure for the frame was constructed from aluminum profiles.

The belt tensioning mechanism was designed based on a model presented in a YouTube video. It was adapted, as shown in Figure 2.6, to fit the materials used up to that point.

It is important to mention that all hardware components, i.e., the mechanical ones, were created both physically and virtually. This underscores the fact that the project involved not only design but also practical implementation.

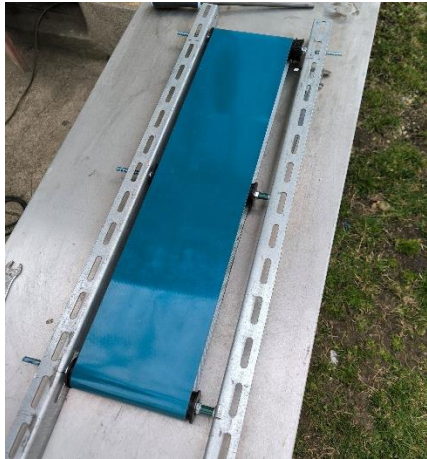


Figure 2.5: Frame for securing rollers

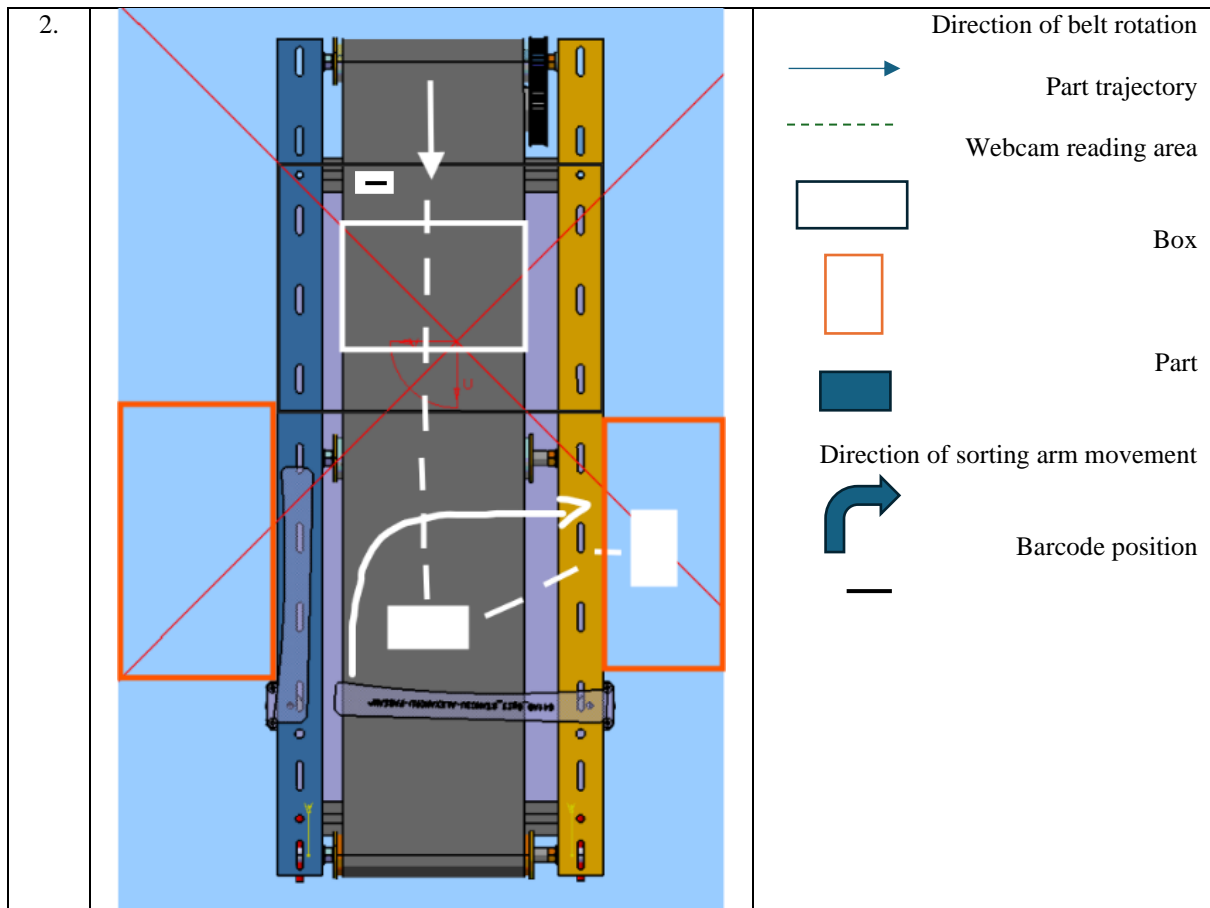


Figure 2.6: Belt tensioning mechanism

3. Sorting Algorithm

Table 1.Sorting Algorithm

Nr.	Sorting System Schematics	Legend
1.		<p> Direction of belt rotation </p> <p> Box illumination system </p> <p> The reading area of the webcam </p> <p> Part </p>



Sorting system operation mode

In the initial sorting system schematic, various essential features can be identified. Firstly, the motor mounting section stands out, featuring integrated channels in the support for adjustment. Additionally, the hubs are secured on a threaded rod, which is held between two bearings placed inside the hub covers. Furthermore, the overall system structure is depicted. The lighting system is mounted in a specific manner, and the reading area of the camera is clearly defined. The initial position of the sorting arms and the direction of the part's movement on the belt are also highlighted.

In the secondary system schematic, the operation mode of the software component can be distinguished, as well as a simulation of the path followed by the identified part. The belt will operate at a constant speed, and the camera will detect the barcode in real-time. This will be compared with the information from the initially configured database. Due to the defined area of the webcam, the barcode will need to be positioned perpendicular to the belt's direction of rotation to detect the code in time and actuate the sorting arm. After a predefined time interval, the arm will return to its initial position, and the part will be directed to the designated box.

4. Execution drawings

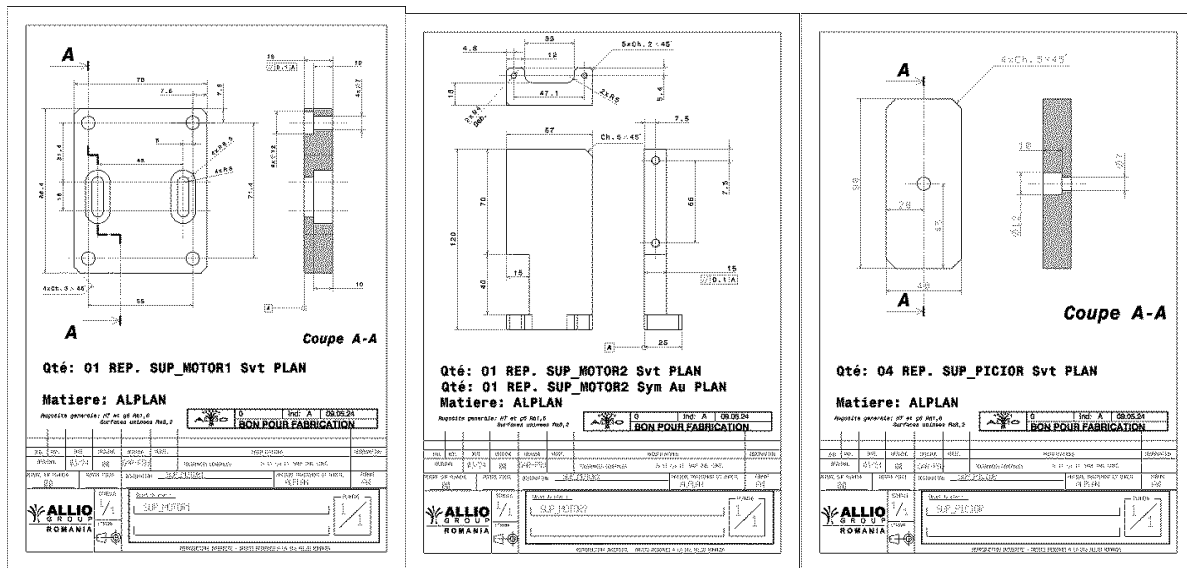


Figure 4.1 Motor mount execution drawing Figure 4.2 Main motor mount execution drawing Figure 4.3 Foot execution drawing

Analyzing figures 4.1, 4.2, and 4.3, it can be observed that positional tolerances were not used for the through-holes and threaded holes. The reason is that they do not require such tolerances. Instead, flatness tolerances were applied between surfaces to ensure proper alignment of the motor and to prevent tilting between the motor seating surface and the machined part. These parts were manufactured within the company from which the project concept was taken. In the following figures 4.4 and 4.5, dimensions for manufacturing the parts on the 3D printer can be observed. They were created to provide information regarding the dimensions of these parts because on a 3D printer, there is no need for an execution drawing; the program automatically knows how to produce the part. All parts and execution drawings were created using CATIA software.

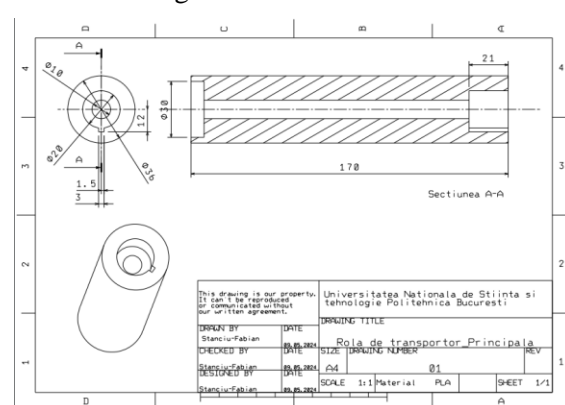
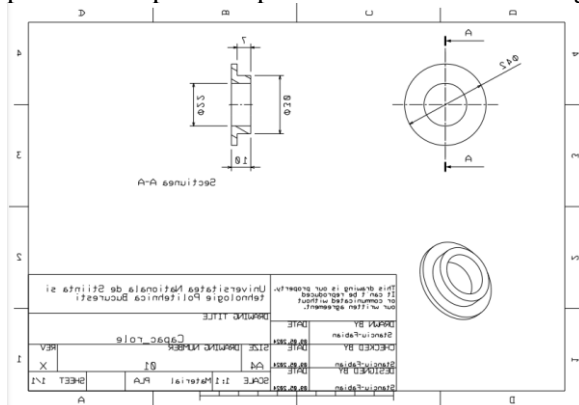


Figure 4.4: Roller cover execution drawings

Figure 4.5: Roller execution drawings

CATIA (Computer Aided Three Dimensional Interactive Application) is a multi-platform software suite for Computer-Aided Design (CAD), Computer-Aided Manufacturing (CAM), Computer-Aided Engineering (CAE), 3D modeling, and Product Lifecycle Management (PLM). It was developed by the French company Dassault Systèmes and is globally marketed by IBM.

5. Conclusions

In conclusion, the project "Design and Implementation of an Experimental Conveyor Model for Product Sorting and a Process Monitoring Application" represents a significant contribution to the field of industrial automation. It demonstrates how modern technology, such as image processing and monitoring, can be utilized to improve efficiency and productivity in various industrial sectors.

The automated sorting system developed in this project not only optimizes the sorting process but also provides a solution for managing products that are not registered in the database. By allowing them to freely fall at the end of the conveyor belt, the system enables better resource management and reduces the risk of errors. Additionally, the use of NEMA motors for driving the conveyor belt and sorting arms ensures reliable and efficient operation of the system.

This project serves as an excellent example of how innovation and technology can be used to address practical problems in the industry.

6. Bibliography

- [1]. Carola. V. (2023) „All you need to know about PLA for 3D printing”
<https://www.3dnatives.com/en/pla-3d-printing-guide-190820194/#!>
- [2]. Michael Dwamena (2021), “How to 3D Print PLA Filament Like a Pro – Ultimate Guide & FAQ”, <https://3dprinterly.com/filament-printing-guide/pla/>
- [3]. Mary Bellis (anul), “Coduri de bare”, <https://ro.eferrit.com/coduri-de-bare/>
- [4]. Mihai Balescu. (2019), “Istoria unei inventii care a revolutionat economia mondiala: codul de bare”, <https://www.manager.ro/articole/economie-139/istoria-unei-inventii-care-a-revolutionat-economia-mondiala-codul-de-bare-99495.html>
- [5]. Eastey (2022). „EC Series Conveyors - Belt Tension Adjustment”,
<https://www.youtube.com/watch?v=7LGnIZRyOV4&t=1s>
- [6]. <https://ro.wikipedia.org/wiki/CATIA>

EXPERIMENTAL MODEL OF AN AERODYNAMIC WING FOR ACTIVE VEHICLE STABILITY ASSISTANCE AND CONTROL

APOSTOL Mihai, ALUPEI COJOCARIU Ovidiu Dorin

Facultatea: Inginerie industrială și robotică, Specializarea: Informatică aplicată în inginerie industrială, Anul de studii: IV, e-mail: mihaiaapostol9@gmail.com

ABSTRACT: The aim of this project is to develop a real-time aerodynamics modification system for vehicles, where decisions are consistently and autonomously made, adapting to the road conditions that it encounters. This system operates intelligently, providing real-time assistance in braking, accelerating, and steering the vehicle by increasing the downforce generated by an active spoiler positioned at the rear of the car, mounted on its trunk. The dynamics of the active spoiler are governed by the tilting of a movable flap into three positions. It is actuated by two linear actuators that translate commands received from the Arduino UNO R3 into mechanical motion, while initiating the entire operation of the system. Decision-making is carried out by a program written in C++, which continuously runs on the Arduino, acquiring and processing data from the accelerometer sensor. Power for the entire system is drawn directly from the car's battery, utilizing multiple electronic components for voltage conversion.

KEYWORDS: spoiler, flap, dynamics, Arduino, actuator

1. Introduction

The project includes all the stages outlined in the guide for preparing the bachelor's thesis. The purpose of the system called Active Spoiler is to modify the car's aerodynamics in real-time according to the situation it is in, significantly improving its performance. These improvements include top acceleration speed, top speed during cornering, and reduced braking distance. This type of active spoiler is primarily intended for sports competition vehicles, as the forces generated by the system are substantial, occurring at higher speeds and during intense accelerations and braking. Of course, its efficiency is also high at lower speeds, but the main segment it targets is motorsport or street sports cars (production cars homologated with a sporty character).

The main objectives of the project are to create a spoiler capable of autonomously adjusting the position of its components in real-time, generating additional downforce at key moments on the vehicle to which it is mounted. The project aims to accomplish all these tasks independently by the spoiler, without any human intervention. The spoiler's decisions are based on input from the acceleration sensor, independently determining, depending on the situation, if and how much to change the flap's inclination. The active spoiler system has been programmed to recognize three road scenarios, critical for improving its performance.

These previously established objectives were initially achieved by using electric actuation systems, namely linear actuators, which are compatible with various electronic components that facilitate the integration of software applications. These applications are excellently suited for the "autonomous" and intelligent character of the active spoiler system.

2. Current stage

The study of aerodynamics on automobiles and the development of technologies to enhance their performance have been adopted from the aerospace industry. This was achieved by reversing the concept applied in aeronautics, namely the creation of lift. Reversing this concept resulted in the creation of additional downforce on the tested object.

Since then, multiple aerodynamic components and systems have been developed to increase downforce, but at a cost. Increasing downforce and thus grip through a spoiler comes with the disadvantage of creating drag, which slows down the vehicle.

The solution is complex: adopting a spoiler with real-time adjustable aerodynamics through the independent actuation of a part of the spoiler, called a flap. This need to increase grip at high speeds led to the invention of the system called DRS (Drag Reduction System), introduced in Formula 1 in 2011.



Fig. 1. DRS System Formula 1 [1]

The particularity of this existing system is that it is operated by the driver by pressing a button on the car's steering wheel, which activates the spoiler's hydraulic system, thereby raising or lowering the flap at the driver's command.

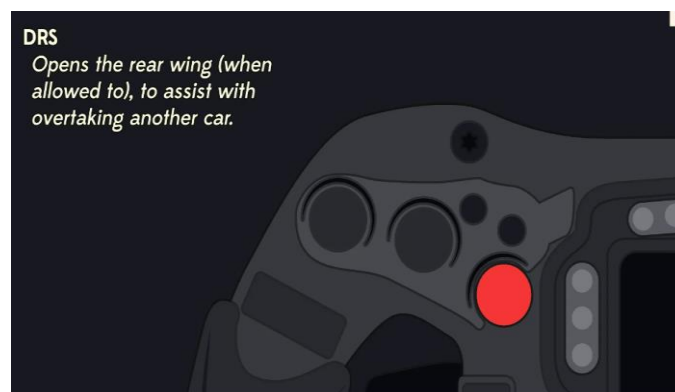


Fig. 2 Localization of the DRS button the steering wheel [2]

The contribution of this project to the development of this system consists of replacing the manual operation of the spoiler's movable components with an automatic one and substituting the hydraulic operation with an electric one using linear actuators. By introducing a fully electric and electronic active spoiler system, this concept advances to a stage where the actuation system becomes completely autonomous, constantly making and adapting decisions based on road conditions.

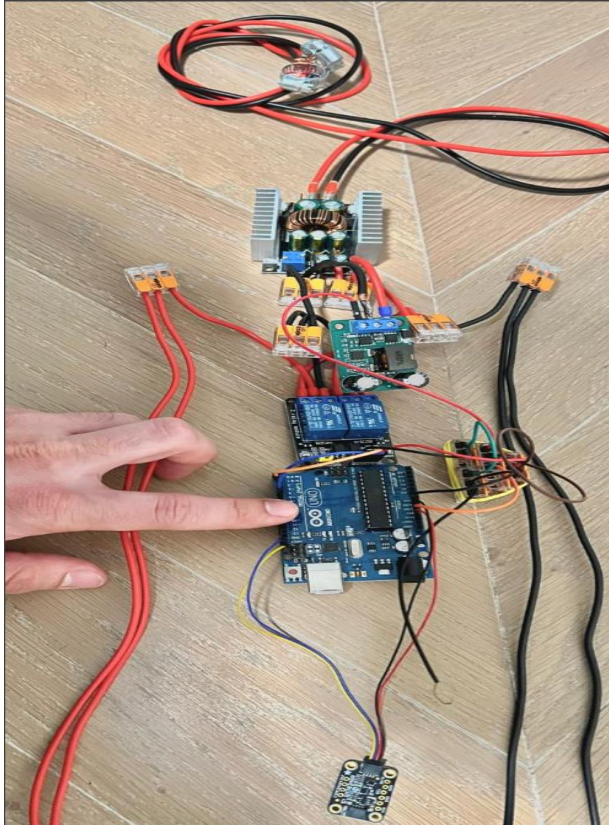


Fig. 3. Localization of the entire autonomous system



Fig. 4. Linear actuators Progressive Automations PA-14P

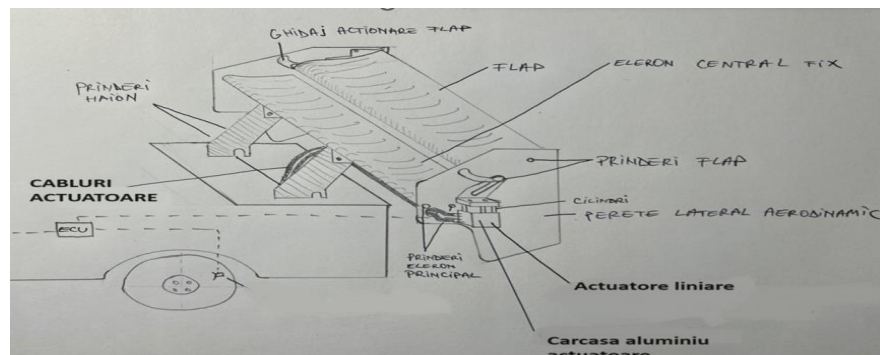


Fig. 5. General scheme of the Active aero wing

3. Stages of assembly and development of the electronic system

The entire system is powered by the car's battery, as it provides a sufficient energy source, constantly recharging from the car's alternator. One initial disadvantage is that the power source is not constant, with its voltage generally varying from 12V to 13.4V. For this reason, I had to use multiple fixed or adjustable voltage converters to stabilize the input voltage to 12V, then lower it to 5V and 3.3V for the accelerometer sensor.

Currents are distributed throughout the entire electronic system via buses. The components used are two linear actuators with integrated feedback, a dual relay module, an Arduino Uno R3 development board, a 9-axis Adafruit LSM303AGR accelerometer-magnetometer sensor, and two voltage converters. The first converter stabilizes the voltage received from the car battery from any value between 12.9V and 13.4V to 12V. Then, the second voltage converter converts from 12V to 5V for the Arduino and the dual relay module. Finally, the voltage is converted to 3.3V through the pin on the Arduino Uno R3 development board for the Adafruit LSM303AGR accelerometer sensor.

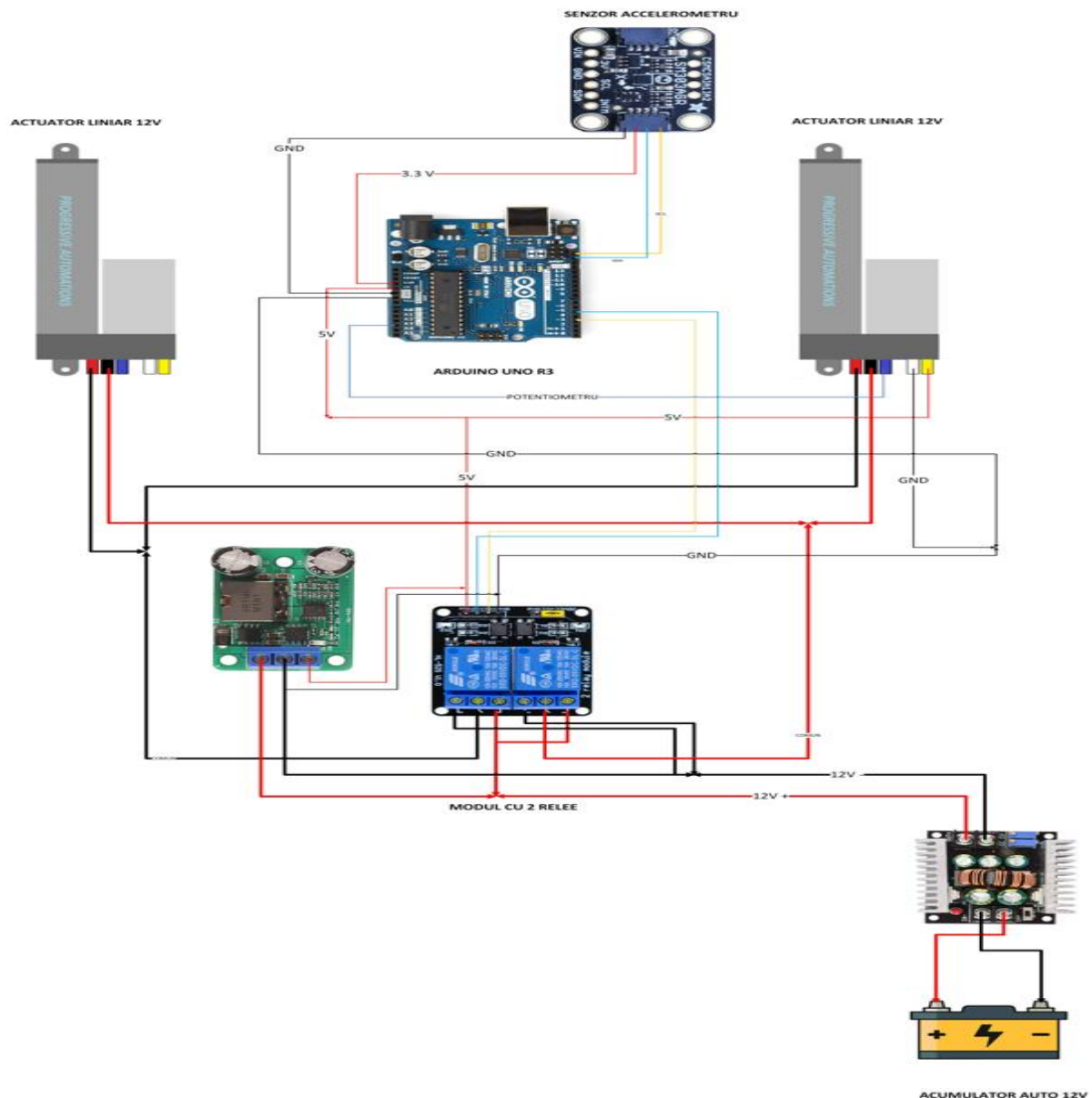


Fig. 6. Electrical scheme of the Active aero wing

4. Design stages for the casing of the entire electronic assembly

For encapsulating the entire electronic assembly, a custom housing was created with individual mounts for securing each component. In the process of creating this housing, a design was developed that allows for good ventilation and heat dissipation of the electronic components without compromising its dimensions. The housing was designed to be compact while ensuring adequate cooling for the system and providing proper pathways for the cables.

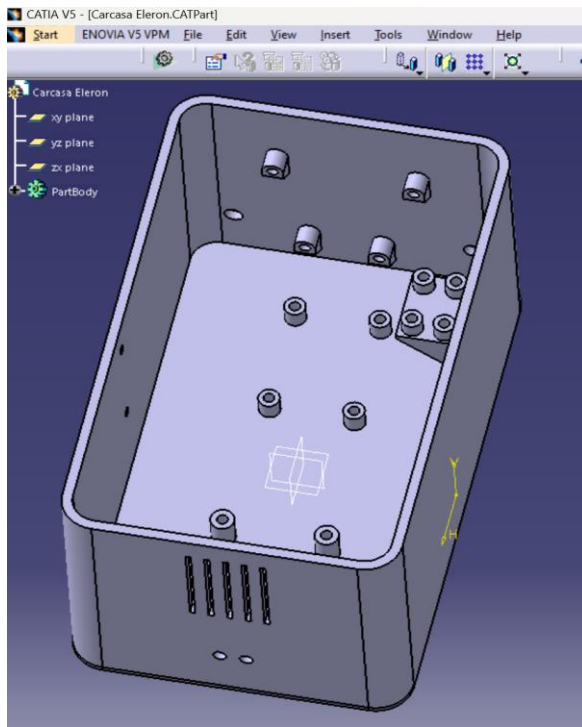


Fig. 7. Electronic components case components

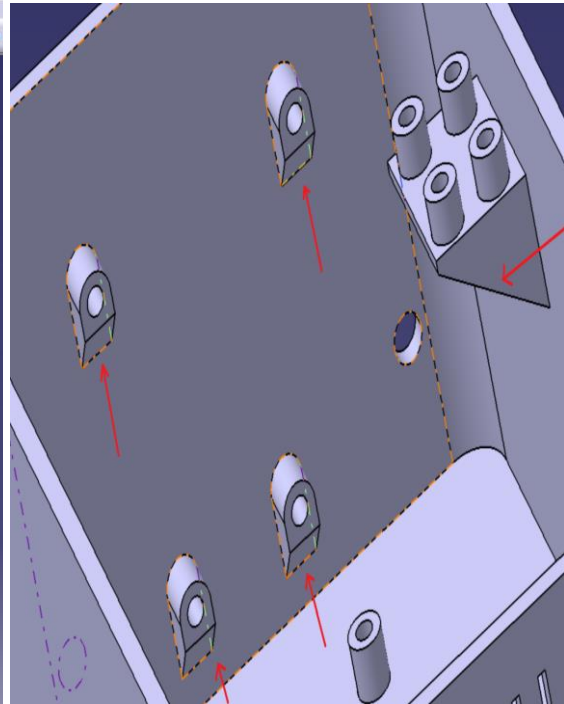


Fig. 8. Side mounts for the electronic components

For the side mount of the 12V to 5V voltage converter, it was necessary to create a separate component that will be secured with two M3 diameter screws. The reason for this adjustment is the high likelihood of failure in printing the three mounts on the wall of the housing due to the inability to create support in that area.

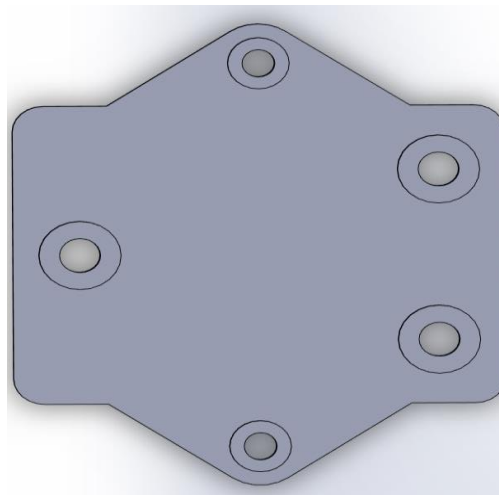


Fig. 9. Side mount for the 12V to 5V convertor

5. Linear actuators coding

The code was written in the C++ programming language using the Arduino IDE.

6. Conclusions

In conclusion, designing an algorithm and creating a fully automated spoiler, with real-time decision-making power based on environmental conditions, directly contributes to the development of a new automated active aerodynamics system, replacing the old and traditional DRS model, operated by human commands, with a modern autonomous system. Implementing this new innovative solution in the automotive field will lead to an exponential increase in competitiveness in any form of competition, raising standards to a new level and setting new records.

7. Bibliography

[1]<https://www.quora.com/How-fast-were-Formula-One-F1-cars-before-they-had-Drag-reduction-System-DRS>

[2]https://www.reddit.com/r/formula1/comments/sl9a9q/explaining_the_various_buttons_of_an_f1_steering/

RESEARCH ON DEVELOPING AN EXPERIMENTAL DRONE MODEL TO ASSIST AUTONOMOUS VEHICLES

POPÎRLAN Robert – Florin, Florin TEODORESCU DRĂGHICESCU

¹Facultatea:de Inginerie Industrială și Robotica, Specializarea:Informatica Aplicată în Inginerie Industrială, Anul de studii:IV, e-mail:robert.popirlan@yahoo.com

ABSTRACT: *The theme of the project is based on developing a drone model for capturing images from various heights and locations. These images are processed on an external computer to identify if there are different objects in the path of autonomous vehicles. This is done to reconfigure their route and avoid potential damage. For the completion of the project, Solidworks was used for creating the 3D model, BetaFlight for configuring the Flight Controller (FC) and Electronic Speed Control (ESC), as well as the power used for takeoff. Furthermore, Arduino IDE will be utilized for establishing communication between the drone and the autonomous vehicle.*

KEYWORDS: *Drone, System, Surveillance, Autonomous Vehicle*

1. Introduction:

In today's modern technological era, the development and implementation of intelligent solutions for urban mobility are becoming increasingly relevant. Among these, drones are beginning to play a significant role, providing a wide range of services and facilities. Therefore, this paper explores the potential and significance of a drone specifically designed to surveil and assist autonomous vehicles in the urban environment. It covers the technical and operational aspects of this technology, highlighting how it can significantly optimize and improve the efficiency and safety of autonomous transport. The goal is to achieve this by thoroughly analyzing the design, characteristics, and usage aspects, providing a comprehensive perspective on the contribution of this emerging technology to the development of urban mobility.

2. Current Status



Figure 1.

The FPV Helion 10 O3 6S HD drone is specially designed for long-distance flights, equipped with an HD O3 video transmission system that ensures superior image quality and a stable connection. It is powered by a 6S battery configuration, which provides enhanced flight duration and high performance.

The long range surveillance UAV

The DeltaQuad Pro #VIEW is designed for organizations who need an eye in the sky.
Its smart features and powerful performance enable effective surveillance & reconnaissance strategies.



Figure 2.

The DeltaQuad Pro #VIEW drone is specialized for long-range surveillance missions, with outstanding autonomy and advanced autonomous tracking capabilities. It is equipped with a wide range of cameras, including thermal imaging options and HD video transmission up to 50 km or unlimited via LTE/4G. It can operate in various weather conditions, including moderate rain or snow, and is ready for flight in less than two minutes.

Helion 10 O3 6S HD Long Range FPV Drone: It is designed for long range and advanced configuration. Key features include powerful performance, HD transmission system, aerodynamic design and durable construction, advanced control system and safety and navigation features. It is ideal for users who want to escape long distances with high-quality real-time image transition.

Autonomous Vehicle Assistance Drone: This is designed to assist autonomous vehicles by monitoring a history that the autonomous vehicles' built-in systems cannot detect. The drone contains a mode of operation that consists of a pilot equipped with FPV goggles to navigate through spaces as non-permissive and provide images in real time from the the drone. The main goal is to provide a flexible and efficient solution for the continuous and safe monitoring of work environments.


Experimental drone for high-altitude imaging: It is designed to be used for high-altitude and multi-area imaging to identify objects in the path of autonomous cars and reconfigure their paths. It is equipped with various sensors to detect and monitor obstacles and areas of interest. Its main purpose is to provide an additional level of safety and assistance to autonomous vehicles in urban and industrial environments.

3. Main components of the system

The system is divided into two distinct components, each with its well-defined role in the operation of the entire system and its efficiency. These components are: The system on the drone: "Drone system"; this party is responsible for collecting data and information from drones. It is equipped with certain sensors and cameras that allow it to supervise and monitor the area of interest. Also, the drone is equipped with a control and navigation system that allows it to move autonomously or through human control. The function of the drone is to collect data from the environment and transmit it to its receiver. The system represented by the transmission mode of drones using radio waves: This component is responsible for receiving and transmitting the data collected by the drone. More specifically, they are used to send to the end user or to accept from end users or other compatible monitoring devices. This mode of transmission is carried out with the help of radio loops that allow an efficient and fast connection. Thus, this transmission system must be robust and use them regularly to ensure efficient data exchange. And the user will receive validated data regarding the dynamic real situation closer to the area of interest. By implementing these two functions, the system becomes complete and allows the user to correlate all data about the surface of interest. The collaboration between the drone and the radio transmission module is essential to ensure effective surveillance and provide accurate and useful data to the end user.

The electronic components are represented in the following table

Table 1. Electronic components

Name of the Components	Characteristics	Representation
SpeedyBee F405 V3 BLS 50A 30x30 FC&ESC Stack	MCU-STM32F405 IMU(Gyro)-BMI270 USB Port Type-Type-C Barometer-Built-in [5]	 <p>Figure 3 [5]</p>








TMOTOR F60 Pro V 2207.5 Brushless Racing Motor – 1950KV	Max power (10s): 1191W. Configuration: 12N14P. Shaft diameter: 4mm. Idle current: 1.19A. Burst (10s): 48.3A. [6]	
FT800 by Tmotor	Power Levels-PIT-25-200-500-800mW Weight-7.58g Channels 48CH Input Voltage 7-36V [7]	
BLAZE 5.8 by TrueRC Canada	Gain: 1.9dBic Polarization: LHCP Cross-Polar Rejection: -15 to -30dB, (1.9%) Bandwidth: 5.4GHz-6.3GHz Radiation Efficiency: 99% [8]	
CADDXFPV Baby Ratel2 Analog Camera	Input voltage: 4.5-36V. Connection method: Connector. Horizontal resolution: 1200TVL. Aspect ratio: 4: 3/16: 9 switchable. [9]	
Receptor FS-A8S 2.4GHz cu 8 Canale, cu Ieșire PPM I-BUS SBUS	8 PPM channels, 18 i-BUS channels; Type: multi-rotor; Frequency range: 2.408-2.475 GHz; Bandwidth: 500 KHz; Lane Number: 135; Sensitivity: -92 dBm; [10]	
PLACA DEZVOLTARE UNO R3 ARDUINO	Operating voltage 5V Input voltage 7-10V (9V recommended) 14 digital input pins (with PWM support) [11]	
HC-12, SI4438, 1KM	Working voltage: 3.2V - 5.5VDC Current consumption during transmission: 100mA at 20dBm Current consumption during reception: 22mA Standby consumption: 16mA [12]	

Figure 4 [6]

Figure 5 [7]

Figure 6 [8]

Figure 7 [9]

Figure 8. [10]

Figure 9. [11]

Figure 10.[12]

4. The operating principle of the drone:

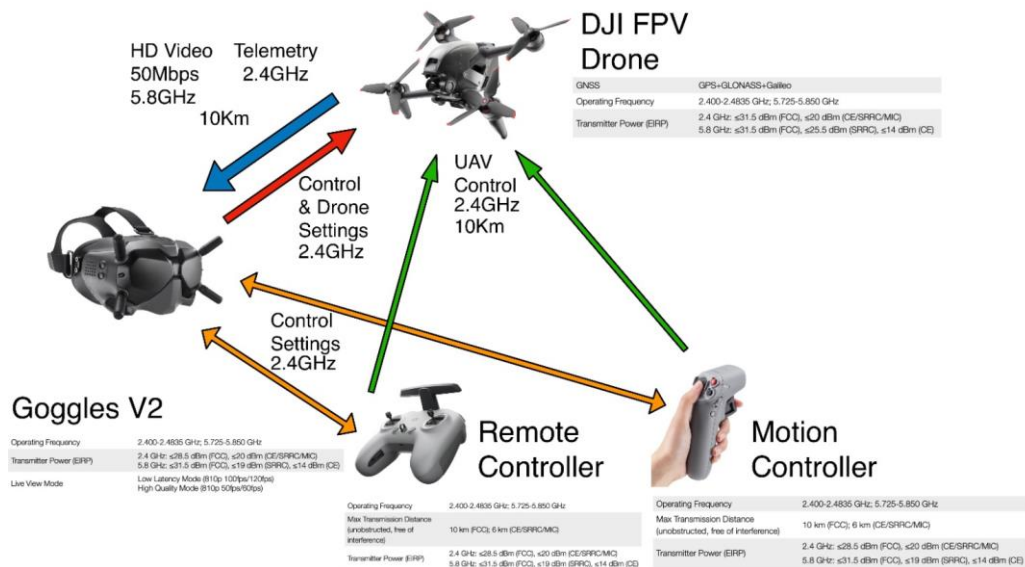


Figure 11.[4]

Drones work by using a set of propellers or motors to generate thrust and maintain flight. They are powered by a power source and controlled by a flight control system. Sensors and electronics monitor and adjust the drone's position, movement and orientation in real time. The information is processed by an on-board computer or flight controller to keep the flight stable and controlled. The drone can be equipped with cameras and other devices to capture images and data while in flight. Communication between the drone and the operator or control system is done via radio or other wireless technologies. Therefore, drones are used in various fields, including aerial photography and filming, as well as in environmental surveillance and monitoring.

5. Mode of operation

It is desired to design the system operation to allow a pilot to use a drone for the purpose of surveillance of various locations of interest that cannot be properly detected or monitored by the embedded systems in autonomous vehicles. This pilot will be equipped with FPV goggles to navigate restricted access spaces and see from the perspective of the drones more easily. To approve the types of equipment needed and to plan how to implement, an organizational chart was created detailing each stage and every component responsible. The flow chart covers everything from identifying the needs and the right equipment to implementation and testing. Each component of the system is properly managed and monitored, thus ensuring efficient deployment and compliance with established objectives. This method aims to create a robust monitoring system. Specifically, it aims to develop a robust and reliable surveillance system that brings tangible benefits in terms of safety and monitoring of specific places, acting as an effective remedy to prevent accidents and improve security.

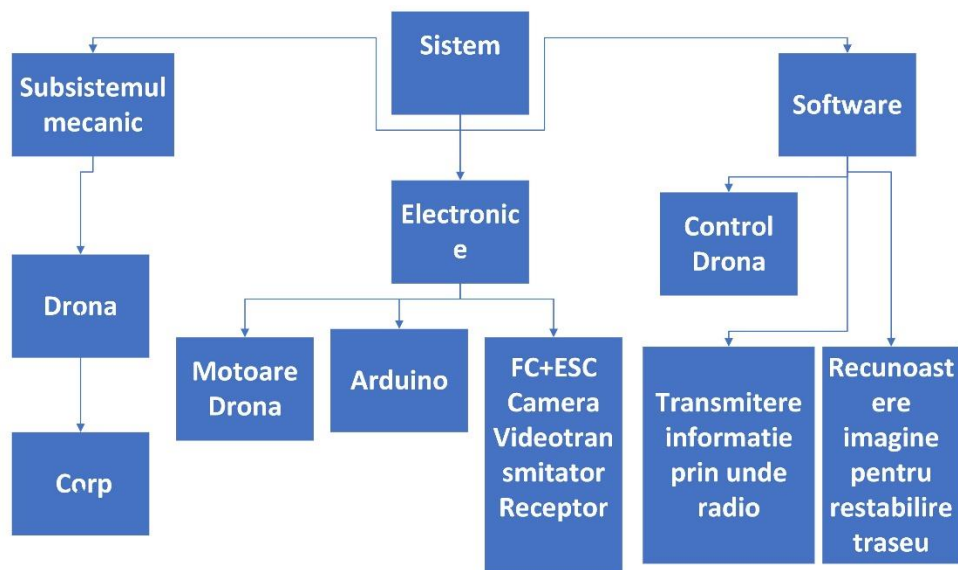


Figure 12. Flux Diagram

6. Software used

Betaflight was used to calibrate the motors, the gyroscope, but also the power adjustment. Betaflight is a configurator for different aircraft models that can edit the data on the main face of the drone. To control the drone, the I-Bus protocol is used, being the most permissive of those present.

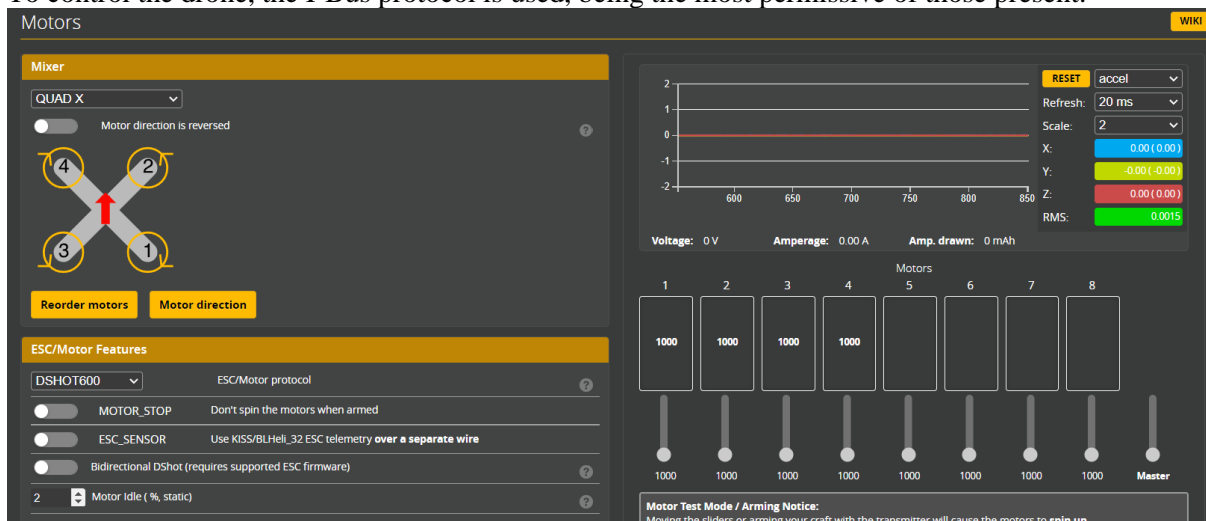


Figure 13

The calibration of the adjustment during the flight was carried out with the help of the PID Tuning window, from where we can change the working mode of the PID controller according to the user's wishes. In this case, only those necessary to have a proper takeoff were edited.

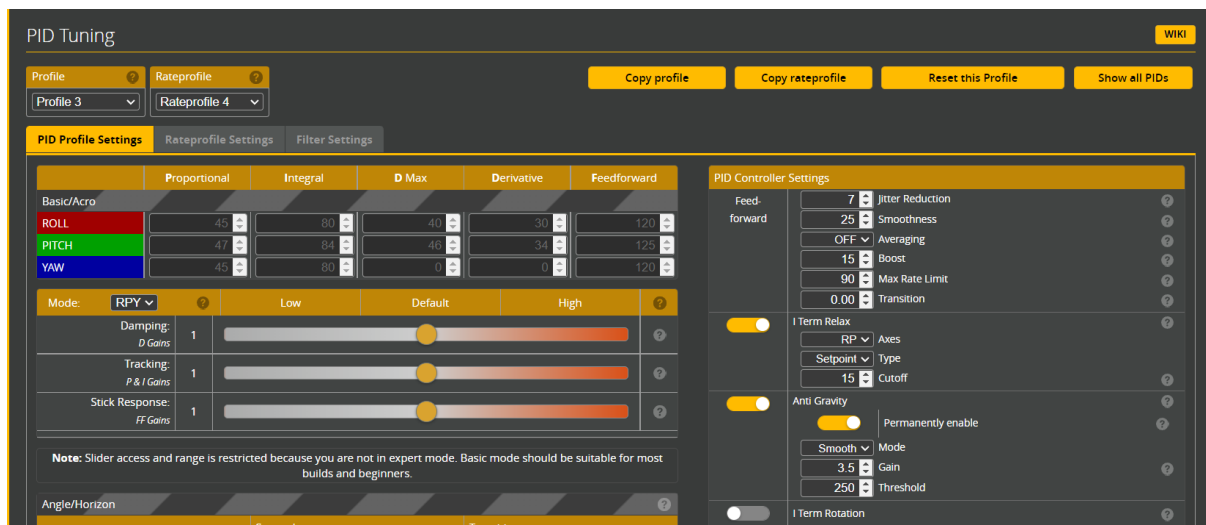


Figure 14

With the help of the VTX we can transmit the image captured by the camera to the FPV glasses. They will help the pilot in maneuvering through inaccessible spaces and with reduced visibility. To transmit the data to the camera, the data of the video transmitter must be recorded, which are generally provided by the manufacturer. Through the CLI (command line interface) the VTX registration is performed.

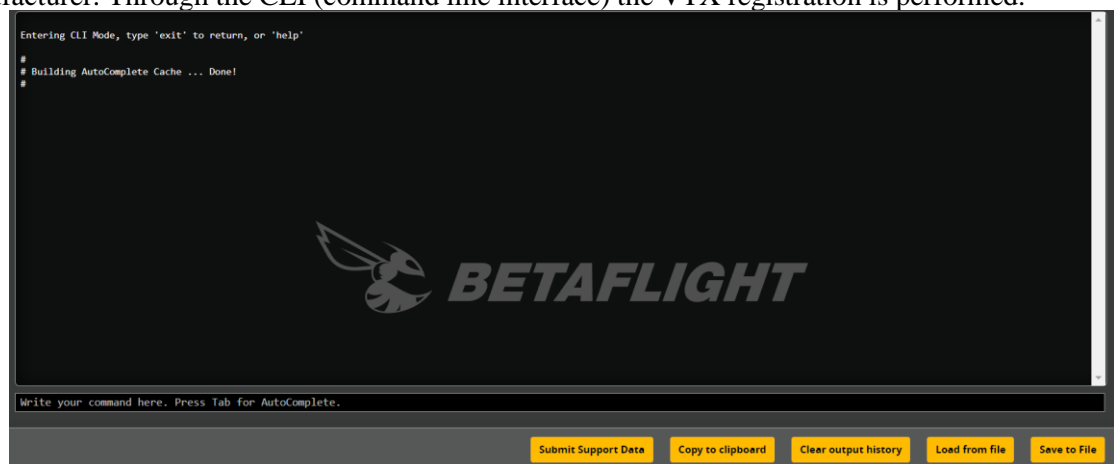


Figure 15

After making these settings, an arming and piloting mode will be declared. They consist of several signals transmitted by the remote control (TX transmitter) to the receiver mounted on the drone (RX receiver). These signals are then processed by the central board and transformed into yaw, roll, power increase commands.

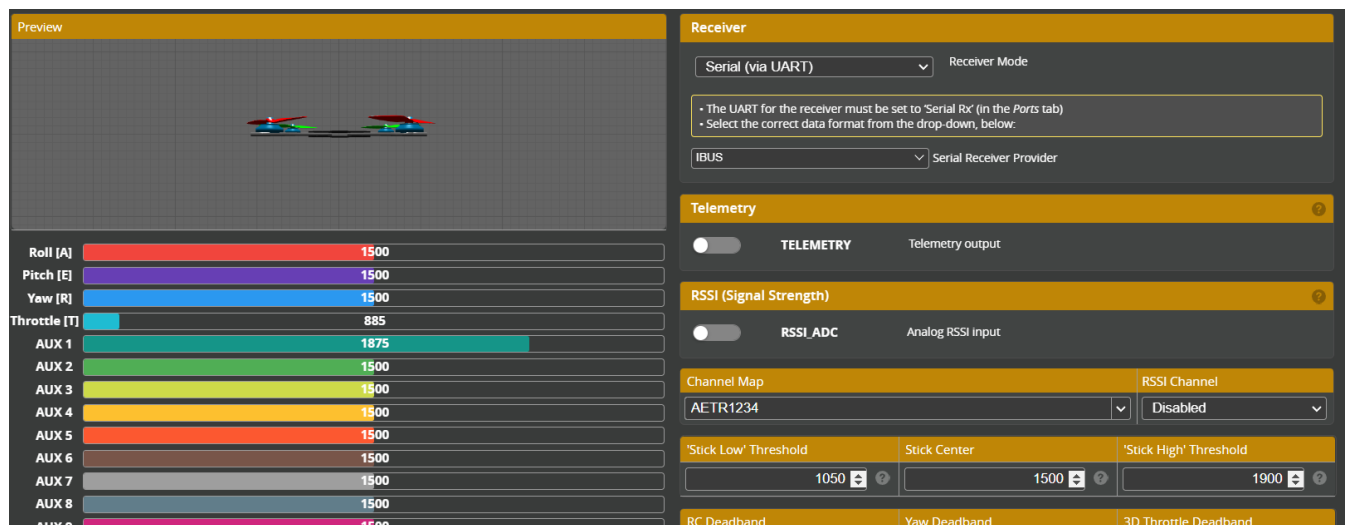


Figure 16

After the full development of the drone, communications will be made using radio waves through the arduino development board, and then the program for recognizing objects or possible dangers will be made using the Python programming language.

7. Conclusion

In conclusion, a surveillance system was developed to increase workplace and traffic safety and to decrease the number of accidents. Its design provides a high standard of safety for a wide range of activities. This highly innovative system opens up new perspectives on the approach to autonomous car monitoring within Industry 4.0. People are also happier to entrust the safety of their lives to this system. This is dynamic, ambulatory and uses less equipment than a static one. In conclusion, mobile monitoring is a more economical mobile and secure solution.

8. Bibliography

- [1]. <https://idrones.ro/produs/fpv-dron-helion-10-o3-6s-hd-za-dalgi-razstoyaniya/>
- [2]. <https://www.deltaquad.com>
- [3]. <https://www.indoor-robotics.com/blog/drone-security-systems-vs-surveillance-cameraschoosing/>
- [4]. <https://forum.dji.com/thread-263359-1-1.html>
- [5]. <https://www.speedybee.com/speedybee-f405-v3-bls-50a-30x30-fc-esc-stack/>
- [6]. <https://tmotorhobby.com/goods-1183-TMOTOR+F60+Pro+V+22075+Brushless+Racing+Motor+-+1750KV1950KV2020KV2550KV.html>
- [7]. <https://store.tmotor.com/product/ft800-vtx.html>
- [8]. <https://www.truerc.ca/shop/5-8ghz-2/transmitter/blaze-5-8>
- [9]. <https://caddxfpv.com/collections/analog-camera/products/caddxfpv-baby-ratel2-analog-camera>
- [10]. <https://www.optimusdigital.ro/ro/aeromodelism/3960-receptor-fs-a8s-24ghz-cu-8-canale-cu-ieire-ppm-i-bus-sbus.html>
- [11]. <https://www.optimusdigital.ro/ro/placi-avr/1685-uno-r3-atmega328p-atmega16u2-placa-de-dezvoltare-compatibila-cu-arduino.html>
- [12]. <https://www.sigmanortec.ro/modul-comunicare-seriala-radio-433mhz-hc-12-si4463-1km>

RESEARCH ON DESIGNING AND IMPLEMENTING AN EXPERIMENTAL MODEL OF AUTOMATIC DOOR OPENING

FLOREA Andrei, DUGĂEȘESCU Ileana

University: Industrial Engineering and Robotics, Specialization: Applied Computer Science in Industrial Engineering,

The year of study: IV, e-mail: floreaandrei77@yahoo.com

***ABSTRACT:** The aim of the project is to develop a system for automatic door opening in the presence of people entering or exiting a room, including counting them. In case the door encounters an obstacle during the opening/closing process, it should not force the system but stop the operation and resume it after a few seconds, assuming the obstacle has been removed. In emergency situations such as fires or evacuations, the doors open automatically, and the system records the number of people leaving the room. After complete evacuation, the door closes automatically to prevent the spread of smoke and fire*

***KEYWORDS:** automatic, opening, counting, evacuation*

1. Introduction

The purpose of automatic doors is to provide a convenient, efficient, and safe solution for accessing public or private spaces. These doors eliminate the need for human intervention to open and close them, thus improving traffic flow in these areas. They emerged in the 19th century. An example of a prototype is represented by the first automatic swinging door designed by engineers Horace H. Raymond and Sheldon S. Roby in 1931 (Fig.1) [1,2]. The invention was patented and installed at Wilcox's Pier restaurant in West Haven, Connecticut, for the benefit of waiters [1]. Another example of an automatic opening door is the model created in 1954 by Dee Horton and Lew Hewitt, specifically designed to allow access for people with disabilities to public buildings. The automatic door used a carpet actuator. In 1960, they co-founded Horton Automatics Inc and introduced the first commercial automatic sliding door to the market [1].



Fig. 1 The first automatic swinging door [1,2]

2. The current stage

The use of automatic opening doors is increasingly widespread today. When choosing the opening system, several factors must be taken into account, including location and context. In heavily trafficked environments such as commercial buildings or public institutions, automatic opening systems are quite common. They are used to facilitate access and enhance accessibility, especially for people with disabilities. [3]

Most swinging automatic doors do not have a secondary power source but can be manually pushed, pulled, or opened in case of emergencies. However, the project also includes a backup battery as an additional feature if needed. Additionally, swinging doors can be connected to the fire alarm and programmed to open upon activation (Fig. 2).

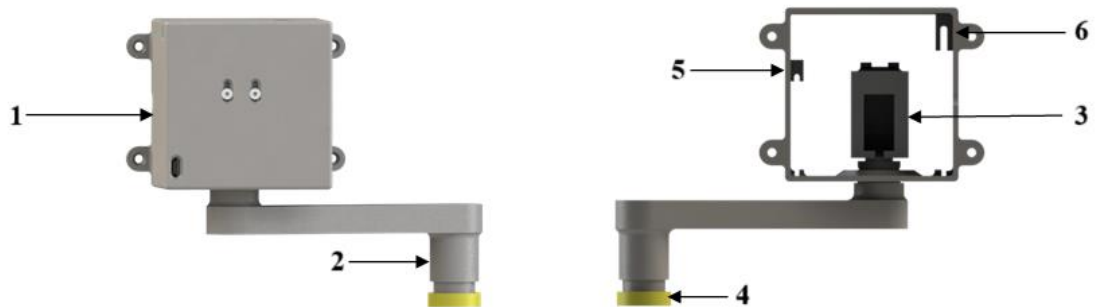


Fig. 2: The assembled components inside the casing

The purpose of developing the system is to efficiently achieve door opening in correct situations and as reliably as possible. At the same time, the system must also ensure the safe evacuation of people only when necessary. Below, all the components presented in Fig. 2 is depicted in Table 1.

Table 1 – Components of the experimental model and sensors




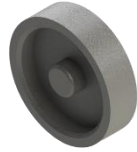


No.	Part name	Representation
1.	Housing	
2.	Arm	
3.	Servomotor bracket	

Table 1 – Components of the experimental model and sensors (continuation)

No.	Part name	Representation
4.	Bearing housing	
5.	Arduino board holder	
6.	Battery holder	

The printed parts were made according to the following printing specifications. After the 3D modeling process of the parts, Creality Ender 3 V2 and Zortrax M300 Plus 3D printers were used. The material used for printing was PLA (Polylactic Acid) with the following characteristics: extruder temperature of 220 degrees Celsius, bed temperature of 60 degrees Celsius, infill of 25%, and a printing speed of 60 mm/s. After assembling the parts made through additive manufacturing, the experimental model is depicted in Fig. 3.

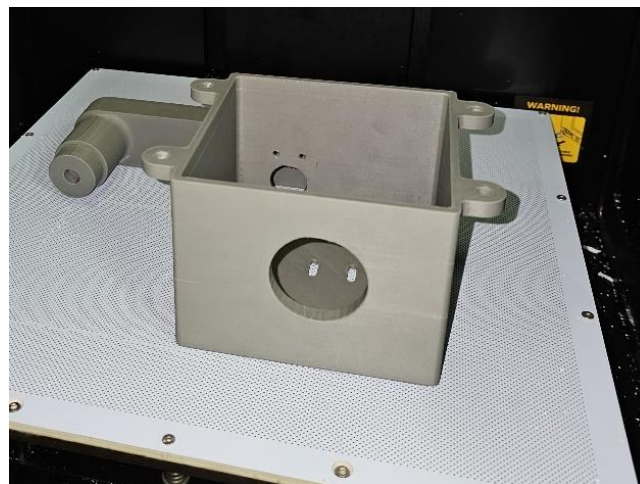


Fig. 3 Experimental model after print

In Fig. 4 is presented the experimental model.

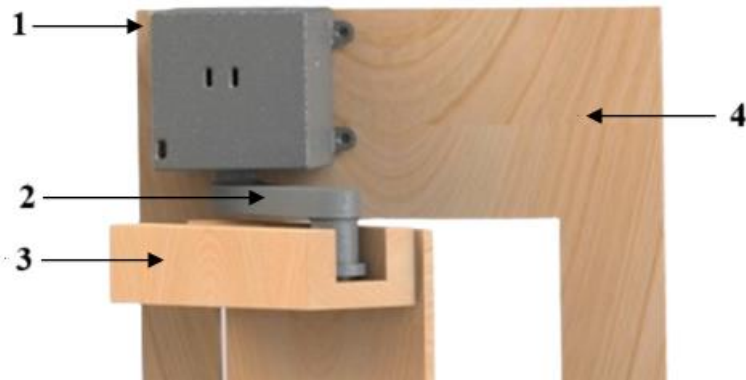


Fig. 4 Final Assembly: 1 - Housing, 2 - Opening arm, 3 - Slide attached to the door, 4 - Door frame

3. Testing the experimental model

For accurate counting of individuals moving inside the room, tests were conducted with multiple motion detection sensors (Table 2). The selection of sensors was based on the consideration of the following aspects:

- A person should be easily detected when entering/exiting the room;
- Sensors should not result in multiple detections;
- Adjustable sensitivity;
- Resistance to interference;
- Precision regardless of the operating environment.

For the development of the experimental model, was used the components shown in Fig. 5.

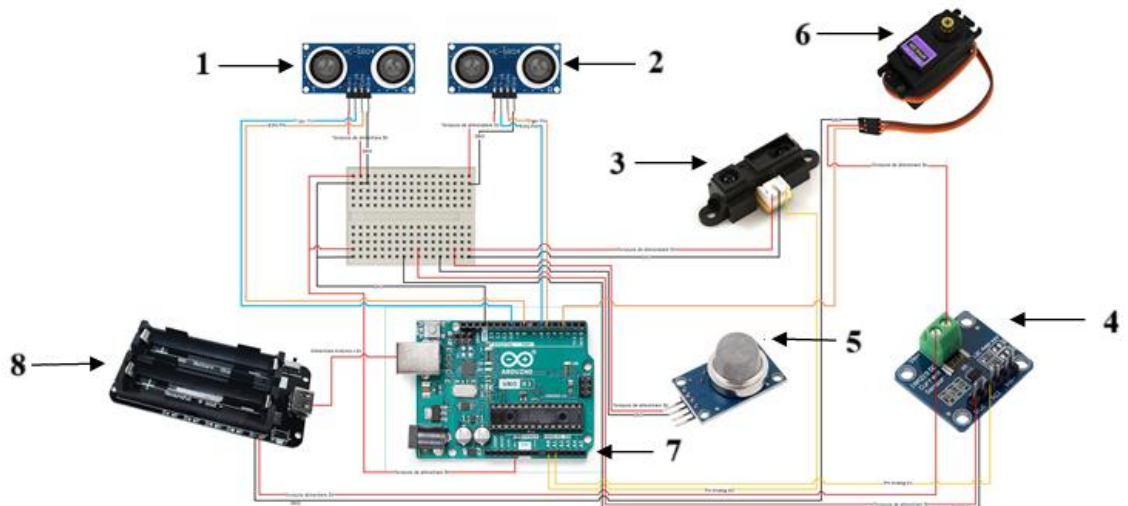


Fig. 5 Wiring diagram: 1, 2 - ultrasonic sensor, 3 - sharp sensor, 4 - current sensor INA219, 5 - smoke sensor MQ2, 6 - servomotor, 7 - Arduino board, 8 - power bank

To open the door are used ultrasonic sensors (1,2), which are connected to digital pins 5, 6 and respectively 7, 8. One sensor is placed inside the room and one outside to open the door for people both

inside and outside the room. The operation of these sensors is as follows: the ultrasonic sensor operates based on two ultrasonic transducers: a transmitter and a receiver. The transmitter emits ultrasonic waves at a frequency of 40,000 Hz. The receiver picks up these waves after they are reflected by an object [4].

```
define trigPin_intrare 6 // entry  
define echoPin_intrare 5 // entry  
define trigPin_iesire 8 // exit  
define echoPin_iesire 7 // exit
```

The sharp sensor (3) counts a person each time the barrier's distance is interrupted and the measured distance is less than 10 cm. This sensor proved to be a suitable option. Detection is precise and occurs when the laser barrier is interrupted, allowing for accurate counting of individuals. This assessment allows to identify the appropriate sensor for project, although adjustments and troubleshooting of technical issues were required.

```
if (distance < 10) { // If the distance is less than 10 cm  
  counter++; // Increment the counter variable by 1  
  Serial.println("Distance is less than 10 cm"); // Print a message for debugging  
  Serial.print("Counter: ");  
  Serial.println(counter); // Print the value of the counter variable for debugging  
  delay(1000); } // Wait for 1 second to prevent rapid multiple increments
```

The INA219 current sensor (4) measures both voltage, with 1% accuracy, and current, monitoring in both directions. This sensor provides the highest precision among all the chosen sensors due to its method of calculating voltage. It features a 0.1 Ohm resistor through which the current flows, allowing for the determination of the current value with very small deviations [5]. The current limit is set to 0.6 amps. If the detected current exceeds the limit, the servo motor will rotate to 125 degrees.

```
if ((current_mA > currentThreshold * 1000){  
  moveServoGradual(125);  
  overloadDetected = true;  
  servoBlocked = true;
```

The MQ2 smoke sensor (5) is used to detect emergency situations and operates at 5V DC. It is capable of detecting concentrations of LPG, smoke, alcohol, propane, hydrogen, methane, and carbon monoxide. The operating principle of the MQ2 sensor is based on the changes in resistance of a sensing element located inside the metal casing [6]. The A1 analog pin for the smoke sensor is assigned. The limit is set to 600. When this limit is exceeded, the servo motor is activated.

```
int smoke_entry = analogRead(A1);  
if (smoke_entry > 600) {
```

The servo motor (6) is connected to the development board as follows: the black wire is connected to GND, the red wire is connected to the power supply (5V) and the third wire is connected to digital pin 9.

To declare the connection between servomotor and board is used the following line code:

```
servo.attach(9);
```

To power the entire door circuit, the power source (8) was used. It consists of two 3.7V 18650 batteries. The battery specifications are as follows: a voltage of 5V and a current of 3.5A [7]. The MG995 servo motor can use up to 3A, but to avoid overloading other components of the assembly, it was limited to 0.6A.

4. Conclusions

In conclusion, the automatic door opening system in case of fire and people counting assembly can be considered a complex "black box" that has been developed to operate in the most reliable and efficient manner possible. Testing and evaluating various types of sensors led to the identification and implementation of an optimal solution that provides both safety and functionality in various scenarios.

5. Bibliography

- [1]. https://en.wikipedia.org/wiki/Automatic_door Accessed on May 8, 2024
- [2]. <https://jmanny.com/when-did-automatic-doors-become-popular-in-the-uk/> Accessed on May 8, 2024
- [3]. <https://ardushop.ro/ro/electronica/45-modul-pir-senzor-de-prezenta-miscare.html> Accessed on May 8, 2024
- [4]. <https://www.bitmi.ro/blog/simuleaza-parcarea-masinii-cu-senzorul-ultrasonic-hc-sr04.html> / Accessed on May 8, 2024
- [5]. <https://www.robofun.ro/tensiune/modul-senzor-cjmcu-219-ina219-pentru-monitorizarea-tensiunii.html> / Accessed on May 8, 2024
- [6]. <https://lastminuteengineers.com/mq2-gas-senser-arduino-tutorial/> Accessed on May 8, 2024
- [7]. https://ardushop.ro/ro/home/2086-two-voltage-18650-lithium-battery-shield-v8-mobile-power-expansion-board-module-5v3a-3v1a-micro-usb-for-arduino-esp32-esp8266.html?gad_source=1&gclid=CjwKCAjw65-zBhBkEiwAjrQRMPfiI3w4BQiNPn97CnNtBr0ScsNYm4KxZCVJfksgEwXOqwdzat4EpBoCQYEQA vD_BwE / Accessed on May 8, 2024

DESIGNING AN ALGORITHM AND DEVELOPING A COMPUTER APPLICATION FOR OPTIMIZING CUTTING REGIMES BASED ON MINIMUM COST PRINCIPLE

STEFAN Mihaela-Alexandra, ALUPEI COJOCARIU Ovidiu Dorin

Faculty: Industrial Engineering and Robotics, Specialization: Applied Informatics, Year of Study: IV,
e-mail: 11mihaelastefan@gmail.com

ABSTRACT: Designing an algorithm and developing a software application for optimizing cutting regimes based on the principle of minimum cost involves creating a software solution to streamline the cutting process in the materials processing industry. The algorithm must take into account parameters such as cutting speed, depth of cut, and the material being processed to minimize the costs associated with the machining operation. Once designed and implemented, the application can be used in various industrial sectors to improve the efficiency of production processes and reduce associated expenses.

KEYWORDS: optimization, minimum cost, cutting, data analysis.

1.Introduction

The purpose of the project titled "Designing an algorithm and developing a computer application for optimizing cutting regimes based on the minimum cost principle" is to develop a computer application with a simple and user-friendly interface that can help me minimize costs in the cutting process. Additionally, designing the algorithm for the application plays an important role in the documentation process. Starting from the calculation formulas for optimizing cutting costs of a piece with the primary operation of face milling, I have constructed a computer application that can be used for data analysis and solving optimization of cutting regimes based on minimum costs principle. The computer application functions correctly and displays results according to the user-input data. From the technical documentation, information regarding the production of the guide piece with face milling as the primary operation and details of the tools used in the manufacturing process are derived. Thus, I was able to estimate the costs for each consumable separately.

I have identified a suitable solution to optimize costs, the first being the analysis of the electricity consumption during idle and loaded operation of the industrial mill used in the production of guide batches. According to the calculations, it can be concluded that it is profitable; therefore, expenses for electricity can be reduced.

2.Current stage

I have accurately calculated the minimum processing cost, and the application is functioning by running the initial data. Additionally, I have documented the manufacturing process of the chosen piece, namely the guide within the milling machine. I have started testing the components of the electrical stand for measuring electrical energy and am proceeding to assemble the components with appropriate connections between pieces.

3. Determining the Minimum Cutting Cost

The minimum cutting cost involves optimizing technological parameters such as cutting speed, depth of cut, and feed rate to minimize production expenses. This also includes proper tool selection to maximize efficiency and durability in the manufacturing process. Material waste reduction and production time optimization are essential in achieving minimum costs.

The calculation of the minimum cost for a piece is determined by the formula:

$$C_p = C_{smu} \left(\frac{t_{pi}}{n} + t_a \right) + C_{smu} * t_b + \frac{t_b}{T} (C_{smu} * t_s + C_{st}) \quad [lei] \quad (1)$$

$$t_b = \frac{l \cdot A_p}{n \cdot a_p \cdot f} \text{ [min];} \quad (2)$$

For a minimum processing cost:

$$C = C_{sf} + C_{amu} + C_{sdv} + C_{en} + C_{sa} * \frac{R1+R2}{100} \text{ [lei];} \quad (3)$$

The feed represents the distance the tool travels relative to the workpiece in the direction of feed motion. It is expressed in millimeters per revolution of the workpiece.[1]

$$s = K_s * C_s * D^{0.6} \text{ [mm/rot]} \quad (4)$$

The calculation of coefficients C_1, C_2, C_3 for each speed step:

$$C_1 = C_{smu} \left(\frac{t_{pi}}{n} + t_a \right) \quad (5)$$

$$C_2 = C_{smu} * \frac{\pi \cdot d \cdot l}{f \cdot v_c} \quad (6)$$

$$C_3 = \frac{\pi \cdot d \cdot l}{f \cdot v_c \cdot T} * C_{smu} * t_s + C_{st} \quad (7)$$

$$C_p = C_1 + C_2 + C_3 \quad (8)$$

3.1. Detailed calculation of the formulas and their verification

To test the formulas mentioned above, I used MathCAD software. I entered the values for each term and observed how the number of pieces affects the cost per manufactured product. Increasing the number of pieces brings changes to the setup time, as well as costs related to employee salaries (large volume of production = large number of employees), equipment depreciation, machinery, and electricity consumption. Therefore, in Figure 3, the difference in price for the same product can be observed following the specifications mentioned above, modified.

3.2. Graphical representation of the obtained values

According to the calculations performed in MathCAD, I analyzed the values of the cost of a piece depending on the values of T. The increase in the cost per piece can be observed according to the first two values of T (durability) (Figure 3.2). Therefore, if the time increases, then the minimum cost per piece also increases because other costs are involved, such as equipment and machinery depreciation, electricity consumption costs, employee salaries, and the number of sharpenings.

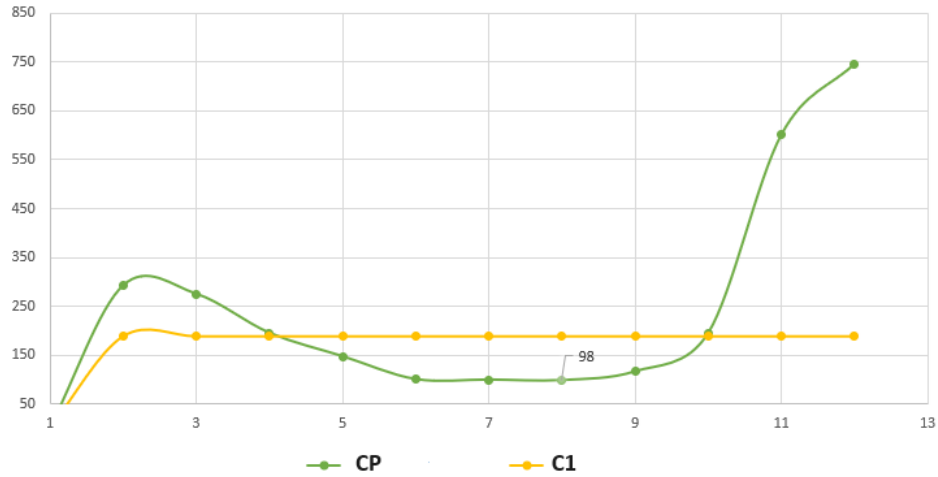


Fig.3.2. Graphical representation of durability values.

4. Implementation of the computer application in optimizing cutting regimes for minimum cost

4.1. Operational schema of the computer application

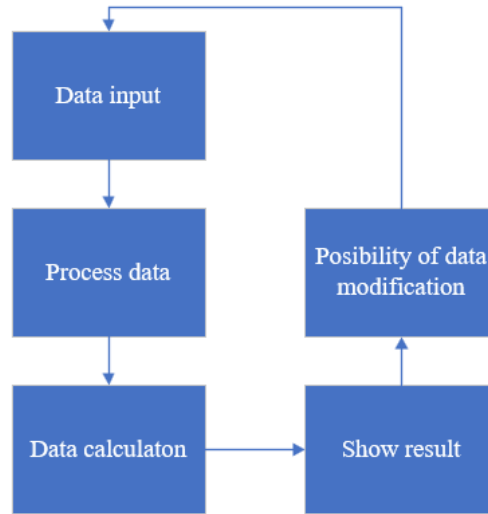


Fig.4.1.Operational scheme

4.2. Description of the application

We have constructed the application with an interactive and user-friendly interface for any user, as depicted in Figure 4.2. The purpose of the application is to assist the user in obtaining the minimum processing cost of a piece through cutting. After clicking the button marked in green, aptly named "Open Calculator", which will disappear once the calculation form opens as shown in Figure 4.2., the application has predefined data in the form to provide the user with a model for completion and, at the same time, an example of calculation. At the end of the form, there is a yellow button that, when pressed, will calculate the minimum cutting cost with face milling as the primary operation. The cost displayed will be in lei and will be located below the button.

The screenshot shows the 'APLICAȚIE INFORMATICĂ PENTRU OPTIMIZAREA REGIMURILOR DE AȘCHIERE PE PRINCIPIUL COSTULUI MINIM' (Computer Application for Optimizing Cutting Regimes on the Principle of Minimum Cost). The interface features a background image of a CNC machine. A green button labeled 'NEW' is visible. Below it, a text box says 'Te voi ajuta să calculezi cu precizie costul minim!'. The form contains several input fields with predefined values: 'Bucăți/Lot: 50', 'Diametru(mm): 15', 'Lungime prelucrare(mm): 50', 'Cost Așchiere(Lei): 3', 'Cost Scula(Lei): 15', 'Salariu Angajat(Lei): 3800', 'Rugozitate: 0.57', 'Timp Auxiliar(min): 15', and 'Timp schimbare(min): 15'. A yellow button labeled 'Afișează rezultat!' is at the bottom. Below the button, the text 'Rezultatul este: 292.320 Lei' is displayed.

Fig.4.2. Cost Calculator Interface of the Application

4.2.1. Application Development

For writing the code, I used Visual Studio Code as the text editor. I began developing the application by outlining the HTML tags, where I wrote its name.. I created the button for opening the calculator and assigned it the same name, as well as the "hideUnhide" function with the corresponding specifications in the JavaScript document, aimed at hiding the button after its press and displaying the calculation form. For text and webpage styling, I added a suggestive background in the CSS document. For ease of use, the user does not need to input specific variables to calculate the minimum cutting cost, as it requires

more advanced documentation to determine the exact necessary values. Therefore, I set these data as implicit and hidden from the user within the code.

5. Technological Design and Technical Documentation of the "Guide" Reference within the "Milling Machine" Assembly

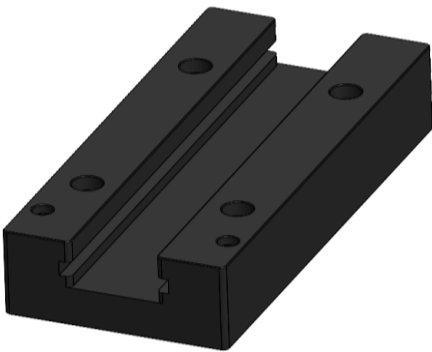


Fig.5. 3D CAD Model of the Guide Piece

5.1. Assembly Sketch

ITEM NO.	PART NUMBER	DESCRIPTION	STANDARD	QTY.
1	reper_1(falca menghina)			1
2	reper_2(falca menghina)			1
3	reper_3(ghidaj)			1
4	reper_4(surub cu bile)			1
5	reper_5(surub cu bile)			1
6	reper_6(bucsa)			1
7	reper_8(stift)			4
8	piulita			2
9	reper_9(stift)			1
10	reper_10(surub cu cap hexagonal)			1
11	reper_11(surub cu cap hexagonal)			1
12	PartIAVise Master			1

Proiectat și Desen original v1

SM11

Desenat v2

STEFAN MIHAELA

Universitatea Națională de Știință și Tehnologie POLITEHNICA București

Facultatea IIR

Departament AD/ 642AD

Verificat

Ansamblul, MENGHINA

Reper, GHIDAJ

Cod proiect, SM AD01.05

Control standarde

Material produs, FONTA

Masă produs, 7.43 kg

Format, A3

Aprobat

Scară, 1 : 1

Desen nr., SM11 AD01.05_2

Data/ Aprobare

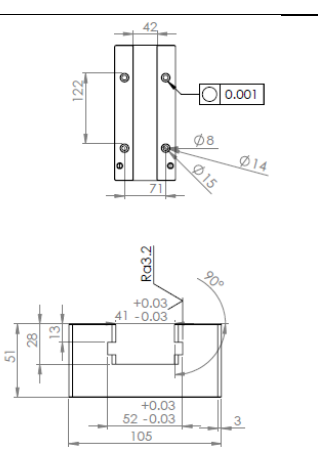
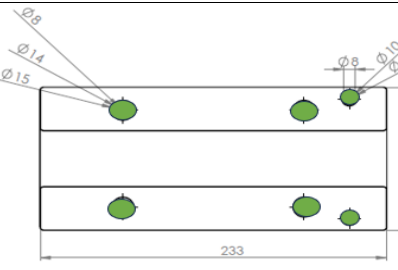
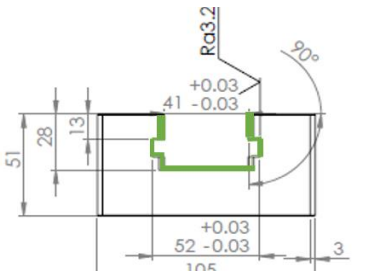
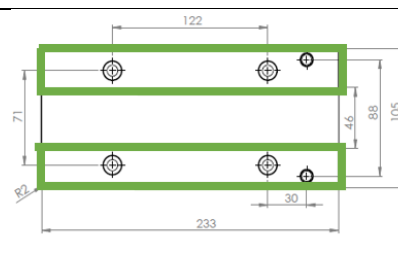
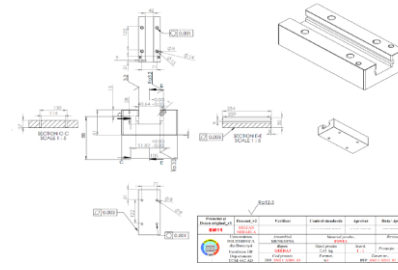
Revizuire,

Protecție:

Fig.5.1. The exploded assembly sketch.

5.2. Manufacturing Technological Processes

Table 5.2. Manufacturing Technological Process

Order Number and Operation Name	Preliminary Sketch of the Operation	Equipment and Tools
0. Casting		<p>U: Casting Installation D/S: Casting Mold V: Caliper</p>
1. Milling Drilling		<p>U: Drilling Machine D: Special Device S: Drill Bit V: Caliper, Thread Gauge</p>
2. Rough Milling		<p>U: Vertical Milling Machine S: Milling Cutter D: Special V: Surface Roughness Gauge, External Micrometer</p>
3. Finishing Milling		<p>U: Vertical Milling Machine S: Milling Cutter D: Special V: Surface Roughness Gauge, External Micrometer</p>
4. Final Inspection		

6. Computerized Measurement and Control Systems

To optimize costs, I created an electric stand to monitor the electric current consumption of the industrial mill during idle and under load. I used a 12 Volt motor with 5.5 Amperes equipped with an N-coder, to which I associated a compatible motor drive, necessary for precision and efficiency. In addition to these components, I utilized an Arduino Uno board, a voltage and current sensor, as well as a 12 Volt power supply. Therefore, I aimed to achieve a positive impact in the industry, with the goal of reducing costs and electricity consumption.

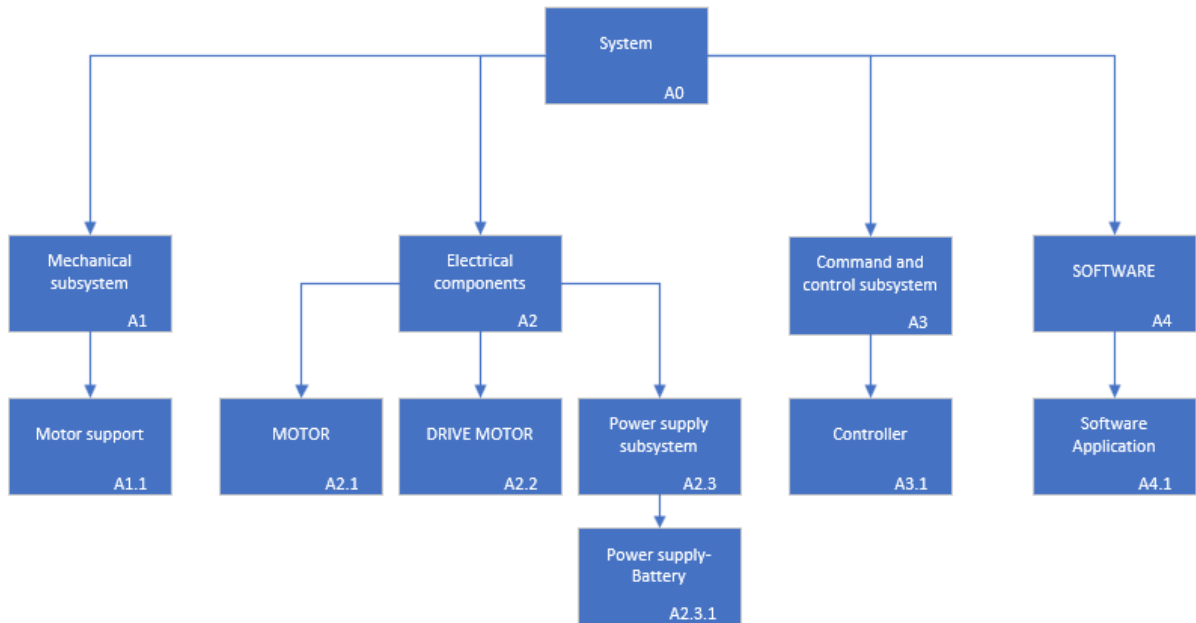


Fig.7.Component Diagram Used in the Electric Stand

6.1. Electrical Diagram of the Components

I have created the electrical diagram of the components, where I have established the corresponding connections.

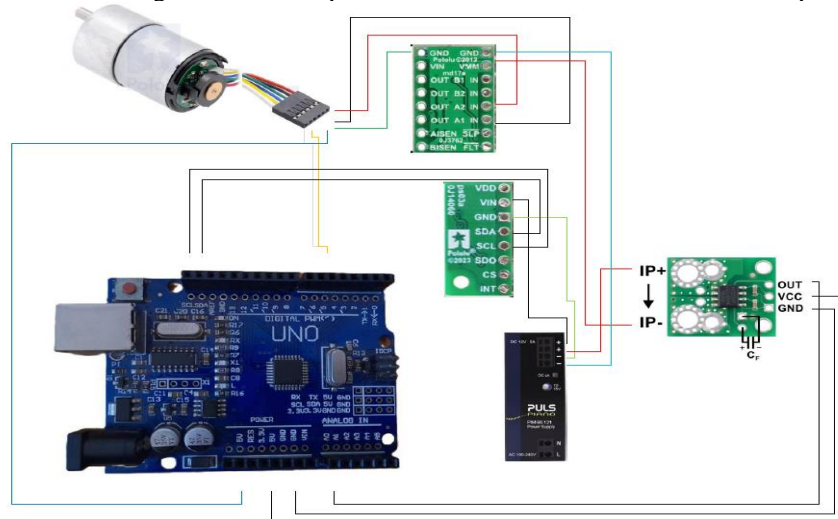


Fig.7.1.Electrical scheme

6.2. The 3D model of the components.

I introduced the components into SolidWorks to create a realistic model. In addition to the components from the electrical diagram, I added a motor mounting bracket and a housing to hold all components to provide stability to the electric stand. Their positioning is done according to the electrical diagram.

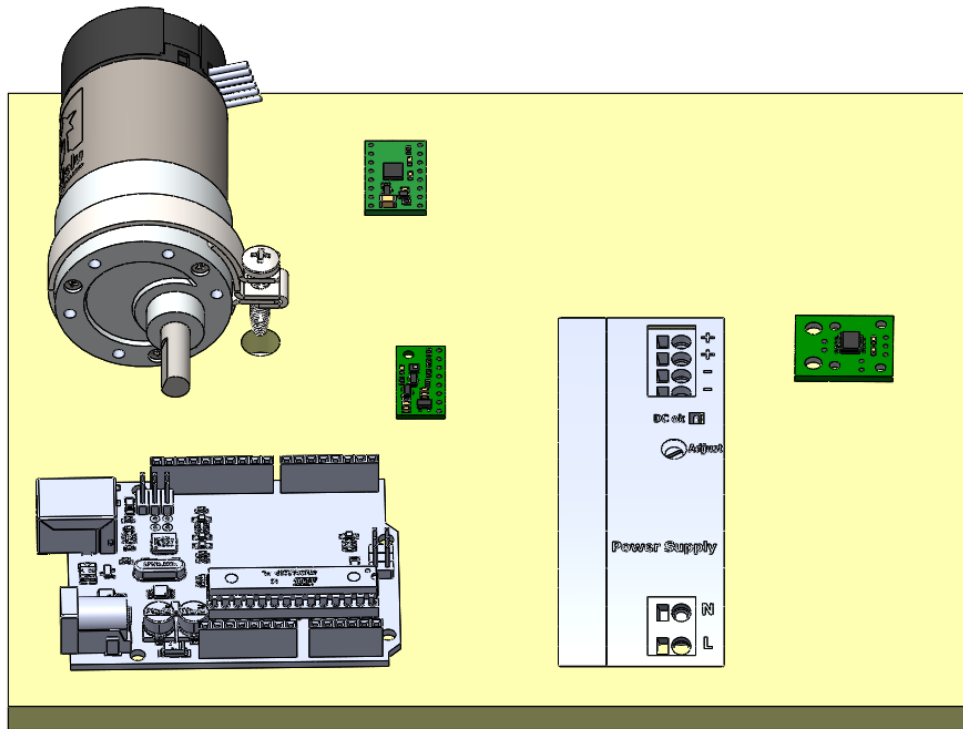


Fig.7.2.3D model of the components

6.Conclusions

I have developed a functional application that can be easily used by the user, where the entered data runs and displays the correct result. Additionally, I have implemented an option to minimize costs by calculating the electric energy consumption of the industrial mill during idle and under load.

7.Bibliography

- [1] <https://ro.scribd.com/document/177176563/Regimuri-de-Aschiere>
- [2] https://www.w3schools.com/css/css_form.asp
- [3] <https://www.w3schools.com/js/>
- [4] <https://www.w3schools.com/html/>
- [5] <https://www.pololu.com/product/2825/specs>

DESIGNING AND IMPLEMENTING A DEVICE FOR PRODUCT IDENTIFICATION IN A SELF-SERVICE

CONSTANTIN Darius-Costin; Tom SAVU

University: Industrial Engineering and Robotics, Specialization: Applied Informatics, Academic year: IV, e-mail: darius.constantin@stud.fiir.upb.ro

***ABSTRACT:** The purpose of this project is to design and develop an intelligent device that utilizes image recognition algorithms to automatically identify products in a self-service setting. By integrating image processing technology, the goal is to optimize menu management, facilitating customer choice and ensuring better inventory and production management. This project proposes an innovative approach to optimize operations in canteens and restaurants, with significant benefits for both operators, through increased efficiency and cost reduction, and consumers, through improved service experience and diversified options available. Therefore, by developing the entire system, both the process of purchasing products by customers and the process of updating and editing the software, which contains useful information for running the entire application, will be simplified for self-service staff.*

KEYWORDS: Image processing, LabVIEW, Ni Vision Assistant, Arduino, DB Access

1. Introduction

Within the project, the objective was to design and implement an experimental model of equipment for product identification in a self-service environment, through the integration of various hardware and software technologies [1]. To achieve this goal, advanced knowledge from fields such as image processing, hardware and software development, database management and web service technologies was applied. For the operation of the entire system, various equipment was required, such as: laptop as the main working platform, a stand equipped with LED lights and a webcam for image acquisition, a PoS (Point of Sale) system and an intelligent utensil serving device. Additionally, software tools such as NI Vision Assistant were used for image processing [2], LabVIEW for user interface development and system integration, Microsoft Excel for data management and report generation, Microsoft Access for creating a product database, Arduino for programming electronic components and HTML-CSS-JavaScript for creating a web page.

The interactions and connections between hardware and software components have been carefully managed to ensure efficient system operation. Data obtained from hardware components is processed and interpreted by software and the results are displayed and optimally utilized for user interaction. Additionally, input and output variables and parameters are clearly defined and managed throughout the project. Input data, such as acquired images, product information, and transactions, are processed and analyzed to generate relevant output data, such as identified products, inventory updates, and statistical reports.

Overall, this project represents an intelligent approach to optimizing the process of product identification in a self-service environment, integrating advanced knowledge and modern technologies to provide an efficient and automated solution, with benefits for both customers and self-service staff.

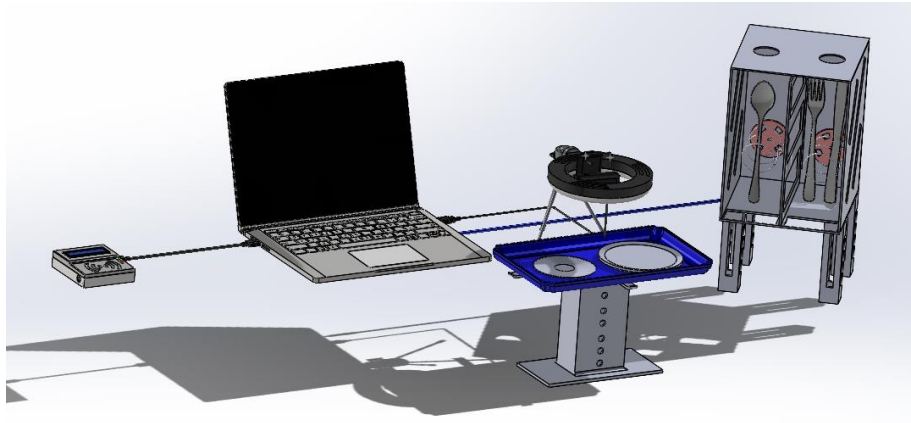


Fig. 1 Equipment for product identification in a self-service environment

2. The structure and operational principles of experimental model

In this chapter, we will explore in detail the overall structure and operating principles of the system designed for product identification in a self-service environment, according to the information provided earlier. We will analyze the global functions of the system, which include interaction with customers and self-service staff, data capture and processing methods, as well as database generation and updating.

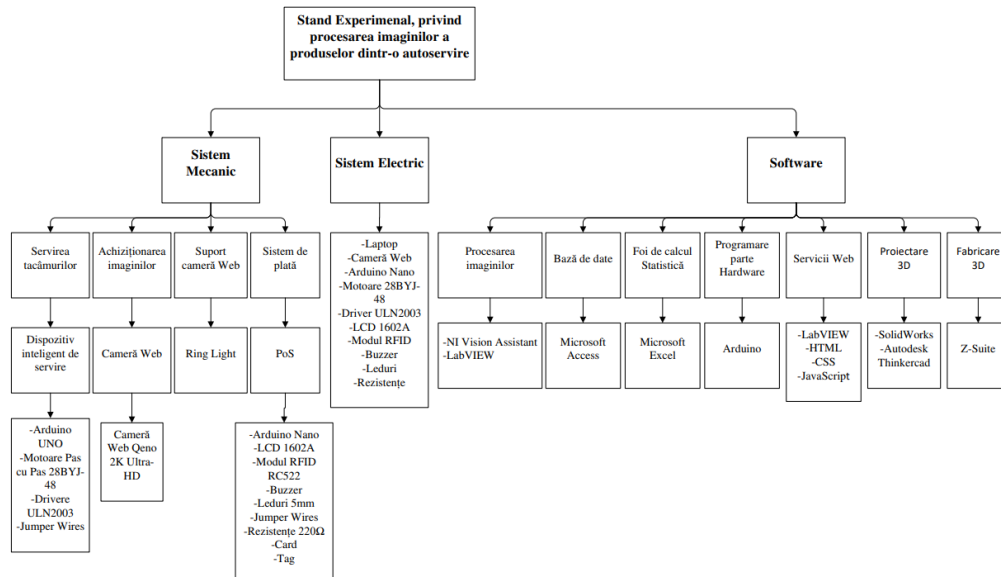


Fig. 2 The architectural diagram of the system

Additionally, the interface with web services is presented, which enables communication between the various components of the system, the way the system interacts with hardware and software environments, such as the webcam, payment terminal, and intelligent utensil serving device.

So, starting from a data flow diagram, this product identification project comprises two parts:

- The serving application
- The training application

The serving application is a software designed for the customer, intended to provide them with an efficient service of automatic processing of selected products, including identifying types of food, instantly calculating the payment amount, and automatically serving utensils.

The training application was created to support the services provided by self-service staff, providing them with tools for automatically inserting images into the food classification file and writing them into the database. This software enables efficient writing and management of new types of food in the application, allowing customers to purchase recently added meal options. Additionally, qualified staff have the ability to directly edit the product database from the application and can also view statistics of products sold.

So, the entire system presents both input and output data:

For the customer serving application, the input data consists of:

- Images acquired using the webcam.
- Information regarding payment transaction: payment button and PoS card.
- Products manually added by the customer through the available menu.

On the other hand, the output data includes:

- Identified products: the names and prices of products identified in the images captured by the webcam.
- Transaction confirmation for payment.
- Utensil serving based on the identified products.

For the training application, the input data consists of:

- Product information: the names and prices of products manually entered by self-service staff, whether as new additions or updates to the system.
- Image acquired using the webcam.

As the same time, the output data consists of:

- Database updates.
- Writing the CLF file.

The common output data for both applications consists of:

- Inventory updates.
- Statistics and reports.

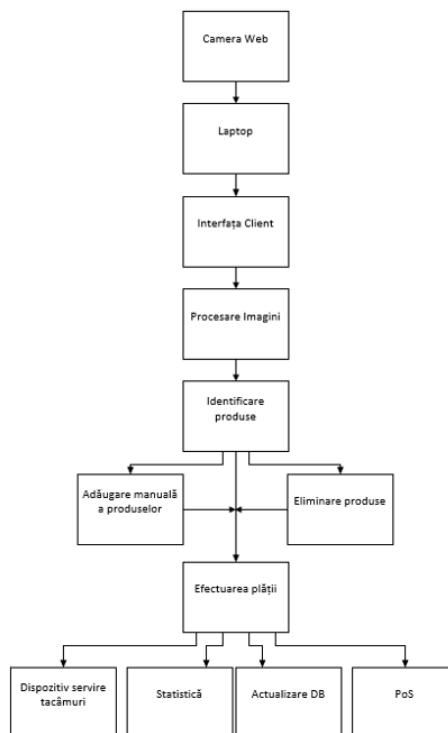


Fig. 3 Assembling the software components for running the client application

As depicted in the above diagram, the client application operates as follows:

The application is started, the board with products is placed on the specially designed stand and then the processing button is pressed.



Fig. 4 Testing the client application

Following the calculation process, on the right side of the screen, the identified products are displayed along with their respective prices. Below the list of identified products, a total payment for all purchased items is displayed. If manual addition of products not found on the tray is desired, the "Menu" button is pressed, which opens a new page.



Fig. 5 Choosing products using the menu

The products are chosen one by one and by accessing the "Add" button, each is added to the main list of purchased items. Pressing the "Home" button closes the menu page, returning to the initial interface. Additionally, if a product needs to be removed from the main list, the "X" button next to the intended product can be pressed for deletion. Finally, after all desired products have been selected, pressing the payment button concludes the entire process. During payment, the quantities of products are decremented by one unit from the database, and sales reports are updated in real time.



Fig. 6 Making the payment

By using the payment terminal, the aim was to simulate the real transaction process with the help of cards. If the customer has a valid card, in this case, the white card, the payment is successfully made. This is

signaled by a suggestive message, the illumination of a green LED, and the initiation of a sound through a speaker.

If the customer's card doesn't have sufficient funds or is not valid, a specific informational message appears, and a red LED lights up. This is simulated through a tag, as can be observed in the third image.

After the payment has been made, the order is sent to the cutlery serving device. Depending on the products in the shopping list, motor 1, which serves spoons, motor 2, which serves forks and knives, or both motors will start. Motor 1 starts when products that can be served with a spoon are identified in the list, while motor 2 starts when products that can be served with a fork and knife are identified.

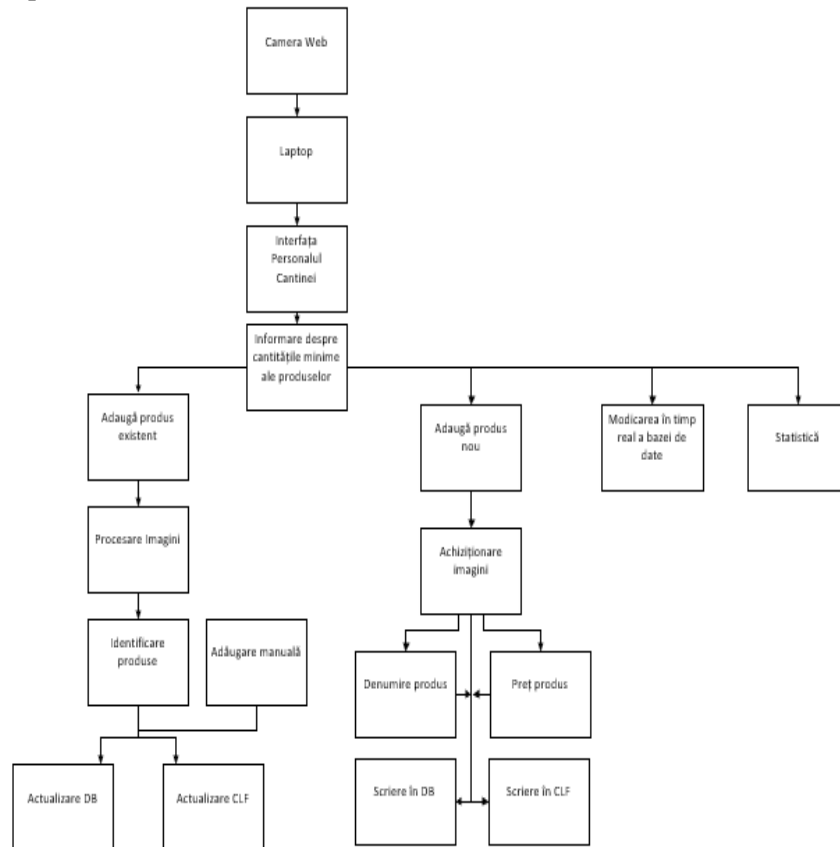


Fig. 7 Assembling the software components for running the application with the self-service staff

As can be observed, the second application functions as follows: the application is started, and based on a created script, a dialog window displaying products whose quantity is below the minimum limit, less than or equal to 3, is shown from the beginning. At this point, authorized personnel confirm receiving the message and are required to update the quantities in the database. To do this, they click on the dedicated edit button, and a new page opens for them.

Ciorbe	Feluri principale	Garnituri	Salate	Desert	Bauturi
Ciorba_pui	Carnati	Cartofi_prajiti	Salata_de_castraveti	Amandina	Apa_minerala
Ciorba_de_perisoare	Ceafa_de_porc	Cartofi_la_cuptor	Salata_rosii_castraveti	Ecler	Apa_plata
	Chiftele_cu_sos	Legume_mexicane	Salata_de_gogosari	Tiramisu	Coca_cola
	Noodles_cu_pui	Orez	Salata_de_sfecla	Trio-Mouse-Ciocolata	Fanta
	Piept_de_pui	Piure_de_cartofi	Salata_de_varza		Sprite
	Pomana_porcului				
	Pulpe_de_pui				
	Snitel_de_pui				

Produs selectat	Pret	Cantitate
Pulpe_de_pui	12	50

Fig. 8 Editing the database directly from the application

Now, any product from the respective list can be selected and both a price and a quantity can be assigned to it. After assigning these, the 'Edit' button is pressed to make the changes and finally, the exit button is pressed to return to the main page.

Furthermore, if there's a need to add a new product, the suggestive button for this operation is pressed, which triggers the algorithm to extract the circular zone, including the identified plate. For the chosen product, to introduce it into the customer-serving application, its name and price are entered. By pressing the 'Add' button, the extracted image of the product is added to the classification file, automatically creating the product class. At the same time, the database undergoes modifications by inserting the new product into the table, including its name, price, and default quantity of one unit. For the application to perform optimally with this added product, the classification file needs to receive multiple images of the product, in various shapes and angles. To achieve this, we utilize the second utility of the application, which is to add an existing product.

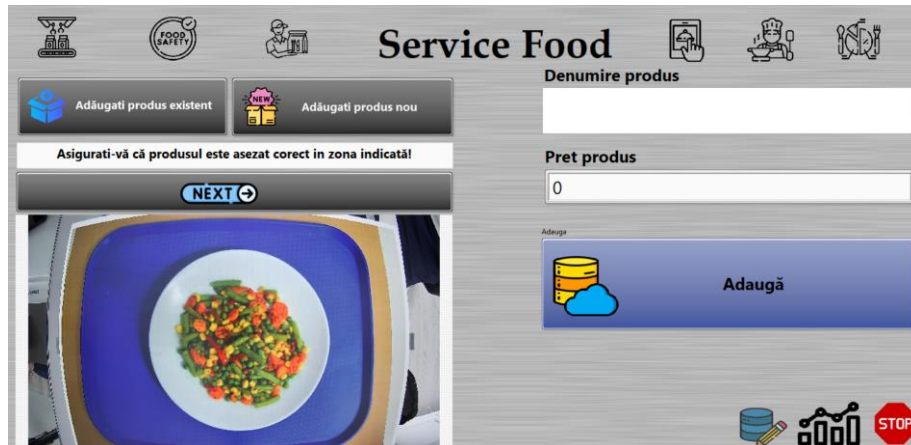


Fig. 9 Inserting new products

Similar to the customer-serving application, an existing product that has already been introduced into the application is chosen, and the product identification algorithm is applied. If the product is correctly identified, the 'Correct Add' button can be pressed, which inserts the extracted image into the classification file, in the class with the same name as the product. Additionally, the quantity of the product is updated in the database by one unit.



Fig. 10 Adding existing products

If we proceed with the other scenario, where the product is not correctly identified, the 'Incorrect Add Manually' button is pressed, which opens a new page where the correct product can be chosen. Additionally, within the same application, we can view statistics for certain operations, such as the quantity of products sold, the date and amount collected, and the quantity of products sold on a specified day.

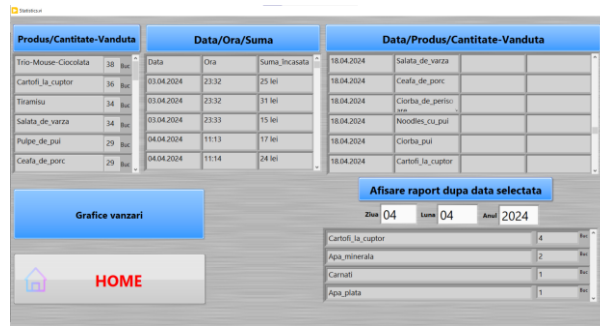


Fig. 11 Generated Reports

One final functionality of the experimental model involves reading data from the internet using a created web page.

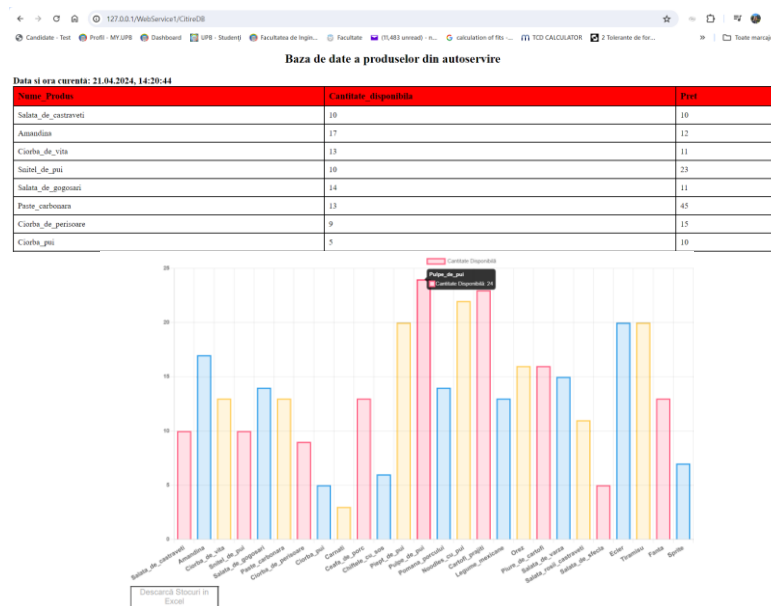


Fig. 12 Reading data from the Internet

3. Conclusions

By implementing this experimental automation model, the aim is to simplify all activities within self-service setups and minimize the working time required.

4. Bibliography

- [1] <https://logmeal.com/api> (Accessed on 05.09.2023)
- [2] <https://forums.ni.com/t5/LabVIEW/LabVIEW-Analytics-and-Machine-Learning-Toolkit-2018/m-p/4137391> (Accessed on 05.02.2024)
- [3] <https://users.utcluj.ro/~tmarita/IPL/IPCurs/C1.pdf> (Accessed on 10.03.2024)

DESIGN AND REALIZATION OF AN EXPERIMENTAL CHESS PLAYING ROBOT MODEL

GHENA Flaviu; SAVU Tom

Faculty: Industrial Engineering and Robotics, Specialization: Informatică Aplicată, Year of study: 4,
e-mail: ghen.flaviu@gmail.com

ABSTRACT: Robotic arms have been proven to be extremely useful in a lot of applications and domains such as assembly industry, handling machine tools, welding, die casting etc. The proposed system aims to demonstrate the integration of the Stockfish v16.1 chess engine and the KINOVA Gen3 Lite Robot Arm, using image processing. During gameplay, the robotic arm's movements are controlled using the graphical programming environment LabVIEW and the input is received from the Python program that makes the Stockfish engine program calls. The image processing is achieved by the LabVIEW NI Vision Assistant's processing functions that were integrated and further processed into the LabVIEW program.

KEYWORDS: LabVIEW, Python, șah, procesare imagini;

1. Introduction

Robotic arms are increasingly being used outside industrial factories, not just inside them, to perform repetitive tasks in certain jobs, to provide assistance services to people with disabilities and beyond, and to carry out certain complex activities. This project titled 'DESIGN AND IMPLEMENTATION OF AN EXPERIMENTAL MODEL OF A CHESS PLAYING ROBOT' aims to undertake such a complex activity, specifically the programming of the KINOVA Gen3 Lite robotic arm to act as an opponent in a chess game. It will be capable of observing whether the chessboard is positioned and oriented correctly based on the color of the pieces it is playing with, making moves in accordance with the chosen difficulty level, and pressing the clock button to complete its move and switch turns to the other player.

2. Details of the robotic arm

The KINOVA Gen3 Lite robotic arm consists of a base, actuators, forearm, wrist, and gripper (see Fig.1) [1].

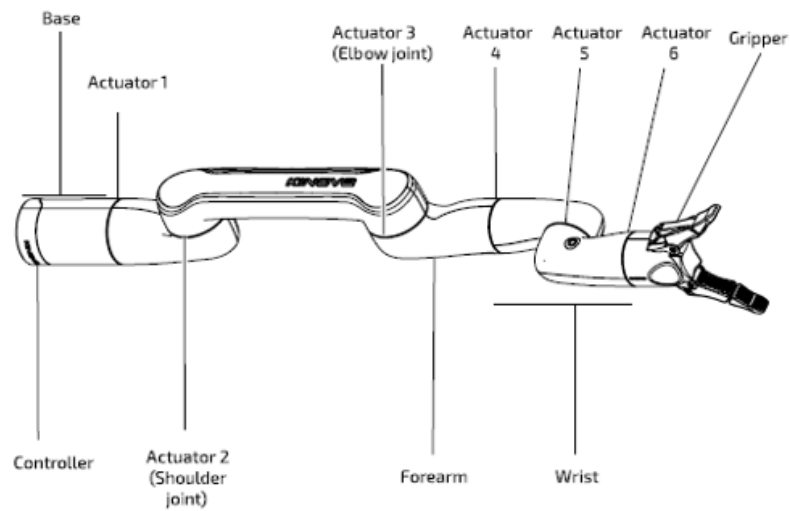


Fig. 1. The main components of the robotic arm

Table 1. Characteristics of the KINOVA Gen3 Lite robotic arm

Degrees of Freedom	6
Payload	0.5 kg
Total Mass	5.4 kg
Maximum Reach	760 mm
Maximum Speed	25 cm/s
Actuator Angle	± 155 to 160°
Power Supply Voltage	21 to 30 VDC, 24 VDC nominal
Average Power	20 W
Protection Rating	IP22
Operating Temperature	0°C to 40°C
Degrees of Freedom	6

3. Objectives

Given that the robotic arm needs to make precise moves that do not disturb the other pieces on the board, both the size and correct positioning of the pieces must be taken into account, maintaining a constant level of brightness throughout the game. The logic of the LabVIEW program [2] consists of multiple While loops and executes a series of frames within a main Flat Sequence, as presented below:

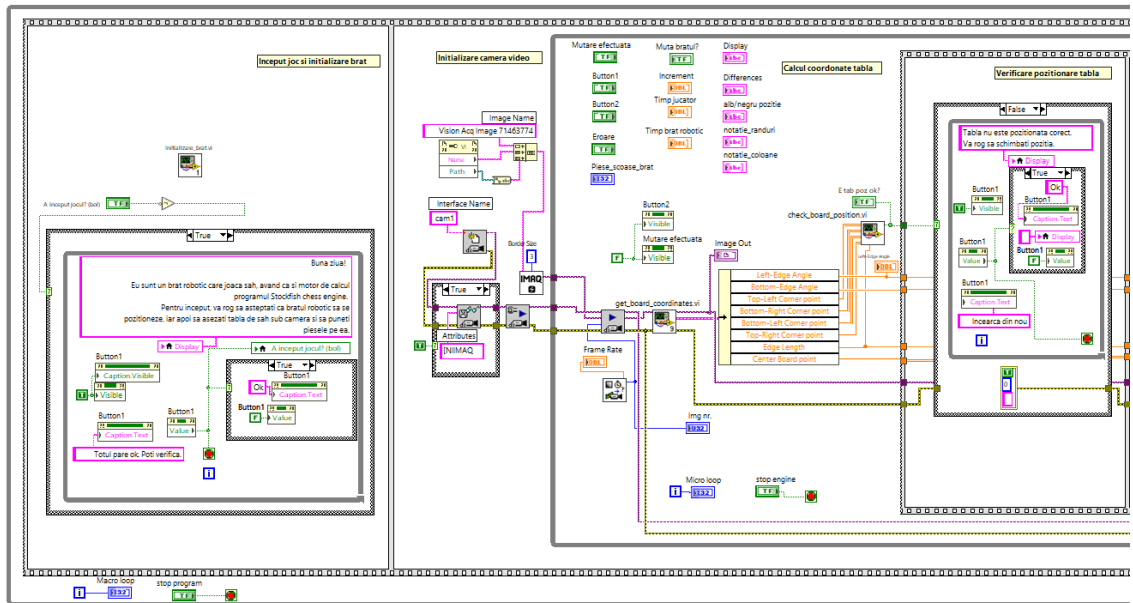


Fig. 2. First part of the LabVIEW program

Here you can see, from left to right, the logic of the LabVIEW program for the chess game:

- **Game start and arm initialization:** the robotic arm is initialized, and the player is asked to position the chessboard under its camera if they haven't done so already.
- **Camera initialization:** the camera mounted on the robotic arm will capture images of the chessboard.
- **Chessboard coordinate calculation:** data such as the angle of the left edge and bottom edge of the chessboard, corner coordinates, average edge length in pixels, and center coordinates are obtained. At this step, the position of the chessboard is checked to verify if the algorithm can continue.
- **Board positioning check:** The positioning of the chessboard is verified, and if the board is not correctly positioned, the user is asked to adjust its position.

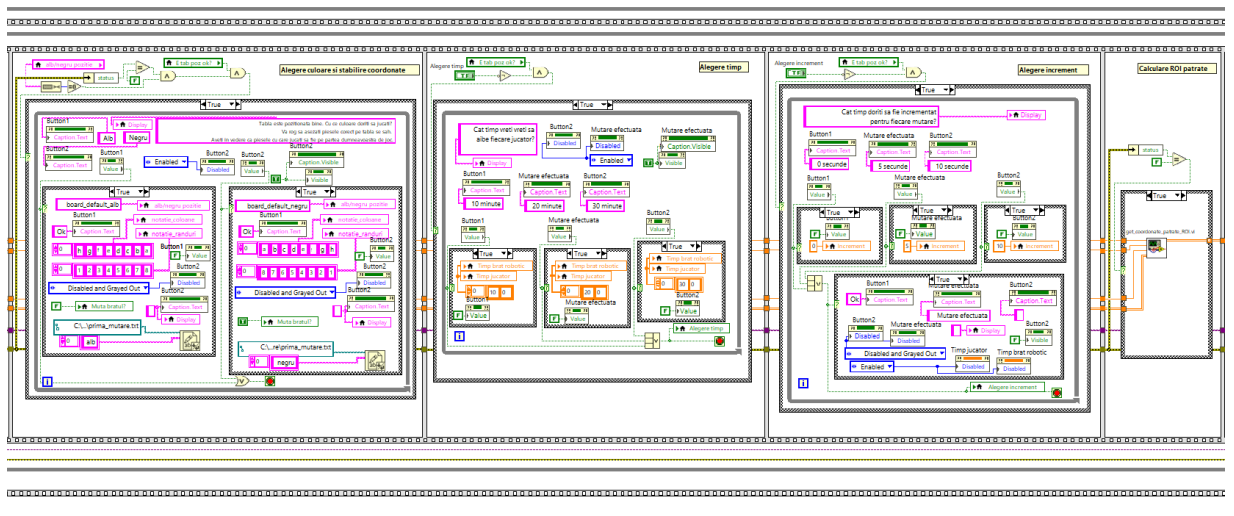


Fig. 3. Second part of the LabVIEW program

- **Color selection and coordinate establishment:** The user is asked to choose the color they want to play with. Here, the coordinates of the chessboard are initialized, and it is determined who will make the first move. These data are then transferred to the Python program through text files.
- **Time selection:** The user is asked to choose the game time.
- **Increment selection:** The user is asked to choose the increment time for each move.
- **Calculation of ROI squares:** The matrix of coordinates of the game squares is calculated.

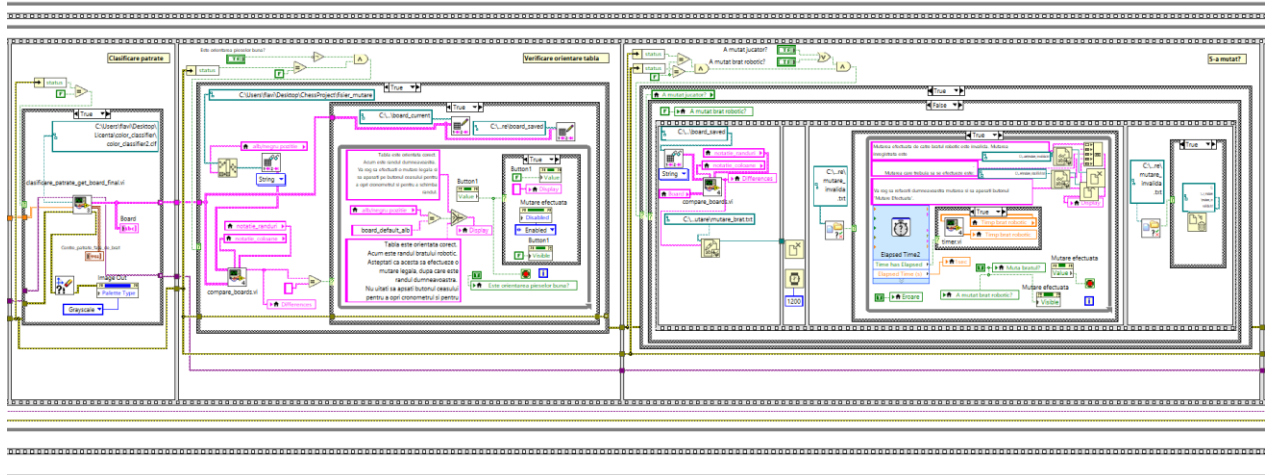


Fig. 4. Third part of the LabVIEW program

- **Square classification:** Each square of the chessboard is classified using the CLF file, and the matrix of the chessboard with all squares classified is created.
- **Board orientation check:** If the orientation of the chessboard is correct, the game can continue. Otherwise, the user is asked to adjust the board's position.
- **Has a move been made?:** At this step, it is checked whether one of the players has made a move, and this move is transmitted to the Python program [3], which decides whether it is legal or not. This step becomes active after the second iteration of the program when one of the users makes a move.

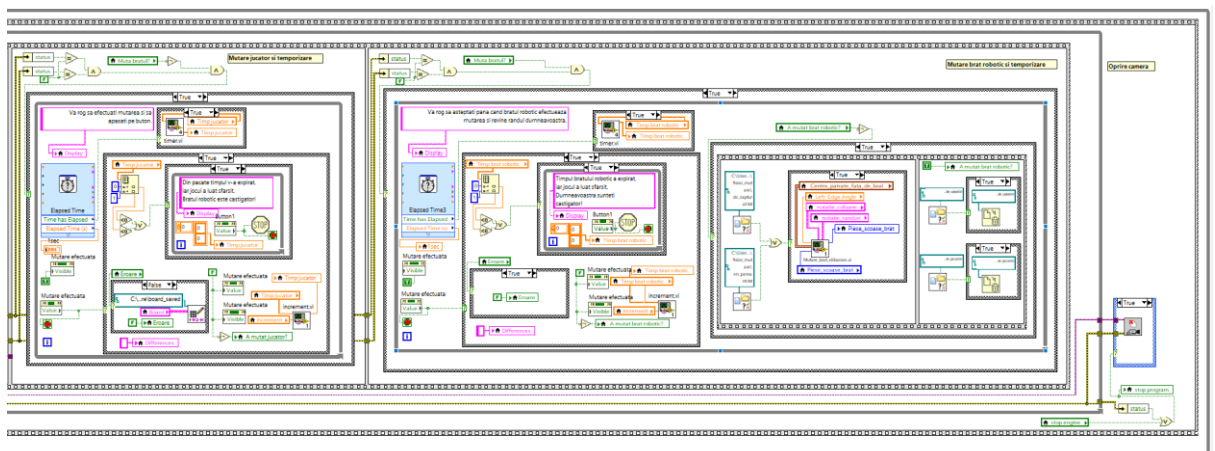


Fig. 5. Fourth part of the LabVIEW program

- **Player move and timing:** In this stage, the user must make a move and press a button if it's their turn to move, while their game time is running out.
- **Robotic arm move and timing:** In this stage, the robotic arm executes the move transmitted by the Python program and presses a button if it's its turn to move, while its game time is running out
- **Camera shutdown:** At the end of the game, the camera session is terminated.

These things were made possible through image processing using a camera attached to the robotic arm. These images were processed using image processing functions from the NI Vision Assistant module [4] in LabVIEW. The data provided by these images were further processed in a LabVIEW Instrument program to create a matrix of regions of interest for each square of the chessboard. These were classified using the Color Classification function from the NI Vision Assistant, using a CLF file trained with pictures of the chessboard taken from the initial position of the robotic arm for different brightness levels. Since the Stockfish chess engine v16.1 [5] program does not require specifying the moved piece but only the squares where the move was made, it was sufficient to classify the squares in images based on the color of the piece and the color of the square it was on. This resulted in the following categories: "Alb", "Alb_pe_alb", "Alb_pe_negru", "Negru", "Negru_pe_alb", "Negru_pe_negru" (see Fig. 6).

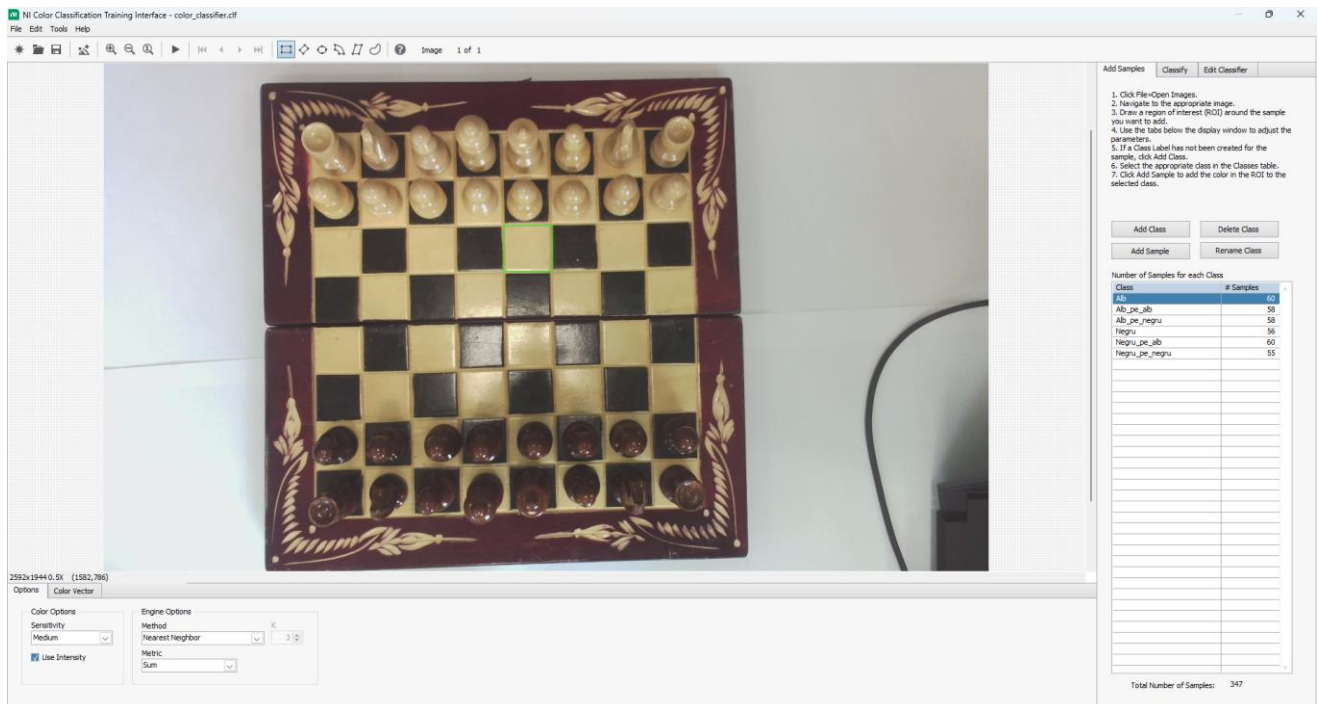


Fig. 6. Training of the CLF file

To obtain the matrix of chessboard squares and the matrix of their center points, the following functions from the NI Vision Assistant program were used, and their data were subsequently processed:

- **Find Straight Edge:** This function is used to locate a straight line within a region of interest, based on parameters such as direction and others like "Edge Polarity," "Minimum Edge Strength," "Projection Width," "Gap," etc. This function was used four times to find the edges of the chessboard, as well as their angle, to calibrate the matrix of squares for the chess game and to transmit precise moves to the robotic arm.
- **Caliper:** This function is used to perform measurements on certain points. It was used to obtain the corner points of the chessboard, the length of the edges in pixels, the midpoints of the edges, and the center of the chessboard.

The commands for the robotic arm were executed using functions from the KINOVA.llb library (see Fig. 7).

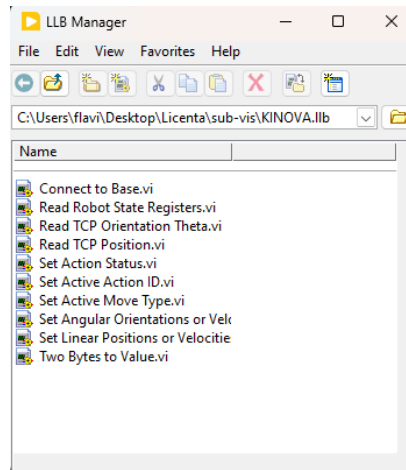


Fig. 7. The KINOVA library in LabVIEW

To obtain the movements of the robotic arm, the LabVIEW Instruments program used to control the robotic arm communicates throughout the game with the Python program containing the functions of the Stockfish chess engine v16.1 program by writing and deleting text files from a common location in the laptop's memory (see Fig. 8). Here, it also checks whether the moves made are legal or not.

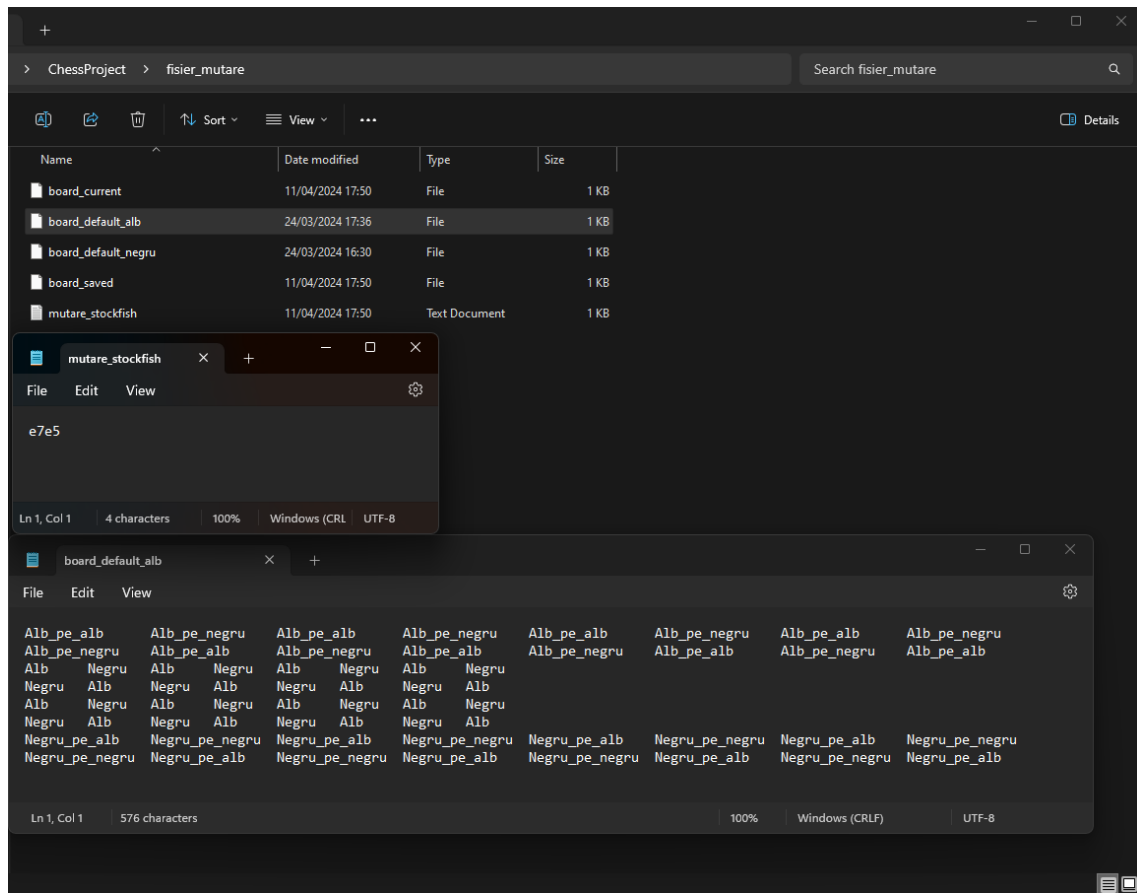
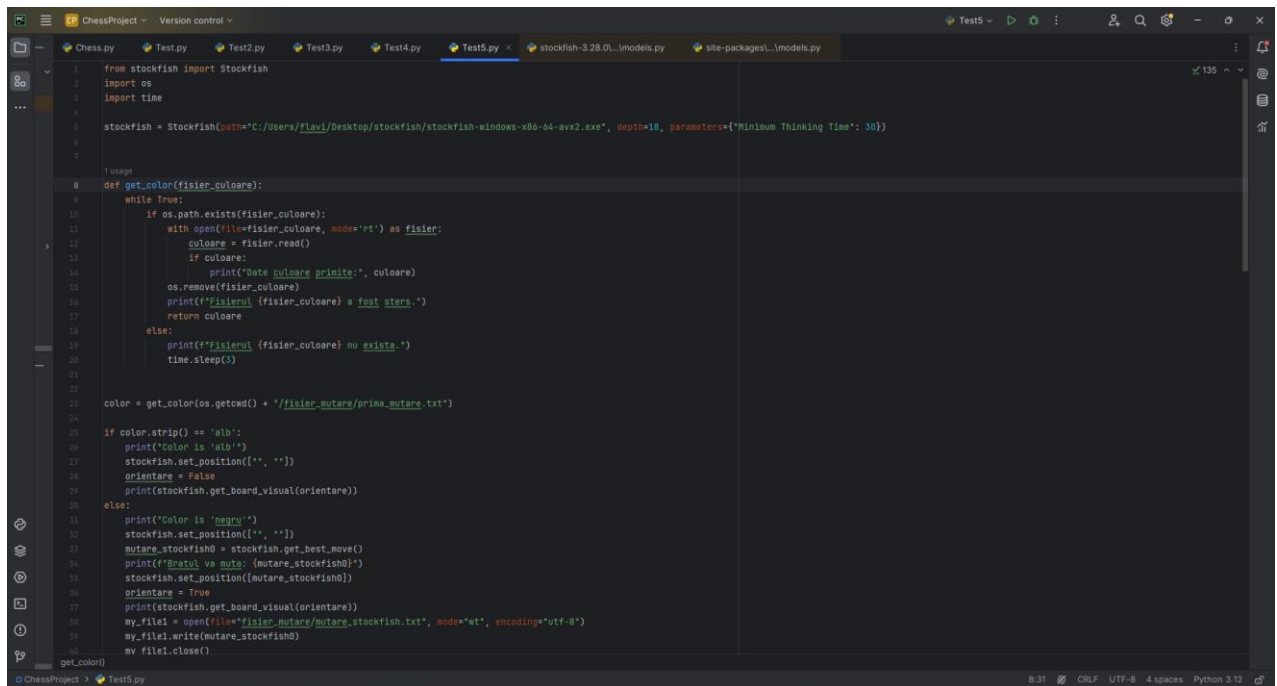


Fig. 8. Communication between the LabVIEW program and Python

The Python File program used to call the Stockfish chess engine v16.1 utilizes the `os`, `time`, and `stockfish` [6] libraries. It contains the location of the engine itself, as well as parameters for difficulty, "depth," "minimum thinking time," etc. It includes a function that retrieves the color chosen by the user from the Front Panel of the LabVIEW Instruments program to synchronize the column and row notations with those in LabVIEW. Additionally, it includes a function that constantly checks whether a move has been made or not by verifying the existence of the user's move file in the common folder. It processes, deletes, and writes the move that the robotic arm is about to make. In case of an error, such as an incorrectly made move, the program generates a file indicating this, and the steps to resolve the issue will be displayed on the Front Panel display of the LabVIEW Instruments program.



```
1 from stockfish import Stockfish
2 import os
3 import time
4
5 stockfish = Stockfish(path="C:/Users/Flavi/Desktop/stockfish/stockfish-windows-x86-64-avx2.exe", depth=18, parameters={"Minimum Thinking Time": 50})
6
7
8 def get_color(fisier_culoare):
9     while True:
10         if os.path.exists(fisier_culoare):
11             with open(file=fisier_culoare, mode="rt") as fisier:
12                 culoare = fisier.read()
13                 if culoare:
14                     print(f'Date culoare printate:', culoare)
15                     os.remove(fisier_culoare)
16                     print(f'Fisierul {fisier_culoare} a fost sters.')
17                     return culoare
18             else:
19                 print(f'Fisierul {fisier_culoare} nu exista.')
20                 time.sleep(3)
21
22 color = get_color(os.getcwd() + '/fisier-mutare/prima_mutare.txt')
23
24 if color.strip() == 'alb':
25     print('Color is ' + 'alb')
26     stockfish.set_position(['', ''])
27     orientare = False
28     print(stockfish.get_board_visual(orientare))
29 else:
30     print('Color is ' + 'negru')
31     stockfish.set_position(['', ''])
32     mutare_stockfish0 = stockfish.get_best_move()
33     print(f'Bestul va muta: {mutare_stockfish0}')
34     stockfish.set_position([mutare_stockfish0])
35     orientare = True
36     print(stockfish.get_board_visual(orientare))
37     my_file1 = open(file="fisier-mutare/mutare_stockfish.txt", mode="wt", encoding="utf-8")
38     my_file1.write(mutare_stockfish0)
39     my_file1.close()
40
41 get_color()
```

Fig. 9. First part of the Python program

4. Conclusions

The objective of this project is promising considering that robotic arms are becoming increasingly common in everyday life, and it may be of genuine interest to chess enthusiasts as well as exhibitions or tournaments of this kind. As long as the CLF file is calibrated for lighting conditions, the robotic arm can function without impediments.

5. Bibliography

- [1] <https://www.kinovarobotics.com/product/gen3-lite-robots>
- [2] <https://www.ni.com/en/shop/labview.html>
- [3] <https://www.python.org/>
- [4] <https://www.ni.com/docs/en-US/bundle/ni-vision-assistant-help/page/visionassist.html>
- [5] <https://stockfishchess.org/>
- [6] <https://pypi.org/project/stockfish/>

DESIGN AND BUILDING OF AN EXPERIMENTAL MODEL OF A ROBOT SYSTEM FOR HANDLING SOME CONTAINERS IN A CHEMISTRY LABORATORY

PAVEL Mirel-Ionut; ROSU Maria Magdalena; SAVU Tom

Faculty: Industrial and robotics engineering, Specialization: Applied informatics, Year of studies: 4,
email: office.pavelionut@gmail.com

ABSTRACT: The chosen work proposes the building of an image detection algorithm and the designing of a sequence of movements using an articulated robotic arm in order to manipulate some containers in a chemistry laboratory. The objective will be achieved using as main components an articulated robotic arm, equipped with a video camera for image detection and various supports made using additive manufacturing.

KEYWORDS: Robotic arm, image processing, additive manufacturing, robotic arm movement sequence

1. Introduction

The project consists in the development of an experimental model of a robotic system consisting mainly of an articulated robotic arm that will work in the field of chemical laboratory experiments. The project includes two major categories of components, namely: the hardware component and the software component. The hardware component will be composed of a Kinova articulated robotic arm, a web camera, an Arduino-type unsoldering board and related elements, travel limiters, a web camera support made through additive manufacturing and Berzelius cup holders also made through additive manufacturing. The software component it will be composed of Solid Edge 2022 design software, Prusa Slicer software for programming a 3D printing machine and the suite of software programs from National Instruments, namely NI Vision Assistant and Labview.

2. The current state of the analyzed situation

A robotics application has been developed at the University of Liverpool that uses a fully autonomous mobile robot to assist scientists in research. The robotic system has been designed to run continuously for weeks on end, allowing it to analyze data and make decisions regarding what to do next. Using a custom gripper as a flexible arm, it has been calibrated to interact with most standard lab equipment and machinery, as well as having safety measures implemented to safely navigate around human colleagues and obstacles.

The mobile robot platform is shown in **Fig. 1a** and Extended Data Fig. 1. It can move around the lab and locates its position using a combination of laser scanning coupled with touch feedback for fine positioning. This gave a positioning accuracy (x, y) of ± 0.12 mm and an orientation accuracy of $\theta \pm 0.005^\circ$ in a standard laboratory environment with dimensions of 7.3 m \times 11 m (Fig. 1b).

This precision allows the robot to perform object manipulations at the various stations in the laboratory (Fig. 1c – 1e). These object manipulations are comparable to those performed by human researchers, such as handling sample vials and operating instruments. The robot has dimensions and radius similar to a human operator (Fig. 1a, d) and can therefore operate in a conventional, unmodified laboratory.

Taking into account the time required to recharge the battery, the robot can work up to 21.6 hours/day with optimal programming. The robot uses laser scanning and tactile feedback, and does not

guide itself using a vision system. Therefore, it can operate in complete darkness if necessary, which is an advantage when performing light-sensitive photochemical reactions. The robot arm and mobile base meet safety standards for collaborative robots, allowing human researchers to work in the same physical space. In **Figs 1.a - 1.e** are show the main operations performed by the autonomous robotic platform. [1]

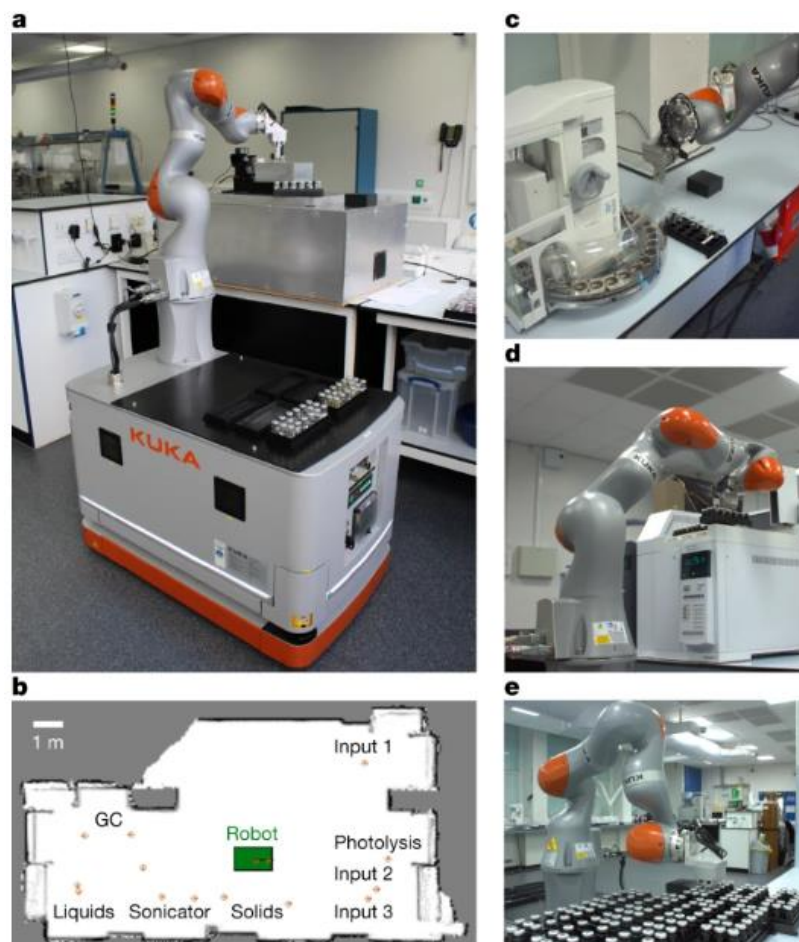


Fig. 1a-1e The main operations performed by the autonomous robotic platform

3. Product development, programming and testing of the IT application

In this chapter, the hardware and software components of the project will be detailed and the rationale behind the choice of each individual component will be explained. After analyzing the final objective of the project, suitable components were selected to fulfill the project objectives as easily as possible.

The technical specifications of the Kinova gen3 Lite articulated robotic arm recommend it as suitable for this type of robotic application because the 6 degrees of freedom, the range of action of 760mm and the maximum load of 0.5kg are sufficient for the successful completion of any sequence of movements bounded by a narrow space. More technical specifications are presented in **fig. 2**.

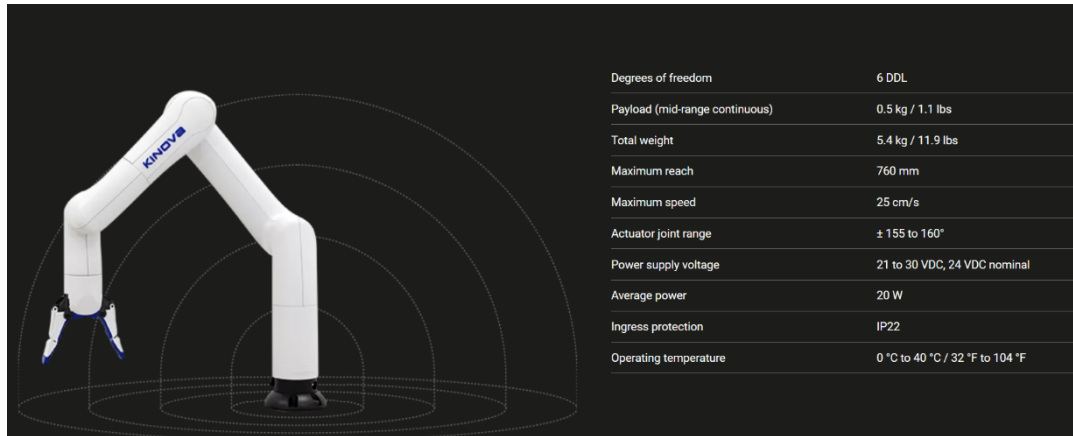


Fig. 2. The technical specifications of the Kinova gen3 lite robotic arm

The Arduino type development board and the stroke limiter were chosen for the ease with which they can be integrated into any robotic, automation or mechatronics application. Within the project, they will be used to acquire digital signals from the field and integrate them into the sequence of movements that the robotic arm will perform. **Fig. 3** shows the hardware configuration used to connect the acquisition board and the stroke limiter.

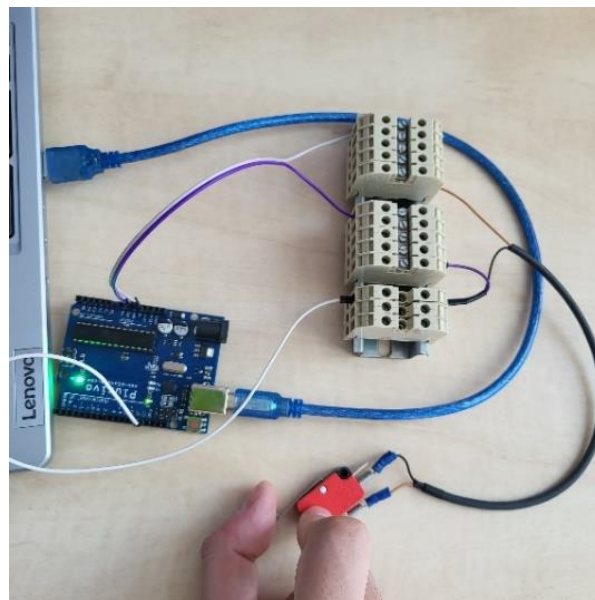


Fig 3 Hardware configuration used for connecting the acquisition board and the stroke limiter

The hardware part is completed by 2 Berzelius cup holders made using additive manufacturing. One of the supports will be composed of 6 different items and will be used to support 3 Berzelius glasses. The other cup holder will be used for mixing chemical solutions. The 3D modeling was carried out in the Solid Edge 2022 software with a view on maximizing the reduction of material used and shortening of the printing time. The maximum volume of liquid contained in each Berzelius glass will not exceed 125ml. **Fig. 4 and 5** shows the isometric views of the 2 cup holders.



Fig. 4 Isometric view of the cup holder

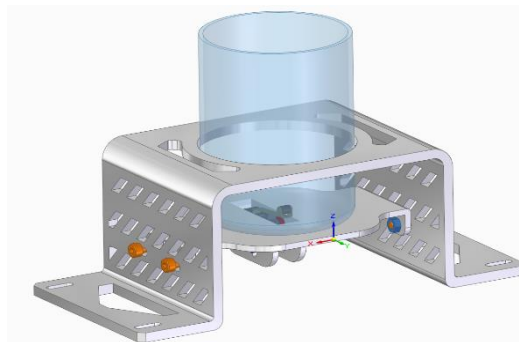


Fig.5 Isometric view of the mixture cup holder

In order to achieve the proposed scenario in which the robot will form a chemical solution by mixing two separate substances, the robotic application will perform a series of steps that will consist of moving the robotic arm in previously programmed fixed positions but also creating a detection algorithm so that the robotic arm will move in positions that can vary. To program the robotic arm and ensure communication between all the devices, the Labview software from the National Instruments suite of programs was used. A project was created that contains a collection of Vi's also created individually to serve for the movements of the robotic arm in each step of the program. In **fig. 6** you can see the code section for moving the robotic arm in a fixed position. Once started, the program will call an ID of an action already programmed in the robotic arm programming platform.

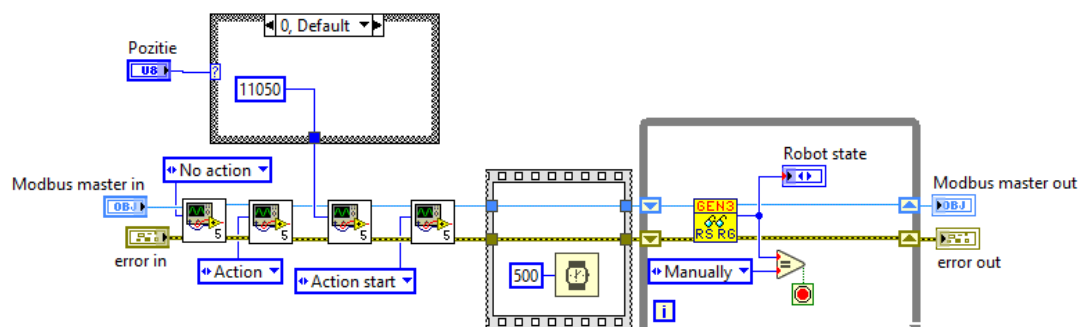


Fig. 6 Code section for moving the robotic arm in a fixed position

In order to move in a variable position determined by the coordinates of the QR code, the robotic arm will move in two previously described intermediate positions from where it will calculate the variable position based on two pictures that will be taken using the web camera attached to the robot. Following the detection from two positions of a QR code mounted on the Berzelius cup holder, the robotic arm will automatically move to the first cup, it will grip it and move to a separate holder for mixing substances. **Fig. 7** describes the code section related to the detection and processing of the QR code image. **Fig. 8** shows the code section related to the calculation of the distance and orientation of the cup holder in relation to the robotic arm.

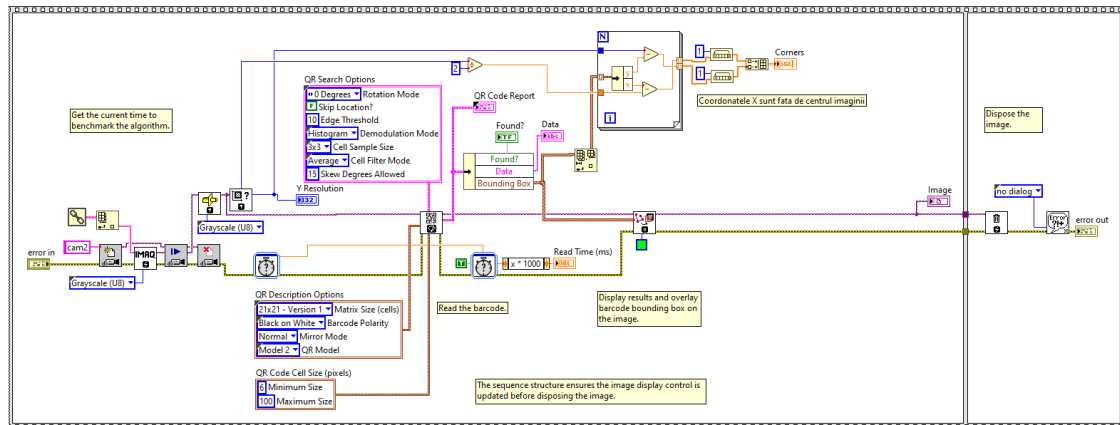


Fig 7 Detection and processing of the QR code

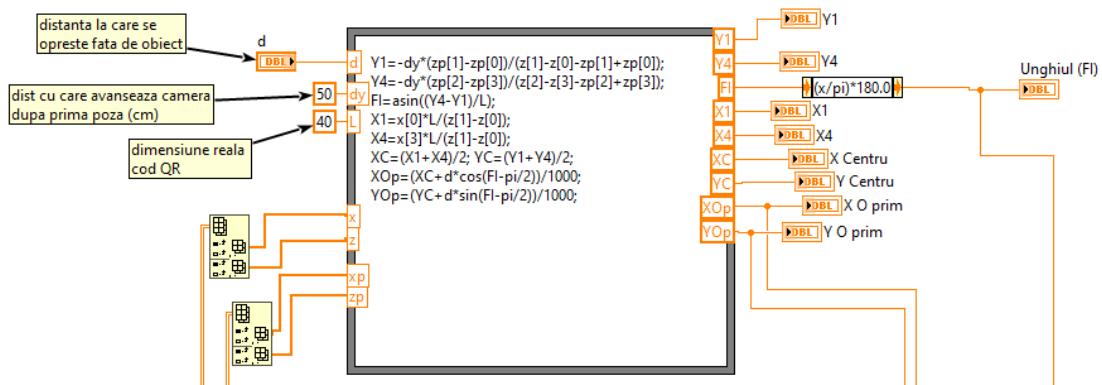


Fig.8 Calculations of the distance and orientation of the cup holder in relation to the robotic arm

Afterwards, the arm will move with the first empty Berzelius glass in a predetermined position and will wait for feedback from the program regarding the correct positioning of the glass in the support. After receiving this feedback, the program will automatically continue moving the robotic arm to the position from which will take over, in turn, the next two glasses with liquid to mix them in the area of the mixing stand. **Fig.9** shows the part of the program in which the feedback of the correct positioning of the glass is obtained by means of a stroke limiter mounted at the base the mixing stand.



Until now, all hardware components have been purchased, manufactured, assembled and tested. Regarding the testing part of the computer application, the program is complete until the step where the computer application obtains the coordinates of the QR code necessary to determine the distance and orientation of the cup holder in relation to the robotic arm.

The final objective of the project is to succeed with the help of the developed robotic system in reducing the need for the presence of a human operator in the performing of laboratory chemical experiments where harmful or dangerous substances for humans are present. As future development directions and for the robotic system to operate in ideal conditions, the entire robotic system will be isolated in a controlled atmosphere room so that, following chemical experiments, any hazardous substances/gases emitted will be filtered and separated from the atmosphere in the rest of the laboratory.

- [1] Burger, B., Maffettone, P.M., Gusev, V.V. *et al.* A mobile robotic chemist. *Nature* **583**, 237–241 (2020). <https://doi.org/10.1038/s41586-020-2442-2>
- [2] Conf.dr.ing Tom SAVU, .. 06-FIIR-L-A1-S1: Programarea calculatoarelor și limbaje de programare 1 (Seria IAI - 2020)
- [3] Conf.dr.ing Tom SAVU, .. 06-FIIR-L-A2-S2: Analiza și prelucrarea imaginilor (Seria IAI - 2021)
- [4] Conf. dr.ing Mihaela-Elena ULMEANU, .. 06-FIIR-L-A2-S2: Bazele proiectării tehnologice asistate de calculator (Seria IAI - 2021)
- [5] Conf. dr.ing Cristian-Vasile DOICIN, .. 06-IIR-L-A4-S1: Tehnologii și echipamente pentru fabricare aditivă (Seria AD - 2023)

RESEARCH ON THE DESIGN OF AN ALGORITHM AND DEVELOPMENT OF A SOFTWARE APPLICATION FOR INTELLIGENT RECOGNITION OF MOVING PRODUCT TYPES AND THEIR SORTING USING A BILATERAL ELECTRIC PLUG UNLOADER COMMAND

CIOBANU Marius-Sebastian; BIGAN Cristin

Faculty:FIIR Specialization:IAII, Year of Study:4, e-mail: c.sebastianm07@gmail.com

ABSTRACT: The main goal of this project is to design an algorithm and develop a software application that allows for the intelligent recognition of various types of products moving on a conveyor belt. The algorithm will use data obtained from optical and video sensors to identify the distinctive characteristics of each product such as shape, size, color, and markings. Based on this information, the products will be automatically sorted according to predefined specifications. This will be achieved with the help of an Arduino UNO R3 acquisition board equipped with a Sensor Shield V5.0, a webcam, and proximity sensors, components that will be connected to a computing system equipped with Matlab.

KEYWORDS: conveyor belt, Arduino, intelligent recognition, programming, algorithm

1. Introduction

The project will contain all the methodological steps provided in the diploma project guide. The initial part of the project will present information about the types and models of conveyor belts used in the industry, models for sorting various types of objects used in the industry, and the progress regarding their evolution. To optimize the process of identifying and sorting objects, the conveyor will be equipped with 3D printed accessories but will also have purchased components for the entire assembly, such as various servomotors, certain sensors, or supports for accessories.

The algorithm and the software part will be implemented in Matlab and Simulink programs, as well as Arduino IDE for executing certain commands from the control board compatible with the Matlab and Simulink environment. The specific board is the Arduino UNO R3 equipped with a Sensor Shield V5, which will contribute to the proper functioning of the servomotors that operate the sorting device and the proximity sensors that will ensure the correct sorting of products by correcting errors according to the electrical diagram in Figure 1.

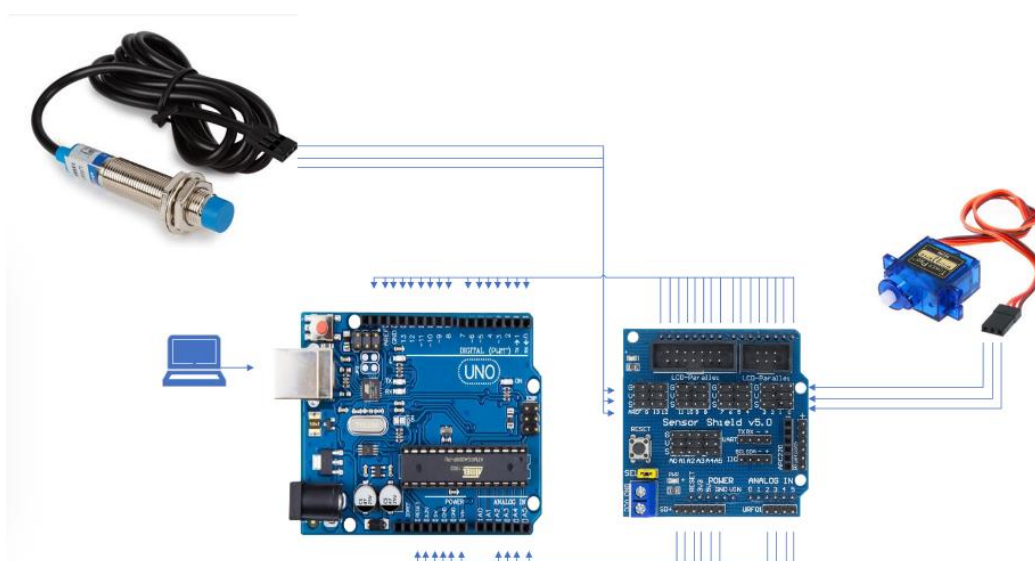


Fig.1.Electrical Diagram

2. Current Status

Sorting devices on conveyor belts have come a long way from simple systems based on magnetic tapes or photoelectric cells in the early days of automation. Nowadays, a wide range of advanced technologies are used to sort a variety of products with high precision and efficiency.

Examples of sorting devices include optical ones that use video cameras and algorithms to identify and classify products based on their visual characteristics such as shape, size, or color; laser devices that create detailed 3D profiles that are subsequently processed and classified; X-ray or magnetic devices.

The available offerings include various types of sorting depending on customer requirements. The most common method is the one that uses video cameras and various algorithms, having high efficiency.

3. Design Stages and Implementation of Neural Networks for Object Identification

The project's objective is that when three types of objects are successively placed on the belt as follows: screw-nut, letter L-letter I, and large volume piece-small volume piece, they will be recognized by the system consisting of a webcam that sends a signal to a computer running a Matlab algorithm that commands Arduino boards to sort objects into two containers by operating the plug according to the functional diagram in Figure 2

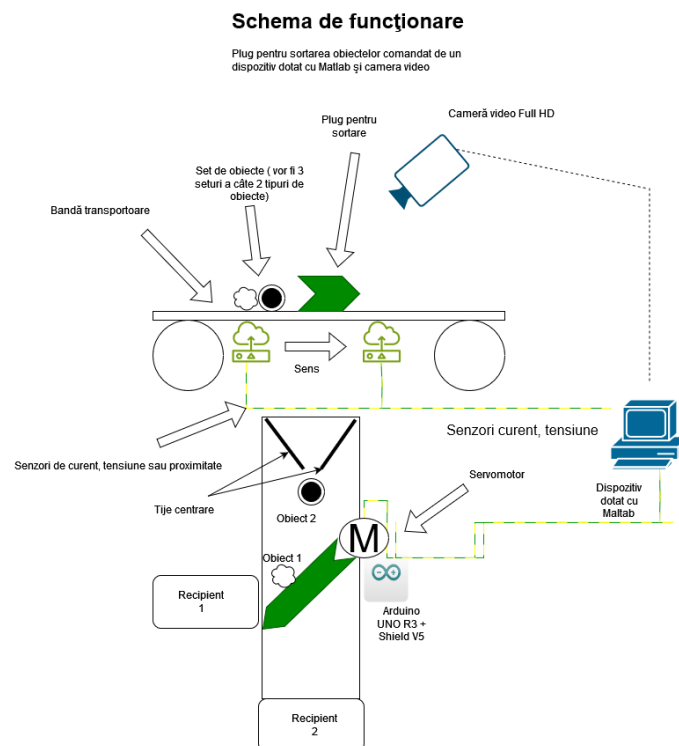


Fig.2. Project Functional Diagram

A first step in realizing the device was choosing, verifying, and testing the components necessary for the system's functionality: Arduino UNO R3 board, Sensor Shield V5.0, proximity sensor. The next step was the 3D design of the belt to establish the positioning of peripheral components and simulate various scenarios. For testing the functionality of the board, connections were made and an LED light was turned on via the Matlab development environment.

To accomplish this step, it was necessary to download a package that allows the use of Arduino in Matlab, downloaded from MathWorks[1]. Subsequently, a network was created and trained based on 39 pictures of various objects to study the network's behavior when presenting objects, being initialized in the Matlab working environment according to Figures 3 and 4.

```
camera =  
webcam with properties:  
    Name: 'Integrated Camera'  
    AvailableResolutions: {'1280x720' '960x540' '848x480' '640x480' '640x360' '424x240' '352x288' '320x240' '320x180' '176x144' '128x96' '64x48'}  
    Resolution: '1280x720'  
    Pan: 0  
    ExposureMode: 'auto'  
    Sharpness: 3  
    WhiteBalance: 4600  
    Zoom: 100  
    BacklightCompensation: 1  
    Contrast: 32  
    ColorEnable: 1  
    Saturation: 64  
    Gamma: 120  
    Tilt: 0  
    Roll: 0  
    Brightness: 128  
    WhiteBalanceMode: 'auto'  
    Hue: 0  
    Exposure: -6
```

Fig.3. Initialization of the Webcam and Trained Network

camera	1x1 webcam
inputSize	[224,224]
net	1x1 DAGNetwork
trainedNetwork_1	1x1 DAGNetwork
trainInfoStruct_1	1x1 struct

Fig.4 Initialization of the Webcam and Trained Network

For training the network, the "Deep Network Designer" toolbox from MathWorks[2] was used. The first task was creating multiple layers for image processing where various values and specifications were set (see Figure 5), followed by verifying their compatibility and finally training the network according to Figure 6.

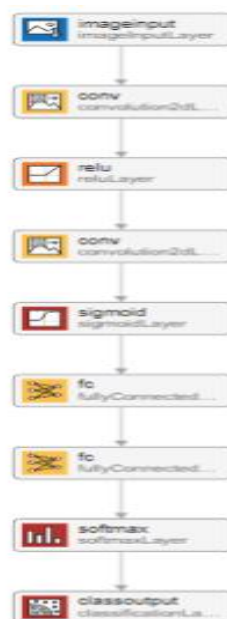


Fig.5 Creating Image Processing Layers

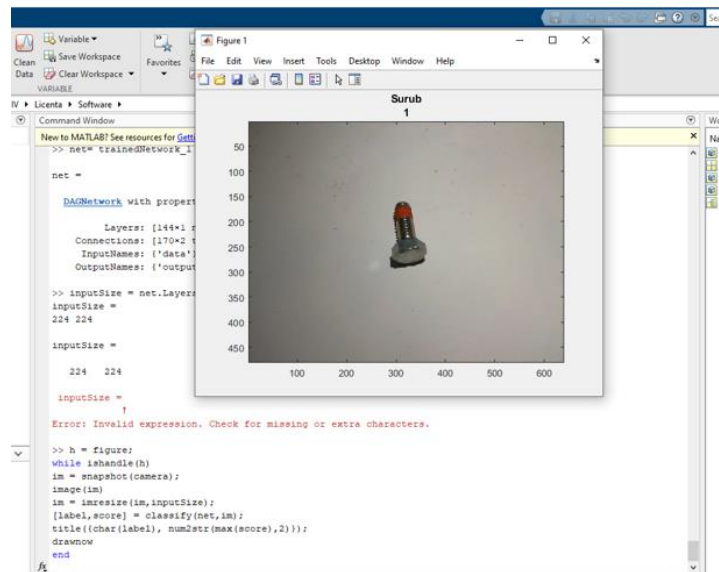


Fig.8 Identification of the “Screw” Piece

To identify objects in real-time, a code sequence was run using a package included in Matlab for the proper functioning of peripheral devices (see Figure 9).

```
>> h = figure;
while ishandle(h)
    im = snapshot(camera);
    image(im)
    im = imresize(im,inputSize);
    [label,score] = classify(net,im);
    title([char(label), num2str(max(score),2)]);
    drawnow
end
```

Fig.9 Implementing the Code Sequence for Real-time Object Identification

The design of the belt and accessories representing the final product was done using the SolidWorks application, with peripheral components assembled according to Figure 10.

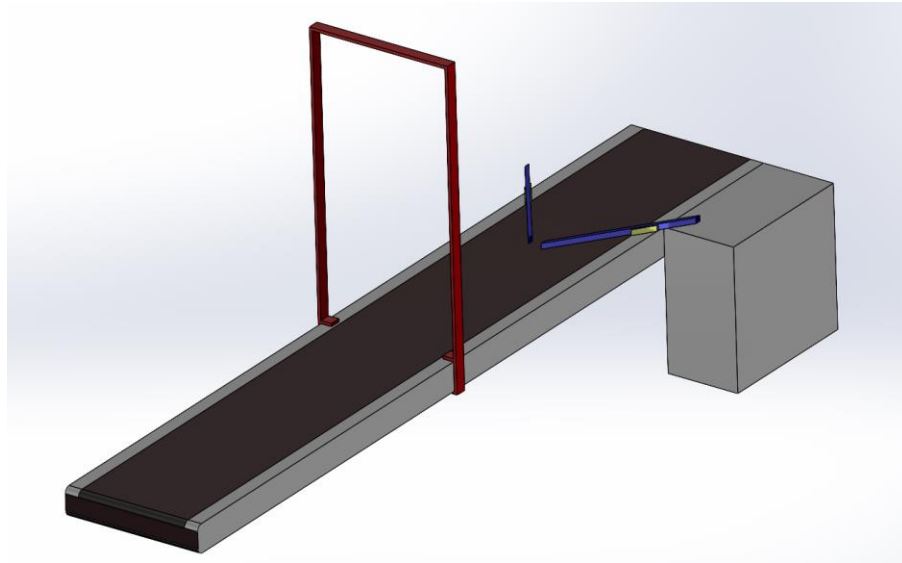


Fig.10 Final Product Design

Currently, it remains to optimize the previously trained network and complete the connections and assembly that allow the sorting of objects using bilateral plug paddles.

4. Conclusions

In conclusion, designing an algorithm and developing a software application for the intelligent recognition of moving products and their sorting has the potential to revolutionize storage and logistics operations. Successful implementation of this project will lead to a significant increase in efficiency, accuracy, and safety while providing a scalable solution for managing a large volume of products.

Bibliography

- [1] https://www.mathworks.com/matlabcentral/fileexchange/47522-matlab-support-package-for-arduino-hardware?s_tid=srchtitle_support_results_2_arduino
- [2] <https://www.mathworks.com/help/deeplearning/gs/get-started-with-deep-network-designer.html>
- [3] Matthias Aßenmacher Multimodal Deep Learning <https://medium.com/@mlblogging.k/14-awesome-free-books-for-machine-learning-deep-learning-reinforcement-learning-8f1d3a90a394>

DESIGN OF AN EXPERIMENTAL MODEL FOR THE OPERATION OF AN AUTOMATIC WASHING MACHINE

HELMIS Gabriel-Alexandru; SAVU Tom

Faculty: Inginerie Industrială și Robotica, Specializarea: Informatică Aplicată în Inginerie Industrială,
Year of study: 4, e-mail: helmisalexandru@gmail.com

ABSTRACT Automation represents the process of using technology to perform tasks or processes with minimal human intervention. It involves the use of various technologies such as robotics, artificial intelligence, machine learning, and software systems to streamline and optimize workflows, improve efficiency, and reduce the need for manual labor.

In industries, automation can range from simple repetitive tasks like data entry to complex operations such as manufacturing, logistics, and even decision-making processes.

KEY WORDS: robot, image processing, Python, LabView

1. Introduction

Household chores represent all activities and responsibilities associated with maintaining and managing a home and the daily life of a family. These tasks can include cleaning, cooking, laundry, shopping, managing household finances, caring for children or other family members, repairing or maintaining the home, and many other activities. Household chores are essential for the functioning of a household and contribute to the comfort, well-being, and functionality of a family.

Automating a process such as laundry can result in more free time spent with family and loved ones. Therefore, the title of the thesis project I have chosen to elaborate on is “DESIGN AND DEVELOPMENT OF AN EXPERIMENTAL MODEL OF A ROBOT FOR LOADING AND OPERATING A WASHING MACHINE.”

To realize this project, I needed knowledge that I gradually acquired during my studies. For creating the mount for the camera and infrared sensor, I needed CAD design skills. Using the infrared sensor and an Arduino Uno Rev3 SMD acquisition board was possible due to the knowledge accumulated during the “Senzori și traductoare” labs. Furthermore, to calibrate the image and program the robot to move to specific coordinates, knowledge of LabView and Python was necessary.

2. Current stage

The project is in the testing, verification, and optimization stage, aiming to provide precise and consistent functionality for the end user. Being an automation process, it involves the use of software and hardware components and an experimental setup. These components are interconnected and depend on each other to ensure the correct functioning of the entire process.

The list of components used in this project includes:

A. Software Components

- Kinova web page
- LabView
- Python
- Arduino IDE

B. Hardware Components

- Kinova Gen3 Lite robotic arm

- GP2Y0A21YK0F infrared sensor
- Sensor mount
- Camera
- Camera mount
- Arduino Uno Rev3 SMD

An infrared sensor and a camera are mounted on the Kinova Gen3 Lite robotic arm. Initially, the robot is positioned above a pile of clothes. Using the camera, it can perform image acquisition, allowing for detailed detection and analysis of objects in its environment. This image-capturing capability is essential for the efficient functioning of the robot in activities such as sorting or handling clothes.



Fig. 1. Kinova Gen3 Lite robotic arm

Through the program developed in Python, the robot can detect the presence of clothes in a specific area and provide the coordinates of their center. Figure 2 highlights this capability by displaying a "Colored" label above the area where the center of the shirt is located. This feature indicates an additional functionality, allowing for the sorting of clothes based on color, thus offering the potential for greater efficiency in organizing and handling them.

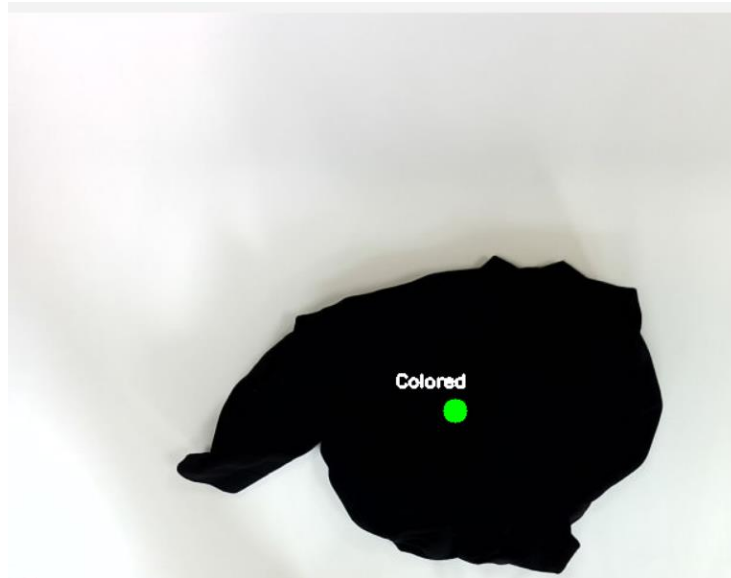


Fig. 2. Black colored t-shirt detected

The robotic arm positions itself at a 90-degree angle above the clothes to measure the distance to the first piece of clothing, thereby calculating the coordinates on the Z-axis it needs to descend to for grasping. To ensure the sensor does not erroneously measure the distance to the clothes, five measurements are taken, as shown in Figure 3, and the most frequently repeated value represents the correct distance. Once it has reached the position where it can grasp the clothing, the gripper closes, and the cloth can be moved to the washing machine.

```
Distance: 41.0 cm
Distance: 41.0 cm
Distance: 41.0 cm
Distance: 41.0 cm
Distance: 41.0 cm
Most Common Distance: 41.0 cm
```

Fig. 3. Reading distance to clothes

3. Experimental setup

Using the components and equipment mentioned above, I developed an experimental setup that follows the steps outlined for loading a washing machine with clothes. In Figure 4 below, the robotic arm is shown in the position for detecting clothes.



Fig. 4. Detecting clothes position

4. Conclusions

In recent years, technological advancements have revolutionized the way we manage household chores. Through the continuous development of new products and innovative technologies, the goal is to completely eliminate the need for human intervention in these repetitive activities. This project aims to completely redefine the way we handle daily tasks, allowing people to use their time and energy for more valuable and fulfilling activities. As a further development, sorting clothes based on color and material should be implemented before they are loaded into the washing machine.

5. Bibliography

- [1]. <https://www.kinovarobotics.com/product/gen3-lite-robots>
- [2]. Gen3 Lite user guide
- [3]. <https://ro.wikipedia.org/wiki/Robot>
- [4]. https://ro.wikipedia.org/wiki/Robot_industrial
- [5]. <https://docs.kinovarobotics.com/>
- [6]. <https://en.wikipedia.org/wiki/Kinova>
- [7]. Tom Savu, „Analiza si prelucrarea imaginilor”, course

RESEARCH ON THE RESISTANCE TO STRESS OF A ROBOT GRIPPER PRODUCED IN DIFFERENT CONSTRUCTIVE - TECHNOLOGICAL CONDITIONS

PÎRVULESCU Sorin-Cristian¹, GHEORGHE² Marian, ZAHARIA² Cristin, LAZĂR³ Dan

Faculty of Industrial Engineering and Robotics, Industrial Engineering Programme,
4th Study Year, e-mail: pirvulescu_sorin@tuta.io

²NUST Politehnica Bucharest, Faculty of Industrial Engineering and Robotics,
Manufacturing Eng. Department (TCM)

³ TF Service Impex SRL

ABSTRACT: There are a variety of type-dimensional robot grippers, with components made of metals, plastics, etc. In this thesis, a robot gripper will be developed for small loads, with specific components element manufactured through 3D printing from different plastic materials, which would allow experimental research of ,mainly, the rigidity aspects associated with bending.

KEYWORDS: Gripper, 3D printing, plastic material, bending strength, rigidity.

1. Introduction

Grippers, main components of robots, are made in a wide rage of: actuation – mechanical, pneumatic, magnetic etc.; general structure – number for fingers, joint elements etc.; component materials: metals, plastics, etc.;

Grippers are continuously researched and developed for constructive-functional and technological optimisation.

2. General considerations

There are a variety of grippers used in different industries: with two parallel fingers or three fingers for handling complex shaped objects [1], with vacuum suction cups for handling boxes in palletizing applications, open finger grippers for handling food products, magnetic grippers for handling ferromagnetic products, etc. [2,3].

As an example, the ROBOTIQ 2F - 85 Gripper (Fig. 1) consists of: a base, two bins, two NBR rubber bin tips, two bars, a palm rest, two distal phalanges, two proximal phalanges and two plastic vanes designed for adaptation to a pick-and-place application of products manufactured by binder jet technology [3-6].

Also, the 9g Micro Servo Gripper (Fig. 2) consists of: a base, two fingers, two simple articulating rods, two toothed driven-transmission connecting rods, a 9g servo motor [7].



Fig. 1. Gripper ROBOTIQ 2F – 85 [2]

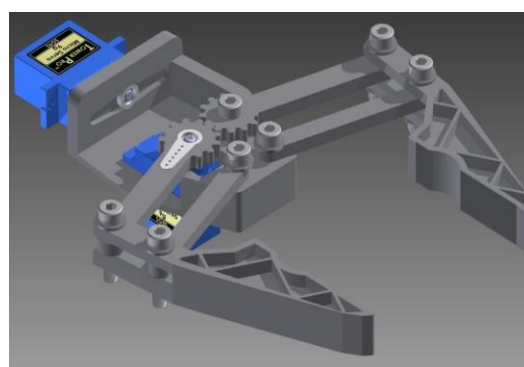


Fig. 2. Gripper 9g Micro Servo [3]

3. Case Study

The problem of developing a small-load robot gripper, Gripper GR 01.00, with specific components manufactured by 3D printing from different materials, allowing experimental investigation of the stiffness associated with bending stress is considered.

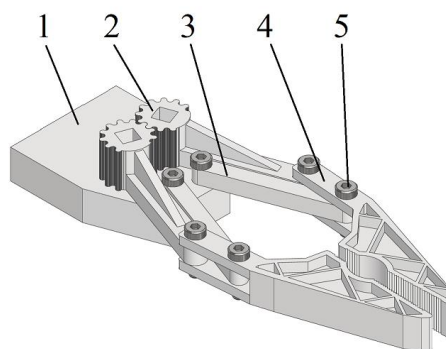
3.1. Main constructional and functional characteristics

The product, Gripper GR 01.00, has been designed based on some characteristics of the reference gripper shown in Fig. 2, but in such a way that it can be operated with a torque wrench.

The structure and components of the Gripper GR 01.00 are as shown in Fig. 3.

In order to ensure high values of bending strength and stiffness, Gripper GR 01.00 components are designed with similar shapes to the reference Gripper components, but with greater thicknesses. Particularly noticeable is the ribbed structure of elements 2 and 4.

The material prescribed for the specific component parts of the Gripper GR 01.00 product is, among the 3D printable materials, in 4 variants (M1 - M4), respectively, with properties as shown in Table 1.



1 - Base plate, 2 - Toothed driven rod (2x),
3 - simple articulating rods (2x), 4 - Finger (2x), 5 - Assembly elements (screw - washer - nut)

Fig. 3. Product structure and components of Gripper GR 01.00 (based of [7])

Tabel 1. Characteristics of materials prescribed for component parts specific to Gripper GR 01.00 (based of [8-11])

Material	M1	M2	M3	M4
	PLA (polylactic acid)	PETG (polyethylene terephthalate glycol)	HIPS (high-impact polystyrene)	TPU95 (thermoplastic polyurethane)
Manufacturer	Crealitiy3D	Polymaker	Formfutura	Polymaker
Density, g/cm ³	1,24	1,25	1,04	1,22
Tensile strength, MPa	51	31,9	22	...
Bending strength, MPa	86	53,7
Young Modulus, MPa	2120	1472	2000	29
Impact resistance, J/m ²	10,5	5,1

A summary of the material, gauge dimensions and mass of specific Gripper GR 01.00 components is given in Table 2.

Tabel 2. Material, gauge dimensions and mass of elements specific components of Gripper GR 01.00

Poz.	Denumire	Material				Dimensiuni de gabarit, mm	Masa, kg
		M1	M2	M3	M4		
1	Placă de bază	PLA	PETG	HIPS	TPU95	61 x 47 x 13	0,013-0,025
2	Bară dințată de acționare					63 x 18 x 6	0,005-0,006
3	Bară de articulare					6 x 6 x 56	0,001-0,002
4	Bac					90 x 24 x 13	0,007-0,009

3.2. Recommended 3D printing technology conditions

A series of recommended technological conditions for 3D printing of specific Gripper GR

Tabel 3. Recommended 3D printing technology conditions (based of [8-11])

Material	M1	M2	M3	M4
	PLA	PETG	HIPS	TPU95
Nozzle temperature, ° C	190-230	230-240	220-260	210-230
Build plate temperature, ° C	0-60	70-80	85-100	25-60
Printing speed, mm/s	40-120	30-50	20-40	20-40

01.00 components are shown in Table 3.	Threshold overhang angle, °	45	60	45	35
	Environmental temperature	Room temperature			

3.3. Manufacturing technological parameters and actual specific components

The technological parameters, i.e. the printing settings in the slicer (based on [12,13]), for 3D printing of specific Gripper GR 01.00 product components are shown in Table 4.

Tabel 4. 3D printing technology parameters (based of [12, 13])

Material		M1	M2	M3	M4
		PLA	PETG	HIPS	TPU95
Nozzle temperature, ° C		200	235	240	220
Build plate temperature, °C		55	72	100	60
Printing speed, mm/s		50	30	25	25
Infill percentage	Of base plate, %	30	30	30	30
	Of other components, %	100	100	100	100

Basically, the specific components of the Gripper GR 01.00 were manufactured on a Creality Ender 3 V2 Neo machine, corresponding to the materials considered and the required number of pieces, as appropriate. Examples of actual specific components of the Gripper GR 01.00 are shown in Fig. 4.



Fig. 4. Actual specific components of the product Gripper GR 01.00 of material M1, M2, M3, M4 respectively

By assembling the actual specific component parts from M1, M2 or M3 material (Fig. 4), the product Gripper 01.00.M1, Gripper 01.00.M2 or Gripper 01.00.M2 respectively can be formed, Gripper 01.00.M3 (Fig. 3).

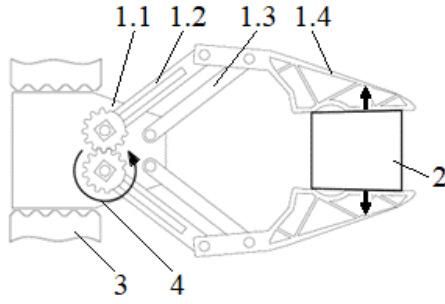
3.4. Experimental testing

A first experimental test was carried out by actuating Gripper 01.00.M1 in an experimental working system [12], as shown in Fig. 5. By driving the torque wrench on one of the toothed bars, the component parts of Gripper 01.00.M1 were stressed in torsion, bending, etc., as appropriate. At a certain value of the actuating moment, *one of the simple articulating rods broke*.

Next, an experimental study on the bending stress of articulating rods was prepared and carried out. Thus, 3 articulating rods of each material M1 - M4 were printed and an experimental working system [12] was structured as shown in Fig. 6. It is noted that the stress mass, m , was realized, from the mass of the bead wire of 0.22 kg and the masses of steel bushings, each of 0.394 kg, added progressively. Correspondingly, the stress force F is:

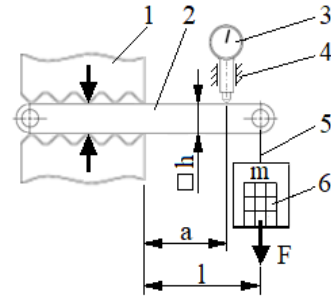
$$F = 10^{-1}mg \Leftrightarrow F = 0,981m, \text{ în daN} \quad (1)$$

where mass m is in kg, and g , the acceleration of gravity, is 9.81 m/s^2 .



1 - Gripper GR.01.00.M1/ 1.1 – Base plate, 1.2 - Toothed driven rod (2x), 1.3 – Simple articulating rod (2x), 1.4 - Finger (2x), 2 – Technological object, 3 – Vise, 4 – Torque wrench

Fig. 5. Stress system on Gripper GR 01.00.M1



1 - Vise, 2 - Simple articulating rod, 3 - Dial gauge, 4 - Magnetic holder, 5 - Thread with thaler, 6 - Stress table

Fig 6. Stress to bend articulating rod

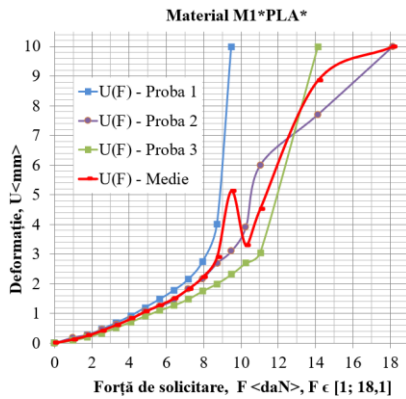
During the stressing of a simple articulating rod: for given values of mass, m_i , respectively, stress force, F_i , the values of rod deformation, U_i , in mm, $i = 1, 2, \dots$ were recorded. The values F_c , U_c at which *rod cracking* starts - material M1, M2 or M3, respectively, rod deformation intensification - material M4; the values F_r , U_r at which *rod breakage* occurs - material M1, M2 or M3, respectively, rod deformation intensification - material M4 (which did not fail during the possible stress).

Based on the experimental data (F_i , U_i), functions defined by points (2) as well as trend functions (3) were determined [14], as shown in Fig. 7 - 12.

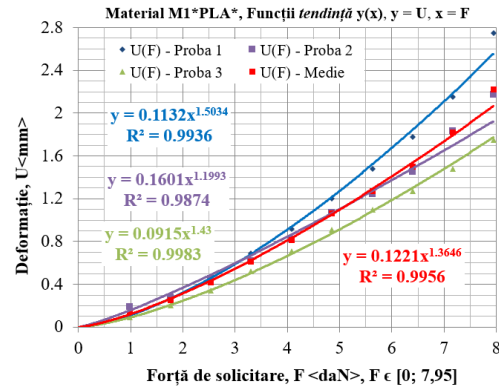
vb

$$U = U(F), F \in [0; F_r] \quad (2)$$

$$U = U(F), F \in [0; F_c] \quad (3)$$

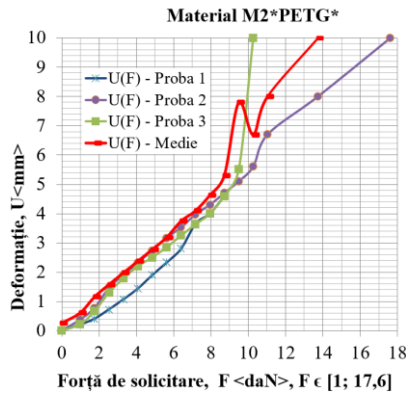


a.

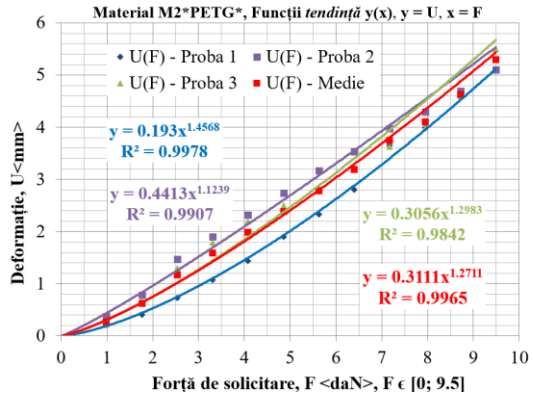


b.

Fig. 7. Trend functions (2) and (3)/ Material M1*PLA* respectively



a.



b.

Fig. 8. Functions (2) and (3)/ Material M2*PETG* respectively

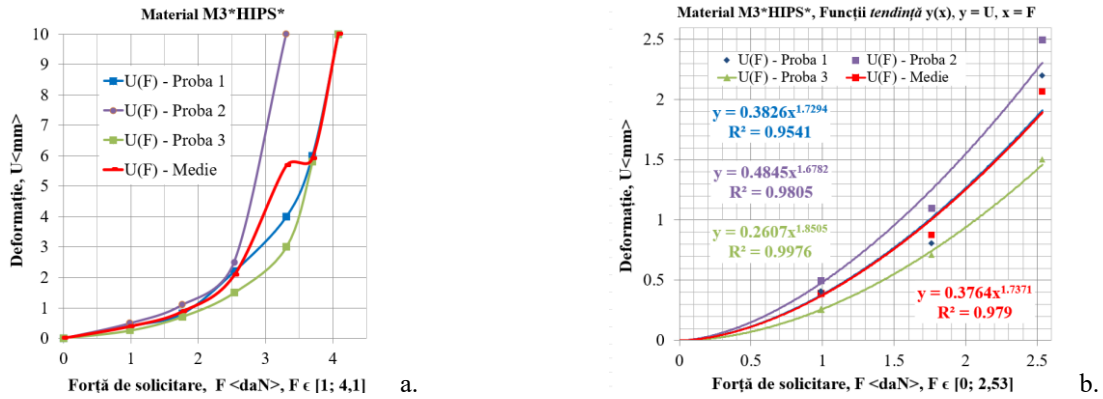


Fig. 9. Functions (2) and (3)/ Material M3*HIPS* respectively

Overall, the following is found for the investigated joint rods:

- The functions $U = U(F)$, $F \in [0; F_r]$ are nonlinear (Fig. 7a, 8a, 9a, 10a);
- at rods of material M1, M2 or M3, the appropriate trend functions, $U = U(F)$, $F \in [0; F_c]$, are nonlinear, power-type (Fig. 7b, 8b, 9b);
- at the rods in material M4, the trend function, $U = U(F)$, $F \in [0; F_c]$ appropriate is linear (Fig. 10 b).

For the characterization of the investigated joint rods based on the trend functions (3) associated with the characteristics $U(F)$ - Mean (Fig. 7b, 8b, 9b, 10b), the effective stiffness K is also determined [15]:

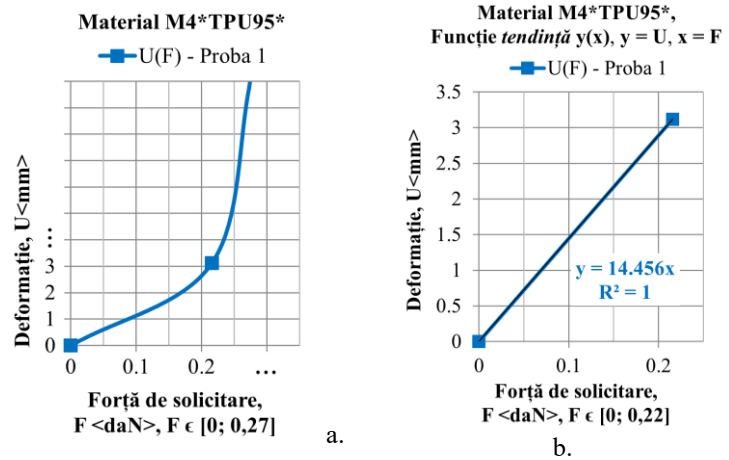


Fig. 10. Funcții (2) și, respectiv, (3)/ Material M4*TPU95*

$$K = F/U, \text{ în daN/mm} \quad (4)$$

as shown in Table 5.

Tabel 5. Effective stiffness K a of the investigated hinge bars

Material	Trend function	F, daN	U, mm	K, daN/mm
M1*PLA*	$U = 0.1221F^{1.3646}$, $F \in [0; 8]$	0,5 ... 7,5	0,05 ... 1, 91	10,5 ... 3, 93
M2*PETG*	$U = 0.3111F^{1.2711}$, $F \in [0; 9,5]$	0,5 ... 9,0	0,13 ... 5,08	3,88 ... 1, 77
M3*HIPS*	$U = 0.3764F^{1.7371}$, $F \in [0; 2,5]$	0,2 ... 2,2	0,21 ... 1,48	0,97 ... 1, 49
M4*TPU95*	$U = 14.456F$, $F \in [0; 0,22]$	0.1 ... 0,18	1,45 ... 2,60	0,069

The following is found: • the effective stiffness K decreases significantly when the load force F increases, except for the articulating rod made of M4 material whose stiffness is constant • the effective stiffness K decreases significantly from the value corresponding to the rods of material M1 to the value corresponding to the rods of material M2, M3, M4 respectively, in the same direction as the variation of specific material characteristics (see Table 1).

For the comparative analysis of the investigated hinge bars, the theoretical stiffness K_0 is also determined, which under the considered working conditions (see also Fig. 6) is [15]:

$$K_0 = 10^{-1} \frac{6EI}{a^2(3l-a)} \Leftrightarrow K_0 = \frac{Eh^4}{20a^2(3l-a)}, \text{ în daN/mm} \quad (5)$$

where: E is Young's modulus, in MPa, I - moment of inertia, $I = h^4/12$, in mm⁴, as shown in Table 6.

It is found that, for rods of a given material, the theoretical stiffness K_0 is constant, and it decreases significantly from the value corresponding to rods of

Tabel 6. Theoretical stiffness K_0 a of the investigated hinge bars

Material	E,	h	a	l	K_0 ,
----------	----	---	---	---	---------

material M1, to the value corresponding to rods of material M2, M3, respectively M4, in the same direction as the variation of specific material characteristics (see Table 1).

	MPa	mm			daN/mm
M1*PLA*	2120	6	22	25	5,35
M2*PETG*	1472				3,72
M3*HIPS*	2000				5,05
M4*TPU95*	29				0,073

Also, from the comparative analysis of the investigated rods, based on the determined K and K₀ magnitudes, the following is found (see Tables 5, 6): • for articulated rods made of M1, M2 or M3 material, the effective stiffness K differs significantly from the theoretical stiffness K₀ by approx. 97.1 ... -26.6%, 4.3 ... -52.4% or -70.5 ... -80.8% respectively • for articulated rods made of M4 material, the effective stiffness K is lower by approx. 5.2% than the theoretical stiffness K₀.

The above results show that for each of the articulated rods - material M1*PLA*, M2*PETG*, M3*HIPS* or M4*TPU95* investigated, the effective stiffness depends on the material characteristics achieved under the experimentally applied 3D-printed fabrication and bending stress conditions (see Table 4, 6).

Looking ahead, it is considered appropriate to develop research to optimise the design and manufacture of robot grippers.

4. Conclusions

- The effective deformation and, correspondingly, the effective stiffness of the studied rods depend on the material characteristics achieved under experimentally applied 3D-printed fabrication and bending stress conditions.
- Further research is needed to optimize the design and fabrication of high-performance robot grippers.

5. Bibliography

- [1] Ligutan D.D., Ai R.T., Bandala A., Vicerra R.R.P., Design of a 3d-printed three-claw robotic gripper end-effector, ResearchGate, 2021, DOI: 10.11113/aej.v11.17865.
- [2] ***, Types of grippers used in manufacturing, Universal Robots, <https://www.universal-robots.com/blog/types-of-grippers-used-in-manufacturing>, accessed at 10.04.2024.
- [3] ***, Schunk, Gripping Systems, High quality and reliability for your production, https://schunk.com/se/en/gripping-systems/c/PUB_8293, accessed at 12.04.2024.
- [4] Muktadir M.A., Yi S., Elliot A.M., Design of robot grippers for binder jet products handling, *Scientific Reports*, 14(1), 2024, DOI:10.1038/s41598-024-56385-8.
- [5] ***, Catalogue of tips for grippers ROBOTIQ, https://blog.robotiq.com/hubfs/Fingertips_bundle_EN_2021-09.pdf, accessed at 13.04.2024.
- [6] ***, User manual for grippers ROBOTIQ, https://assets.robotiq.com/website-assets/support_documents/document/online/2F-85_2F-140_TM_InstructionManual_HTML5_20190503.zip/2F-85_2F-140_TM_InstructionManual_HTML5/Content/1.%20General_Presentation.htm, accessed at 16.04.2024.
- [7] ***, Robot Gripper 9g Micro Servo, <https://www.thingiverse.com/thing:715525>, accessed at 8.03.2024.
- [8] ***, Technical details specified by the PLA manufacturer, https://store.creality.com/products/cr-1-75_mm-pla-3d-printing-filament-1kg?variant=f3eff5ac-1216-46bb-b9ed-8eaf772eece1 accessed at 02.05.2024
- [9] ***, PETG filament datasheet, https://c.cdnmp.net/490505258/custom/prod/1_fisa_tehnica_1832.pdf?rv=1715115600 accessed at 02.05.2024
- [10] ***, HIPS filament datasheets, https://c.cdnmp.net/490505258/custom/prod/1_fisa_tehnica_1251.pdf?rv=1715115600 accessed at 02.05.2024, <https://sangir.com/wp-content/uploads/2022/03/HIPS-SHEETS-TDS.pdf> accessed at 02.05.2024.
- [11] ***, Datasheet filament TPU95, https://c.cdnmp.net/490505258/custom/prod/1_fisa_tehnica_1448.pdf?rv=1702219676, accessed at 02.05.2024.
- [12] ***, Industrial systems, TF Service Impex SR, 2024, <https://tfservice.ro/>
- [13] Ulmeanu M., Additive manufacturing technologies, Curs, UNSTPB, 2023.
- [14] ***, Microsoft Excel, Microsoft Office 365

[15] Gheorghe M., Production process engineering and management 1, Course notes, UNSTPB, 2022

RESEARCH AND CASE STUDIES ON ORIENTATION FOR CHOICE AND DEVELOPMENT OF PROFESSIONAL CAREER IN THE FIELD OF INDUSTRIAL ENGINEERING

ISPAS Elena-Andreea¹, GHEORGHE²Marian, DIMA³ Eustațiu

¹Faculty of Industrial Engineering and Robotics,
Specialization: Industrial Economic Engineering, 4th study year, e-mail: ispas.andreea24@yahoo.com

²NUST Politehnica Bucharest, Faculty of Industrial Engineering and Robotics,
Manufacturing Eng. Department (TCM)

³ Scopeworker Bucharest

ABSTRACT: Career optimization has become a necessity, given the rapid evolution of technology and the dynamic nature of the job market. At the same time, due to lack of information, many students end up exploring other fields, despite their engineering knowledge. Graduates increasingly need counseling to find the right position, a process that involves identifying individual potential and skills. Through a dedicated website, they will not only get to know themselves better, but also receive useful information regarding the hiring process from recruitment teams and experienced engineers.

KEYWORDS: algorithm, interview, website, recruitment, career

1. Introduction

In the current period, we can observe the beneficial effects of specializations/professions in the field of industrial engineering on transforming the functioning of modern industry. They deal with production processes, design, implementation, and services, aiming for efficiency, competitiveness, and technological progress. All these contribute to sustainable development by minimizing waste and efficiently using resources.

2. General considerations

Starting points: the existence of other career guidance websites online, but which do not meet students' expectations, either because they are not in their field [1], or because they were created to promote paid sessions by trainers [2], or because they ask irrelevant questions about career choice [3].

We cannot say that there is no webpage to guide graduates at all [4], but it is precisely from here that we were able to create and develop a platform suitable for them. We are talking about current advice from engineers in the field or from recruitment teams, about the succession of existing positions on the market that they do not know about due to lack of research, technical and economic tests designed to highlight their level, and also an algorithmic part that can generate a specific position in line with the skills they have.

In accordance with the COR (Classification of Occupations in Romania) 2024 (based on [5]), the positions related to the Industrial Economic Engineering specialization can be displayed. This way, students can gather information from a single source without having to give up their engineering studies. Some of these positions are presented in Table 1.

Table 1. Codes and job titles in the field, in Romania [5]

Code	Subcode	Occupation Title
COR 2141 Engineers in Technology and Production	214110	CAD (Computer-Aided Design) Designer
	214115	Business Manager
	214116	Building Manager

	214136	Manufacturing Programmer/ Production Launcher
COR 2144 Mechanical Engineers	214401	Mechanical Engineer
	214408	Machine Tools Engineer
	214412	Automotive Engineer
	214438	Mechanical Engineer Designer
	214442	Vehicle Performance Specialist
	214467	Research Engineer in Machine Construction Technology
COR 2310	231001	Assistant Professor, etc.
COR 1211 Leaders in the financial field	121102	Chief Economist
	121105	Head of Department, Bank / Deputy Head of Department
	121128	Head of Financial Office
	121130	Head of Economic Analysis Office
COR 1212 Human Resources	121205	Chief Human Resources Officer
	121207	Human Resources Manager
	121209	Head of Human Resources Office

A major advantage of graduating in Industrial Economic Engineering is the formation of technical and economic skills and competencies. This combination prepares students to tackle the complex challenges of modern industry, propelling them towards valuable positions within any company.

3. Developing a platform for career guidance

3.1. Career Guidance Analysis

Career guidance involves a dynamic process consisting of setting and developing goals, seeking information, planning and executing behaviors, as well as monitoring and processing feedback. Employees need to be able to cope with unpredictable and dynamic professional environments that require more guidance [6].

Being a student employee involves a dynamic mindset, along with the joy of working on projects with people from various organizations and the excitement of participating in new experiences. Developing employability skills, considered an essential factor in subjective career success, offers significant advantages. Moreover, students who can overcome academic challenges can develop positive attitudes toward the academic process and remain optimistic about career success [7].

University graduates occupy an interesting position in the economy, and there are still competing interpretations regarding their outcomes when entering the labor market. Policy continues to present them as a social and occupational elite group that will have access to an initial salary and will fulfill their potential through careers as "knowledge workers".

However, there are still inequalities among graduates regarding their outcomes in the labor market. It was evident that while some of them developed idealized visions, the majority of students anticipated a much more challenging career progression. For the most part, students seemed to interpret the labor market as increasingly flexible but also riskier. This was commonly translated as "the end of lifelong employment" [8].

The current research includes the responses of four graduates, presented in Table 2, followed by responses from a recruitment team and a technical director. that will contribute to informing and guiding the career future. Considering that engineers in the field are already facing technological changes, they were able to provide valuable advice to prepare students for these developments.

Table 2. Interview with Experienced Engineers

Question	Answers	Names
How do you think your field will evolve, and how can students prepare for it?	"The automotive field will evolve according to environmental restrictions and regulations (energy and green technology), and students will adapt to these changes through constant information."	Andreea STAN
	"The field is evolving more and more; unfortunately, the freely available resources are limited, and you cannot have access to what is happening behind the scenes without working in the field. However, with the minimum required knowledge acquired from various resources (websites, videos, online courses), you can easily obtain a junior position."	Bogdan HĂȚIȘ
What were the biggest challenges you faced in your first job?	"At my first job, the biggest challenge was interacting with as many people as possible and learning to fulfill my tasks."	Andreea STAN
	"The biggest challenge was to quickly learn new information and retain as many functionalities of the machine as possible."	Anca DUCA
	"At my first job, the biggest challenge was the large volume of information that needed to be acquired, which was different from what was taught in college."	Cosmin OLTEANU
	"At my first job, the biggest challenge was learning to manage and solve problems in a very short amount of time."	Bogdan HĂȚIȘ
What valuable lessons have you learned so far in your career, and how can graduates and students apply them?	"We never know too much, but we must have enough confidence that we are the best in our field. Honesty and the ability to ask for help when needed are very important."	Andreea STAN
	"Patience and attention are the most important assets in a successful career. Graduates and students should be open and expose their problems to find solutions."	Anca DUCA
	"Theory and practice are fundamental in an engineer's career. It is important to assimilate the knowledge from college and apply it in practice."	Cosmin OLTEANU
	"Patience and perseverance are the keys to success in an engineering career. It's important not to be discouraged by failures and to continue learning and developing."	Bogdan HĂȚIȘ

They also say that graduates can stand out in an interview through "sincerity, motivation, adaptability, communication, acquired knowledge, the desire to get the job, and quickly assimilating information."

3.2. Platform creation

For creating the website, Visual Studio was used for coding, along with JavaScript, HTML, and Tailwind CSS technologies. The project was structured through distinct components for various elements, such as the header, content sections, and contact area. Navigation between different pages in the application was managed through React Router (based on [11]).

At the same time, careful organization was needed, based on the needs of students and graduates. Thus, after analyzing the existing platforms, the reasons why many give up engineering were identified, and we were able to include as many important elements as possible to encourage graduates.

The website includes a section with tips (Fig. 1), a test section (Fig. 2) with technical tests and economic tests (Table 3), along with the profession generation form (Fig. 3), and I plan to create a feedback form as well.



Fig. 1. Tips from Engineers, Recruitment Teams, and Directors



Fig. 2. Tests reflecting students' level

Table 3. Technical and Economic Tests

Technical Test (based on [9])	Economic Test (according to [10])
<p>(1). If a prescribed diameter $\varnothing X h6$ has tolerance T and the lower deviation is EI, then $T + EI$ is:</p> <ol style="list-style-type: none"> of value equal to 0 of strictly positive value of strictly negative value 	<p>(1). What is the definition of interest?</p> <ol style="list-style-type: none"> The amount paid by the creditor to the debtor The amount paid by the debtor to the creditor The amount paid by the debtor to use the borrowed sum The amount received by the creditor for providing a loan
<p>(2). In the design of technological processes, the requirement regarding the economic characteristic associated with production includes:</p> <ol style="list-style-type: none"> cost, productivity, and efficiency cost and productivity productivity 	<p>(2). What is the main effect of bank credit on the economy?</p> <ol style="list-style-type: none"> Reduction of demand Reduction of consumption Stimulating economic activity Increase in inflation

<p>(3). For a technological product, the degree of concordance between the prescribed characteristics and the necessary characteristics is:</p> <p>a. of value equal to 0 b. of subunitary value c. of value equal to 1</p>	<p>(3). What is the necessary condition to achieve monetary equilibrium in the money market?</p> <p>a) Money supply equals money demand b) Money demand is greater than money supply c) Money demand is less than money supply d) The interest rate is maximum</p>
<p>(4). A technological system includes a cutting machining center and tools such as:</p> <p>a. die b. abrasive wheel</p>	<p>(4). What does the absolute advantage of producing a good represent?</p> <p>a. Higher opportunity cost. b. Lower opportunity cost.</p>

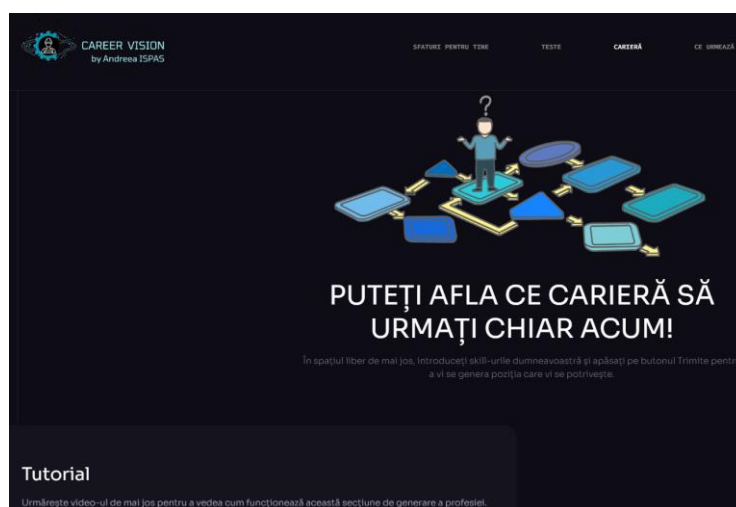


Fig. 3. Profession Generation Form Based on Skills

3.3. Future Developments

After completing the website, future developments will bring more useful information for students and graduates, for all fields of the Faculty of Industrial Engineering and Robotics, and then at the level of the entire University, as presented in Fig. 4.

Students will have the opportunity to directly contact major employers in Engineering through the platform (Fig. 4) and to obtain a job more easily.



Fig. 4. Future research for career guidance

4. Conclusions

- The aim of this research has been to make a significant contribution to the career guidance of future engineers. The platform provides concrete and up-to-date information, testing methods that assess the real level at which students are and the profession generation form, which provides a practical and useful tool in finding a job.

- Plans to expand the platform will help even more students from other majors and even at the university level by adding contacts and available positions of large companies.

- It is essential that young people are validated, encouraged and made aware of their potential and the future opportunities available to them in Engineering.

5. References

- [1]***, Edmundo, Free vocational quiz, <https://edmundo.ro/descopera-directiile-de-cariera-care-ti-se-potrivesc/>, *** , <https://www.integraledu.ro/news/ce-job-ti-se-potrivate-sustine-un-test-de-cariera>, accessed on 8.03.2024.
- [2] Haapaniemi D., Career counselling and advice, <https://careerpartner.ro/consiliere-si-consultanta-in-cariera/>, accessed on 8.03.2024.
- [3]***, KUDIKA, What career really suits you, https://www.kudika.ro/quiz/test_30000-ce-cariera-ti-se-potrivate-cu-adevarat/index.html, *** , Career test, <https://www.unica.ro/test/test-de-cariera>, accessed on 23.03.2024.
- [4]***, Hipo, Find out which fields suit your personality, https://www.hipo.ro/locuri-de-munca/targabsolventi/quiz_cariera/ , *** , European Career Test, <https://testcariera.ro/test-de-cariera.php>, accessed on 27.03.2024.
- [5]***, Classification of Occupations in Romania, <https://codcor.ro/>, accessed on 02.04.2024.
- [6] Hirschi A., Koen J., “Contemporary career orientations and career self-management: A review and integration”, University of Bern and University of Amsterdam, 22 October 2020.
- [7] Ozturk U., Yildirim E., “Attitudes Towards New Career Approaches among Working Students: A Comparative Analysis with Nonstudent Employees”, Bitlis Eren University, Sakarya University Turkey, 10 March 2024.
- [8] Tomlinson M. (2007), “Graduate employability and student attitudes and orientations to the labour market”, ISSN 1363-9080.
- [9] Gheorghe M., Production Process Engineering and Management 1, Lecture Notes (In Romanian), UNSTPB, 2022-2023.
- [10] Ioniță I. R., Economics Basics, Lecture Notes (In Romanian), UNSTPB, 2021-2022.
- [11] YU A., THE COMPLETE WEB DEVELOPMENT BOOTCAMP, [HTTPS://WWW.UDEMY.COM/COURSE/ THE-COMPLETE-WEB-DEVELOPMENT-BOOTCAMP/](https://www.udemy.com/course/the-complete-web-development-bootcamp/), ACCESSED THROUGHOUT 2023.

RESEARCH ON EVALUATING THE EFFICIENCY AND IMPACT OF STAFF TRAINING PROGRAMS ON OPERATIONAL PERFORMANCE

**TATU Alexandra-Ioana¹, CANORIȚĂ Ioana-Mălina¹, GHEORGHE² Marian, IACOB
Viviana-Maria³**

Faculty: Industrial Engineering and Robotics, Specialization: Industrial Economic Engineering,
Year of study: IV, e-mail: alexandra.ioana2310@gmail.com

²NUST Politehnica Bucharest, Faculty of Industrial Engineering and Robotics,
Manufacturing Eng. Department (TCM)

³ SC Automobile Dacia SA

***ABSTRACT:** This paper focuses on the impact of staff training programs on operational performance within SC Automobile Dacia SA company. Different elements of the employee training process are analysed, including the methods used and the frequency of training sessions to provide relevant conclusions about their impact on the organization.*

***KEYWORDS:** performance, efficiency, staff, impact*

1. Introduction

Investment in the development and improvement of human resources is an essential element of the strategy for growth and success on the market, at SC Automobile Dacia SA. Through training sessions, courses and online webinars made available to employees, the company aims to improve their skills and abilities. Such programmes are designed to provide them with the tools to meet the demands and challenges of the changing work environment and to support them in achieving individual and organisational goals.

2. General considerations

Proper staff management is of crucial importance for many companies. As labour costs are one of the largest cost components for firms, even a marginal decrease in costs resulting from a more efficient use of staff, through proper planning or scheduling, could result in benefits [1].

In addition, due to the shortage of (qualified) staff, it is very important to meet the demand for tasks as efficiently as possible without using more staff than the minimum necessary and/or to provide training whenever necessary. In this context, the issue of staffing is extremely relevant.

However, most of the research has focused either on the staffing decision, given a predefined mix of skills, or on budgeting and planning for the necessary training, but neglects the consequences of worker learning and training on the staffing decision and the associated dynamic changes in employee skill levels. Training and team development has become a requirement of the current economic period [2].

Education and training are key determinants of both the implementation of core company values - integrity, authenticity, respect, innovation - and performance improvement. Continuous training is also an important factor for the professional and personal development of the team, strengthening cohesion and, not least, delivering new knowledge and skills.

SC Automobile Dacia SA is firmly focused on enriching the knowledge and skills of its employees [6]. In addition to technical training and refresher courses, training programs are also dedicated to improving certain key areas: communication, management, team cohesion, leadership and sales. Such a wide range of training and development needs may seem chaotic, but they are all contained in an annual training and development plan [7].

In each company there are departments specifically dedicated to identify the training needs of employees as well as the types of training required for each individual employee/ team. For such planning

of courses and trainings at SC Automobile Dacia SA, the Youth Council was established [5]. This is a complex development and volunteering project developed by the Procurement team. The main focus of the project is the employee experience part so that new colleagues feel the support of the team in all the important moments of their career - from the recruitment process, onboarding to development and autonomy in the job. It is an original project, and that is due to the experience, empathy and dedication of all Youth Council members. Each experience is tailored for both newcomers and people with extensive experience. Participants are convinced that in a global competitive environment, operational performance and staff development are the interdependent keys to sustainable growth of a company [5].

In 2022, a profound transformation process began for this team, with the Group's decision to transfer an important part of its Corporate Procurement activities to Romania. Thus, in just two years, the number of employees in the department has increased by 32%, while most of the existing positions have gone through a transformation process from a local to an international dimension.

Both the management and HR teams have welcomed the Youth Council project with great enthusiasm and have worked closely in all phases from strategy to post implementation. The challenge and main focus were, of course, the *employee experience* part [4].

3. Participatory elements

3.1. Staff training programs

The Youth Council team, together with the management and HR team, provide to the other departments, at the beginning of each year, a portfolio of trainings as shown in Fig. 1 (compulsory and optional) of several types: e-learning, operational, classroom, webinar. Several platforms are made available to employees to carry out these trainings (e.g. LinkedIn, Alliance-learning, Teams).

The capacity of organisations to accumulate and apply new knowledge is a decisive factor in meeting new competitive standards. The ever-changing diversity, coupled with the need to adapt to changes in the external environment accelerate the rhythm of evolution and learning. The need to survive in the marketplace requires organisations to learn at an ever-increasing pace. New information and communication technologies accelerate the pace of change and increase the need for learning, subjecting it to an increased flow of information. For interns, the learning alliance platform (Fig. 2) is a real support. This platform is dedicated to finding the right training (face-to-face or digital), monitoring courses, selecting topics of interest and accessing recommended content [4].

NEW COMERS BOP	Training code	3 MONTHS BOP
1. Purchasing Foundations e-learning	A-040227	1. A-SMA teams - inscrire en afara L@A
2. APO Core Process - Sourcing e-learning		2. A-RFQ teams - inscrire en afara L@A
3. APO Core Process-The Panel e-learning		3. ONE VIEW CONSULTARE in sala - optional
4. APO Core Process-Performance Review e-learning		4. BOP COGS in sala
5. NEW COMMERS BOP in sala	A018416	5. Management de la Conformite - Caracteristiques Specifiques Reglementaire et Securite e-learning
6. SCOPP SCA+ECO in sala	A018411	6. How to Prepare for Your Negotiations e-learning
7. SCOPP Utilaje in sala	A018410	7. COST modul 1 (Standard Quotation) in sala
8. ESSENTIALS OF THE ANQP STANDARD - EN e-learning	A-000165	8. SRM - SUPPLIER RISK MANAGEMENT ESSENTIALS e-learning
9. e-PDS SOFTWARE e-learning	A-144891	9. SRM - SUPPLIER RISK MANAGEMENT MISSIONS e-learning
10. SCOPP DEV teams - inscrire en afara L@A		10. SRM - SUPPLIER RISK MANAGEMENT OPERATIONAL e-learning
11. Renaulution : Strategie developpement durable e-learning		11. Fundamentals of Customs e-learning
12. Electronic part file inscripitor	https://ins.ope...	12. ASC IP PB (English version) annua exista https://ins.ope...
13. E-sqis video		13. e Conf Circular Economy for APO video
14. Standard Quotation e-learning	A-021692	14. CSR Ecovadis Replay 2023 numal exista video
15. ESSENTIALS OF THE V3P DEVELOPMENT LOGIC - EN e-learning		15. Sourcing achat in sala
		16. Master class IC : EC crisis inscripitor
		17. Master class IC : Energy video
		18. MEI Macroeconomy & Inflation video
		19. Raw Material Management 2023 video

Fig 1. Training passport example (based on [3])

The screenshot shows the Learning Alliance platform interface. The top navigation bar includes links for Home, Learning, Regulations, and L&A Guides. The main content area is divided into several sections:

- Hi LISETTE! What would you like to learn today?**: A search bar with the placeholder text "Search by keywords".
- Digital Learning Offer**: A carousel of training actions with images and titles like "Discover your Learning", "Soft Skills - Acquire", "Language skills", and "Leadership training".
- Your Subjects**: A section with a list of subjects (e.g., CHANGE MANAGEMENT, COMPANY CULTURE & BENEFITS) and a dropdown menu for selecting languages.
- Your Playlists**: A section with a list of playlists and a dropdown menu for selecting languages.
- Your Trainings**: A section with a list of trainings and a dropdown menu for selecting languages.
- ASSIGNED / NO DUE DATE**: A button indicating the status of the training.

Annotations on the left side of the interface provide additional context:

- Your Subjects:** Don't forget to add your subjects of interest. The system will suggest trainings.
- Your Language(s):** Select the languages you want your training to be.
- Your Playlists:** that you have selected by clicking on the follow button.
- The Transcript:** Includes all your Trainings status (active & completed)
- The Assigned/ No due date:** Your assigned training with or without due date

An annotation on the right side of the interface says: "Browse the carousel for various training actions."

Fig. 2. Navigating the Learning Alliance platform (based on [3])

Staff training is a systematic and planned activity underpinning this goal, aimed at acquiring and improving the skills and knowledge of employees. A modern training system thus becomes a vital necessity for any organisation in order to develop and maintain the professional standards of its human resources [8].

The objectives of these training sessions are to learn how to carry out the activities and the functionality of the working systems. One of the benefits is that the employee knows the operating system(s) of the company in which they work. Another benefit would be that they learn various tactics for negotiating, marketing or selling the products the company produces.

3.2. Methods of performance evaluation

Performance indicators are measures used to assess and monitor the achievement of objectives and results within organisations or individual activities. These indicators provide an objective way to measure the success and effectiveness of an action, process or strategy [2]. Performance indicators are more applicable to the training department and consist of tracking attendance, volume of training completed by employees and satisfaction level.

This level of satisfaction is evidenced by the evaluation methods (Fig. 3) which consist of taking certain tests at the end of the evaluation or completing feedback forms.

Employee feedback is very important as it identifies future training needs or satisfaction levels as well as feedback on the quality of training sessions delivered by trainers.

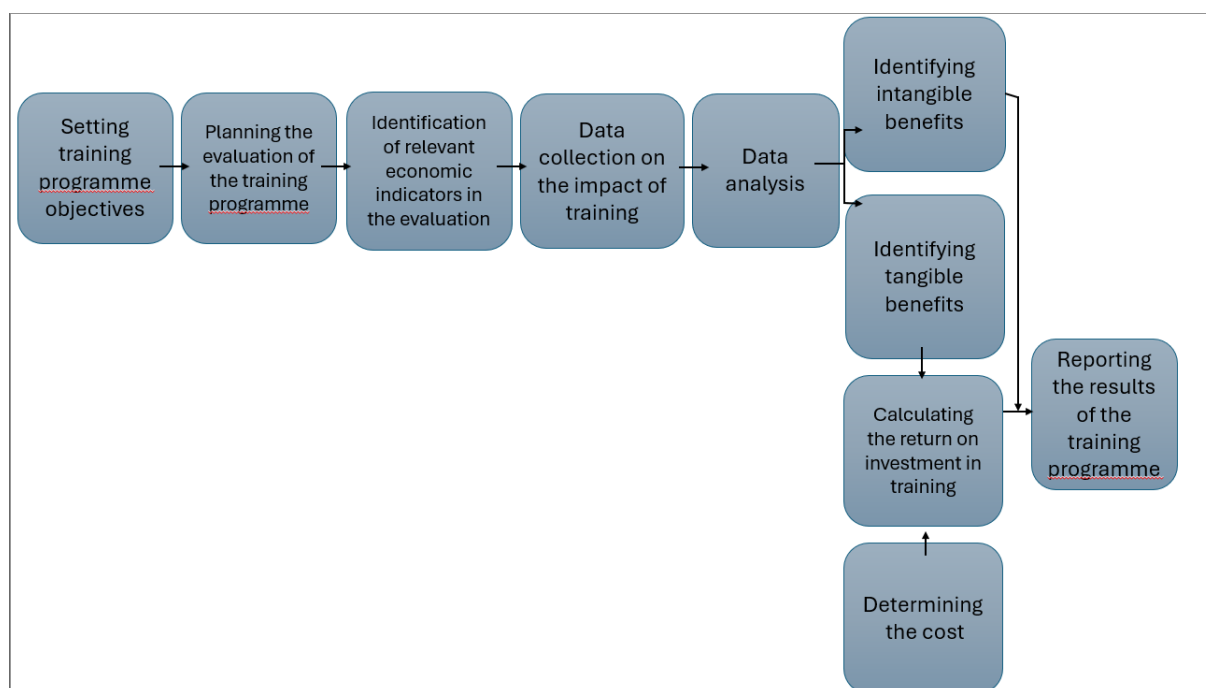


Fig. 3. Model for evaluating training programs (based on [7])

More broadly, performance appraisal is considered to be an action, a process or some type of cognitive activity, by which an appraiser assesses or estimates a person's performance with respect to standards, as well as his or her own mental representation, value system or conception of performance [6].

The involvement of leaders and managers in promoting and supporting training programs is very important, as they can be role models for employees by actively participating in these programs [9]. This

commitment is not just a formal thing, but also an important step in building an organisational culture where continuous learning is essential.

Leaders are in charge of planning training and encouraging employees to attend as many training sessions as possible as part of each employee's training passport. Production-focused leaders set high performance standards and make sure they are met, organise tasks carefully and indicate working patterns, and closely monitor the work of team members. People-centred leaders encourage employee participation in goal setting and other group decisions, building trust and mutual respect. Studies at the University of Michigan have concluded that people-centred leaders perform better [7].

Teams of managers are the ones who step in when leaders fail on their own to encourage employees to participate in the training provided for in the training passport.

4. Conclusions

- Participating in the wide range of training and education is not only a service obligation for company employees, but also a form of recognition and reward.

- The specialised nature of the knowledge acquired leads to an employee's increased value and performance within the team and the company.

- Trainings contribute to the personal development of team members, to their inner enrichment and to increasing team cohesion. For some courses, being nominated as a participant is an achievement and a form of motivation, given the limited number of places available. At the same time, it is a motivating factor that increases engagement. Also, the direct impact of training on individual and team performance is visibly significant.

5. Bibliography

[1] ***, Importance of training programmes for employee development <https://revistacariere.ro/leadership/management/importanta-programelor-de-formare-pentru-dezvoltarea-angajatilor>, accessed at 25.04.2024.

[2] ***, The importance of training programmes and career development, <https://bia.ro/importanta-programelor-de-training-si-dezvoltarea-carierii/>, accessed at 13.03.2024.

[3] ***, Documentation within the company SC Automobile Dacia SA, 2024.

[4] ***, Committing together for sustainable growth and development <https://www.industrialunion.org/renault-the-renault-group-works-council-and-industrial-global-union-sign-a-global-framework>, accessed at 05.04.2024.

[5] ***, <https://www.renaultgroup.com/en/>, accessed at 24.04.2024.

[6] Cole, G. A. (1997). Personnel Management (In Romanian), Editura Codecs S.A., București.

[7] Virgă, D. (2004). Performance assessment, Bogáthy, Z. (coord.), Handbook of work and organizational psychology (In Romanian), Editura Polirom, Iași.

[8] Borgonjon T., Maenhout B. The impact of dynamic learning and training on the personnel staffing decision, Computers & Industrial Engineering, Volume 187, January 2024, 109784, DOI: 10.1016/j.cie.2023.109784.

[9] Fraile F., Psaromatis F., Alarcón F., Joan J., A Methodological Framework for Designing Personalised Training Programs to Support Personnel Upskilling in Industry 5.0, *Computers*, 12, 224, DOI: 10.3390/computers12110224, 2023

PRODUCT DEVELOPMENT BASED ON ONLINE DATA ANALYSIS OF USER SEARCH TRENDS

BUTUC Mihai-Alexandru¹, ISPAS Elena-Andreea¹,
GHEORGHE² Marian, TIRIPLICĂ² Petre

¹Faculty: Industrial Engineering and Robotics,
Specialization: Industrial Economic Engineering,
Year of study: IV, e-mail: butucalexandru65@gmail.com

²NUST Politehnica Bucharest, Faculty of Industrial Engineering and Robotics,
Manufacturing Eng. Department (TCM)

ABSTRACT: This paper investigates the analysis of search trends in the field of engineering part design using data-driven research methods based on online data. The main goal of the study is to identify patterns and changes in user preferences and requirements for part design. To achieve this, a diverse set of data sources will be used, such as search engines and social media platforms, to collect relevant information about search terms, consumed content, and online discussions. By analyzing this data, we will gain a deeper understanding of market requirements and expectations for part design. The results of this study can be used to guide the product development process, identifying emerging user needs and directing design strategies in the proper direction to meet these ever-changing requirements.

KEYWORDS: marketing, analysis, users, data, search engines

1. Introduction

Google Trends, accessible through [1], provides information about queries submitted. This tool is based on a representative random sample of all queries that are handled by Google on a daily basis.

Search normalization is done based on the location of the request and the time. Each data point for a given time and location is divided by the sum of all searches to obtain the relative popularity which is scaled on a range from 0 to 100, considering the proportion of a query to the total searches from the total queries. The index is called Google Trends Index and is denoted as GTI. Two main advantages are: providing data for indicators that are published infrequently from official sources and low sensitivity to the biases of small samples.

Even though it is a powerful tool, Google Trends has several limitations. It depends on the level of internet penetration, the social and economic status of individuals, and the age category. Young people and students are more likely to use Google to search for software programs, which are needed during their studies and later in their careers. On the other hand, people with a high level of poverty and/or illiteracy are less interested in using the internet/Google.

The objective of this paper is to compare and analyze the usefulness of users' online search trends in the way of product design and development.

2. General considerations

In order to carry out this study, data was collected on the most popular software tools used in the design and development of products.

At the national level, the frequency of data is monthly, starting with the first month of 2022 until December 2023. The data is provided by Google Trends platform using the keywords/ application name: 'AutoCAD', 'Fusion 360', 'SolidWorks', 'CATIA' [2].

At county level, the analysis is conducted annually, for the years 2022 and 2023 respectively, based on the same keywords/ applications name as in the national analysis.

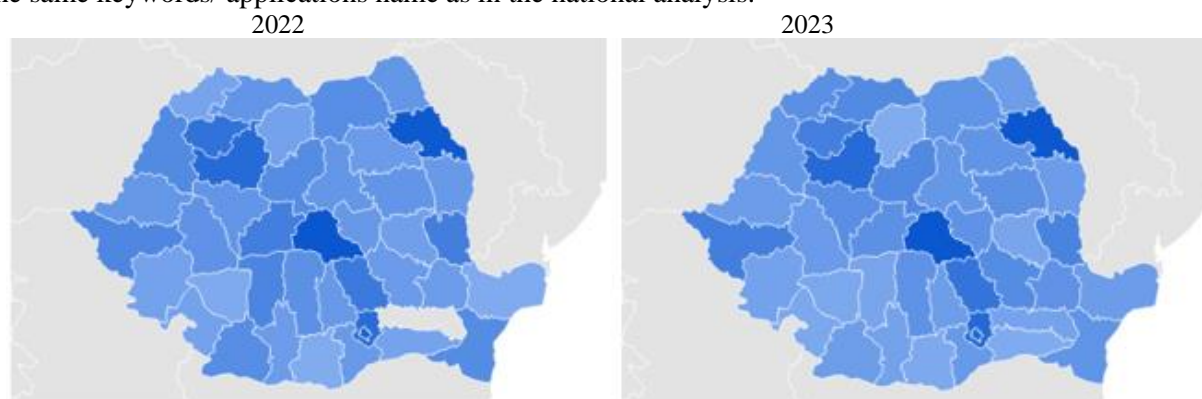


Fig. 1. AutoCAD [1]

According to Fig. 1, there are significant differences between counties in the distribution of the number of searches [3]. It can be seen that for the keyword "AutoCAD" the most searches in 2022 are in Brasov county, this level keeping its position at the top of searches in 2023. This is followed by the largest urban centers in development in Romania (Iasi, Bucharest, Cluj). The fact that the cities are university centers positively influences the number of searches.

According to the analysis of searches in Ialomita county, there is a significant increase in interest in AutoCAD software, which is probably due to the increased need for design systems or qualified personnel (Fig. 1).

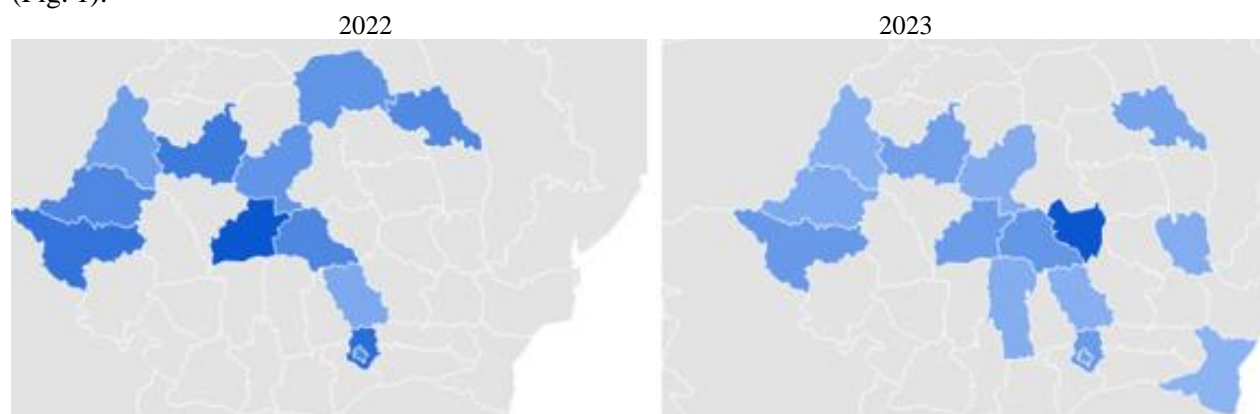


Fig. 2. Fusion 360 [1]

Considering the case of the keyword "Fusion 360", it can be seen that the number of searches is significantly higher in the more developed counties of the country. The number of searches is relatively constant over the two years analysed, resulting in a low level of demand (Fig. 2).

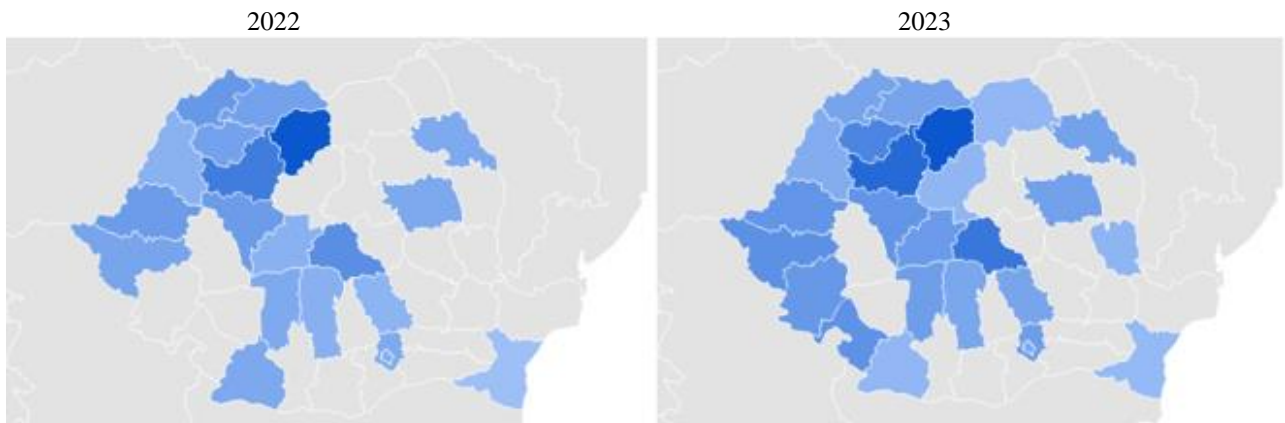


Fig. 3. SolidWorks [1]

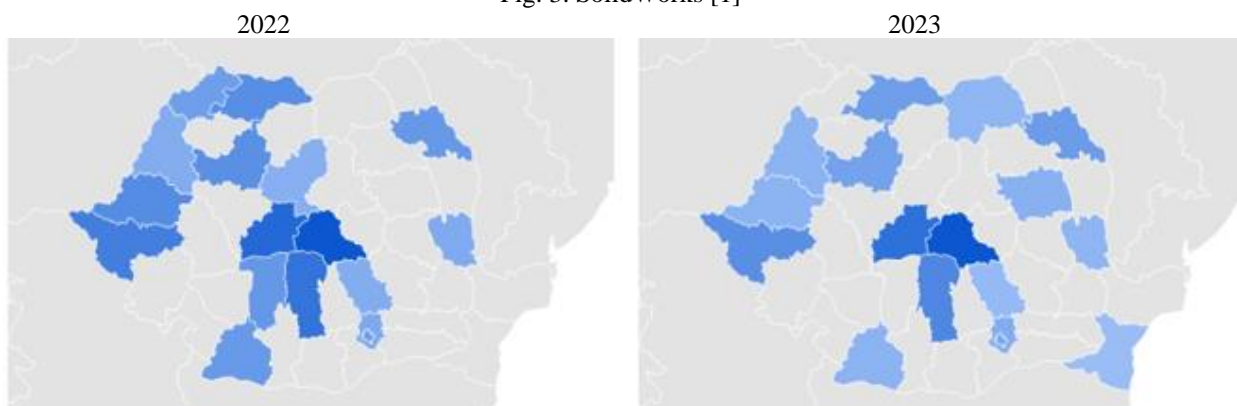


Fig. 4. Catia [1]

The keywords/ applications name "SolidWorks", "CATIA" show a steady growth, involving more and more counties in continuous development (Fig. 3, 4).

Analysing at national level, in 2023, the most searched keywords/ applications among counties are "AutoCAD", "SolidWorks". Thus, it is possible to estimate the user trend for these two design and product development software programs.

3. Comparative analysis between the four keywords/ applications names

According to Fig. 5 and 6, it can be seen that there has not been a major change when referring to the number of searches. Thus, it can be assumed that AutoCAD is the market leader in the field of product design and development.

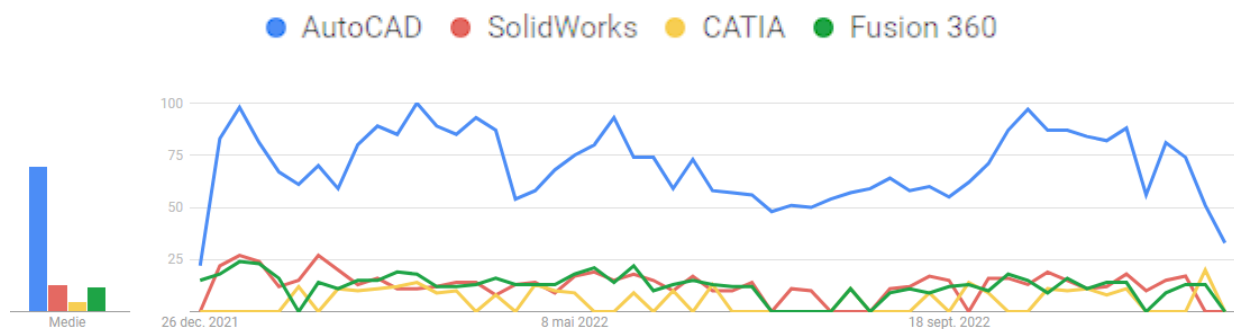


Fig. 5. Number of searches for the four keywords/applications names in the year 2022 [1].

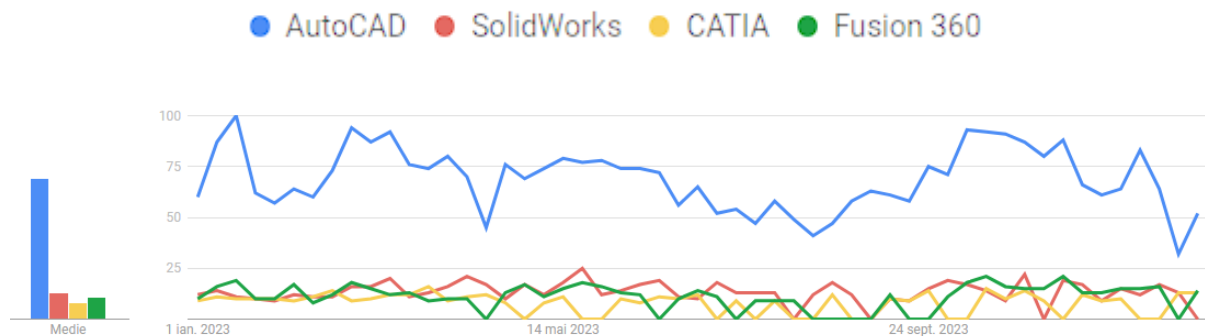


Fig. 6. . Number of searches for the four keywords/ applications names in the year 2023 [1].

However, a decrease in user interest during the summer period is noted for 2022 and 2023 respectively, thus reinforcing the idea that these programs are also used to a large extent by pupils/students.

4. Predictions for product development

As the data provided from the online environment shows, econometric models can be estimated for the market for software for product design and development.

A new term, Artificial Intelligence (AI), is being introduced to describe a possible development path for design software, which is also showing an increase in user interest (Fig. 7).

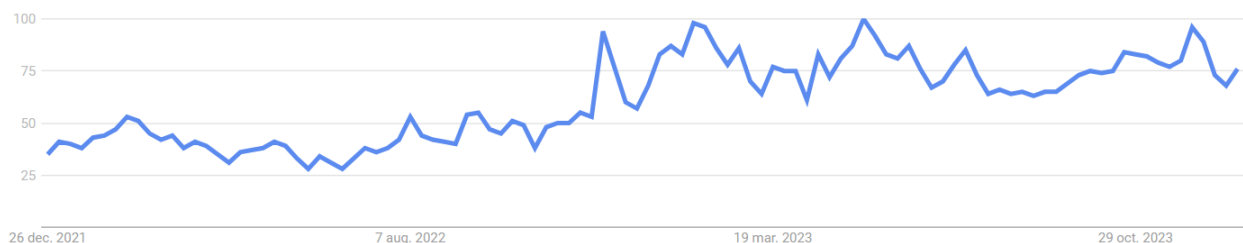


Fig. 7. Evolution of the number of searches for the term "Artificial Intelligence" over the period 2022-2023 [1]

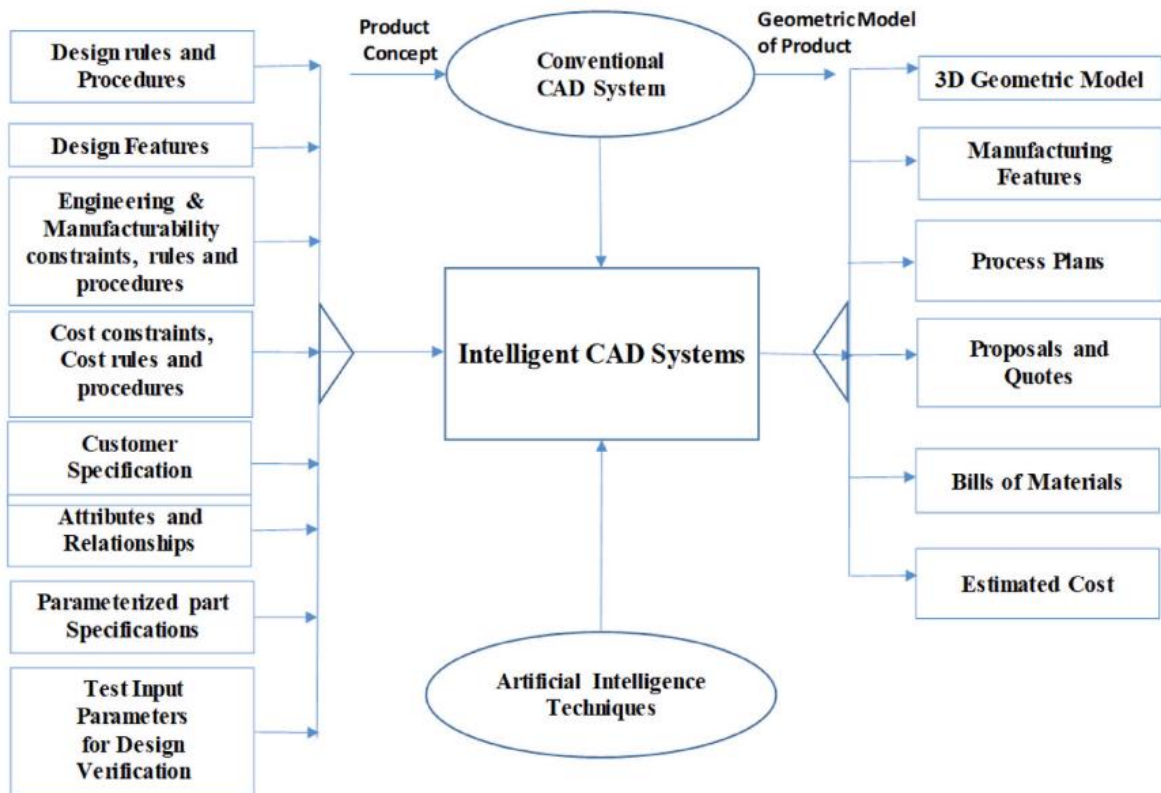


Fig. 8. Conventional CAD to intelligent CAD [4, 8]

Conventional CAD systems can be transformed into intelligent ones [4, 8] (Fig. 8).

Model-based reasoning (MBR) is the process by which CAD can be merged with Artificial Intelligence (AI). Through quantitative and qualitative analysis, MBR forecast the interactions which could exist between the different parts of the design [5, 8].

The MBR characteristics can be expressed as follows: the component parts of the product are stored hierarchically in order to know the relationships between them; knowledge-based reasoning and decision-making procedures are expressed by design experts; the reasoning and methodology system defines the rules for the links between the parts of the product; the analysis of qualitative and quantitative simulation defines the efficiency of the developed product; simple installation procedure in the database.[8].

On this principle, programs such as SOLIDWORKS x Design, which is the first integrator of AI in design, have been developed. Thus, operators can implement different solutions to their instant design challenges through cloud collaboration, solutions generated by an AI tool. First, the operator creates the model and defines the constraints. Then, SOLIDWORKS x Design will instantly generate the part via AI integrated into its system, based on the user-defined constraints [6, 7, 8].

Also, the cooperation between the technologies Augmented Reality (AR), Virtual Reality (VR), Mixed Reality (MR) and programming software systems can bring a new growth in the trend of their use.

In augmented reality technology, the CAD model is loaded into VR, AR, and MR platforms for simulation and conceptualization. However, in present, CAD applications still do not offer visualization and simulations like those in VR, AR and MR. There are many complex elements in real systems that require detailed conceptualization [8].

5. Conclusions

- By comparing the trends in 2022, respectively, 2023 regarding the number of searches for the design and product development software programs "AutoCAD", "Fusion 360", "SolidWorks", "CATIA", it can

be stated that they are continuously growing, gradually increasing the number of users interested in them. In order to continue the upward trajectory, these products must be constantly improved.

- In perspective, integrating AI, AR, VR, MR into product design and development systems will facilitate the design process and the associated activities.

6. Bibliography

- [1]**, Search engine, <https://trends.google.com/trends/>, accesed at 15.03.2024.
- [2] Manolache D.-S., Computer Aided Design 2, Lecture Notes, UNST Politehnica Bucharest, 2022-23.
- [3] Tiriplica P.-G., Probability Theory and Mathematical Statistics, Lecture Notes, UNST Politehnica Bucharest, 2021-22.
- [4] X.F. Zha, “Artificial intelligence and integrated intelligent systems in product design and development”, *Intelligent Knowledge-Based Systems*, Springer, Boston, MA, 2005, pp. 1067–1123.
- [5] Khan S., Awan M. J., A generative design technique for exploring shape variations, *Advanced Engineering. Informatics.* 38 (2018) 712–724. DOI: 10.1016/j.aei.2018.10.005, WOS:000454378700053, Elsevier B.V., 2018.
- [6] N. Le, “Product Design with Cloud Based and Desktop CAD Software, A comparison between SolidWorks and Onshape”, 2018.
- [7] B. Duan, “Analysis on the value of 3D printing in jewelry design based on artificial intelligence”, *Journal of Physics: Conference Series*, vol. 1744, IOP Publishing, 2021, February, 42132, 4.
- [8] Hunde B.R., Woldeyohannes A.D., “Future prospects of computer-aided design (CAD) – A review from the perspective of artificial intelligence (AI), extended reality, and 3D printing”, *Results in Engineering*, Volume 14, DOI: 10.1016/j.rineng.2022.100478, WOS: 000815966600004, Elsevier B.V., 2022.

DEVELOPMENT OF A WEB APPLICATION FOR INTERNATIONAL STANDARDS USED IN TECHNOLOGICAL PROCESSES

FRÎNCU Roxana-Iuliana¹, Nicolae TUNSOIU², Cristin ZAHARIA²

¹Faculty: Industrial Engineering and Robotics,

Specialization: Industrial Economic Engineering, Year of study: IV, e-mail: roxanafrincu760@gmail.com

²NUST Politehnica Bucharest, Faculty of Industrial Engineering and Robotics,
Manufacturing Eng. Department (TCM)

ABSTRACT: Standify.eu is an online platform dedicated to providing relevant international standardized resources for documenting technological processes. Platform users have access to a wide range of essential technical documents and standards for the industrial sector. In addition to these resources, Standify.eu also offers specialized online courses designed to facilitate the proper understanding and application of these standards. The intuitive interface and efficient navigation menu facilitate access to relevant information and resources. A distinctive aspect of the platform is the free access to these standardized resources in electronic format (PDF), which is a significant advantage for researchers, professionals, and students conducting research in the industrial field who may be hindered by the costs associated with acquiring these resources. Essentially, Standify.eu aims to become an essential and accessible tool for all those interested in studying and applying standards in the industrial sector, thus contributing to the promotion of knowledge and practices according to international standards.

KEYWORDS: Website, Standard, Courses, Accessibility.

1. Introduction

This paper focuses on creating a successful online platform in the context of the observed difficulty in accessing standardized resources in the technical field. Existing resources are often only available in printed form or require payment for access to digital versions. The platform presented in this paper, Standify.eu, aims to solve this problem by providing simple and free access to relevant standardized resources. The sections specific to each functionality already implemented on the Standify.eu site reflect this approach by including a library of standardized resources and a section dedicated to online courses where teachers can add additional materials to facilitate the learning process and the realization of technical projects. Thus, this paper explores the importance and utility of such a platform in the context of the technical industry and the educational process, with the main objective being to assist students and professionals in the technical field. This updated version highlights even better the implementation and existing functionalities of the Standify.eu platform as well as its purpose to serve both students and professionals in the technical field.

2. Current status

1. The Standify.eu web platform (As illustrated in Figure 1) has already been implemented and is functional, being published on the internet after purchasing the domain Standify.eu on the GoDaddySites platform [10]. All the functionalities of a website are operational, offering users a complete navigational experience. However, work on the standardized resource library is still ongoing. Currently, there are only a few PDF documents with specific names that are visual demos because it is necessary to create a database and complete it with all the relevant data. Regarding the course area, it is not yet filled with the correct video resources but only with some on the respective subject. The intention is to

find more video resources as close as possible to the addressed subject. Additionally, it is desired to create a blog section and a newsfeed for the community that will form around this platform to allow the sharing and discussion of resources by users. Overall, the Standify.eu platform is in an initial stage of development, and the next step is to continue working on specific functionalities to offer a complete and valuable experience to its users.

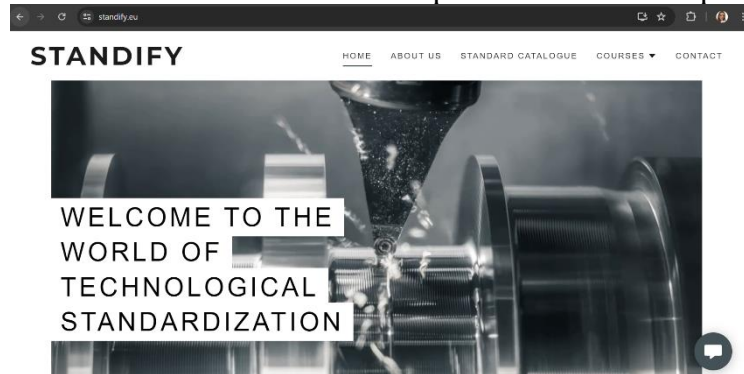


Fig. 1 Standify.eu

3. Development Process of the Standify.eu Platform

The Standify.eu platform was developed in a series of planned and coordinated stages to ensure the successful implementation of the proposed objectives. The development process included the following main steps:

1. Domain Purchase and Name Availability Verification

The first step in developing the platform was purchasing the Standify.eu domain and verifying the availability of the website name. Choosing a distinctive and suitable name was essential for the platform's identity and market recognition [10].

2. Defining Platform Objectives and Design

The objectives and functionalities of the platform were clearly defined and listed at this stage in parallel with the elaboration of the website design. Special emphasis was placed on creating an intuitive and attractive interface for users to facilitate navigation and access to available resources [9].

3. Implementation of Necessary Functionalities Through an Easy-to-Use Interface

The next step involved implementing the essential functionalities of the platform through an easy-to-use interface. Features such as the standardized resource library and the online course section were developed and integrated [8].

4. Platform Verification and Testing

The Standify.eu platform was subjected to a rigorous verification and testing process to ensure proper functionality and performance. Any errors or issues encountered during the tests were identified and rectified.

5. Platform Publication

The final step involved the official publication of the Standify.eu platform on the internet, making it available to users.

This detailed development process ensured the successful implementation of the Standify.eu platform and contributed to achieving the proposed research objectives. However, as described above, there are still steps to follow to complete the platform and achieve the final objectives.

4. Used Resources

The development process of the Standify.eu platform involved the use of a variety of specialized resources divided into specific categories:

Resources for Domain Purchase and Name Availability Verification

For this crucial stage, we relied on the GoDaddy platform to purchase the Standify.eu domain and verify the availability of the website name, ensuring that we have a distinctive and recognized online identity [2]. (See Figure 2)

Product	Quantity	Term	Price
EU Domain Registration standify.eu	1 Domain	1 Year	€3.99
Subtotal:			€3.99
Tax:			€0.76
Total:			€4.75

Fig. 2 Domain standify.eu

Resources for Defining Objectives and Platform Design

For defining the platform's objectives and elaborating its attractive and functional design, we used the Canva platform for websites, which provided inspiration and flexible tools for this creative stage [1].

Resources for Implementing Functionalities and User Interface

For implementing the essential functionalities and creating an easy-to-use interface, we integrated video resources from platforms such as YouTube and Vimeo, ensuring that users have access to relevant and quality multimedia content [8].

Resources for Obtaining Visual and Graphic Elements

To obtain high-quality icons and images with a transparent background, we used the Remove.bg and Freepik.com platforms, thus offering a professional and attractive aspect to the platform.

Resources for Documentation and Training

During the platform verification and testing process, the resources and tools provided by ChatGPT were essential for documentation and obtaining clear and concise usage instructions for all these mentioned platforms.

5. Platform Sections

The following lines will present the most important sections of the platform mentioned earlier in the form of figures. (See Figure 3 and 4)



Fig. 3 Online courses provided by the platform

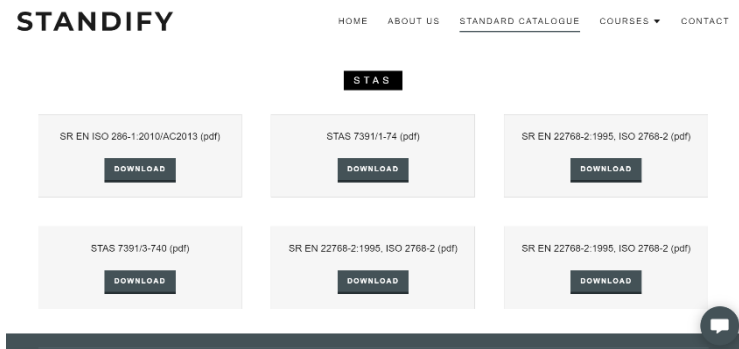


Fig 4. Standardised resources

6. Conclusions

The Standify.eu platform has been successfully published, offering access to standardized resources and online courses in the technical field. This represents an essential solution for education and professional development in a digital era, which is why it is necessary to complete the platform through the most suitable implementation methods.

7. Bibliography

- [1]. Canva "How to build a website." Accessed April 12, 2024. <https://www.scribbr.com/category/citing-sources/>.
- [2]. GoDaddy "Search Domain." Accessed April 15, 2024. <https://websites.godaddy.com/>.
- [3]. Gross, D., & Yellen, J. (2004). Graph Theory and Its Applications. Chapman & Hall/CRC, Boca Raton, ISBN 978-1-58488-505-4.
- [4]. Pressman, R. S. (2014). Software Engineering: A Practitioner's Approach (8th Edition). McGraw-Hill Education, New York, ISBN 978-0078022128.
- [5]. Nielsen, J. (2000). "Designing Web Usability: The Practice of Simplicity". New Riders Publishing, ISBN 978-1562058104.
- [6]. Krug, S. (2014). "Don't Make Me Think, Revisited: A Common Sense Approach to Web Usability". New Riders Publishing, ISBN 978-0321965516.
- [7]. Feldman, S. (2018). "Introduction to Information Retrieval". Cambridge University Press, ISBN 978-0521865715.
- [8]. Mozilla Developer Network (2024), "Web technology for developers." Accessed May 6, 2024. <https://developer.mozilla.org/en-US/docs/Web>.
- [9]. Google Developers (2024), "Web Vitals." Accessed May 6, 2024. <https://web.dev/vitals/>.
- [10]. Bootstrap Documentation (2024), "Bootstrap 5 Overview." Accessed May 6, 2024. <https://getbootstrap.com/docs/5.0/getting-started/introduction/>.

ARTROBO: USING COLLABORATIVE ROBOTS FOR AUTOMATED DRAWING TRANSPOSITION ONTO PAPER

STOICA Bogdan-Cristian¹, HANGA Mihail², COSTEA Ionuț Bogdan² and CAZACU Carmen Cristiana³

¹Faculty: Industrial Engineering and Robotics, Digital Production Systems Specialization, Year of study: I, e-mail: stoicabogdancristian19@gmail.com

²Faculty: Industrial Engineering and Robotics, Applied Informatics in Industrial Engineering Specialization,

³Faculty: Industrial Engineering and Robotics, Department: Robots and Production Systems

ABSTRACT: *ArtRobo is robotic arm that can automate the replication of hand drawn paintings and sketches using industry standard robotics. This approach combines the creativity of a human brain with mechanical precision. By streamlining the laborious tasks, it allows artists to focus more on their creativity, debunking the notion that industrialization compromises artistic expression. ArtRobo is a tool for creativity that enhances the human-machine cooperation through industrialization. This pushes the boundaries of “The creative” starting a new era of hand&machine art-making, proving that art and robotics can coexist, showcasing that both sides can coexist efficiently and accurately while keeping the human creativeness.*

KEYWORDS: *ArtRobo, Collaborative Robots, Automated Transposition, Robotic Precision, Artistic Digitalization*

1. Introduction

The digital era is in constant evolution, and the intersection of art and technology offers fertile ground for innovation and creativity. This paper explores the potential and implications of integrating robotic technology into the artistic creation process. While digital technology has advanced considerably in recent years, manually transferring drawings onto paper remains an essential aspect of many artistic and creative fields. Traditional printing offers an alternative, but it is limited to standard printing techniques and cannot recreate the unique trace of a brush or other drawing tool. Therefore, developing a robotic system capable of taking over these tasks and performing them automatically represents a significant step towards optimizing the creation process.

This work focuses on developing a robotic arm capable of transferring hand-drawn designs onto paper, opening up new horizons in the field of art and robot-assisted manufacturing. The project unfolds in two main stages:

1. *Research Stage:* This stage involves defining the technical and functional requirements, acquiring the equipment, and designing or developing additional equipment as needed.
2. *Implementation Stage:* This stage encompasses assembling the equipment, developing the paper transfer program, and testing the functionality of the entire assembly. The expected outcome is a functional system that demonstrates the feasibility of the concept and allows for further evaluation of its performance and usefulness.

2. Current State

The use of robotic systems in drawing and painting has gained significant attention from researchers in recent years. For instance, [1] proposes a new method for designing a controller for dual-arm manipulation, applicable to various tasks like drawing. To create a visual-mental-physical circuit for communication between human and non-human actors, [2] combined a generative adversarial network, a co-robotic arm, and a five-year-old child. Additionally, [3] developed inverse kinematic models using an artificial neural network technique to adjust the movement of a 3DOF drawing robot arm. A 3DOF robotic arm made from LEGO NXT bricks was used for drawing on paper in [4] and was considered suitable for educational projects on robotics and robot programming.

In the field of trajectory planning, traditional methods often involve manual trajectory design by artists. Only recently have automated trajectory planning methods been proposed. However, these recent approaches still have limitations [5], resulting in drawings that feel more like prints rather than organic creations. Fig.1 & Fig.2 illustrate such drawings made by an arm and highlight areas for improvement.



Fig .1. Drawing made by a robot with 3DOF

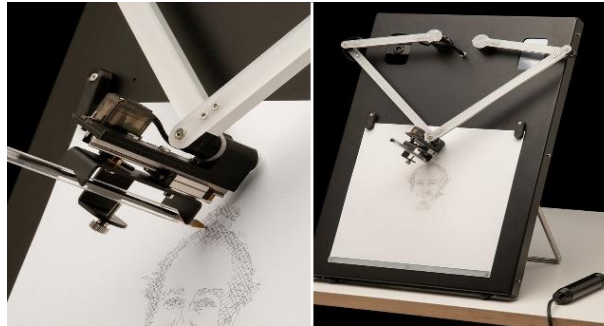


Fig.2. Drawing made by an assembly with 2DOF

3. Equipment Used

The UFactory Lite 6 robotic arm was chosen for this task. Its ability to combine precision (repeatability of ± 0.2 mm) with rapid speed (500 mm/s) is essential for accurately reproducing drawings while ensuring quick completion. The 1 kg payload allows for the use of a variety of brushes and colors, offering flexibility. Compatibility with standard I/O interfaces facilitates integration with the intuitive UFACTORY Studio software, simplifying arm programming and control. Its 6-degree-of-freedom (DOF) kinematic configuration provides a wide range of motions, allowing for the accurate recreation of drawing details on the paper surface. An inverse kinematics algorithm translates digital commands into precise physical movements, guiding the arm to specific points on the paper. Motion planning algorithms are used to generate smooth and efficient trajectories. Precise control of these trajectories is ensured by implementing PID controllers Fig. 3 & Fig. 4.[6]

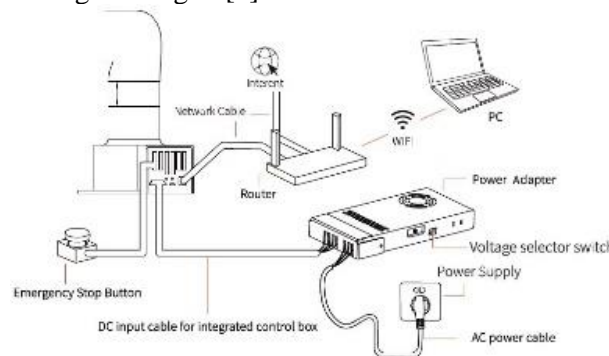


Fig.3. Set-up UFactory Lite 6

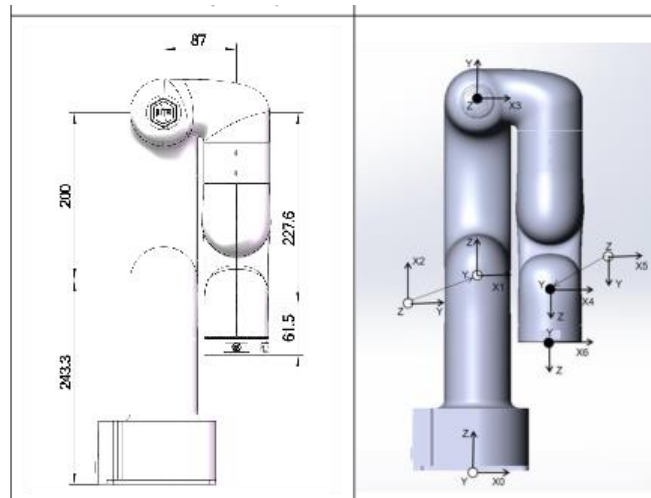


Fig.4 Parameters UFactory Lite 6

A custom brush holder was designed and 3d printed with a focus on functionality and adaptability. It prioritizes stability without weighing down the arm, achieved through printing parameters (PLA+: Layer height: 0.2 mm; Nozzle 0.4 mm @ 210°C; Bed 60°C; Max print speed: 200 mm/s; Max Accel: 1500 mm/s²). Precise adjustment mechanisms are integrated to allow for fine-tuning of the brush height, angle, and orientation in relation to the paper. The brush is secured by a secure clamping mechanism, which also allows for quick release for color changes. The holder's compatibility with various art brushes provides flexibility in the choice of creative tools. The rigid connection of the holder to the robotic arm ensures maximum stability and precise transfer of digital commands into physical movements of the brush. Fig.5.



Fig.5 Custom brush holder

The UFactory Lite 6 robotic arm, designed for interaction with flat and rigid surfaces, was not optimized for drawing on paper. Paper, being a flexible and sensitive surface, presented specific challenges regarding the precision and control of the arm's movements. To overcome these challenges, a custom holder was designed and made from lightweight and resistant materials. The holder features a flat and rigid surface, similar to the environment for which the robotic arm was originally optimized. A paper fixation system was also included to ensure stable and precise positioning (Fig.6).

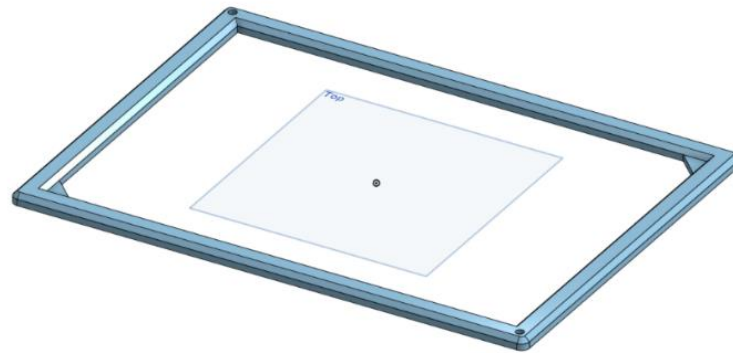


Fig.6 Paper holder 3DPrinted

4.Programming

The 6DOF robotic arm with integrated kinematics allows for flexibility in the coding approach. Here's a breakdown of the steps involved:

1. *Image Processing and Transfer:*
 - Image acquisition
 - Processing to find and extract the contour of the image
 - Processing the contour to define coordinates
 - Sorting coordinates for efficient transfer
 - Arm movement based on coordinates for transferring the image onto paper
2. *Hand-Drawn Digital Transfer:*
 - Creating a digital drawing interface
 - Using a mouse tracker to capture the drawing
 - Defining a colouring canvas
 - Sorting coloured pixels for efficient transfer
 - Transforming pixel coordinates to UFactory Lite 6 specific coordinates (mm)

These approaches were developed after multiple code iterations. To transfer an image, an algorithm traces the outline and chooses points to connect for precise rendering. While initial code worked for simpler images, it lacked precision for complex paths. To address this, a variant using Bezier curves was implemented to create smoother transitions between points on the contour. Transferring a hand-drawn digital drawing was achieved using Python libraries like easygui and pygame for creating the mouse tracker and drawing functions. Colored pixels are then sorted and grouped for efficient transfer, with their coordinates converted to a format compatible with the robotic arm.

Finally, both programs were combined into a single code with a "case" text file enabling switching between image and hand-drawn drawing modes. The code was further optimized with custom functions for improved efficiency. Here's a deeper look into specific functionalities:

Image_processor.py:

This file forms the foundation for understanding the drawing itself. Let's analyse the `process_image()` function step by step:

1. *Input Validation:* Ensures the function receives a valid path to the image file.
2. *Image Loading:* OpenCV, a powerful image processing library, is used to load the image in grayscale mode for simplified processing.
3. *Standardization by Scaling:* The image is resized to a fixed size using OpenCV functionalities for consistent processing regardless of the original image dimensions.
4. *Smoothing Details:* A Gaussian filter attenuates the image, mitigating noise or minor inconsistencies in the drawing.

5. *Thresholding*: This essential step creates a binary image by distinguishing drawing lines from the background. Pixels exceeding a specific intensity threshold are considered part of the drawing (typically white), while everything below falls into the background (typically black).
6. *Line Thickening*: Mitigates potential line imperfections by expanding the foreground (drawing lines) by a few pixels, making them appear thicker.
7. *Refining Lines*: A slight erosion is applied to counteract the thickening from the previous step, achieving a balance between clear and well-defined lines.
8. *Contour Identification*: Contours are identified using OpenCV's contour finding algorithms, essentially creating a digital representation of the drawing's outlines.
9. *Saving the Plan*: The identified contours, representing the digital sketch of the drawing, are stored for later use by the arm control component.

arm_draw.py:

This file plays a central role in controlling the UFactory Lite 6 robotic arm. It provides a class called `Arm_draw` equipped with methods for configuring and manipulating the arm, transforming the digital sketch into a physical masterpiece.

Tools at your disposal:

1. *move_to(x, y, z, w, r, p)*: Instructs the arm to move to a specific position in 3D space, defined by x, y, z coordinates and arm orientation (w, r, p).
2. *stop_arm()*: Gracefully stops the arm's operation and disconnects it upon completion or in case of emergencies.
3. *reset_arm()*: Returns the robotic arm to its original designated position, ensuring a predictable starting point for each drawing.
4. *suicide()*: An emergency stop measure that sends the arm to a pre-configured safe position to prevent unintended movements.
5. *set_magic_number()*: Defines a scaling factor that adjusts the drawing size to fit the dimensions of the paper used.
6. *set_write_height()*: Controls the height at which the pen touches the paper, significantly impacting the outcome of the drawing.
7. *set_offset()*: Defines an offset value for adjusting the starting location of the drawing on the paper, crucial for precise reproduction.
8. *set_contour()*: Bridges the digital and physical worlds by providing the `Arm_draw` class with the processed contours extracted from the image, offering the robotic arm the plan to follow.
9. *set_is_separated()*: Informs the class whether the provided contours represent separate elements or a single continuous drawing, allowing for appropriate arm control. 1
10. *draw()*: Instructs the robotic arm to translate the digital sketch (stored as contours) into a physical drawing on paper. It meticulously follows the provided contours, transforming the digital lines into lines drawn with the pen in the real world.

main.py:

The `main.py` file acts as the conductor of the ArtRobo program, bringing together the functionalities of `image_processor.py` and `arm_draw.py` to achieve the ultimate goal - automatic drawing on paper (Fig.7&Fig.8):



Fig.7. First successful test



Fig.8. Exposition at Polifest2024 and user interaction

User Input:

The program starts by interacting with the user, prompting for an operating mode selection:

- **"IMAGE"**: Uses a pre-existing image as the source for the drawing.
- **"USER"**: Captures the user's drawing using a designated input method (possibly a tablet or touchscreen).
- **"STOP"**: Gracefully stops the operation of the robotic arm.

Image Processing (if applicable):

If "IMAGE" mode is selected, main.py calls functions from image_processor.py to process the selected image. This step extracts the crucial contours that represent the essence of the drawing.

Configuration and Control (For All Modes):

Next, main.py interacts with the Arm_draw class from arm_draw.py. It uses the provided methods to configure the robotic arm, including:

- Setting the scaling factor (set_magic_number) to adjust the drawing size.
- Defining the writing height (set_write_height) for optimal pen pressure.
- Specifying the offset (set_offset) to precisely position the drawing on the paper.

Providing the Plan (For "IMAGE" and "USER" Modes):

Depending on the chosen mode, main.py retrieves the contours:

- Processed contours from the image (image_processor.py) for the "IMAGE" mode.
- User-drawn contours captured through the input method for the "USER" mode.

Then, it provides these crucial contours to the Arm_draw class using the set_contour method, offering the robotic arm the necessary instructions.

Execution:

main.py calls the draw() method from the Arm_draw class. This method instructs the robotic arm to meticulously follow the provided contours, translating the digital representation into a physical drawing on paper.

Safety:

main.py prioritizes safety. In case of unforeseen situations, it ensures the proper shutdown of the robotic arm using the stop_arm() method from arm_draw.py.

5. Added Value Study

With this robotic arm that draws, we participated in the POLIFEST 2024 event, where it enjoyed real success at our faculty's booth. Figure 9 shows part of the "activity" of the robotic arm at this event.

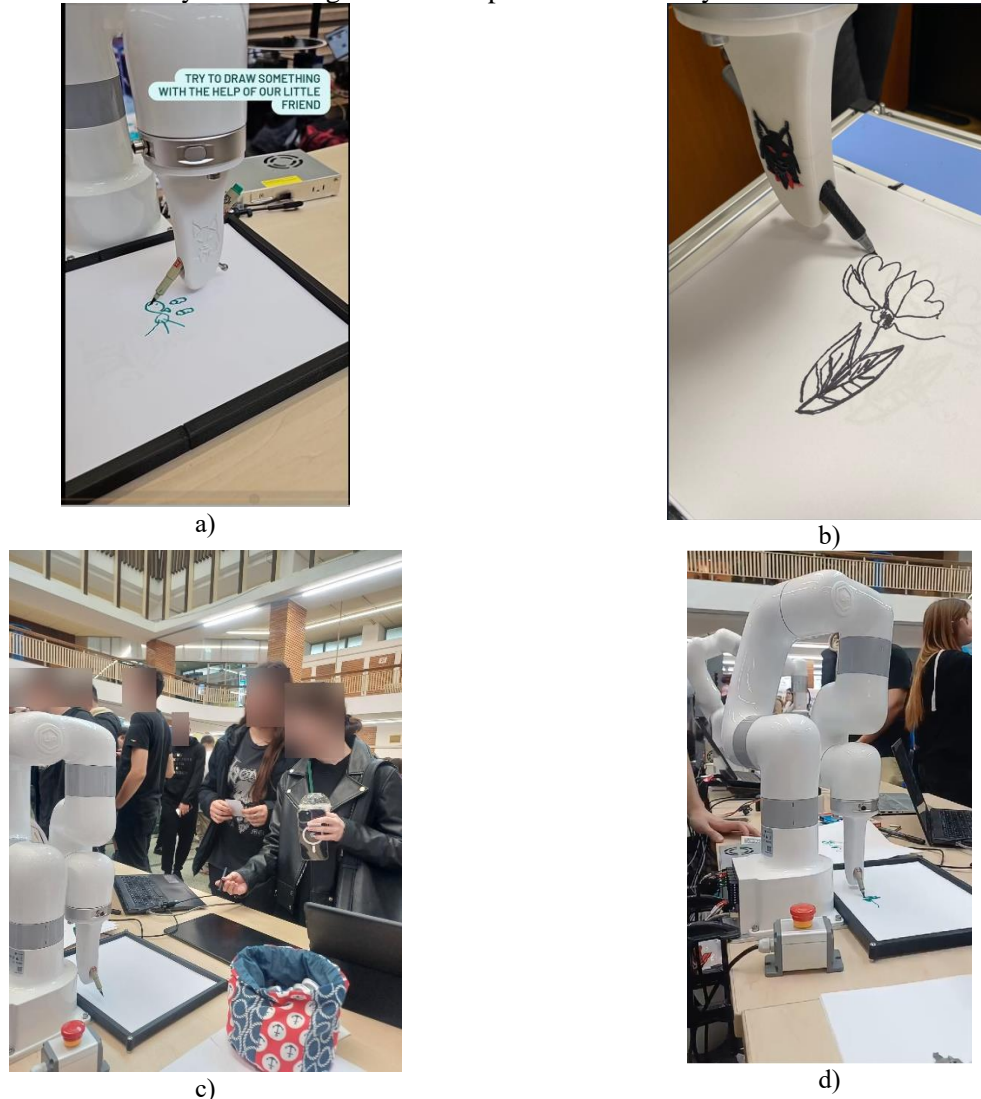


Fig. 9 – POLIFEST2024

6. Conclusions

Our study, investigated the effectiveness and implications of integrating robotic technology into the creative process. By using collaborative robots, we demonstrated that the automatic transfer of hand-drawn drawings onto paper can be achieved with significantly improved precision and efficiency. This opens up new perspectives in artistic production and robot-assisted manufacturing, allowing artists and creators to focus more on the creative aspects of their process, while robotic technology handles the repetitive and technical aspects. Thus, ArtRobo not only accelerates the creation process but also enriches the dialogue between humans and machines in the context of artistic production.

Considering the success at the POLIFEST 2024 event, we aim to identify other events where we can participate and promote the faculty.

7. Bibliography

- [1] Almeida, D.; Karayiannidis, Y. A Lyapunov-Based Approach to Exploit Asymmetries in Robotic Dual-Arm Task Resolution. In Proceedings of the 2019 IEEE 58th Conference on Decision and Control (CDC), Nice, France, 11–13 December 2019. [\[Google Scholar\]](#) [\[CrossRef\]](#)
- [2] TWOMEY, R. Three Stage Drawing Transfer. Available online: <https://roberttwomey.com/three-stage-drawing-transfer/> (accessed on 10 May 2023).
- [3] Putra, R.Y.; Kautsar, S.; Adhitya, R.; Syai'in, M.; Rinanto, N.; Munadhif, I.; Sarena, S.; Endrasmono, J.; Soeprijanto, A. Neural Network Implementation for Invers Kinematic Model of Arm Drawing Robot. In Proceedings of the 2016 International Symposium on Electronics and Smart Devices (ISESD), Bandung, Indonesia, 29–30 November 2016. [\[Google Scholar\]](#)
- [4] Baccaglini-Frank, A.E.; Santi, G.; Del Zozzo, A.; Frank, E. Teachers' Perspectives on the Intertwining of Tangible and Digital Modes of Activity with a Drawing Robot for Geometry. *Educ. Sci.* **2020**, *10*, 387. [\[Google Scholar\]](#) [\[CrossRef\]](#)
- [5] Shaw J-S, Lee S-Y. Using genetic algorithm for drawing path planning in a robotic arm pencil sketching system. Proceedings of the Institution of Mechanical Engineers, Part C: Journal of Mechanical Engineering Science. 2024;0(0). doi:10.1177/09544062241230171
- [6] <http://download.ufactory.cc/xarm/en/xArm%20Developer%20Manual.pdf?v=1600992000052>
- [7] [https://en.wikipedia.org/wiki/B%C3%A9zier_curve#:~:text=A%20B%C3%A9zier%20curve%20\(%2F'b,by%20means%20of%20a%20formula.](https://en.wikipedia.org/wiki/B%C3%A9zier_curve#:~:text=A%20B%C3%A9zier%20curve%20(%2F'b,by%20means%20of%20a%20formula.)
- [8]. <https://docs.opencv.org/4.x/>
- [9]. <https://devdocs.io/pygame/>
- [10]. <https://www.sciencedirect.com/topics/engineering/inverse-kinematics#:~:text=Inverse%20kinematics%20is%20just%20opposite,for%20arm%20in%20sagittal%20plane.>

DEVELOPING TRIBOELECTRIC GENERATORS FOR ENERGY CONSERVATION

GEORGESCU Alexia-Ioana, CIOBOTARU Felicia-Ionela, ALEXANDRU Tudor

Facultatea: Inginerie Industrială și Robotica, Specializarea: Robotica, Anul de studii: IV, e-mail:
alexia.georgescu@stud.fiir.upb.ro

SUMMARY: The paper aimed to develop a triboelectric generator as a solution for energy conservation. It reviews energy consumption and the current state of triboelectric nanogenerator technology, presenting two types of such generators and examples of their implementation. An experimental setup was proposed, consisting of a copper strip and a Kapton element. When these materials are rubbed together, they produce electrical energy that can be used to power LEDs.

KEYWORDS: triboelectric nanogenerator, energy conservation, copper strip, Kapton element, electrical energy

1. Introduction

In the contemporary world, energy protection has turned into a basic issue, driven by both natural worries and the rising interest for electrical power. As customary energy sources exhaust and their ecological effect turns out to be more evident, the investigation of option, supportable energy sources has heightened. Among these, the triboelectric nanogenerator (TENG) stands apart as a promising arrangement because of its capacity to reap energy from mechanical developments, for example, vibrations and rubbing, which are bountiful in ordinary conditions.

The worldwide utilization of electrical energy has seen a predictable ascent throughout the course of recent many years, driven by industrialization, urbanization, and the multiplication of electronic gadgets. This flood sought after overburdens existing power matrices and increases the direness to foster new energy arrangements. The customary techniques for energy creation, principally founded on petroleum derivatives, contribute considerably to ozone depleting substance emanations, requiring a shift towards cleaner options. Sustainable power sources like sunlight based, wind, and hydropower are gaining ground, yet they frequently require significant framework and are dependent upon natural constraints. In this manner, there is a developing interest in creative advancements like triboelectric generators that can supplement these sources and upgrade generally speaking energy proficiency.

Triboelectric generators influence the triboelectric impact, where certain materials become electrically charged in the wake of coming into contact with an alternate material and afterward being isolated. This peculiarity can be tackled to change over mechanical energy into electrical energy. The innovation behind TENGs is moderately straightforward yet profoundly compelling, including materials with various electron affinities that, when scoured together, make a charge irregularity. This irregularity produces an electric flow when associated through an outside circuit. TENGs offer a few benefits, including minimal expense, simplicity of creation, and the capacity to produce power from various mechanical sources, making them flexible for various applications.

Nanogenerators, a subset of energy reaping gadgets, come in different structures, including piezoelectric, pyroelectric, and triboelectric generators. Among these, triboelectric nanogenerators are especially significant for their proficiency and straightforwardness. There are two essential sorts of TENGs: contact-detachment mode and sliding mode. In the contact-partition mode, the surfaces of two materials come into contact and afterward discrete, making an occasional charge move. In the sliding mode, the materials slide against one another, creating persistent electric heartbeats. Each type has its own arrangement of uses and advantages, contingent upon the particular prerequisites of the energy collecting situation.

The exploratory arrangement proposed in this study includes a copper strip and a Kapton component. These materials were chosen for their reasonable triboelectric properties. At the point when the copper and Kapton are scoured together, they produce an electric charge due to the triboelectric impact. This arrangement is intended to exhibit the reasonableness of TENGs in producing usable electrical energy. The created power can be utilized to control low-energy gadgets like LEDs, exhibiting the capability of TENGs for limited scope energy applications.

2. Current status

Energy efficiency is crucial for reducing environmental impact, decreasing energy dependence, and enhancing economic resilience. Linares & Labandeira, 2010 discuss the critical role of energy efficiency in mitigating climate change and reducing energy vulnerabilities. It highlights the importance of specific policies to promote energy conservation, focusing on economic instruments and consumer information to drive energy efficiency improvements [1].

Triboelectric nanogenerators represent an innovative approach to energy efficiency by converting mechanical energy into electrical energy. Lin et al., 2015 introduces a highly efficient TENG that utilizes rolling electrification and electrostatic induction to harvest mechanical energy. The study demonstrates an instantaneous energy conversion efficiency of approximately 55%, highlighting the potential of TENGs to improve energy efficiency in various applications. The design features rolling motion, which minimizes material wear and mechanical energy consumption, making it a robust solution for sustainable energy harvesting [2].

Molnar et al., 2018 reviews the main types of triboelectric generators, focusing on their technical parameters and schematic solutions. It discusses the construction and application of triboelectric nanogenerators in various devices, highlighting their high efficiency when combined with other energy sources and super capacitors. The paper details the different types of generators within triboelectricity, including the contact-separation mode and sliding mode, and their potential for high efficiency in energy harvesting applications [3].

Cui et al., 2015 highlights the practical application of triboelectric generators in clothing, showcasing their potential to power portable electronic devices through body movements [4].

3. Energetic efficiency

In today's world, electric power is indispensable for carrying out the everyday activities of any individual. There is always talk about the need for energy on a large scale, but it is overlooked that everything starts on a much smaller scale. The phone is a good example because it uses small electronic components, including sensors. These components can be found in medical equipment, technical instruments for environmental monitoring, as well as in IoT devices. Sensors are fundamental to the operation of any technology, playing the role of collecting data. They have a high energy consumption, and since batteries are the main power source, the surrounding environment is prone to pollution.

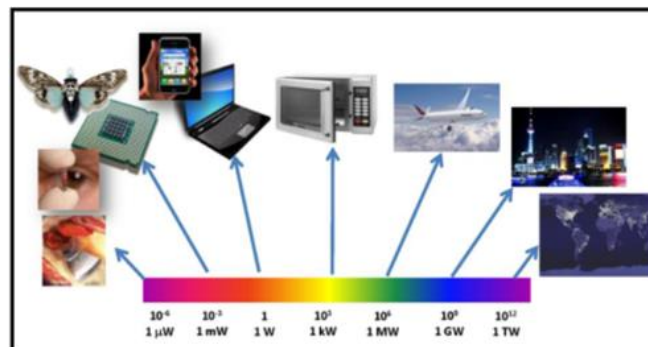


Fig.1. Magnitude of power and its corresponding applications

4. Research on triboelectric nanogenerators

Professor Zhong Lin Wang's group, from the Georgia Institute of Technology, demonstrated for the first time in 2012 the possibility of converting energy generated during motion into electrical energy through the triboelectric nanogenerator. This technology can thus reduce the use of batteries, reducing the impact on the environment.

5. The main types of triboelectric nanogenerators

- Triboelectric nanogenerator operating through vertical pressing

This operates through the periodic change in induced potential difference caused by the cyclic separation and re-contact of opposing electrical charges on the inner surfaces of the two materials. When a force is applied to the device, the surfaces of the two materials come into contact, causing charge transfer and generating a potential difference. This potential difference generates alternating current (AC) signals. At least one of the materials must be an insulator to maintain charges on the inner surface of the material and induce the flow of electricity.

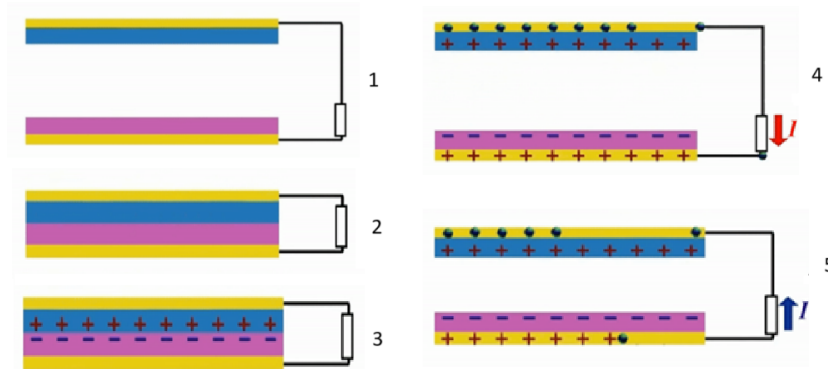


Fig.2.

- Triboelectric nanogenerator operating through sliding friction

It relies on the lateral sliding between two surfaces. During this process, there is a periodic change in the contact area, which generates a separation of charge centers, producing a voltage that drives the flow of electrons. This cycle produces a symmetric alternating current.

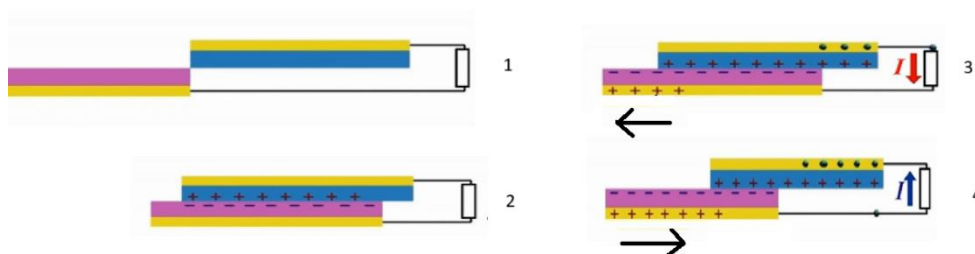


Fig.3

6. Examples of implementation

The transformation of energy produced by humans into electrical energy through textiles (Fig.4.)

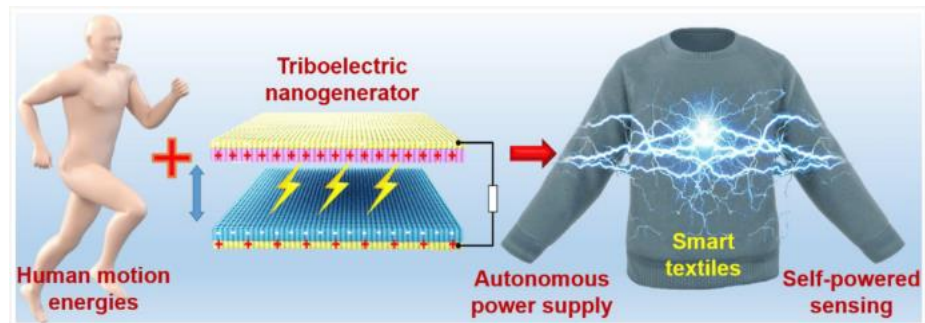


Fig.4.

Motion detection alarm powered directly by pressing the contact surface (Fig.5.)

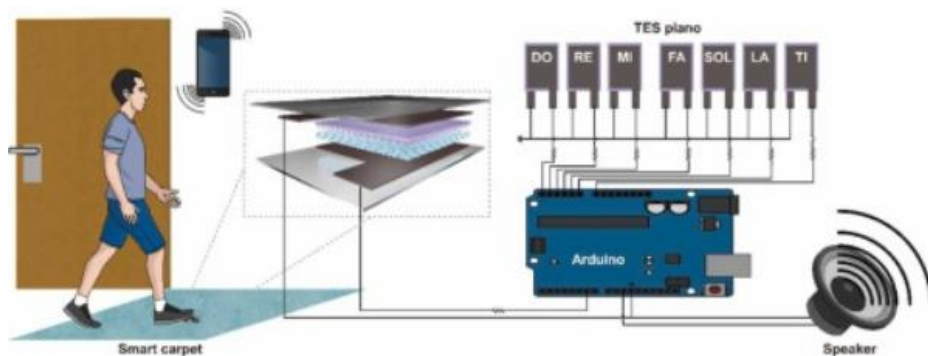


Fig.5.

Experiment to measure the voltage produced as a result of the force exerted on the surface of the carpet (Fig.6)

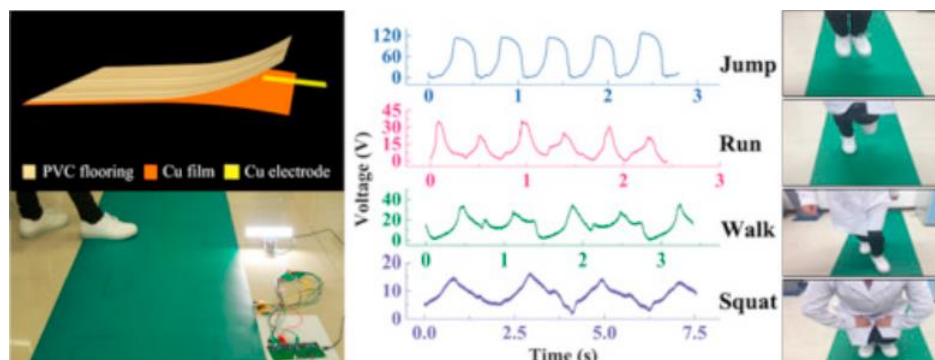


Fig.6.

7. Experiment

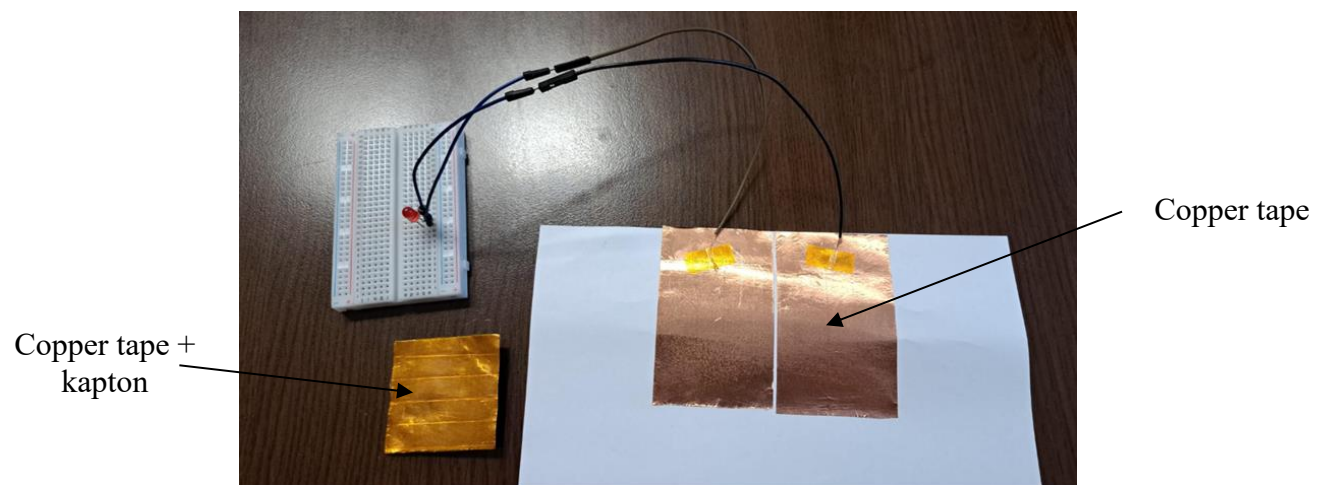


Fig.7. Materials used



Fig.8. Measured value during the experiment

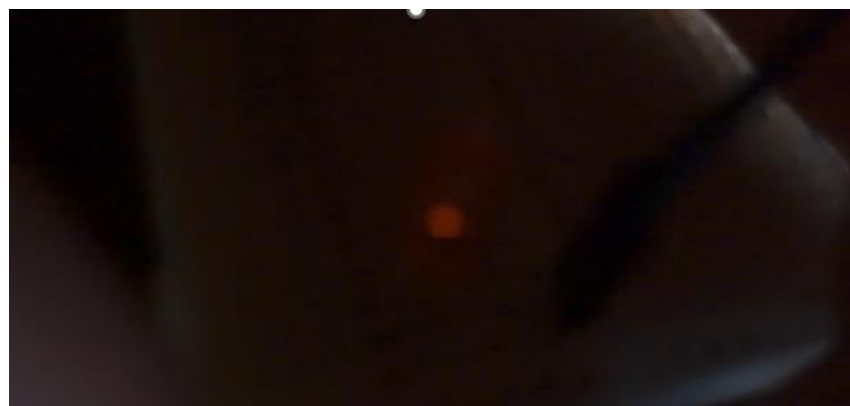


Fig.9. The LED lit during the experiment

8. Conclusions

The study demonstrates that triboelectric generators (TENGs) are an effective solution for energy conservation, capable of harvesting energy from everyday mechanical movements. The materials and technology required for TENGs are low-cost and straightforward to fabricate, making them accessible for widespread adoption and implementation. The proposed experimental setup, utilizing a copper strip and a Kapton element, successfully demonstrated the practical generation of electrical energy through the triboelectric effect. This validates the theoretical principles and highlights the feasibility of TENGs for small-scale energy applications. The study opens avenues for further research into optimizing TENG materials and configurations, improving energy conversion efficiency, and expanding their applications. Continued innovation in this field can significantly impact global energy conservation efforts.

9. Bibliography

- [1]. Lin, L., Xie, Y., Niu, S., Wang, S., Yang, P. K., & Wang, Z. L. (2015). Robust triboelectric nanogenerator based on rolling electrification and electrostatic induction at an instantaneous energy conversion efficiency of~ 55%. *ACS nano*, 9(1), 922-930.
- [2]. Molnar, O., Gerasimov, V. V., & Kurytnik, I. (2018). Triboelectricity and construction of power generators based on it.
- [3]. Cui, N., Liu, J., Gu, L., Bai, S., Chen, X., & Qin, Y. (2015). Wearable triboelectric generator for powering the portable electronic devices. *ACS applied materials & interfaces*, 7(33), 18225-18230.
- [4]. Wiese, C., Larsen, A., & Pade, L. L. (2018). Interaction effects of energy efficiency policies: a review. *Energy Efficiency*, 11(8), 2137-2156.